ABSTRACT

Nguyen, Anh Quynh, Pyruvate Intervention for Brain Injury Inflicted by Cardiac Arrest-Resuscitation. Doctor of philosophy (Integrative Physiology), April 2016.

Fewer than 10% of the 360,000 people who suffer out-of-hospital cardiac arrest annually in the U.S. survive to hospital discharge. Many suffer brain injuries that greatly affect their daily activities and quality of life. Despite improvements in clinical outcomes from cardiac arrest as a result of therapeutic hypothermia, survival rates are still dismal. Additional interventions to be used alone or in combination with therapeutic hypothermia could potentially save many lives.

The intermediate metabolite pyruvate has been proven to be neuroprotective when given acutely. The goal of this investigation is to examine the neuroprotective capabilities and mechanisms of pyruvate in a large animal model of cardiac arrest, closed-chest cardiopulmonary resuscitation (CPR) and countershock induced defibrillation. The central hypothesis is that pyruvate therapy suppresses matrix metalloproteinase (MMP) activity and thereby preserves blood-brain barrier (BBB) integrity, increases expression and content of the cytoprotective cytokine erythropoietin (EPO), and dampens inflammation following cardiac arrest, and, thus, improves neurobehavioral recovery from cardiac arrest.

Experiments were conducted in Yorkshire swine, subjected to cardiac arrest, closed-chest cardiocerebral resuscitation (CCR), defibrillation by trans-thoracic countershock, and recovery. The project was divided into two studies with different durations of cardiac arrest, producing

different intensities of brain damage. In the first study, swine were subjected to 6 min of untreated cardiac arrest and 4 min of CCR, following by defibrillation and recovery of spontaneous circulation (ROSC). In the second study, untreated cardiac arrest was extended to 10 min before 4 min CCR. Animals were euthanized at 1, 4, and 72 h ROSC, and the brain was biopsied for histological and biochemical analyses. For animals in 72 h ROSC groups, neurological assessment and testing were performed at 24, 48, and 72 h ROSC.

At 3 d ROSC, the number of viable cerebellar Purkinje cells fell by 30% vs. Sham control, but pyruvate infusion during CCR and the first 60 min ROSC preserved these neurons. EPO mRNA abundance was sharply increased at 4 h ROSC and in the non-arrest Sham, indicating the surgical protocol, hyperoxic ventilation and anesthesia induced neuroprotective EPO, which may have limited brain injury. There were no differences in neurological scores among Sham, CPR, and CPR+Pyruvate, prompting study of more prolonged cardiac arrest to intensify brain injury.

At 4 h ROSC in 10 min untreated cardiac arrest group, cardiac arrest unexpectedly decreased hippocampal and cerebellar MMP-2 activities and cerebellar EPO content, regardless of treatment. 72 h survival rate fell from 100% in study one (6 min pretreatment arrest) to only 2 of 6 pigs in study two (10 min pretreatment arrest), which wide disparity in neurological function among the 2 survivors. Collectively, these results indicate the prolonging pre-intervention arrest from 6 to 10 min sharply intensified brain injury, depleted cytoprotective EPO, and inactivated oxyradical-sensitive enzymes. Pyruvate treatment did not exert favorable effects on these variables, indicating that pyruvate may have had limited ability to traverse the blood brain barrier and protect the brain parenchyma in this large animal model of cardiac arrest and CCR.

PYRUVATE INTERVENTION FOR BRAIN INJURY INFLICTED BY CARDIAC ARREST-RESUSCITATION

Anh Quynh Nguyen, M.S.

APPROVED

Major Professor : _____
Robert T. Mallet, Ph.D.

Committee Member : _____
Albert H. Olivencia-Yurvati, D.O., Ph.D.

Committee Member : _____
Peter B. Raven, Ph.D.

Committee Member : _____
Shaohua Yang, M.D., Ph.D.

Committee Member : _____
Caroline Rickards, Ph.D.

University Member : _____
Bruce Budowle, Ph.D.

Graduate Advisor : _____
J. Thomas Cunningham, Ph.D.

Department Chair : _____
Steve Mifflin, Ph.D.

Accepted:

Graduate Dean : _____
Meharvan Singh, Ph.D. *Date*

PYRUVATE INTERVENTION FOR BRAIN INJURY INFLICTED BY CARDIAC ARREST-RESUSCITATION

DISSERTATION

Presented to the Graduate Council of the

Graduate School of Biomedical Sciences

University of North Texas Health Science Center

For the Degree of

DOCTOR OF PHILOSOPHY

By

Anh Quynh Nguyen

Fort Worth, TX

April 15, 2016

ACKNOWLEDGEMENTS

This work was supported by the research grant R01 NS076975 from the National Institute of Neurological Disorders and Stroke. Fellowship support to Anh Quynh Nguyen was provided by the D.O./Ph.D. program at the University of North Texas Health Science Center at Fort Worth.

This work would not be possible without the guidance, mentorship, encouragement, patience, and support from my Major Professor, Dr. Robert T. Mallet. His teaching and leading-by-example have always been an inspiration of a scientist I want to become one day. I am thankful for my co-mentor, Dr. Albert H. Olivencia-Yurvati for his support throughout the project, Dr. Peter B. Raven for all his teaching, and my committee members whose feedback and expertise in their respective fields have made this project better-rounded: Dr. Shaohua Yang, Dr. Caroline Rickards, and Dr. Bruce Budowle.

I also would like to thank Dr. Myoung-Gwi Ryou Dr. J. Thomas Cunningham, Dr. Gourav Roy Choudhury, Roger Hollrah, Arthur Williams Jr., Tito Nelson and DLAM staff for their help with animal surgeries, biochemical and histology techniques in this project.

The myocardial MMP-2 data in the appendix A is the result from the collaboration with Dr. Rick Schulz lab (University of Alberta).

I am grateful for my parents, Tan Nguyen and Ngoc Tran, and my whole family (my sister, aunts, uncles, cousins) who have always been there for me and believed in me during my long academic journey. Last but not least, I would like to thank my little family: my husband for his love and support, and my 3-month old Noah BaoLong for being such a great and happy baby.

TABLE OF CONTENT

TABLES

CHAPTER III

CHAPTER IV

FIGURES

CHAPTER III

Figures

CHAPTER IV

APPENDIX A

APPENDIX B

PUBLICATIONS and PRESENTATIONS

Peer-reviewed reports

Nguyen AQ, Cherry BH, Scott GF, Ryou MG, Mallet RT. Erythropoietin: Powerful protection of ischemic and post-ischemic brain. *Exp Biol Med* 2014: 1-15. DOI: 10.1177/1535370214523703.

Cherry BH, Nguyen, AQ, Hollrah RA, Olivencia-Yurvati AH, Mallet RT. Modeling cardiac arrest and resuscitation in the domestic pig. *World Journal of Critical Care Medicine* 2015 Feb 4; **4(1)**: 1-12.

Cherry BH, Nguyen AQ, Hollrah RA, Williams AG Jr., Hoxha B, Olivencia-Yurvati AH, Mallet RT. Pyruvate stabilizes electrocardiographic and hemodynamic function in pigs recovering from cardiac arrest. *Exp Biol Med* 2015; **240**(12): 1774 – 1784

Scott GF, Nguyen, AQ, Cherry, BH, Hollrah RA, Williams, AG, Ryou MG, Mallet, RT. Pyruvate preserves cerebroprotective anti-glycation machinery after cardiac arrest in swine. *Journal of neurotrauma* 2016. In submission.

Abtracts

Nguyen, AQ, Cherry, BH, Ryou, MG, Hollrah RA, Williams, AG, Scott GF, Olivencia-Yurvati, AH, Mallet, RT. Cytoprotective and Anti-glycation defenses in porcine brain after cardiac arrest and cardiocerebral resuscitation. *FESEB J*. 2016. Accepted.

Nguyen, AQ, Cherry, BH, Ryou, MG, Hollrah RA, Williams, AG, Scott GF, Olivencia-Yurvati, AH, Mallet, RT. Pyruvate suppresses hippocampal MMP-2 activity following cardiac arrest-resuscitation. *FESEB J. 2015*; **29**: 834.3

Nguyen AQ, Cherry BH, Ryou MG, Hollrah RA, Williams AG Jr., Scott GF, Olivencia-Yurvati AH, Mallet RT. Pyruvate suppresses hippocampal MMP-2 activity in swine following cardiac arrest and resuscitation. Brain Research Conference, Washington DC, November, 2014.

Nguyen AQ, Cherry BH, Ryou MG, Williams AG Jr., Hollrah RA, Baker C, Choudhury GR, Olivencia- Yurvati AH, Mallet RT. Delayed Neuronal death in swine following cardiac arrest and resuscitation. *FESEB J*. 2014; **28**: 877.12.

Cherry BH, Nguyen AQ, Williams Jr. AG, Scott GF, Hollrah RA, Ryou M, Hoxha B, Olivencia-Yurvati AH, Mallet RT. Vasopressin Instead of Epinephrine Enhances Efficacy of CPR Without Causing Tachycardia. *FESEB J*. 2014; **28**: 1150.5..

Cherry BH, Nguyen AQ, Hollrah RA, Ryou MG, Williams AG Jr., Hoxha B, Olivencia-Yurvati AH, Mallet RT. Pyruvate improves electrolyte homeostasis following cardiac arrest. *Resuscitation Science Symposium* 2013; 8: 127.

Cherry BH, Nguyen AQ, Ryou MG, Williams AG Jr., Hoxha B, Olivencia-Yurvati AH, Mallet RT. Intravenous pyruvate for cardiac arrest does not cause persistent hypernatremia. *FASEB J.* 2013; **27**: 1206.6.

Oral Presentation

Nguyen, AQ. Blood-Brain Barrier: Pathophysiology and Prevention. *Frontiers in Cardiology Symposium*, Winter Park, Colorado. January, 2013.

ABBREVIATIONS

ANOVA	Analysis of variance
ATP	Adenosine Triphosphate
ADP	Adenosine Diphosphate
AMP	Adenosine Monophosphate
BBB	Blood-brain barrier
Ca^{2+}	Calcium ion
CA1	*Cornus ammonis* region 1 of hippocampus
CPR	Cardiopulmonary resuscitation
CCR	cardiocerebral resuscitation
CYTc	Cytochrome c
EKG	Electrocardiogram
EPO	Erythropoietin
GAPDH	Glyceraldehyde-3 phosphate dehydrogenase
GR	Glutathione reductase
GPx	Glutathione peroxidase
HCO_3^-	Bicarbonate iron
HIF-1α	Hypoxia inducible factor-1
K^+	Potassium ion
MAP	Mean aortic pressure
MMP	Matrix metalloproteinase
MPO	Myeloperoxidase
Na^+	Sodium ion

NAD^+/ NADH	Nicotinamide adenine dinucleotide
$NADP^+$/NADPH	Nicotinamide adenine dinucleotide phosphate
ROS	Reactive oxygen species
ROSC	Recovery of spontaneous circulation
qPCR	Real-time polymerase chain reaction
TUNEL labeling	Terminal deoxynucleotidyltransferase mediated dUTP-biotin nick-end
ZO-1	Zona occludens-1

CHAPTER I

INTRODUCTION

1. Cardiac arrest: a lethal clinical presentation

In the US, approximately 550,000 cases of cardiac arrest occur annually. Of those, 63% (~360,000 cases) occur outside the hospital setting, and of these out-of-hospital cases, approximately 40% are witnessed and received bystander chest compression, or cardiopulmonary resuscitation (CPR). Unfortunately, less than 10% of these victims survive to hospital discharge. These survival rates are persistently dismal despite community CPR education and more effective emergency response networks, which speaks to the challenge of effective and efficient delivery of lifesaving resuscitation to cardiac arrest patients (Go et al., 2013). Timely CPR, especially outside of healthcare settings, has been associated with increase in 30 d survival (Wissenberg et al., 2013). CPR quality is heterogeneous among healthcare providers and settings, and in many cases CPR did not meet published recommendations, even when performed by well-trained hospital staff (Abella et al., 2008). Because of its vital role, CPR quality and effectiveness has been scrutinized in recent years, and there has been a call for more frequent CPR training sessions for skill improvement in health care and non-healthcare settings. The high mortality and morbidity of cardiac arrest as a result of brain injury has prompted the American Heart Association (AHA) to emphasize quality chest compression as the utmost priority in resuscitation (Kleinman et al., 2015). Moreover, so-called rescue breathing is no longer recommended for bystander CPR, as the brain damage caused by interruption in chest

compressions outweighs the limited benefits of mouth-to-mouth ventilation. The term *cardiocerebral resuscitation* (CCR) more accurately represents this ventilation-free approach.

Clinical presentation of brain injury due to cardiac arrest-resuscitation varies with duration of arrest, quality of resuscitation, comorbidity, and other factors. Many survivors report severe difficulties with daily activity, motility, and memory. A survey of 400 persons, who had survived at least six months after cardiac arrest, reported difficulties with memory and stair climbing, even though more than three-fifths of those who had been working before their illness returned to work (Bergner et al., 1984). In another study, 308 survivors of out of hospital cardiac arrest and age-matched myocardial infarction controls were evaluated to assess sleep and rest, emotional behavior, body care and movement, household management, mobility, social interaction, ambulation, alertness, communication, work, recreation and pastimes, eating behavior, physical activity, and psychosocial status. The cardiac arrest group scored worse in 11 of 12 categories, twice as many reported poorer memory functions, and 15 % fewer were able to return to work (Berger, 1985).

Neuropathological deficits in cardiac arrest survivors worsen as the duration of cardiac arrest is prolonged. In a pig model of cardiac arrest-resuscitation, Hogler *et al.* (2010) evaluated damage in brain regions at 72 h of recovery after 7, 10, or 13 min of cardiac arrest and correlate the histological injuries to neurological outcome. These authors reported appreciable differences in edema and necrosis in cerebral cortex, hippocampus, and cerebellar cortex in pigs subjected to 7 or 10 min arrest vs. non-arrested controls, while none of the pigs subjected to 13-min arrest survived. Of note, marked degeneration of Purkinje cells in the cerebellar cortex was identified in the 7 and 10 min cardiac arrest groups, and the number and density of neurons in the cerebellar granular cell layer were decreased in the 10-min cardiac arrest group.

Among many areas and cell types in the brain, the neurons of the hippocampal CA1 region and cerebellar Purkinje cells are among the most vulnerable to ischemic insult (Ng et al., 1989). The hippocampus is critically involved in memory and spatial navigation (Squire, 1992; Mizuseki et al., 2012), and the cerebellum coordinates motor control and posture. The loss of cerebellar Purkinje cells is associated with many movement and posture disorders, such as Huntington's disease (Venkatesan, 2006). Recent research has shown the cerebellum to contribute to more than motor and postural functions. Anatomical studies demonstrated that cerebellar neurons project to the prefrontal and posterior parietal cortices, and cerebellar interactions with the frontal, parietal, temporal and occipital lobes, as well as neuroimaging and neuropsychological data support involvement of the cerebellum in movement and cognition, attention, executive control, working memory, and learning (Strick, 2009). Post-ischemic Purkinje cell degeneration is gradual, and can be detected at 2-3 days after reperfusion (Horn et al., 1992; Sato et al, 1990). Interestingly, in dogs subjected to global ischemia by aorta clamping for 18 minutes, neuronal damage followed a bimodal pattern: the majority of Purkinje cells and hippocampal CA1 neurons had condensed, darkened nuclei (a sign of damage) at 15 min ROSC, appeared to recover at 1h, but disintegrated 2-3 days after ROSC (Sato et al., 1990). Considerable research effort has focused on mitigating damage in these two brain regions.

2. Mechanisms of brain injury inflicted by cardiac arrest-resuscitation:

Within seconds of cardiac arrest, mitochondrial oxidative phosphorylation in brain neurons is impaired, intracellular acidosis develops, lactate accumulates, and reactive oxygen and nitrogen derivatives (ROS and RNS) are produced (Chalkias, 2012). In the ischemic environment, excessive ROS and RNS trigger signaling cascades resulting in disruption of the blood-brain barrier (BBB), a structure essential for controlling and regulating movement of

substances between the brain and the cerebral circulation. Introduction of "foreign" components can harm neurons and supportive cells. Brain ischemia and reperfusion activates matrix metalloproteinases (MMPs), a family of proteases known to degrade extracellular matrix, thus disrupting BBB, enabling inflammatory signals and cells to invade the brain microenvironment (Figure 1). Matrix metalloproteinase -9 (MMP-9) is known to mediate BBB destruction (Gidday, 2005) and inhibition of MMP-9 by endogenous tissue inhibitors of MMPs (TIMPs) affords neuroprotection in mice experiencing focal cerebral ischemia (Fujimoto, 2008). MMP-2 is upregulated after focal cerebral ischemia and is proposed to contribute to extracellular matrix destruction and neuronal damage (Heo et al., 1999).

There are many activators of MMPs, including the "Redox Switch" mechanism, in which the redox state of sulfhydryl groups in the MMP molecule is modulated by changes in the intracellular glutathione (GSH): glutathione disulfide (GSSG) concentration ratio (Okamoto et al., 2004). In mice subjected to 20 min global cerebral ischemia by bilateral occlusion of the common carotid arteries, MMP-2 and MMP-9 activities and hippocampal neuronal death were increased 3 days after transient global ischemia. When MMP-9 knock-out mice were subjected to the same ischemic insult, hippocampal MMP-2 and MMP-9 activities and neuronal damage were appreciably decreased (Lee et al., 2004).

Suppression of MMP-2 and/or MMP-9 activity in brain after ischemia-reperfusion insult is an important mechanism to mitigate brain injuries. Indeed, inhibition of MMPs has been shown to reduce neuronal damage following brain ischemia. Extensive research has been conducted to identify an effective and specific novel MMP inhibitor (Devy et al., 2011). So far, doxycycline is the only FDA approved MMP inhibitor and has been used in clinical trials for many clinical diseases such as chronic obstructive pulmonary disease (Dalvi et al., 2011).

However, doxycycline is a broad-spectrum MMP inhibitor; it is administered orally and chronically at low doses in order to achieve therapeutic effect, and thus is not a suitable intervention for acute ischemic events.

Reactive oxygen species (ROS), abundant during ischemia and reperfusion, cause damage to cellular metabolic and ion transport machinery (Idris et al, 2005). ROS also activate platelets and endothelial cells, leading to thrombus formation and resulting vascular occlusion. ROS also trigger neurons to secrete inflammatory cytokines, leading to recruitment of resident microglia, activation of astrocytes, and infiltration of non-resident inflammatory cells (particularly neutrophils and macrophages) to the brain. The resident and infiltrating cells secrete harmful enzymes and proteases, which further damage brain infrastructure (Shichita et al., 2012). Biochemical and gene expression changes inflicted by ischemia could be observed within minutes (e.g. heat shock proteins) to days (apoptotic proteins.) (Akins et al., 1996). Specifically, inflammatory cells release MMPs, which degrade extracellular matrix and tight junctions at the BBB, thereby potentiating edema and facilitating extravasation of leukocytes and, thus, exacerbating brain injury (Yang et al., 2007). Oxidative stress caused by IR induces dissociation of BBB tight junction proteins, such as occludin, in a rat model of hypoxia and reoxygenation (Lochhead et al., 2010). In an *in vitro* experiment, incubation of intact cerebrovascular endothelial monolayers, a model of BBB, with the pro-inflammatory cytokines TNF-α, IL-1β or IL-6 resulted in decreased transendothelial electrical resistance (TEER), an indicator of BBB disruption (Vries et al., 1996). This result was confirmed *in vivo*, where intracerebral injection of TNF-α causes increased BBB permeability and increased expression of MMP-9 (Rosenberg et al., 1995).

Cardiac arrest has been shown to activate an intense systemic inflammatory response. In patients suffering from cardiac arrest-resuscitation, plasma IL-8 and TNF-α peaked at 12 h and 6 h ROSC, respectively. Elevation of IL-8 seemed to reflect clinical outcome: those who died or became brain dead within 1 week of cardiac arrest had significant higher circulating IL-8 compared to survivors. (Ito et al., 2001). Other pro-inflammatory cytokines such as IL-6, IL-10, IL-1ra, and endotoxin were reported to increase and were correlated with adverse outcomes in humans (Adrie et al., 2002). In pigs subjected to 7 min ventricular fibrillation, plasma TNF-α reached its maximum concentration at 15 min ROSC, and IL-1β at 2 h; there was no involvement of IL-6 within the first 6 h ROSC (Niemann et al., 2009). Inflammation persists even with therapeutic hypothermia. In pigs with 15 minutes of pre-intervention ventricular fibrillation followed by intra-arrest cardiopulmonary bypass cooling for 1, 3, 5 min achieving brain temperature of 30.4±1.6, 24.2±4.6, and 18.8±4.0^{o}C, it was found that pro-inflammatory cytokines such as plasma IL-6 and TNF-α increased significantly at 1h after resuscitation but returned to normal within 24 h (Sipos et al., 2010).

Injury inflicted by cardiac arrest and resuscitation can trigger pro-apoptotic signaling cascades. Cytochrome c (CYTc), an electron carrier indigenous to the mitochondrial intermembrane space, is released into the cytosol upon ischemic-reperfusion due to opening of the mitochondrial permeability transition pore. The presence of cytochrome c in the cytoplasm initiates an intrinsic signaling pathway culminating in apoptosis. Release of CYTc into the blood stream has been suggested to be a prognostic biomarker in cardiac arrest (Chalkias et al., 2015). In rats subjected to 8-min untreated ventricular fibrillation (VF), plasma CYTc did not exceed 2μg/ml in survivors, returning to baseline within 48 to 96 h, but was more elevated and remained so for more prolonged periods in rats that subsequently succumbed to post-arrest brain injury

(Ayoub et al, 2008). This finding that CYTc release varied with survival suggests interventions that prevent mitochondrial damage may foster post-arrest brain recovery and survival.

Brain damage from cardiac arrest is complex and multifactorial, representing the impact of decreased blood flow to the entire brain and/or release of factors from other ischemic organs. Cardiac arrest initiates several neuronal injury mechanisms, including apoptosis, necrosis, inflammation, and excitotoxicity. Of the many pathways culminating in apoptosis, the intrinsic pathway, which involves disruption of the outer mitochondrial membrane due to release of proapoptotic factors such as caspases and cytochrome c, is of particular interest in this project. Many chemical factors have been implicated in neuronal injury; a partial list includes glutamate, acidic amino acid toxicity, nitric oxide, free radicals, dopamine, and norepinephrine. Extensive research effort has been devoted to developing pharmacological interventions to prevent brain damage from cardiac arrest, yet none has entered mainstream clinical practice due to failed clinical trials (e.g. Calcium channel antagonist, barbiturates) or undesirable side effects (such as N-methyl-D-aspartate-receptor antagonists) (Harukuni et al, 2006).

Damage to the internal organs during cardiac arrest-resuscitation is due in large part to harmful effects of reperfusion, as well as the effects of ischemia per se. In fact, studies have demonstrated that reperfusion may inflict even more severe injury than ischemia alone; accordingly, interventions such as therapeutic hypothermia and post-ischemic conditioning by influencing injury mechanisms initiated by reperfusion, most notably ROS formation, intracellular Ca^{2+} overload and glutamate excitotoxicity, may exert robust brain protection (Horn, 1992; Kalogeris, 2012).

Advances in cardiac care have not improved the in-hospital and out-of-hospital cardiac arrest mortality and morbidity rates appreciably in the past few decades. The most important

advancement is the application of therapeutic hypothermia (TH) following restoration of sinus rhythm and recovering of arterial pressure. TH has been shown to be brain protective and improves neurological outcome. Mild therapeutic hypothermia (32^oC – 34^oC) has become a standard post-resuscitation treatment in many hospitals across the U.S. It is the only therapy that improved neurological outcome after cardiac arrest in a randomized, controlled trial (Holzer et al., 2002). Complications of mild hypothermia include immunosuppression, electrolyte disorders such as hypernatremia, hypokalemia, hypomagnesmia, hypophosphatemia, and hypocalcemia, suppression of the clotting cascade causing higher risk of bleeding, hemodynamic disturbances such as bradycardia, and interfering with drug metabolism, especially that catalyzed by cytochrome P450. Optimal intensity and duration use of hypothermia and rate of rewarming are still controversial (Janata et al, 2009). In a rat model of asphyxia-induced cardiac arrest and CPR, hypothermia, initiated 8 h after ROSC, improved Purkinje cell survival compared to the normothermic group, and the outcome was not significantly different when TH was initiated even earlier (Paine, 2012). Additionally, the effect of hypothermia is controversial, and the treatment option is limited to comatose patients (Bernard, 2002), and its effects and mechanisms are being elucidated in many experimental preparations and by many research groups worldwide. TH protocol must be precisely followed and can only be carried out in advanced critical care units due to potential adverse effects. In most out-of-hospital cardiac arrest cases, the delay in patient transportation to the hospital restricts the immediate intervention of TH. In addition, TH has not been shown to be effective in cases with shockable rhythm and severe acidemia (pH< 7.20) (Ganga et al., 2013), and rebound pyrexia of > 38.7^oC following TH was associated with worse neurological outcome (Leary et al., 2013). Efforts to mitigate reperfusion injury prompted experiments in pigs in which the brain was cooled within minutes to 30^oC, after 15 min of non-

intervened ventricular fibrillation, followed by a 20-min period of rewarming to mild hypothermia (33^{o}C), then defibrillation. Unfortunately, the result was not favorable due to large number of mortality to myocardial failure within the first 24 h of recovery (Weihs et al, 2010).

Besides many pharmacological efforts, mechanical interventions, including impedance threshold device (ITD), have been intensely studied in an attempt to develop an effective adjunct to the current resuscitation protocols to improve survival as well as neurologic (Yannopoulos et al., 2013). Keeping the patient in head-up position during CPR has been shown to increase cerebral perfusion compared to planar or head-down position, and thereby decrease intracranial pressure. However, the optimal degree of head-up tilt and duration of CPR in the head-up position have not been established (Debaty, 2015).

Therefore, it is crucial to have a therapeutic modality that is readily available to the paramedic team, is easy to use, and has potential benefit to cardiac arrest patients. Many substances have been tested, such as the nitric oxide (NO) donor sodium nitroprusside (Yannopoulos, 2011), the inhaled anesthetic sevoflurane, and a nonionic copolymer blocking pores on membranes caused by severe cellular stress, Poloxamer 188 (P188). Bartos *et al*. (2015) showed in pigs subjected to 17 min cardiac arrest that a bundle therapy of CPR, ITD, sevoflurance, and P188 improved hemodynamics during resuscitation, reduced the need for epinephrine and repeated defibrillation, and achieved higher rates of ROSC, and recovery with mild to no neurologic deficit (42%) at 48h after 17 min of untreated cardiac arrest in pigs.

Our aim is to identify an intervention agent that fosters neurological recovery after cardiac arrest. Pyruvate meets these requirements. It is a natural cellular metabolite, easily dissolved and stable in aqueous solution, and can be administered *iv*, so it can be infused as soon as an intravenous access is established. This project is particularly important because it

contributes to the body of knowledge on the impact of cardiac arrest and resuscitation on brain histology and biochemistry as well as the mechanisms by which pyruvate protects brain from ischemia and reperfusion. Erythropoietin (EPO), a hematopoietic cytokine, has been shown to be endogenously expressed in the brain and is cytoprotective. EPO, however, does not readily cross the BBB, so intravenous EPO is of limited efficacy. We propose that pyruvate dampens IR - induced brain inflammation in part by inducing endogenous EPO formation, which initiates other neuroprotective cascades. We propose pyruvate as a new agent that can easily cross the BBB and stimulate beneficial molecular pathways to protect the cells. This work is intended to develop a new intervention to promote neurological and cognitive function recovery in cardiac arrest patients. Specifically, this study is directed toward elucidating mechanisms by which pyruvate may protect brain function. If pyruvate proves effective, its use could allow immediate intervention to protect the brain from ischemia-reperfusion injuries in out-of-hospital and in-hospital cardiac arrest.

3. Erythropoietin

Erythropoietin protects many cell types in the central nervous system. EPO has been shown to be protective when given before, during, or after ischemic events. Many effectors of EPO have been elucidated. Overall, there seems to be redundancy in protection and cross-talk among signaling pathways downstream of EPO. For example, EPO augments beneficial gene expression that is activated by ischemia. In neuronal cell culture, EPO exerted cytoprotection via Jak2 signaling that activated nuclear translocalization of NF-κB and its DNA binding (Digicayliogiu, 2001). NF-κB is a transcription factor that activates expression of many cytoprotective genes under ischemia (Kaltschmidt et al, 2010). In an *in vivo* rat model of stroke, Mengozzi *et al* (2012), using microarray technology, demonstrated further upregulation of genes

implicated in synaptic plasticity- Arc, BNDF, Egr1, and Erg2, and EPO activated Erg2 in particular. Thus, EPO may minimize brain injury by potentiating the brain's reparative processes.

On the other hand, EPO has been shown to decrease neuronal apoptosis. In mice, transgenic over- expression of human EPO in brain decreased infarct volume by 84%, diminished edema, and ameliorated neurological deficit following 90 min of middle cerebral artery occlusion with 24 h reperfusion. In the transgenic mice, the number of apoptotic cells and activities of NOS-1 and NOS-2 were markedly reduced compared to wild-type. Increased endogenous EPO expression sharply increased phosphorylation of the signaling kinases ERK-1, ERK-2, AKT, JNK-1, and JNK-2. Indeed, activation of both ERK-1/-2 and PI3K/Akt is necessary for neuroprotection by hEPO. Although EPO over-expression dampened NOS-1 and NOS-2, this effect was not mediated by ERK-1/-2 and PI3K/Akt (Kilic et al, 2005). Another group (Wen et al., 2002) confirmed the anti-apoptotic effect of EPO treatment on a different effector Bcl-X_L. Content of Bcl-X_L, an anti-apoptotic member of the Bcl-2 family, was markedly increased in hippocampus of Mongolian gerbils treated with EPO after ischemic insult. Moreover, in ischemic cultured cortical neuron treated with EPO, they also demonstrated an increase in mRNA expression of Bcl-X_L.

In addition to neurons, other cell types including astrocytes and cerebrovascular endothelium, and white matter are fundamental to brain function and, therefore, merit protection from ischemic insult. Incubation of cultured rat astrocytes in 5-20 U/mL EPO for 16 h before being exposed to cytotoxic concentration of staurosporine attenuated cell death. In addition, EPO treatment was correlated with elevated expression of heme oxygenase-1 (HO-1), a potential mediator of EPO's cytoprotective mechanism (Diaz et al, 2005). EPO also protects cerebral

microvascular endothelial cells from oxidative stress produced by reoxygenation following oxygen-glucose deprivation. EPO treatment of cultured endothelial cells 1 h before oxygen-glucose deprivation leads to increased nuclear translocation of SIRT-1, which activates Akt1, maintains phosphorylated Fox03a in the cytoplasm, dampens mitochondrial cytochrome c release and caspase activation, culminating in decreased apoptosis (Hou et al., 2011).

In a mouse model of periventricular leukomalacia, a condition prevalent in premature infants, where cerebral white matter is damaged due to hypoxia-ischemia and inflammation, *i.p.* EPO treatment attenuated cerebral white matter damage after 96 h of ischemia-hypoxia stress (Liu et al., 2011). Moreover, neurobehavioral performance scores were significantly higher within the first 10 d of recovery in the EPO-treated vs. control mice. The protection by EPO in this model was demonstrated to be mediated by mitigating microglial activation of poly-(ADP-ribose) polymerase-1 (PARP-1), a signaling protein associated with cellular injuries (Liu et al, 2011).

Another effector of EPO treatment is reduced Zn^{2+} accumulation. Zn^{2+} has been demonstrated to play an important role in neuronal injury caused by prolonged ischemia. Exposure to 200μM Zn^{2+} solution induced death of cultured hippocampal neurons, but pretreatment with EPO for 24 h increased neuronal survival. Additionally, *in vivo* experiments in a rat model of traumatic brain injury confirmed that rhEPO inhibited excitotoxic Zn^{2+} intracellular translocation in CA3, dentate gyrus, and hilar regions of the hippocampus (Zhu et al., 2009).

4. Effect of oxidative stress on Krebs cycle and glycolytic enzymes

a. Aconitase

Aconitase, a key component of the Krebs cycle, is a well-known target of ROS activity. Aconitase activity was found to be markedly decreased in a cellular model of oxidative stress and in many brain conditions such as Huntington diseases (Fitzmaurice, 2002; Kim, 2005). Aconitase is inactivated by ROS-induced disassembly of its catalytic $[4Fe\text{-}4S]^{2+}$ cluster in a manner reversible by GSH and other reductants (Vasquez-Vivar et al., 2000) or by oxidation of a sulfhydryl moiety near its active site (Buldeau et al., 2005). On the other hand, pyruvate-enriched cardioplegia restored myocardial aconitase activity in a porcine model of cardiopulmonary bypass (Knott et al., 2006).

b. Glyceraldehyde-3-phosphate dehydrogenase (GAPDH)

The glycolytic enzyme GAPDH has been found to mediate apoptosis. Specifically, overexpression of GAPDH and its accumulation in the nucleus leads to neuronal and non-neuronal cell death (Sawa et al., 1997). The underlying mechanism is a matter of speculation. It was postulated that nuclear translocation of GAPDH may be the signal to initiate the mitochondrial apoptotic cascade (Shashidharan et al., 1999, Tanaka et al., 2002).

5. Pyruvate: cytoprotection from ischemia-reperfusion via multiple cellular pathways

Pyruvate, an intermediate metabolite generated by glycolysis, has been shown to bolster cellular defense mechanisms against oxidative stress. A direct antioxidant, pyruvate scavenges reactive oxygen species such as hydrogen peroxide and peroxynitrite (Desagher et al., 1997). In rat astrocytes subjected to oxygen-glucose deprivation, pyruvate treatment improves GSH/GSSH and NADPH/NADP+ redox status and prevents cell death through suppression of caspase-3 activation, decreased Cytochrome c, and by preventing pro-apoptotic PARP cleavage (Mongan

et al., 2002, Sharma et al, 2003). Pyruvate activates the mitochondrial pyruvate dehydrogenase, thereby increasing carbohydrate oxidation to generate ATP. In goats subjected to hemorrhagic shock, systemic resuscitation with pyruvate-fortified Ringer's solution for 90 min was associated with decreased formation of the lipid peroxide 8-isoprostane, a product of oxidative stress and indicator of antioxidant deficiency in tissues (Gurji et al., 2014). Pyruvate also preserved creatine kinase, and aconitase activities, and augmented the ATP energy state of reperfused hindlimb muscle. Importantly, these effects persisted for 3.5h after pyruvate administration (Gurji et al., 2014).

Previous work from our laboratory in a canine model of cardiac arrest and open-chest cardiac massage resuscitation showed that *iv* treatment of pyruvate upon reperfusion is associated with markedly decreased MMP activity in the brain and favorable neurological outcome (Sharma et al., 2008). The effect of MMP on brain subjected to cardiac arrest induced global ischemia is poorly understood. However, this study showed that pyruvate can be administered *iv* acutely during ischemia to protect the brain from ischemia-reperfusion injury in an emergency setting.

A prospective, randomized, semi-blinded human trial demonstrated pyruvate's safety and efficacy in patients undergoing cardiac surgery with cardiopulmonary bypass (Olivencia-Yurvati et al., 2003). In this clinical study, the use of pyruvate-fortified cardioplegia solution to arrest the heart for coronary revasculization afforded robust recovery of cardiac mechanical function post cardiopulmonary bypass surgery, in a manner markedly superior to conventional lactate-fortified cardioplegia. Specifically, in the pyruvate cardioplegia group, left ventricular stroke work increased vs. lactate cardioplegia 4-12 h after bypass, and coronary sinus troponin I and creatine phosphokinase-MB release, markers of myocardial injury, were sharply lowered compared to the

lactate cardioplegia. Importantly, the patients receiving pyruvate met criteria for hospital discharge on average 1-2 days sooner than the lactate cardioplegia patients.

6. Hypotheses and goal:

The most recent American Heart Association guidelines (2015) continue to support the C-A-B (compression, airway, breathing) sequence of resuscitation. Total preshock and postshock pauses in chest compressions should be as short as possible because shorter pauses are associated with greater shock success and achievement of ROSC. Manual chest compression remains the standard of care and presently there is no benefit recommendation regarding use of the impedance threshold device (ITD). Usage of ITD did not significantly improve satisfactory neurological outcome in out-of-hospital cardiac arrest (Sufderheide et al., 2011). Vasopressin was removed from ACLS Cardiac Arrest Algorithm as a vasopressor therapy for the simplicity of approach toward cardiac arrest when 2 therapies (vasopressin vs. epinephrine) were showed to be equivocal. A high-quality randomized controlled trial did not identify any superiority of targeted temperature management at 36^{o}C compared with 33^{o}C; hypothermia treatment in comatose patients are recommended at either temperature (AHA guidelines, 2015). Despite these refinements and extensive research, no new pharmacological or mechanical intervention has been added to the guidelines. Thus there is an important and unmet need for facile, rapidly acting pharmacological agents for acute intervention for cardiac arrest.

Our long term goal is to identify a treatment that preserves BBB integrity during global brain ischemia-reperfusion to potentially mitigate the adverse, often lethal neurological consequences of cardiac arrest. Our central hypothesis is that pyruvate therapy suppresses MMP activity, thereby preserving BBB integrity, increases EPO expression, and dampens inflammation following cardiac arrest, and, thus, improves neurobehavioral recovery from

cardiac arrest. To address the central hypothesis and thereby help accomplish our long term goal, the following specific hypotheses were tested in a domestic swine model of cardiac arrest, closed-chest CPR, electrical defibrillation and recovery:

Hypothesis 1: Oxidative stress due to cardiac arrest results in inflammation, which degrades BBB

Hypothesis 2: Pyruvate dampens BBB damage by mitigating inflammation caused by matrix metalloproteinases

Hypothesis 3: Pyruvate dampens ischemia-reperfusion via HIF-1α/Erythropoietin pathway

Hypothesis 4: Pyruvate treatment fosters neurocognitive recovery

REFERENCES

2015 American Heart Association Guidelines Update for Cardiopulmonary Resuscitation and Emergency Cardiovascular Care. *Circulation* 2015; **132**:S315-S367.

Abella BS, Alvarado JP, Myklebust H., Edelson DP, Barry A, O'Hearn N, Vanden Hoek Tl, Becker LB. Quality of cardiopulmonary resuscitation during in-hospital cardiac arrest. *JAMA* 2005; **293**(3): 305 – 310.

Adrie C, Adib-Conquy M, Laurent I, Monchi M, Vinsonneau C, Fitting C, Fraisse F, Dinh-Xuan AT, Carli P, Spaulding C, Dhainaut JF, Cavaillon JM. Successful cardiopulmonary resuscitation after cardiac arrest as a "sepsis-like" syndrome. *Circulation* 2002; **106**: 562 – 568 .

Akins PT, Liu PK, Hsu CY. Immediate early gene expression in response to cerebral ischemia: friend or foe? *Stroke* 1996; **27**: 1682 – 1687.

Aufderheide TP, Nichol G, Rea TD, Brown SP, Leroux BG, Pepe PE, Kidenchuk PJ, Christenson J, Daya MR, Dorian P, Callaway CW, Idris AH, Andrusiek D,Stephens SW, Hostler D, Davis DP, Dunford JV, Pirrallo RG, Stiell IG, Clement CM, Craig A, Van Ottingham L, Schmidt TA, Wang HE, Weisfeldt ML, Ornato JP,Sopko G; Resuscitation Outcomes Consortium (ROC) Investigators. A trial of an impedance threshold device in out-of-hospital cardiac arrest. *N Engl J Med.* 2011 Sep 1; **365**(9):798-806.

Bak IJ, Misgeld U, Weiler M, Morgan E. The preservation of nerve cells in rat neostriatal slices maintained in vitro: a morphological study. *Brain Res* 1980, **197**: 341 – 353.

Bareyre F, Wahl F, McIntosh TK, Stutzmann JM. Time course of cerebral edema after traumatic brain injury in rats: effects of riluzole and mannitol. *J Neurotrauma* 1997; **14**(11): 839 – 849.

Bartos JA, Matsuura TR, Sarraf M, Youngquist ST, McKnite SH, Rees JN, Sloper DT, Bates FS, Segl N, Debaty G, Lurie KG, Neumar RW, etzger JM, Riess ML, Yannopoulos D. Bundled postconditioning therapies improve hemodynamics and neurologic recovery after 17 min of untreated cardiac arrest. *Resuscitation* 2015; **87**: 7 – 13.

Bergner L, Bergner M, Halistrom A, Eisenberg M, Cobb L: Health status of survivors of out-of-hospital cardiac arrest six months later. Am J Public Health 1984; 74:508.

Berger L, Hallstrom A, Berger M, Eisenberg MS, Cobb LA. Health status of survivors of cardiac arrest and of myocardial infarction controls. Am J Public Health 1985; 75: 1321- 1323.

Bergmeyer HU, Bergmeyer J, Graβl M. Methods of enzymatic analysis. Weinheim: Verlag Chemis 1983; VI: S70 – S77.

Bernard SA, Gray TW, Buist MD, *et al.* Treatment of comatose survivors of out-of-hospital cardiac arrest with induced hypothermia. *New Engl J Med*, 2002; **346**: 557–563.

Bulteau Al, Lundberg KC, Ikeda-Saito M, Isaya G, Szweda LI. Reversible redox-dependent modulation of mitochondrial aconitase and proteolytic activity during in vivo cardiac ischemia-reperfusion. *Proc Natl Acad Sci USA* 2005; **102**: 5987 – 5991.

Bunch TJ, White RD, Gersh BJ, Meverden RA, Hodge DO, Ballman KV, Hammill SC, Shen WK, Packer DL. Long-term outcome of out-of-hospital cardiac arrest after successful early defibrillation. *N Engl J Med* 2003; **348**:2626-2633.

Bu¨nger R, Mallet RT, Hartman DA. Pyruvate-enhanced phosphorylation potential and inotropism in normoxic and post ischemic isolated working heart. *Eur J Biochem* 1989;**180**:221–33.

Bu¨nger R, Mallet RT. Mitochondrial pyruvate transport in working guinea-pig heart: work-related vs. carrier-mediated control of pyruvate oxidation. *Biochim Biophys Acta* 1993; **1151:223**–36.

Burchell SR, Dixon BJ, Tang J, Zhang JH. Isoflurane provides neuroprotection in neonatal hypoxic ischemic brain injury. *J Investig Med*. 2013; **61**(7): 1078 – 1083.

Chalkias, A. *et al*. Post-cardiac arrest brain injury: Pathophysiology and treatment. *Journal of Neurological Sciences* 2012;doi:10.1016/j.jns.2011.12.007.

Chalkias A, Kuzovlev A, Noto A, d'Aloja E, Xanthos T. Identifying the role of cytochrome c in post-resuscitation pathophysiology. *The American Journal of Emergency Medicine* 2015; **33**(12): 1826 – 1830.

Cherry BH, Sumien N, Mallet RT. Neuronal injury from cardiac arrest: aging years in minutes. *Age* 2014; **36**(4): 9680.

Cherry BH, Nguyen AQ, Hollrah RA, Olivencia-Yurvati AH, Mallet RT. Modeling cardiac arrest and resuscitation in the domestic pig. *World J Crit Care Med.* 2015 Feb **4**; 4(1):1-12.

Cherry BH, Nguyen AQ, Hollrah RA, Williams AG Jr, Hoxha B, Olivencia-Yurvati AH, Mallet RT. Pyruvate stabilizes electrocardiographic and hemodynamic function in pigs recovering from cardiac arrest. *Exp Biol Med* (Maywood). 2015 Dec; **240**(12):1774-84.

Cronberg t, Lilja G, Rundgren M, Friberg H, Widner H. Long-term neurological outcome after cardiac arrest and therapeutic hypothermia. *Resuscitation* 2009; **80**: 1119 – 1123.

Dalvi PS, Singh A, Trivedi HR, Ghanchi FD, Parmar DM, Mistry SD. Effect of doxycycline in patients of moderate to severe chronic obstructive pulmonary disease with stable symptoms. *Annals of Thoracic Medicine* 2011; Vol **6**, Issue 4: 221-226.

Debaty G, Shin SD, Metzger A, Kim T, Ryu HH, Rees J, McKnite S, Matsuura T, Lick M, Yannopoulos D, Lurie K. Tilting for perfusion: Head-up position during cardiopulmonary resuscitation improves brain flow in a porcine model of cardiac arrest. *Resuscitation* 2015; **87**: 38-43.

Devy L, Dransfield DT. New strategies for the next generation of matric-metalloproteinase inhibitors: selectively targeting membrane-anchored MMPs with therapeutic antibodies. *Biochemistry research international* 2011; Volume **2011**, Article ID 191670, 11 pages.

Eisenburger P, List M, Schorkhuber W, Walkwe R, Sterz F, Lagger AN. Long-term cardiac arrest survivors of the Vienna emergency medical service. *Resuscitation* 1998; **39**: 137-143.

Fitzmaurice PS, Bamsey CL, Ang L, Guttman M, Rajput AH, Furukawa Y, Kish SJ. Brain aconitase activity is not decreased in progressive supranuclear palsy. *Neurology* 2002; **59**: 137 – 138.

Fujimoto, M. *et al*. Tissue inhibitor of metalloproteinases protect blood-brain barrier disruption in focal cerebral ischemia. *Journal of Cerebral Blood Flow & Metabolism*. 2008; **28**: 1675 – 1685.

Ganga HV, Kallur KR, Patel NB, Sawyer KN, Gowd PB, Nair SU, Puppala VK, Manandhi AR, Gupta AV, Lundbye JB. The impact of severe academia on neurological outcome of cardiac arrest survivors undergoing therapeutic hypothermia. *Resuscitation* 2013; Vol. **84**, Issue 12: 1723 – 1727.

Gidday, J. *et al*. Leukocyte-derived matrix metalloproteinase-9 mediates blood-brain barrier breakdown and is proinflammatory after transient focal cerebral ischemia. *Am J Physiol Heart Cir Physiol*. 2005; **289**: 558 – 568.

Go et al. Heart disease and stroke statistics- 2013 update, a report from the American Heart Association. *Circulation* 2013; **127**:000-000.

Grosebaugh DA, Muir WW. Cardiorespiratory effects of sevoflurane, isoflurane, and halothane anesthesia in horses. *Am J Vet Res* 1998; **59** (1): 101 – 106.

Gurji HA, White DW, Hoxha B, Sun J, Olivencia-Yurvati AH, Mallet RT. Pyruvate-fortified resuscitation stabilizes cardiac electrical activity and energy metabolism during hypovolemia. *World J Crit Care Med* 2013; **2:56**–64.

Gurji HA, White DW, Hoxha B, Sun J, Harbor JP, Schulz DR, Williams AG Jr, Olivencia-Yurvati AH, Mallet RT. Pyruvate-enriched resuscitation: metabolic support of post-ischemic hindlimb muscle in hypovolemic goats. *Exp Biol Med* 2014; **239:240**–9.

Harukuni I, Bhardwaj A. Mechanisms of brain injury after global cerebral ischemia. *Neurologic Clinics* 2006; **24**(1): 1 – 21.

Heo JH, Lucero J, Abumiya T, Koziol JA, Copeland BR, Zoppo GJ. Matrix metalloproteinases increase very early during experimental focal cerebral ischemia. J of Cerebral Blood Flow and Metabolism 1999; **19**: 624 – 633.

Hogler S, Sterz F, Sipos W, Schratter A, Weihs W, Holzer M, et al. Distribution of neuropathological lesions in pig brains after different durations of cardiac arrest. *Resuscitation* 2010; **81:1577**–83.

Holzer et al. Mild therapeutic hypothermia to improve the neurologic outcome after cardiac arrest. *N Engl J Med* 2002; **346**: 549 – 556.

Horn M, Schlote W. Delayed neuronal death and delayed neuronal recovery in the human brain following global ischemia. *Acta Neuropathol* 1992; **85**: 79 – 87.

Ito T, Saitoh D, Fukuzuka K, Kiyozumi T, Kawakami M, Sakamoto T, Okada Y. Significance of elevated serum interleukin-8 in patients resuscitated after cardiopulmonary arrest. *Resuscitation* 2001; **51**(1): 47 – 53.

Idris AH, Roberts LJ, Caruso L, Showstark M, layon AJ, Becker LB, Hoek TV, Gabrielli A. Oxidant injury occurs rapidly after cardiac arrest, cardiopulmonary resuscitation, and reperfusion. Crit Care Med 2005; 33(9): 2043 – 2048.

Janata A, Holzer M. Hypothermia after cardiac arrest. *Progress in cardiovascular diseases* 2009; **52**(2): 168 – 179.

Kalogeris T, Baines CP, Krenz M, Korthuis RJ. Cell biology of ischemia/reperfusion injury. *Int Rev Cell Mol Biol*. 2012; **298**: 229 – 317.

Kim SY, Marekov L, Buubber P, Browne SE, Stavrovskaya I, Lee J, Steinert PM, Blass JP, Beal MF, Gibson GE, Cooper AJL. Mitochrondrial aconitase is a transglutaminase 2 substrate: transglutamination is a probable mechanism contributing to high-molecular-weight aggregates of aconitase and loss of aconitase activity in Huntington Disease Brain. *Neurochemical Research* 2005; **30**(10): 1245 – 1255.

Kleinman ME, Brennan EE, Goldberger ZD, Swor RA, Terry M, Bobrow BJ, Gazmuri RJ, Travers AH, Rea T. Part 5: Adult basic life support and cardiopulmonary resuscitation quality: 2015 American Heart Association Guidelines update for cardiopulmonary resuscitation and emergency cardiovascular care. *Circulation.* 2015 Nov 3; **132** (18 Suppl 2):S414-35.

Knott EM, Ryou MG, Sun J, Heymann A, Sharma AB, Lei Y, Baig M, Mallet RT, Olivencia-Yurvati AH. Pyruvate-fortified cardioplegia suppresses oxidative stress and enhances phosphorylation potential of arrested myocardium. *Am J Physiol Heart Circ Physio*l 2005; **289:H1123**–30.

Knott EM, Sun J, Lei Y, Ryou MG, Olivencia-Yurvati AH, Mallet RT. Pyruvate mitigates

oxidative stress during reperfusion of cardioplegia-arrested myocardium. Ann Thorac Surg. 2006; 81(3): 928 – 934.

Kragholm K, Wissenberg M, Mortensen N, Fonager K, Jensen SE, Rajan S, Lippert FK, Christensen EF, Handen PA, Lang-Jensen T, Hendriksen OM, Kober L, Gislason G, Torp-Pedersen C, Rasmussen BS. Return to work in out-of-hospital cardiac arrest survivors: A nationwide register-based follow-up study. Circulation 2015; 131: 1682-1690. DOI: 10.1161/CIRCULATIONAHA.114.011366.

Leary M, Grossestreuer AV, Iannacone S, Gonzalez M, Shofer FS, Povey C, Wendell G, Archer SE, Gaieski DF, Abella BS. Pyrexia and neurologic outcomes after therapeutic hypothermia for cardiac arrest. *Resuscitation* 2013; Vol. **84**, Issue 8: 1056 – 1061.

Lee SR, Tsuji K, Lee SR, Lo EH. Role of Matrix Metalloproteinases in delayed neuronal damage after transient global cerebral ischemia. *The Journal of Neuroscience*, 2004: **24**(3): 671 – 678.

Lochhead JJ, McCaffrey G, Quigley CE, Finch J, DeMarco KM, Nametz N, Davis TP. Oxidative stress increases blood-brain barrier permeability and induces alterations in occluding during hypoxia-reoxygenation. *J of Cerebral Blood Flow & Metabolism* 2010; **30**: 1625 – 1636.

Olivencia-Yurvati AH, Blair JL, Baig M, Mallet RT. Pyruvate-enhanced cardioprotection during surgery with cardiopulmonary bypass. *J Cardiothorac Vasc Anesth.* 2003 Dec; **17(6)**:715-20.

Mallet RT. Pyruvate: metabolic protector of cardiac performance. *Proc Soc Exp Biol Med* 2000; **223:136**–48.

Mallet RT, Sun J, Knott EM, Sharma AB, Olivencia-Yurvati AH. Metabolic cardioprotection by pyruvate: recent progress. *Exp Biol Med* 2005;**230**:435–43.

Mallet RT, Sun J. Pyruvate enhancement of cardiac function and energetics requires its mitochondrial metabolism. *Cardiovasc Res* 1999; **42:149**–61.

McCullough LD, Hurn PD. Estrogen and ischemic neuroprotection: an integrated view. *Trends in endocrinology and metabolism* 2003; **24**(5): 228 – 235.

Mellergard P, Bengtsson F, Smith ML, Riesenfeld V, Siiesjo BK. Time course of early brain edema following reversible forebrain ischemia in rats. *Stroke* 1989; **20**(11): 1565 – 1570.

Mizuseki K, Royer S, Diba K, Buzsaki G. Activity dynamics and behavioral correlates of CA3 and CA1 hippocampal pyramidal neurons. *Hippocampus* 2012; **22**(8): 1659 – 1680.

Mongardon N, Dumas F, Ricome S, Grimaldi D, Hissem T, Pene F, Cariou A. Postcardiac arrest

syndrome: from immediate resuscitation to long-term outcome. *Annals of Intensive Care* 2011; **1**:45.

Mongan PD, Fontana JL, Chen R, Bu¨nger R. Intravenous pyruvate prolongs survival during hemorrhagic shock in swine. *Am J Physiol Heart Circ Physiol* 1999; **277**: H2253–63.

Nannelli A, Rossignolo F, Tolando R, Rossato P, Longo V, Gervasi PG. Effect of β-naphthoflavone on AhR-regulated genes (CYP1A1, 1A2, 1B1, 2S1, Nrf2, and GST) and antioxidant enzymes in various brain regions of pig. *Toxicology* 2009; **265**: 69 – 79.

Ng T, Graham DI, Adams JH, Ford I. Changes in the hippocampus and the cerebellum resulting from hypoxic insults: frequency and distribution. *Acta Neuropathol* 1989; **78**: 438 – 443.

Nguyen AQ, Cherry BH, Scott GF, Ryou MG, Mallet RT. Erythropoietin: powerful protection of ischemic and post-ischemic brain. *Exp Biol Med* 2014; **239**(11): 1461 – 1475.

Nichol G, Stiell IG, Hebert P, Wells GA, Vandemheen K, Laupacis A. What is the quality of life for survivors of cardiac arrest? A prospective study. *Acad Emerg Med* 1999; **6**:95-102.

Mengozzi M, Cervellini I, Villa P, Erbayraktar Z, Gokman N, Yilmaz O, Erbayraktar S, Manohasandra M, Hummelen PV, vandenabeele P, Chernajovsky Y, Annenkov A, Ghezzi P. Erythropoietin-induced changes in brain gene expression reveal induction of synaptic plasticity genes in experimental stroke. *PNAS* 2012; **109** (24): 9617 – 9622.

Niemann JT, Rosborough JP, Youngguist S, Shah AP, Lewis RJ, Phan QT, Filler SG. Cardiac function and the proinflammatory cytokine response after recovery from cardiac arrest in swine. *J Interferon Cytokine Res*. 2009; **29** (11): 749 – 58.

Okamoto T, Akuta T, Tamura F, Van Der Vliet A, Akaike T. Molecular mechanism for activation and regulation of matrix metalloproteinases during bacterial infections and respiratory inflammation. *Biol. Chem*. 2004; Vol. **385**, Issue 11: 997 – 1006.

O'Reilly SM, Grubb N, O'Carroll RE. Long-term emotional consequences of in-hospital cardiac arrest and myocardial infarction. *Br J Clin Psychol 2004*; **43**:83-95.

Paine MG, Che D, Li L, Neumar RW. Cerebellar Purkinje cell neurodegeneration after cardiac arrest: effect of therapeutic hypothermia. *Resuscitation* 2012; Vol. **83**, Issue 12: 1511 – 1516.

Passonneau JV, Lowry OH. Enzymatic analysis: a practical guide. Totowa: Humana Press 1993. Print.

Pierce AE, Roppolo LP, Owens PC, Pepe PE, Idris AH. The need to resume chest compressions

immediately after defibrillation attempts: An analysis of post-shock rhythms and duration of pulselessness following out-of-hospital cardiac arrest. *Resuscitation* 2015; **89**: 162-168.

Piscator E, Hedberg P, Goransson K, Djarv T. Survival after in-hospital cardiac arrest is highly associated with the Age-combined Charlson Co-morbidity index in a cohort study from a two-site Swedish University hospital. *Resuscitation* 2016; **99**: 79 – 83.

Rosenberg GA, Estrada EY, Dencoff JE, Stetler-Stevenson WG. Tumor necrosis factor-α-induced gelatinase B causes delayed opening of the blood-brain barrier: an expanded therapeutic window. *Brain Research* 1995; **703**: 151 – 155.

Ryou MG, Flaherty DC, Hoxha B, Gurji H, Sun J, Hodge LM, OlivenciaYurvati AH, Mallet RT. Pyruvate-enriched cardioplegia suppresses cardiopulmonary bypass myocardial inflammation. *Ann Thorac Surg* 2010; **90:1529**–35.

Ryou, M-G *et al*. Pyruvate protects the brain against ischemia-reperfusion injury by activating the erythropoietin signaling pathway. *Stroke*. 2012; **43**: 1101-1107.

Sato M, Hashimoto H, Kosaka F. Histological changes of neuronal damage in vegetative dogs induced by 18 minutes of complete global brain ischemia: two-phase damage of Purkinje cells and hippocampal CA1 pyramidal cells. *Acta Neuropathol* 1990; **80**: 527 – 534.

Sawa A, Khan AA, Hester LD, Snyder SH. Glyceraldehyde-3-phosphate dehydrogenase: Nuclear translocation participates in neuronal and nonneuronal cell death. *Proc Natl Acad Sci* 1997; **94**:11669–11674.

Shichita T, Sakaguchi R, Suzuki M, Yoshimura A. Post-ischemic inflammation in the brain. *Frontiers in immunology* 2012; Vol. **3**, Article 132: 1 – 7.

Sharma AB, Knott EM, Bi J, Martinez RR, Sun J, Mallet RT. Pyruvate improves cardiac electromechanical and metabolic recovery from cardiopulmonary arrest and resuscitation. *Resuscitation* 2005; **66:71**–81.

Sharma AB, Barlow MA, Yang SH, Simpkins JW, Mallet RT. Pyruvate enhances neurological recovery following cardiopulmonary arrest and resuscitation. *Resuscitation* 2008; **76:108**–119.

Shashidharan P, Chalmers-Redman RME, Carlile GW, Rodic V, Gurvich N, Yuen T, Tatton WG, Sealfon SC. Nuclear translocation of GAPDH-GFP fusion protein during apoptosis. *Neuroreport* 1999; **10**:1149–1153.

Sipos W, Duvigneau C, Sterz F, Weihs W, Krizanac D, Bayegan K, Graf A, Hartl R, Janata A, Holzer M, Behringer W. Changes in interleukin-10 mRNA expression are predictive for 9-day survival of pigs in an emergency preservation and resuscitation model. *Resuscitation* 2010; **81**(5):603-608.

Soede NM, Langerdijk P, Kemp B. Reproductive cycles in pigs. *Animal reproduction science* 2011; **124**(3-4): 251 – 258.

Stefanon I, Valero-Munoz M, Fernandes AA, Ribeiro RF Jr, Rodriguez C, Miana M, Martinez-Gonzalez J, spalenza JS, Lahera V, Vassallo PF, Cachofeiro V. Left and right ventricle late remodeling following myocardial infarction in rats. PLOS One, 2013: DOI: 10.1371/journal.pone.0064986.

Strick PL, Dunn RP, Fiez JA. Cerebellum and nonmotor function. *Annu Rev. Neurosci.* 2009; **32**:413 – 34.

Squire LR. Memory and the hippocampus: A synthesis from findings with rats, monkeys, and humans. *Psychol Rev.* 1992; **99**:195–231.

Tanaka R, Mochizuki H, Suzuki A, Katsube N, Ishitani R, Mizuno Y, Urabe T. Induction of glyceraldehyde-3-phosphate dehydrogenase (GAPDH) expression in rat brain after focal ischemia/ reperfusion. *J Cereb blood flow metab* 2002; **22**(3): 280 – 288.

Tejero-Taldo MI, Sun J, Caffrey JL, Mallet RT. Pyruvate potentiates badrenergic inotropism of stunned guinea-pig myocardium. *J Mol Cell Cardiol* 1998; **30:2327**–39.

Tejero-Taldo MI, Caffrey JL, Sun J, Mallet RT. Antioxidant properties of pyruvate mediate its potentiation of b-adrenergic inotropism in stunned myocardium. *J Mol Cell Cardiol* 1999; **31:1863**–72.

Vasquez-Vivar J, Kalyamaraman B, Kennedy MC. Mitochondrial aconitase is a source of hydroxyl radical. An electron spin resonance investigation. *J Biol Chem* 2000; **275**: 14064 – 14069.

Venkatesan A, Frucht S. Movement disorders after resuscitation from cardiac arrest. *Neurologic Clinics* 2006; **24**(1): 123 – 132.

Vries HW, Bloom-Roosemalen MCM, Oosten MV, Boer AG, Berkel TJC, Breimer DD, Kuiper J. The influence of cytokines on the integrity of the blood-brain barrier in vitro. *Jounal of Neuroimmunology* 1996; **64**: 37 – 43.

Weihs W, Krizanac D, Sterz F, Sipos W, Hogler S, Janata A, Holzer M, Losert UM, Behringer W. Outcome after resuscitation using controlled rapid extracorporeal cooling to a brain temperature of 30^{o}C, 24^{o}C, and 18^{o}C during cardiac arrest in pigs. *Resuscitation* 2010; **81**(2): 242 – 247.

Wissenberg M, Lipert FK, Folke F, et al. Association of national initiatives to improve cardiac arrest management with rates of bystander intervention and patient survival after out-of-hospital cardiac arrest. *JAMA* 2013; **310**(13): 1377 – 1384.

Xiao F, Arnold T, Zhang S, Imtiaz N, Khan A, Alexander JS, Conrad S, Carden D. Matrix metalloproteinases are not involved in early brain edema formation after cardiac arrest in rats. *Acta Neurochir Suppl.* 2003; **86**: 75 – 78.

Yuan HB, Huang Y, Zheng S, Zuo Z. Hypothermic preconditioning reduces Purkinje cells death possibly by preventing the over-expression of inducible nitric oxide synthase in rat cerebellar slices after an *in vitro* simulated ischemia. *Neuroscience* 2006, **142**: 381 – 389.

Yang Y, Estrada EY, Thompson JF, Liu W, Rosenberg GA. Matrix metalloproteinase-mediated disruption of tight junction proteins in cerebral vessels is reversed by synthetic matrix metalloproteinase inhibitor in focal ischemia in rat. *Journal of Cerebral Blood Flow & Metabolism* 2007; **27**: 697 – 709.

Zheng S and Zuo Z. isoflurane preconditioning induces neuroprotection against ischemia via activation of P38 mitogen-activated protein kinases. *Molecular Pharmacology* 2004; **65**(5): 1172 – 1180.

CHAPTER II

METHODS

1. Surgical Preparation:

This prospective, randomized, single center and controlled study was designed to elucidate the mechanism by which prolonged out-of-hospital cardiac arrest affects neurological injuries and how pyruvate mitigates this damage. Vivarium care and experimental procedures were strictly followed in accordance with the National Research Council's 1996 Guidelines for the Care and Use of Laboratory Animals, and the ARRIVE guidelines (Kilkenny, 2010), and were approved by the University of North Texas Health Science Center Institute for Animal Care and Use Committee (protocol # 2012/13-29-A10). A certified and licensed veterinarian assured that the protocol followed the National Research Council's guidelines.

Yorkshire swine (25 kg – 35kg) were purchased from local USDA approved breeders. Animals were habituated to the animal facility for at least 2 days (acute protocol) or a week (recovery protocol) before the experiments. Pigs were anesthetized with intramuscular 5.56 mg/kg Telazol (Tiletamine HCl and zolazepam HCl, NADA 106-111) and 1.11 mg/kg Anased (xylazine, NADA 139-236) cocktail. An endotracheal tube (7-8mm) was advanced into the trachea, and the animals were mechanically ventilated with a volume-controlled ventilator (MDS Matrx, Model 3000), with tidal volume of 12-15 ml/kg, 12 – 16 cycles per minutes, and end tidal PCO_2 kept within 35 - 40 mmHg. Surgical anesthetic plane was maintained by continuous administration of 1-3% isoflurane (Isothesia, NDC 11695-6776-2, Narkovet Delux Anesthesia System) in oxygen. Anesthesia plane was confirmed by the absence of pedal reflex (withdrawal

response to pinching the hooves), and pinnal reflexes (insert a pinky into the external ear canal and observe for the ear movement), and by monitoring heart rate and blood pressure.

The pig was positioned dorsal recumbent on the surgical table. Body temperature was maintained at 37 – 38 ^{o}C by heating pads throughout the surgical preparation and the experiment. Core body temperature was monitored with a rectal probe. Right forelimb, left and right hind limbs were secured caudalaterally. The left forelimb was positioned rostrolaterally. Adhesive foam electrodes (Coviden) were placed on the left and right forelimbs, and the left hind limb for electrocardiogram (EKG) monitoring. To access the right jugular vein, a 7-cm incision was made in the skin at the right jugular furrow. The cutaneous colli at the incision site was cut, exposing a groove underneath, formed by sternohyoideus muscle to the medial and cutaneous colli to the lateral side. Dissecting through the fascia reveals the right external jugular vein. A catheter containing a pacing wire was inserted and advanced into the right ventricle. Catheter position was confirmed by the typical ventricular waveform monitored with a pressure transducer. Once the heart was arrested, the pacing wire was withdrawn, leaving a patent catheter for treatment solution administration. The treatment solutions, prepared randomly by a designated personnel not participating in the experimental protocol, were either sterile 2M sodium pyruvate or 2M sodium chloride. Solutes were dissolved in deionized-distilled H_2O and sterilized by filtration through 0.3 µm pore size membranes in a sterile polyethersulfone container (Stericup® Filter Units, Cat# SCVPU02RE, EMD Milipore). Pyruvate or NaCl infused *iv* at the rate of 0.1 mmol/kg/min, which achieved plasma pyruvate concentrations of 3.5 – 4 mM in the systemic circulation (Sharma et al., 2005). A retrograde catheter was inserted rostrally to measure the jugular venous pressure and to collect venous blood.

Femoral vein and artery location was approximated at the sheath between the lateral (rectus femoris, vastus medialis) and medial thigh muscles (adductor femoris, semimembranosus, semitendinosus). The fascia was cut, revealing the femoral artery underneath. A 7-Fr polyurethane catheter was passed through a small incision in the femoral artery and advanced into the abdominal aorta for arteria blood collection. The catheter was connected to a transducer for blood pressure and heart rate measurement by BPA blood pressure analyzer (Digi-Med) and Grass Model 7D polygraph (Grass instrument Co., Quincy, Mass., USA). The electrocardiogram (EKG), mean arterial pressure (MAP), and jugular venous pressure were continuously monitored and recorded by a data acquisition system (Windaq) at a sample rate of 200 Hz. The femoral vein was cannulated for medication and fluid administration.

2. Cardiac arrest protocol:

In acute experiments, i.e. 1h or 4h post-arrest recovery, 7000 units of heparin (Heparin sodium injection, USP) were injected via femoral vein to prevent blood clots after completion of surgical preparation and prior to cardiac arrest protocol. $NaHCO_3$ (Butler Schein, 002484) was injected 10 mEq boluses *iv* via femoral vein as needed. 0.167 to 0.267 U/kg vasopressin (Pitressin, 20 units/ml, NDC 42023-117-25) was bolus-injected into the jugular catheter to provide vasoconstrictor support during CPR. Defibrillatory countershocks were delivered by external paddles (Medtronic Lifepak 12) starting at 200 J and goes up to 360 J. Shocks (1-3x 200J, 1-3x 300J, and 1-3x 360J, sequentially) were delivered at 30s intervals with intervening chest compressions, and were abandoned after 9 attempts, if appreciable arterial pressure and spontaneous electrical rhythm were not achieved. After successful cardioversion, 1ml (20mg/ml) Lidocaine (Lidoject 2%, Henry Schein, NDC 11695-4147-1) was injected into the jugular vein

for prophylaxis of arrhythmias. The sequence and time of drug administration is summarized below:

a. *10-min arrest, 1 h recovery*: cardiac arrest was induced by passing a 4 Hz train of electrical impulses at 60V – 70V to the right ventricle. A monophasic decline in blood pressure, loss of pressure pulsation, and the absence of an organized cardiac electrical rhythm confirmed the arrest. Mechanical ventilation was then suspended. At 5 min of cardiac arrest, 10mEq of $NaHCO_3$ was slowly injected into the femoral vein. Treatments (sodium pyruvate or NaCl) were infused from 5.5 min of cardiac arrest until 60 min of ROSC. Cardiocerebral resuscitation (CCR) was delivered at 6 to 10 min at the rate of 100-110 compression/min at a depth of approximately 2 inches (25% of chest diameter). Vasopressin was injected into the jugular vein at 60s CCR. The defibrillation protocol was begun at 10 min arrest, i.e. 4 min CCR. If ROSC could not be achieved after the first 2 countershocks, a rescue dose of epinephrine was administered before the next shock. The ventilator was reconnected and lidocaine was given as soon as ROSC was achieved. The depth and frequency of ventilator cycles were adjusted to keep end-tidal P_{CO2} between 35-45 mmHg. Mean aortic blood pressure was maintained at a minimum of 70mmHg by administering intravenous 2% diluted phenylephrine drip (phenylephrine HCl, 10 mg/ml, NDC 66758-017-01) in normal saline (Braun, NDC 0264-7800-20). Arterial and venous blood was sampled at the following times: baseline (before cardiac arrest and after completion of surgery), 5’ ROSC, 15’ ROSC, 30’ ROSC, and 60’ ROSC. Blood was immediately analyzed in a blood gas laboratory (Instrumentation Laboratory, GEM Premier 3000). Partial pressures of O_2 and CO_2, and pH of arterial samples informed ongoing management of these variables. 10ml of blood was centrifuged at 7500

rpm for 10 min to sediment formed elements; the plasma supernatant was aliquoted in 1.5ml centrifuge tubes, flash frozen in liquid nitrogen, and stored at -80^{o}C for future analysis.

The animal was euthanized at 1h ROSC for tissue collection. To minimize the interval from sacrifice to sample collection, 15 min prior to euthanization, the dorsal aspect of the scalp was shaved and reflected, and the skull was cut with a bone saw, revealing the dura. Once the animal was euthanized, the dura was cut and brain was removed and placed on ice for regional biopsy. After that, left and right ventricles, left and right lungs, kidneys, and liver were also sampled and biopsied on ice for planned studying of these organs. Further details are described in the euthanasia session below.

b. *10-min arrest, 4 h recovery*: similar to the 10-min arrest, 1 h recovery protocol described above, but the recovery period was extended to 4h ROSC, and then the animal was sacrificed as described above. Additional blood, samples were collected at 2, 3, and 4 h ROSC.

c. *10-min arrest, 3 d recovery*: the cardiac arrest protocol was conducted as described above. Intracatheters (20G x 2" intracatheter, Terumo Surflo) were introduced to the femoral artery and vein instead of a conventional catheter to minimize the size of incision where catheter was inserted. Mean arterial pressure stabilized by 2-3 h ROSC, allowing discontinuation of phenylephrine infusion and catheter withdrawal. The femoral artery, femoral vein, and jugular vein were sutured with 7-0 Prolene blue monofilament (Ethicon). Muscles, fascia, and skin was closed with 3-0 synthetic absorbable sutures (Vedco polyglycolic acid, violet braided-coated synthetic absorbable sutures). Analgesic buprenorphine (Buprenex) was injected intramuscularly to the right hind limb during the

first hour that animal was extubated. The animal was monitored for heart rate and arterial oxygen saturation, and was slowly weaned off of supplemental oxygen. As reflexes returned and the animal became more awake and its gagging reflex returned, the endotracheal tube was withdrawn. Then, the animal was wrapped in a warm blanket, and returned to its pen. Animals were closely monitored until they were fully awake from anesthesia. Vital signs (heart rate, oxygen saturation, ventilatory rate, and skin color) were taken every 30 min until the animals were fully ambulatory. Neurological and cognitive tests were performed as described in the "neurological test" section. The animals were euthanized approximately 72 hours after ROSC, and biopsies of brain and other tissues were collected as described above.

d. *14 min arrest, 4 h recovery*: The animal was surgically prepared and cardiac arrest was induced by electrical pacing as described above. Treatment infusion was started at 9.5 min arrest, and chest compressions were begun at 10 min arrest. Efforts to defibrillate were begun at 14 min arrest and followed the same countershock sequence as described above. After ROSC was confirmed, ventilation immediately resumed, and lidocaine was administered *iv* to prevent arrhythmia. Blood samples were collected at pre-arrest baseline and at the same ROSC times as in 10 min arrest, 4 h recovery group. In this group, after euthanasia, the brain was cross perfused with cold (4^{o}C) saline (0.9% NaCl) at the rate of 1ml/gram/min tissue over 10 min (300 ml/ min) to rinse the cerebral vasculature of blood before tissue biopsy (details in section 3 below).

e. *14-min arrest, 4 h recovery protocol, delayed pyruvate infusion (DP)*: these experiments were conducted to test the effect of pyruvate when its administration was delayed until 1-

2 h ROSC. Pyruvate solution was prepared and its infusion rate was the same as described above.

f. *4h, non-arrested normoxic Sham protocol*: To determine the effects of surgical stress ventilation and anesthesia in the experiments, a non-arrest Sham group was studied. These animals were anesthetized and ventilated with 1-3% isoflurane in 21% compressed air instead of 100% oxygen. Surgical preparation, blood sampling, and tissue biopsy were performed as in the other groups described above. The animals were euthanized at 4 h as stated in the 10-min arrest, 4 h recovery protocol.

3. Euthanasia and Cross-perfusion

The thoracic cavity was accessed by an incision in the left 5^{th} or 6^{th} intercostal space. The pericardium was incised, exposing the heart. To sacrifice the anesthetized animal, a direct electrical current of 60V was applied to the left ventricle epicardium to induce ventricular fibrillation. The descending aorta was cross-clamped. A 0.5 cm incision was made in the ascending aorta, approximately 2 cm rostral to the clamp, for insertion of a catheter to deliver perfusion fluid. Ice-cold (4^oC) 0.9% NaCl + heparin (1000U/L) was delivered via peristatic pump at a rate of 1ml/g tissue/minute for 10 minutes. Afterwards, the brain was exposed by craniotomy, dissected, and biopsies were excised. Other organs were biopsied in sequence: left and right ventricles, left and right atrium, left and right lungs, kidney, and liver. Brain was further dissected to identify and sample frontal, temporal, hippocampus, cerebellum, pons, and medulla. Excised tissues were freeze-clamped with aluminum blocks precooled in liquid N_2 and were stored at -80^oC (Thermo Scientific) for biochemical analysis, or fixed in 10% formalin for paraffin embedding.

4. Protein extraction:

Frozen tissues were pulverized with precooled mortar and pestle under liquid N_2. 100 mg powder was then added to a tube containing 1 ml of phosphate buffer (0.1M KH_2PO_4) and 5 µl protease inhibitor (Sigma-Aldrich, P8340) and then homogenized for 1 minute at 4^oC using a Teflon piston. The suspension was then centrifuged at 25,000 rpm at 4^oC for 20 minutes (Thermo Scientific Ultracentrifuge). The supernatant was saved and the pellet was re-suspended in 0.4 ml of phosphate buffer, and again homogenized and centrifuged. The supernatants were combined, aliquoted, and stored at -80^oC.

5. Measurement of protein concentration in extracts

Protein concentration in aqueous solution was measured using Bradford reagent (Sigma-Aldrich, B6916). A standard curve was constructed with sequential dilutions of bovine serum albumin in ddH_2O (Thermo Scientific, Cat# 23209), diluted in ddH_2O to concentration of 0.25 mg/ml to 2 mg/ml. 5µl of samples and 250 µl Bradford reagent were combined in each well on a 96-well plate, which was then incubated for 30 min at room temperature. Absorbance was read at wavelength 595 nm using a spectrophotometer plate reader (Bio-Tek).

6. Tissue embedding

Fresh biopsies were fixed with 10% formalin for 24 h, then washed three times and stored in 70% ethanol at 4^oC. Biopsies were prepared for paraffin embedding by sequential immersion in the following solutions: 50% ethanol for 2 h, 70% ethanol overnight, 90% ethanol for 2h, 100% ethanol for 2 h twice, 1:1 xylene/ethanol for 1h, xylene for 1 h twice, 1:1 xylene/paraffin for 1h, paraffin for 1h, fresh paraffin for 1h, then embedding tissue in molten paraffin and allowed to solidify overnight.

7. Hematoxylin and eosin (H&E) staining and histological examination

Paraffin blocks were cut into 5μm thick sections and mounted on glass microscope slides (Pearl, Cat# 7105). Slides were submerged sequentially in the following solutions: 2 changes of xylene for 5 min each, 2 changes of 100% ethanol for 5 min each, 95% ethanol for 5 min, and 70% ethanol for 5 min. Next, slides were washed in running water for 2 min, stained in Hematoxylin Gill 3 (Sigma-Aldrich, Cat# GHS332) for 7 min, washed in running water for 1 min, and then dehydrated in 70% ethanol for 1 min, 95% ethanol for 1 min. The slides then were counterstained with eosin (Eosin Y, 1%) for 2 min, and then rinsed briefly in 95% ethanol. Complete dehydration were done in 2 changes of 100% ethanol for 5 min each and two changes of xylene for 5 min each. Samples were mounted with Permount (Fisher Scientific SP15-500), cover-slipped, and air-dried overnight at room temperature.

Morphological examination was performed under light microscope (Zeiss) by an observer blinded to the treatment protocols. Nine random, high powered pictures per section (2 sections total) were read for each experiment. Cerebellar Purkinje cells were identified from their large cell bodies, their characteristic large apical dendrites, and their location at the border between the granular cell and molecular cell layers. Injured neurons were recognized as having one or more of the following hallmarks: cell swelling, vacuolization, or darkened nuclei (Bak et al., 1980, Yuan et al., 2006).

8. Immunoblotting

Running gel (10% SDS-PAGE) and 4% stacking gel were casted. Tissue extracts were electrophoretically separated using the Mini-PROTEAN Tetra cell system (BioRad, Cat#1658001EDU) with the following ingredients: Acrylamide/Bis solution 37.5:1 (BioRad, Cat#1610158), 1.5M Tris: pH 8.8 (BioRad, Cat#1610798), SDS (BioRad, Cat#1610418),

ammonium persulfate (BioRad, Cat#161-0700), and Temed (BioRad, Cat#161-0800). Precision Plus Protein All blue Standards (BioRad, Cat# 161-0373) were utilized for molecular mass (kDa) reference. 30 µg of proteins were loaded into each well and were separated by size and charge at 100V for 100 min in Tris/Glycine/SDS (BioRad, cat# 161-0772).

After electrophoresis, proteins were transferred electrophoretically overnight at 30V in 4^{o}C Tris/Glycine solution (BioRad, Cat# 161-0771) onto nitrocellulose membranes. Complete transfer was confirmed by Ponceau S staining of the membrane (Sigma-Aldrich, Cat#P7170).The membrane was incubated with 5% non-fat milk (Bio-Rad, Cat#1706404XTU) at room temperature for 1 h to block non-specific binding, and then exposed to primary antibodies overnight at 4^{o}C. Appropriate secondary antibodies (1:5000 dilution) were applied at room temperature for 1 h. In order to visualize protein bands, the membrane was first incubated with chemiluminescent substrate (Thermo Scientific, Cat#PI34080). X-ray films of membranes were taken using an imaging system (Thermo Scientific). Densitometry was performed with the AlphaEaseFC (Alpha Innotech) digital program.

Primary and secondary antibodies were purchased from commercial vendors: β-actin (Genscript, Cat# A00702), heat shock protein-70 (Abcam, Cat# Ab59467), HIF-1α (Santa Cruz, Cat# Sc-10790), MPO (R&D, Cat# MAB3174), zona occludens-1 (Santa Cruz, Cat# Sc-10804), erythropoietin (Santa Cruz, Cat# Sc-7956), heme oxygenase-1 (Santa Cruz, Cat# Sc-7695), Nrf-2 (Santa Cruz, Cat# Sc-722), MMP-2 (Santa Cruz, Cat# Sc6838), cytochrome c (Novus, Cat# NB100-56503), caspase-3 (Bioss, Cat# Bs-0081R), caspase-9 (Biovision, Cat# 3016-100). Secondary antibodies included donkey anti-goat horseradish peroxidase (HRP), goat anti-rabbit HRP, and goat anti-mouse HRP (Jackson Immuno Research, Cat# 705-035-0003, 111-035-003, 115-001-003, respectively).

9. Gel zymography of matrix metalloproteinases

Matrix metalloproteinase-2 and -9 (Gelatinase) activities were examined by gelatin zymography as previously described (Frankowski et al., 2012). Briefly, 8% SDS-PAGE with 0.1% gelatin was casted, and extracts (30 µg protein) were run at 100V in 4^{o}C buffer solution for 3 h. The gel was washed in 2.5% TritonX-100 buffer (50 mM Tris-HCl-pH 7.5, 5mM $CaCl_2$, 1 µM $ZnCl_2$) at 37^{o}C for 48 hours to activate MMP proteins. Gels were stained with Coomassie Blue solution (0.25% Coomassie Blue, 45% methanol, 10% acetic acid) for 1-2 h, and destained in 30% methanol, 10% acetic acid for 30 minutes, or until clear bands were revealed. The destained gel was scanned with a digital scanner with grayscale setting for photography.

10. Real-time polymerase chain reaction (RT-PCR)

a. RNA isolation

Tissues from different brain regions were harvested in an RNAse-free environment and flash-frozen in liquid N_2. Total RNA was isolated using ReliaPrep RNA tissue Miniprep system (Promega, Cat# Z6112). Briefly, guanidine thiocyanate was used to disrupt nucleoprotein complexes, allowing RNAs to be released into the solution and isolated free of protein. 1-Thioglycerol inactivates ribonucleases. Nucleic acids in the lysates are bound to the ReliaPrep Minicolumns by centrifugation. DNase I (ThermoFisher Scientific, Cat# 89836) was used to degrade contaminating DNA. RNAs were then eluded from the membrane into distilled and deionized water. Total RNA concentration was measured with NanoDrop (ThermoFisher Scientific, Cat # 2000c).

b. cDNA amplification

cDNA was amplified using Omniscript Reverse Transcription kit (Qiagen, Cat# 205113), oligo dT primer (Qiagen, Cat# 79237), and RNase inhibitor (Qiagen, Cat#129916). Amplification reactions were conducted at 37^{o}C for 60 min.

c. RT-PCR

Reverse transcriptase reactions were conducted with iQ SYBR Green Supermix (Bio-Rad, Cat# 1708882). Primers for HIF-1α (forward: 5′-GCCAGAACCTCCTGTAACCA-3′; reverse: 5′-CCTTTTCCTGCTCTGTTTGG-3′), EPO (forward: 5′-CCAAAGCAGGAGGAATTCAG-3′; reverse: 5′-GCTGTTGTGGGAGTCTCCAT-3′), α-actin (forward: 5′-TCATCACCATCGGCAACG-3′; reverse: 5′-TTCCTGATGTCCACGTCGC-3′) were obtained from Integrated DNA Technologies, Inc., Coralville, Iowa. Denaturation and annealing took place at 94^{o}C and 60^{o}C, respectively, for a total of 40 cycles using a thermocycler (Bio-Rad). Melt curves were obtained to ensure quality of primers. Comparative threshold values (Cq) were used to compare gene expression among experimental groups.

11. Brain water content

Brain edema was assessed indirectly from the difference between wet weight and dry weight of brain tissue, a measure of tissue water content. Approximately 1 cm^{3} of cerebral and cerebellar tissue was collected in glass jars and weighed. The jars were placed in a dry oven and the tissue desiccated at 110^{o}C overnight, and then re-weighed.

12. Terminal deoxynucleotidyl transferase dUTP nick end labeling (TUNEL)

The TUNEL procedure was used to visualize necrotic and apoptotic cells, following protocols for embedded tissues by Promega (G3250). Briefly, tissue slides were washed in

xylene to remove paraffin, hydrated in 100% ethanol, rehydrated sequentially in the following concentrations of ethanol: 100%, 95%, 85%, 70%, 50%, and then washed in 0.85% NaCl and PBS. Afterward, slides were fixed in 4% formaldehyde, washed in PBS, and then submerged in Proteinase K solution (to permeabilize tissues to the staining reagents in subsequent steps). Tissues were stained with Tdt reaction mix. Staining reactions were stopped with SSC solution. Slides were then washed, counterstained with Vectashield® with DAPI (Vector laboratory, Cat# H-1200), and visualized using a fluorescence microscope (Zeiss Observer Z1 fluorescence microscope).

13. Plasma pyruvate concentration measurement

a. Metabolite extraction

Flash-frozen plasma samples were placed on ice and allowed to thaw slowly. Plasma proteins were precipitated by combining thawed plasma with 1 volume of Solution A (1M $HClO_4$ and 2mM EDTA), and then centrifuged at 10,000 rpm for 5 minutes at 4^oC to removed denatured protein precipitate. To neutralize and precipitate the $HClO_4$, 400 µl supernatant was added to 122 µl of solution B (2M KOH + 0.3M MOPS), and chilled on ice for 30 min, and centrifuged again to sediment the $KClO_4$ precipitate. Pyruvate was measured in the supernatant.

b. Pyruvate measurement in the plasma

Plasma pyruvate was measured as a UV-VIS spectrophotometric assay previously described (Bergmeyer et al., 1983; Passonneau et al., 1993). In this assay, the reduction of pyruvate to lactate is stoichiometrically coupled to the oxidation of NADH to NAD^+, monitored as the decrease in absorbance at 339 nm. Lactate dehydrogenase is added to trigger the reaction. The change of absorbance is proportional to the pyruvate concentration in the reaction medium.

$$\text{Pyruvate} + \text{NADH} + H^+ \xleftrightarrow{lactate\ dehydrogenase} \text{lactate} + NAD^+$$

14. Enzyme activity assays in tissues

Glutathione reductase (GR) and glutathione peroxidase (GPx) activities were measured using commercial kits (Cayman Chemical, Ann Arbor, MI, Cat# 703202 and 703102). Briefly, GPx activity was measured indirectly by coupling the GPx reaction to that of GR, which converts NADPH to $NADP^+$. Rate of absorbance decrease at 340nm due to the oxidation of NADPH to $NADP^+$ was used to calculate the GPx and GR enzyme activities.

$$H_2O_2 + 2GSH \xrightarrow{GPx} 2H_2O + GSSG + NADPH \xrightarrow{GR} 2GSH + NADP^+$$

Aconitase and glyceraldehyde-3-phosphate dehydrogenase (GAPDH) activities were measured by spectrophotometric assay following the linear change in absorbance at 340nm at 37^{o}C for 30 min according to an established colorimetric method (Bergmeyer et al., 1983) using a UV spectrophotometer (Shimadzu, UV-1800). In the aconitase assay, the aconitase reaction, which converts citrate to isocitrate, is coupled to the reduction of NAD+ to NADH by isocitrate dehydrogenase. The rate of reduction of NAD^+ to NADH, monitored at 340 nm, is proportional to rate of isocitrate formation, which is directly proportional to aconitase activity.

$$\text{Citrate} \xrightarrow{aconitase,\text{Fe2+}} \text{Isocitrate}$$

$$\text{Isocitrate} + NAD^+ \xrightarrow{Isocitrate\ dehydrogenase} \alpha\text{-ketoglutarate} + CO_2 + NADH + H^+$$

The GAPDH assay monitors the reduction of NAD^+ to NADH in the presence of excess concentration of glyceraldehyde 3-phosphate and inorganic phosphate. The rate of increase in absorbance at 340 nm is proportional to GAPDH-catalyzed conversion of glyceraldehyde 3-phosphate to 1,2-*bis*phosphoglycerate.

$$\text{Glyceraldehyde-3-phosphate} + PO_4^{3-} + NAD^+ \xrightarrow{GAPDH} \text{1,3-}bis\text{phosphoglycerate} + NADH + H^+$$

One unit of enzyme activity was defined as amount of enzyme required to catalyze the conversion of 1µmol of substrate to product per minute. Enzyme activities were expressed per mg of protein.

15. Myeloperoxidase activity

Myeloperoxidase (MPO) activity was measured using a commercial kit (Northwest Life Science Specialties, Vancouver, WA, Cat# NWK-MPO03). Briefly, MPO catalyzes the reaction between H_2O_2 and Cl^- to form HOCl. HOCl reacts with β-amino acid taurine to form a product that reacts with 5-thio-2-nitrobenzoic acid (TNB), a yellow complex with maximal absorbance at 412 nm. The product of the latter reaction is colorless, which results in a reduction of absorbance. The rate of decline of absorbance is proportional to MPO activity.

16. Neurological Exams

a. Cerebral performance categories

Cerebral performance categories were scored using the following scale, which is widely used in clinical practice and in the preclinical laboratory for prognosis (Yannopoulos, 2013): 1=normal; 2= slightly disabled; 3= severely disabled but conscious; 4= vegetative state; and 5: animals that died in the lab due to unachievable ROSC, or died afterward.

b. Neurological examination

The detailed neurological examination was performed in consultation with UNTHSC staff veterinarian, Dr. Egeenee Daniels. Each animal was examined by 2 staff members who were blinded with the treatment groups. Score of 1 to 5 was assigned, in which 1 is the worse and 5 is normal. Scoring the strength of muscle group: 1= no contraction, muscle flicker but no movement; 2= movement possible but not against gravity; 3= movement possible against gravity but not against resistance by the examiner; 4= movement possible against some resistance by the

examiner; 5= normal strength. For reflexes: 1= no reflex; 2= hyporeflexia/ hyperreflexia/ clonus; 3= normal. For gait: 1= cannot walk even with assistance; 2= severe ataxia; 3= moderate ataxia/ veering/ difficult turning; 4= walks with some ataxia; 5= normal. Testing categories include: mental status (bright, alert, and responsive), limb posture, gait, proprioception (response to folding leg underneath), menace response (flinch response to swinging at face), pupil symmetry, pupil light response, pupil size, palpebral reflex, facial sensation (response to pinching or poking), ocular positioning (eyes not crossed or walleyed), nystagmus (no twitching or involuntary movement of eye), positional nystagmus (no head tilt or body twitch). The neurological examination scores range from 57 (completely normal neurological function) to 13 (no neurological function).

c. Cognitive and behavior test

The memory test was modified from a T-arm test in mice (Gieling et al., 2011). Pigs were housed in separate pens and in a different room from testing one. At one end of the testing room, two pods were set up, each containing a food bowl. The food was hidden behind a barrier, and requiring the animal to knock down the barrier to get to the treat (a small piece of marshmallow). The treat was present in both bowls, but was accessible from one side of the barrier, but not the other to mitigate the olfaction attraction.

Twenty-four hours before the cardiac arrest or sham protocol, the pig was transported to the testing room, and kept in a waiting area at one end of the testing room for 15 min before testing. The door was then opened and the pig freely moved around the room to find the treat. If after 5 minutes, the animal could not locate the treat, it was showed the treat location by the examiner. The test was repeated 5 times per session per day with 15 minute rest in between. Time and distance travelled to get to the treat was recorded.

Twenty-four hours after the cardiac arrest or sham protocol, the same test was repeated in mobile animals to assess their memory of the treat location. The initial location of the animal in the testing room was randomized. The trainer/observer was blinded to treatment and protocol.

17. Statistical analysis

Data are expressed as mean values $\pm$ standard error of mean (SEM). Single factor (treatment) analysis of variance (ANOVA) was used to compare biochemical values among groups. An appropriate *post-hoc* test was applied to identify statistically treatment effects. Two-factor ANOVA (time, treatment) with repeated measures on time and appropriate *post hoc* tests were utilized for hemodynamics and plasma chemistry values. P values < 0.05 were required to reject the null hypothesis. Statistical analysis was performed using Sigma Stat 3.5 (Systat Software, Inc.).

Number of animals needed for the project is determined by power analysis with the probability of making a type I error less than 0.05 (α) and probability of correctly rejecting the null hypothesis is at least 0.8 ($1-\beta$). Based on previous data from the lab (Ryou et al., 2010; Ryou et al., 2012), we speculate that cardiac arrest, when treated with pyruvate, will decrease MMP activity and other inflammatory markers by at least 50% and will triple neurological scores (Sharma et al., 2008). At these effect sizes, 10 successful experiments per group will be required to detect statistically significant differences. From our experience with conducting the cardiac arrest experiment, the success rate of recovering the animal is roughly 80% due primarily to failed cardioversion after CPR. Therefore, we anticipate 13 animals per group for this project.

REFERENCES

Frankowski H, Gu YH, Heo JH, Milner R, J.del Zoppo G. Use of gel zymography to examine matrix metalloproteinase (Gelatinase) expression in brain tissue or in primary glial cultures. *Method Mol Biol.* 2012; **814**: 221 – 233.

Gieling ET, Nordquist RE, Van der Staay FJ. Assessing learning and memory in pigs. *Anim Cogn.* 2011; **14**(2):151-173.

Kilkenny C, Browne WJ, Cuthill IC, Emerson M, Altman DG. Improving bioscience research reporting: the ARRIVE guidelines for reporting animal research. *J Pharmacol Pharmacother* 2010:**1**:94-9.

National Research Council (U.S.). *Guide to the Care and the Use of Laboratory Animals*, 8th Ed. Washington, DC: National Academies Press, 2011.

CHAPTER III

DELAYED NEURONAL DEATH IN SWINE FOLLOWING CARDIAC ARREST AND CARDIOCEREBRAL RESUSCITATION

Anh Q. Nguyen[1], Brandon H. Cherry[1], Myoung-Gwi Ryou[3], Arthur G. Williams Jr.[1], Roger A. Hollrah[1], Albert H. Olivencia-Yurvati[1,2], Robert T. Mallet[1,2]

[1]Institute of Cardiovascular and Metabolic Diseases and [2]Department of Surgery, Univ. North Texas Health Science Center, Fort Worth, TX; [3]Medical Laboratory Sciences, Tarleton State Univ., Fort Worth, TX

ABSTRACT

Cardiac arrest, a leading cause of death in the U.S., kills >90% of its victims, and survivors often are disabled by permanent brain injury inflicted by ischemia-reperfusion. Purkinje cells of the cerebellum and CA1 neurons of the hippocampus are especially vulnerable to post-ischemic neuronal death. Increased erythropoietin (EPO) expression is associated with favorable neurological outcome. We tested the hypothesis that cardiac arrest in a domestic swine model causes delayed neuronal death in the hippocampus and cerebellum, and pyruvate treatment mitigates injuries via increased EPO expression. Yorkshire swine (25-35 kg) were subjected to cardiac arrest-resuscitation (n = 9) or non-arrest sham (n = 5) protocols. Ventricular fibrillation was induced by electrical pacing. Precordial compressions (100/min) were given at 6-10 min arrest, and then sinus rhythm was restored with transthoracic countershocks. Sodium pyruvate or control NaCl was infused *iv* at 0.1 mmol/kg/min during CCR and the first 60 min after return of spontaneous circulation (ROSC). At 1h, 4h, or 3 d ROSC, brain regions were biopsied for biochemical analysis, or fixed and stained for histological examination. At 3 d ROSC, more than 30% of the Purkinje cells were shrunken, lacked dendrites and displayed condensed cytoplasm, while in shams, the majority of Purkinje cells retained the characteristic thick dendrites and well-defined nuclei. Pyruvate treatment after cardiac arrest was associated with preserved Purkinje cell number compared to NaCl treatment. This cytoprotection was not associated with changes in inflammation components (MMPs and MPO), cytoprotective mechanisms (hsp70 and HIF-1α/EPO), or apoptotic propteases (caspase-3 and -9). Thus, cardiac arrest-resuscitation produced marked changes in cerebellar neurons evident 3 d after acute insult. Intravenous pyruvate protected the cerebellar Purkinje cells, suggesting that pyruvate administration during and immediately after resuscitation could protect ischemia-vulnerable neurons.

Key words: global ischemia, cardiac arrest, cardiopulmonary resuscitation, cardiocerebral resuscitation, neurological dysfunction, delayed neuronal death

Abbreviations: ANOVA, analysis of variance; CA1, *Cornus ammonis* region 1 of hippocampus; CPR: cardiopulmonary resuscitation; CCR: cardiocerebral resuscitation; CPC: cerebral performance category; CYTc: cytochrome c; EPO: erythropoietin; GR: glutathione reductase; GPx: glutathione peroxidase; HIF-1α: hypoxia inducible factor-1; MAP: mean aortic pressure; MMP: matrix metalloproteinase; MPO: Myeloperoxidase; ROSC: recovery of spontaneous circulation; TUNEL: terminal deoxynucleotidyltransferase mediated dUTP-biotin nick-end labeling; ZO-1: zona occludens protein 1

INTRODUCTION

Cardiac arrest is usually lethal, and survivors often face severe, persistent neurological disability due to irreversible brain injury inflicted by global ischemia/reperfusion. Brain ischemia and reperfusion activates inflammatory cascades, leading to loss of vulnerable neurons such as CA1 pyramidal neurons in the hippocampal CA1 region and cerebellar Purkinje cells. This process takes hours to days before the morphologic outcome is manifested (Kirino, 2000; Nguyen et al., 2014).

Inflammatory cascades, including matrix metalloproteinases (MMPs) and myeloperoxidase (MPO), can damage the brain parenchyma and the blood-brain barrier (BBB), exacerbating damages caused by ischemia (Lakhan et al., 2013). In mice subjected to 40 min bilateral carotid occlusion, elevated MMP-2 and -9 activities and increased neuronal death were observed in the hippocampus at 72 h reperfusion, and treatment with MMP inhibitor, BB-94, significantly reduced MMP activities and neuronal damage (Lee et al., 2004). On the other hand, in rats subjected to 1 h unilateral middle cerebral artery occlusion, increased MPO activity, detected at 72 h reperfusion, was correlated with increased number of neutrophils and brain water content (Matsuo et al., 1994). Cerebral ischemia also activates pro-apoptotic proteases such as caspase-3 and -9, culminating neuronal death (Broughton et al., 2009).

Erythropoietin (EPO), a hematopoietic cytokine, has been shown to be expressed in the brain and to exert cytoprotection. Cerebroventricular infusion of EPO in gerbils protected neurons from ischemia-induced cell death, while infusion of soluble EPO receptor worsened neuronal degeneration and learning ability (Sakanaka et al., 1998). In rats subjected to 20 min bilateral common carotid artery occlusions, intraperitoneal (*i.p.*) administration of 3000 IU/kg of recombinant human EPO (rhEPO) for 24 h decreased permeability of the blood-brain barrier (BBB) in cerebral cortex, hippocampus, and thalamus, and lipid peroxidation in the cortex

(Bahcekapili et al., 2007). In a mouse model of traumatic brain injury, *i.p.* injection of EPO at 1 and 24 h after injury afforded improved motor and cognitive function 3 d after the ischemic insult (Yatsiv et al., 2005). These and other studies provide compelling preclinical evidence of EPO's neuroprotective actions. However, clinical trials to evaluate the efficacy and safety of EPO in stroke patients demonstrated adverse effects of the treatment, indicating increased rate of intracerebral hemorrhages, especially when co-administered with tissue plasminogen activator (Ehrenreich et al., 2009). Results of another trial suggested that EPO administration could potentially lead to recurrent stroke (Pfeffer et al., 2009). Thus, despite the promising results in animal research, EPO's adverse clinical outcomes raise important concerns about use of exogenous EPO for the clinical management of acute cerebral ischemia-reperfusion scenarios. On the other hand, induction of endogenous EPO formation within the brain (Masuda et al., 1994) may obviate the use of massive dosages of exogenous EPO to deliver sufficient amount of EPO across the BBB.

Pyruvate, an energy substrate and antioxidant, is protective against ischemia-reperfusion injuries (Mallet, 2000; Mallet and Sun, 2003; Mallet et al., 2005). Moreover, pyruvate treatment increased endogenous EPO content in the myocardium (Ryou et al., 2009) and brain (Ryou et al., 2012). In a swine model of cardiopulmonary bypass, pyruvate-enhanced myocardial EPO expression was associated with sharply decreased circulating C-reactive protein concentration and activity of the neutrophil pro-oxidant enzyme myeloperoxidase (Ryou et al., 2009, 2010). Furthermore, pyruvate infusion during reperfusion was associated with increased EPO content and mRNA expression, in parallel with sharply decreased brain infarct volume, in a rat model of ischemic stroke (Ryou et al., 2012). Accordingly, this study tested the hypotheses that (1) brain ischemia-reperfusion imposed by cardiac arrest, closed-chest cardiocerebral resuscitation, and

recovery of spontaneous circulation induced pro-inflammatory matrix metalloproteinases and myeloperoxidase, and (2) acute pyruvate infusion during resuscitation and the first 60 min recovery could suppress these inflammatory factors and increase expression of the cerebroprotective cytokine EPO, thereby protecting ischemia-vulnerable neurons.

MATERIALS AND METHODS

Surgical preparation

This preclinical study was designed to elucidate the impact of cardiac arrest and cardiocerebral resuscitation (CCR) on injury in ischemia-susceptible brain regions, and whether intravenous pyruvate treatment mitigates this damage. All animal care, surgery, and experimental procedures were conducted in accordance with the National Research Council's Guide for the Care and Use of Laboratory Animals, and were approved by the University of North Texas Health Science Center Institutional Animal Care and Use Committee (protocol # 2012/13-29-A10).

Surgical preparation and cardiac arrest protocol were conducted as previously described (Cherry et al., 2015). Yorkshire swine (25 kg – 35kg) were anesthetized with *im* 5.56 mg/kg Telazol (Tiletamine HCl and zolazepam HCl, NADA 106-111) and 1.11 mg/kg Anased (xylazine, NADA 139-236) cocktail. The surgical anesthetic plane was maintained by ventilation with 1-3% isoflurane (Isothesia, NDC 11695-6776-2, Narkovet Delux Anesthesia System) in oxygen. Animals were mechanically ventilated (MDS Matrx, Model 3000) at a tidal volume of 12-15 ml/kg, 12 – 16 cycles/min to keep end tidal PCO_2 at 35 - 40 mmHg. Core temperature was monitored with a rectal probe. A catheter was introduced into the right external jugular vein and a pacing wire was advanced via this catheter into the right ventricle. The catheter also was used for treatment solution administration. The left femoral artery and vein were cannulated for blood pressure monitoring and medication/ fluid administration, respectively.

Cardiac arrest was induced by passing a 4 Hz train of 60V – 70V electrical impulses to the right ventricular endocardium. Mechanical ventilation was then suspended and the pacing wire withdrawn. At 5 min of cardiac arrest, 10mEq of $NaHCO_3$ was injected into the femoral vein. Treatments (NaCl or sodium pyruvate) were infused from 5.5 min of cardiac arrest until 60

min after recovery of spontaneous circulation (ROSC) to achieve arterial pyruvate concentration of 3.5 – 5.0 mM during treatment infusion; pyruvate concentration returned to baseline by 2 h ROSC (Cherry et al., 2015). Precordial chest compressions were delivered at 6 to 10 min arrest at the rate of 100-110 compression/min at a depth to approximately 2 inches (25% of chest diameter). 0.167 to 0.267 U/kg vasopressin (Pitressin, 20 units/ml, NDC 42023-117-25) was bolus-injected into the jugular catheter to provide vasoconstrictor support during CCR. The defibrillation protocol was begun at 10 min arrest. Single countershocks were delivered at 30 s intervals with intervening CCR until ROSC was achieved, following this sequence: 1-3 200J countershocks, then 1-3 300 J countershocks, then 1-3 360J countershocks. If the first 2 countershocks did not produce ROSC, epinephrine was administered bolus to the external jugular vein and chest compression given before the next shock. The experiment was terminated if spontaneous cardiac rhythm was not restored by the 9^{th} countershock.

Once ROSC was confirmed by an organized electrical rhythm and a rapid recovery of external pressure, mechanical ventilation was resumed and lidocaine (20mg/ml) was injected *iv*. The depth and frequency of ventilator cycles were adjusted to keep end-tidal P_{CO2} between 35-45 mmHg. Mean blood pressure was maintained at a minimum of 70mmHg by *iv* administration of phenylephrine HCl (10 mg/ml, NDC 66758-017-01) diluted to 0.2 mg/ml in normal saline (Braun, NDC 0264-7800-20). Arterial and venous blood was sampled at pre-arrest baseline, and at 5, 15, 30, 60, 120, 180, and 240 min ROSC, immediately analyzed in a blood gas laboratory (Instrumentation Laboratory, GEM Premier 3000). Partial pressures of O_2 and CO_2, and pH of arterial samples informed ongoing management of these variables. Another 10ml of blood was centrifuged at 7500 rpm for 10 min, and then plasma was aliquoted into 1.5ml centrifuge tubes, flash frozen in liquid nitrogen, and stored at -80^{o}C for future analysis.

Mean arterial pressure stabilized above 70 mmHg by 2-3 h ROSC, allowing discontinuation of phenylephrine infusion and catheter withdrawal. The femoral artery, femoral vein, and jugular vein were sutured with 7-0 Prolene blue monofilament (Ethicon). Muscles, fascia, and skin were closed sequentially with 3-0 synthetic absorbable sutures (Vedco polyglycolic acid). Analgesic buprenorphine (Buprenex) was injected intramuscularly to the right hind limb during the first hour after weaning of mechanical ventilation. The animal was monitored for heart rate and arterial O_2 saturation, and was slowly weaned of supplemental O_2. As the animal became more awake and gag reflex returned, the endotracheal tube was withdrawn. Then, the animal was wrapped in a warm blanket and returned to its pen. Animals were closely monitored until they were fully awake. Vital signs (heart rate, arterial O_2 saturation, ventilatory rate, and skin color) were carefully evaluated at 30 min intervals until animals were fully ambulatory. Neurological and cognitive tests were performed as described in the "neurological test" section.

Animals were euthanized at 72 h after ROSC for tissue collection. To minimize the interval from sacrifice to sample collection, 15 min prior to euthanization, the dorsal aspect of the scalp was shaved and reflected, and the skull was cut with a bone saw, revealing the dura. Once the animal was euthanized, the dura was cut and brain was removed and placed on ice for regional biopsy. After that, left and right ventricles, left and right lungs, kidneys, and liver were also sampled and biopsied on ice for planned studying of these organs

Hematoxylin and eosin (H&E) staining

Morphological examination of the cerebellum was performed under light microscope (Zeiss) by an observer blinded to the treatment protocols. Nine random, high powered pictures per section (2 sections total) were examined for each experiment. Cerebellar Purkinje cells were

identified as large cell bodies with their characteristic large, apically projected dendrites at the border between the granular and molecular cell layers (Esiri and Perl, 2006). Injured neurons were identified as having one or more of the following hallmarks: cell swelling, vacuolization, or darkened nuclei without a clearly defined nucleolus (Bak et al., 1980, Yuan et al., 2006).

Protein extraction

Frozen tissues were pulverized with precooled mortar and pestle under liquid N_2. 100 mg powder was then added to a tube containing 1 ml of phosphate buffer (0.1M KH_2PO_4) and 5 µl protease inhibitor (Sigma-Aldrich, P8340) and then homogenized for 1 minute at 4^{o}C using a Teflon piston. The suspension was then centrifuged at 25,000 rpm at 4^{o}C for 20 minutes (Thermo Scientific Ultracentrifuge). The supernatant was saved and the pellet was re-suspended in 0.4 ml of phosphate buffer, and again homogenized and centrifuged. The supernatants were combined, aliquoted, and stored at -80^{o}C.

Immunoblotting

Proteins in brain extracts were separated by SDS-polyacrylamide gel electrophoresis. Running gel (10% SDS-PAGE) and 4% stacking gel were cast and run using the Mini-PROTEAN Tetra cell system (BioRad, Cat#1658001EDU). 30 µg of total protein were loaded into each well and separated by size and charge at 100V for 100 min in Tris/Glycine/SDS (BioRad, cat# 161-0772). After electrophoresis, proteins were transferred overnight at 30V in 4^{o}C Tris/Glycine solution (BioRad, Cat# 161-0771) onto a nitrocellulose membrane. The membrane was incubated with 5% non-fat milk (Bio-Rad, Cat#1706404XTU) at room temperature for 1 h to block non-specific binding, and then with primary antibodies overnight at 4^{o}C. Next, appropriate secondary antibodies (1:5000 dilution) were applied at room temperature

for 1 h. In order to visualize protein bands, the membrane was first incubated with chemiluminescent substrate (Thermo Scientific, Cat#PI34080). X-ray films of membranes were taken using an imaging system (Thermo Scientific), and analyzed with a digital densitometry program (AlphaEaseFC; Alpha Innotech, San Leandro, CA).

Primary and secondary antibodies were purchased from commercial vendors: β-actin (Genscript, Piscataway, NJ, Cat# A00702), heat shock protein-70 (Abcam, Cambridge, UK, Cat# Ab59467), hypoxia inducible factor-1α (Santa Cruz, Dallas, TX, Cat# Sc-10790), myeloperoxidase (R&D, Minneapolis, MN, Cat# MAB3174), zona occludens-1 (Santa Cruz, Cat# Sc-10804), erythropoietin (Santa Cruz, Cat# Sc-7956), MMP-2 (Santa Cruz, Cat# Sc6838), MMP-9 (Novus, Littleton, CO, Cat# NBP1-57940), cytochrome c (Novus, Cat# NB100-56503), caspase-3 (Bioss, Woburn, MA, Cat# Bs-0081R), and caspase-9 (Biovision, Milpitas, CA, Cat# 3016-100). Secondary antibodies includes donkey anti-Goat horseradish peroxidase (HRP), goat anti-rabbit HRP, goat anti-mouse HRP (Jackson Immuno Research, West Grove, PA, Cat# 705-035-0003, 111-035-003, and 115-001-003, respectively).

Gelatin zymography of matrix metalloproteinases

Matrix metalloproteinases (MMPs) 2 and 9 (Gelatinase) activities were examined by gelatin zymography as previously described (Frankowski et al., 2012). Briefly, 8% SDS-PAGE with 0.1% gelatin was cast and run at 100V in 4^{o}C buffer solution for 3 h. The gel was washed in 2.5% TritonX-100 buffer (50 mM Tris-HCl-pH 7.5, 5mM $CaCl_2$, 1 µM $ZnCl_2$) at 37^{o}C for 48 h to activate MMPs. Gels were stained with Coomassie Blue solution (0.25% Coomassie Blue, 45% methanol, 10% acetic acid) for 1-2 h, and destained in 30% methanol, 10% acetic acid for 30 minutes, or until clear bands were revealed. The destained gel was scanned digitally with grayscale setting for photography.

Real-time polymerase chain reaction (RT-PCR)

a. RNA isolation

Tissues from different brain regions were harvested in an RNAse-free environment and flash-frozen in liquid N_2. Total RNA was isolated using ReliaPrep RNA tissue Miniprep system (Promega, Cat# Z6112). Briefly, guanidine thiocyanate was used to disrupt nucleoprotein complexes, allowing RNAs to be released into the solution and isolated free of protein. 1-Thioglycerol was added to the isolation solution to inactivate ribonucleases. Nucleic acids in the lysates were bound to the ReliaPrep Minicolumns by centrifugation. DNase I (ThermoFisher Scientific, Cat# 89836) was used to degrade contaminating DNA. RNAs were then eluted from the membrane into distilled and deionized water. Total RNA concentration was measured with NanoDrop (ThermoFisher Scientific, Cat # 2000c).

b. cDNA amplification

cDNA was amplified using Omniscript Reverse Transcription kit (Qiagen, Cat# 205113), oligo dT primer (Qiagen, Cat# 79237), and RNase inhibitor (Qiagen, Cat#129916). Amplification reactions were conducted at 37^{o}C for 60 min.

c. RT-PCR

Reverse transcriptase reactions were conducted with iQ SYBR Green Supermix (Bio-Rad, Cat# 1708882). Primers for HIF-1α (forward: 5′-GCCAGAACCTCCTGTAACCA-3′; reverse: 5′-CCTTTTCCTGCTCTGTTTGG-3′), EPO (forward: 5′-CCAAAGCAGGAGGAATTCAG-3′; reverse: 5′-GCTGTTGTGGGAGTCTCCAT-3′), α-actin (forward: 5′-TCATCACCATCGGCAACG-3′; reverse: 5′-TTCCTGATGTCCACGTCGC-3′) were obtained from Integrated DNA Technologies (Coralville, IA). Denaturation and annealing took place at 94^{o}C and 60^{o}C, respectively, for a total of 40 cycles using a thermocycler (Bio-

Rad). Melt curves were obtained to ensure quality of primers. Comparative threshold values (Cq) were used to compare gene expression among experimental groups.

Brain water content

Brain edema was assessed indirectly from the ratio of wet weight to dry weight of brain tissue. Approximately 1 cm^3 of cerebral and cerebellar tissue was collected in glass vials, weighed, desiccated at 110^oC overnight, and then re-weighed. The difference between wet and dry weight is a measure of tissue water content.

Enzyme immunoassay (EIA)

Glutathione reductase (GR) and glutathione peroxidase (GPx) activities were measured using commercial kits (Cayman Chemical, Ann Arbor, MI, Cat# 703202 and 703102). Briefly, GPx activity was measured indirectly by coupled reaction with GR. Rate of absorbance decrease at 340nm due to the oxidation of NADPH to $NADP^+$ was used to calculate the GPx and GR enzyme activity.

$$H_2O_2 + 2GSH \xrightarrow{GPx} 2H_2O + GSSG + NADPH \xrightarrow{GR} 2GSH + NADP^+$$

Myeloperoxidase activity

Myeloperoxidase (MPO) activity was measured using a commercial kit (Northwest Life Science Specialties, Vancouver, WA, Cat# NWK-MPO03). Briefly, MPO catalyzes the reaction between H_2O_2 and Cl^- to form HOCl, which in turn reacts with β-amino acid taurine to form a product that reacts with 5-thio-2-nitrobenzoic acid (TNB), a yellow complex with maximal absorbance at 412 nm. The product of the latter reaction is colorless, producing a decrease in absorbance at 412 nm which is proportional to MPO activity.

Neurological Exams

a. Cerebral performance categories

Cerebral performance categories were scored using the following scale, which is widely used in clinical practice and in the preclinical laboratory for prognosis (Yannopoulos, 2013): 1=normal; 2= slightly disabled; 3= severely disabled but conscious; 4= vegetative state; and 5: animals that died, either in the lab due to unachievable ROSC, or afterward.

b. Neurological examination

Detailed neurological examinations were conducted in consultation with the institution's staff veterinarian. Each animal was examined by 2 staff members who were blinded with the treatment groups. A score of 1 to 5 was assigned, in which 1 is the worse and 5 is normal. Scoring for muscle group strength: 1= no contraction, muscle flicker but no movement; 2= movement possible but not against gravity; 3= movement possible against gravity but not against resistance by the examiner; 4= movement possible against some resistance by the examiner; 5= normal strength. For reflexes: 1= no reflex; 2= hyporeflexia/ hyperreflexia/ clonus; 3= normal. For gait: 1= cannot walk even with assistance; 2= severe ataxia; 3= moderate ataxia/ veering/ difficult turning; 4= walks with some ataxia; 5= normal. Testing categories include: mental status (bright, alert, and responsive), limb posture, gait, proprioception (response to folding leg underneath), menace response (flinch response to swinging at face), pupil symmetry, pupil light response, pupil size, palpebral reflex, facial sensation (response to pinching or poking), ocular positioning (eyes not crossed or strabismus exotropia), nystagmus (no twitching or involuntary movement of eye), positional nystagmus (no head tilt or body twitch).

c. Cognitive and behavior test

The memory test was developed by modifying the T-arm test used to study mice (Gieling et al., 2011). Pigs were housed in separate pens and in a different room from the testing one. At one end of the testing room, two pods were set up, each containing a food bowl. The food was hidden behind a barrier and required the animal to knock down the barrier to get to the treat (a small piece of marshmallow). The treat was present in both bowls, but was accessible from one side of the barrier, but not the other to mitigate the olfaction attraction.

Twenty four hours before the CA/Sham protocol, the pig was transported to the testing room, and kept in a waiting area at one end of the testing room for 15 min before testing. The door was then opened and the pig freely moved around the room to find the treat. If after 5 min, the animal could not locate the treat, it was shown to the treat location. The test was repeated 5 times per session per day with 15 min rest in between. Time and distance travelled to get to the treat were recorded.

24 h after the CA/Sham protocol, the same test was repeated in mobile animals to assess their memory of the treat location. The initial location of the animal in the testing room was randomized. The trainer/observer was blinded to treatment and protocol.

Statistical analysis

All data are presented as mean $\pm$ SEM. Between-group comparisons of MMP, myeloperoxidase activities, densitometry values from zona occludens protein 1, heat shock protein 70, and cytochrome c immunoblots, Purkinje cell counts and morphology, and , cerebral performance categories were accomplished with single-factor analysis of variance (ANOVA). Within group comparisons of cerebral edema, HIF-1α, erythropoietin, glutathione peroxidase and

glutathione reductase activities, and neurological function were achieved by two-factor ANOVA for time and treatment. *Post hoc* Holm-Sidak test was used for pairwise comparison when ANOVA detected statistically significant effects. P values < 0.05 were taken to indicate statistically significant treatment effects.

RESULTS

Brain edema

Cerebral water content was comparable among Sham, cardiac arrest-CCR + NaCl (CPR), and cardiac arrest-CCR + sodium pyruvate (CPR+P) at 1h (P= 0.4), 4h (P= 0.5), and 3d ROSC (P= 0.3). Moreover, cardiac arrest did not produce statistically significant differences in water content at the different time points (Figure 2).

Matrix metalloproteinases and myeloperoxidase

Matrix metalloproteinases and myeloperoxidase activities and contents were measured in the cerebellum and hippocampus at 3 d ROSC (Figure 3). MMP-2 and MMP-9 are gelatinases that degrade extracellular matrix and have been implicated in ischemia-induced tissue inflammation. MMP-2 and MMP-9 activities were similar among Sham, CPR, and CPR+P groups (Figure 3 A -D). MMPs are known to be secreted as pro-enzymes, which have restricted effect and must be proteolytically cleaved to be fully activated. MMP contents, assessed by immunoblot, were not different among the 3 groups in both cerebellum (Figure 3F, H) and hippocampus (Figure 3B, D). Tissue inhibitor of matrix metalloproteinase-2 (TIMP-2) is an endogenous inhibitor of MMPs. There were no differences in TIMP-2 content in the hippocampus (Figure 3I) or the cerebellum (Figure 3J).

There were no appreciable effects of cardiac arrest-resuscitation or intravenous treatment on cerebellar (Figure 4A) or hippocampal (Figure 4B) contents of myeloperoxidase, an enzyme secreted by neutrophils, with ischemia-reperfusion inflicted by cardiac arrest-resuscitation, compared to control (Figure 4). Myeloperoxidase activity in the cerebellum did not change appreciably at 3 d ROSC (Figure 4C).

Zona occludens

Zona occludens-1 (ZO-1) is a structural component of tight junction complex that maintains the integrity of the blood-brain barrier. Its dissociation from the tight junction increases blood-brain barrier permeability, allowing extravasation of materials that are not indigenous to the brain microenvironment. Under oxidative stress inflicted by cardiac arrest, ZO-1 protein content tended to increase in the hippocampus (Figure 5A), although the difference was not statistically significant. In contrast, cardiac arrest-resuscitation tended to lower ZO-1 content in the cerebellum (Figure 5B). Pyruvate treatment had no impact on ZO-1 content in either region.

Heat shock protein

Heat shock protein-70 (Hsp-70), a cytoprotective protein which has been shown to be associated with cell survival and recovery after ischemic injury in the brain, was examined in the hippocampus and cerebellum. Cardiac arrest increased Hsp-70 content in the hippocampus (P= 0.056) with both NaCl and pyruvate infusion (Figure 6A). The same trend was not observed in the cerebellum (Figure 6B).

Pro-apoptotic proteins

The pro-apoptotic proteases, caspase-3 and caspase-9, were evaluated in the cerebellum and hippocampus 3d after the ischemic insult (Figure 7). Active caspase-3 tended to increase with cardiac arrest in the cerebellum (Figure 7C) and hippocampus (Figure 7D), and pyruvate seemed to lessen its content, yet these changes were not statistically significant. Cardiac arrest was not associated with alterations in caspase-9 content in both cerebellum and hippocampus.

Cytochrome c, a protein abundant in the mitochondrial intermembrane space, has been reported to be released into the cytoplasm and extracellular matrix during ischemic insult, and its translocation is associated with apoptosis in neurons (Perez-Pinzon et al., 1999). Cytochrome c content did not markedly change following cardiac arrest/CCR in the hippocampus (Figure 8A) and cerebellum (Figure 8B), regardless of the treatment.

Hypoxia inducible factor-1 and erythropoietin

Gene expression of hypoxia inducible factor-1α (HIF-1α) and erythropoietin (EPO) in the hippocampus were examined at 4 h and 3 d ROSC (Figure 9). HIF-1α mRNA abundance was similar among experimental groups and was comparable at 4 h and at 3 d (Figure 9A). In contrast, EPO mRNA abundance was considering higher at 4 h ROSC vs. 3 d ROSC in both CCR groups as well as in the sham group at the respective time point (Figure 9B).

Glutathione reductase and peroxidase

Glutathione reductase (GR) and peroxidase (GPx) activities were analyzed in the cerebellum at 3 d after cardiac arrest-resuscitation. A trend toward an increase in GPx activity with cardiac arrest/CCR, and even higher activity with pyruvate treatment was observed, but was not statistically significant (P= 0.09, Figure 10A). Cerebellar GR activity was similar in sham, CPR, and CPR+P at 3 d ROSC (Figure 10B).

At 1h ROSC, cardiac arrest/CCR lowered GR activity by 50-60% vs. the sham value (Figure 11); the enzyme recovered by 4 h ROSC. By 3 d ROSC, GR activity in the two cardiac arrest-resuscitation groups recovered compared to the sham value. Pyruvate treatment did not alter in GR activity compared vs the NaCl-treated control group.

Cerebellar Purkinje cells

The cerebellar Purkinje cells are among the most ischemia-sensitive neuron of the brain (Ng et al., 1989). The Purkinje cells were examined by histology 3 d after cadiac arrest-resuscitation vs. sham protocol (Figure 12). Cardiac arrest-resuscitation produced 30% decrease in the number of cerebellar Purkinje cell per high power field at 3 d recovery ($P < 0.05$ vs. sham) , and pyruvate treatment during CCR and the first 60 min ROSC preserved these neurons, in a manner evident at 3d ROSC ($P < 0.05$ vs. CPR).

Neurological and cognitive test

Cerebral performance category, a prognostic tool to assess neurological outcome after cardiac arrest in clinical settings, was used to evaluate neurobehavioral function of animals in all 3 experimental groups. Scores in this test range from 1 to 5, with 1 representing best normal function and 5 representing brain death. All animals consistently scored 1 (Table 1), indicating essentially normal neurological function. Furthermore, there were no differences in neurological outcome among Sham, CPR, and CPR+P at 24h ($P = 0.6$), 48h ($P = 0.7$), and 72h ($P = 0.2$) after ROSC. A more detailed neurological assessment also was conducted on these animals. Details on the categories and total score are reported on Table 2. Again, neither of the cardiac arrest/CCR groups differed from their sham counterparts at 24 h, 48 h, or 72 h ROSC.

Cognitive function of animals after cardiac arrest was investigated by training animals to locate a marshmallow treat before cardiac arrest. The time and travelling distance required to locate the treat, a test of memory, were determined at 24, 48, and 72 h ROSC (Figure 13). Each animal had 5 trials 24 h before cardiac arrest. By the 5^{th} trial, all were able to locate the food source in a short amount of time and with a direct travel path. There were no between-group

differences in distance and time to locate food at 24 h following cardiac arrest/CCR and recovery or the sham protocol. Thus, 6 min of pre-intervention cardiac arrest and 4 min closed chest compression did not produce appreciable neurobehavioral deficits 24 h later.

DISCUSSION

Brain Inflammation after cardiac arrest-resuscitation

Six minutes of untreated cardiac arrest and 4 min closed-chest compression did not result in cerebral edema at 1h, 4h, or 3d ROSC. This outcome was not entirely unexpected as the inflammatory response to global brain ischemia may have peaked between 4 h and 72 h ROSC. Inflammation, which involves blood brain barrier disruption and extravasation of immune cells and plasma, develops gradually and the time of peak intensity is not well-characterized in pigs. A rat study that examined the time course of edema, 15 min of global brain ischemia showed that edema peaked at 30 min reperfusion and normalized at 180 min in frontal-parietal cortex, caudoputamen, and hippocampus, and that an abbreviated 5 min ischemic insult and 30 min reperfusion did not result in appreciable edema (Mellergard et al., 1989). On the other hand, edema has been found to be delayed. In rats subjected to traumatic brain injury. In these areas, brain water content increased within 1-6 h, peaked at 48 h, and resolved by 5-7 days post-trauma (Bareyre et al., 1997).

Intense activation of MMP-2 and MMP-9 is associated with worse neurological outcome. Reactive oxygen species, abundant during ischemia and reperfusion, incite neurons to secrete inflammatory cytokines, leading to recruitment of resident microglia and astrocytes, and infiltration of non-resident inflammatory cells (i.e. neutrophils, macrophages), cytokines, and chemokines to the brain. These cells secrete harmful enzymes and proteases, which further damage the brain infrastructure (Shichita et al., 2012). Specifically, inflammatory cells release MMPs, which degrade extracellular matrix and tight junctions at the BBB in the early stages of ischemic stroke stage, thereby potentiating edema and extravasation of leukocytes, and, thus, exacerbating brain injury (Yang et al., 2007, Xin et al., 2012). In an *in vitro* BBB preparation with isolated rat cerebral endothelial cells, exposure to the pro-inflammatory cytokines, TNF-α,

IL-1β, or IL-6 resulted in decreased transendothelial electrical resistance (TEER), an indicator of BBB disruption (Vries et al., 1996). This finding was confirmed by *in vivo* experiments: intracerebral injection of TNF-α increased BBB permeability and MMP expression (Rosenberg et al., 1995). MMPs are activated by the redox switch mechanism, in which the redox states of sulfhydryls in the MMP molecule are modulated by changes in the intracellular glutathione (GSH): glutathione disulfide (GSSG) concentration ratio (Okamoto et al., 2004). In mice subjected to global cerebral ischemia by bilateral 20 min occlusion of the common carotid arteries, MMP-2 and MMP-9 activities increased and were associated with increased hippocampal neuronal death 3 days after cardiac arrest. In the same study, MMP-9 knock-out mice, when subjected to the same experimental condition, showed significantly reduced MMP-2 and MMP-9 activities and less neuronal damage (Lee et al., 2004). Oxidative stress caused by IR also induces dissociation of tight junction proteins, such as occludin, in a rat model of hypoxia and reoxygenation (Lochhead et al., 2010). Suppression of MMP-2 and/or MMP-9 activity in brain after IR insult is an important mechanism to mitigate brain injuries. On the other hand, MMP-2 and MMP-9, secreted by EPO activated endothelial cells, has been shown to be crucial in promoting neural progenitor cell migration into the damaged area (Wang et al., 2006); thus, activation of these MMPs during post-ischemic recovery may have a neuroprotective function. Endogenous tissue inhibitors of matrix metalloproteinases (TIMPs) also exert neuroprotection. In rats subjected to 2 h middle cerebral artery occlusion and reperfusion, MMP-2 activity and TIMP-2 peaked at day 5, while MMP-9 and TIMP-1 were maximally elevated at 48 h, and treatment with inhibitors of MMPs reduced BBB permeability and brain edema (Rosenberg et al., 1998). In mice subjected to 30 min stroke, TIMP-1 knock-out was associated with increased MMP-9 activity and exacerbated BBB disruption and apoptosis (Fujimoto et al., 2008). In

cardioplegically arrest myocardium maintained on cardiopulmonary bypass, pyruvate-enriched cardioplegia decreased MMP-9 activity and increased TIMP-2 content compared to control cardioplegia (Ryou et al., 2010). Our result indicated that 6 min of untreated cardiac arrest did not alter MMP-2 and MMP-9 activities and content, nor content of TIMP-2, regardless of treatment. Additionally, MPO, an enzyme released by activated inflammatory neutrophils, was unchanged after cardiac arrest vs. non-arrest pigs. Increased MPO activity is associated with increase neutrophil infiltration and brain water content (Matsuo et al., 1994).Thus, the unchanged MPO activity is consistent with the absence of edema. Increased inflammation may compromise the blood brain barrier (BBB), a selective vascular endothelial barrier, formed by tight junction proteins, including zona occludens-1 (ZO-1). Decreased ZO-1 expression and protein content, and compromised BBB have been reported in post-ischemic rat brain at 72 h reperfusion (Jiao et al., 2011).

Cellular protective proteins

Pyruvate has many advantages in protecting the brain from ischemia/reperfusion. Pyruvate readily traverses the blood brain barrier via monocarboxylase transporters in the cerebrovascular endothelium, and neurons and astrocytes also possess these transporters (Oldendorf, 1973; Conn and Steele, 1982; Miller et al., 1986). Pyruvate protects cells by preserving cellular energy state and antioxidant defenses, and directly detoxifies reactive oxygen and nitrogen intermediates in both the myocardium and neurons (Mallet et al, 2005; Ryou et al., 2013). On the other hand, pyruvate treatment was associated with increased EPO expression in myocardium and brain, although the mechanism is elusive. It was postulated that pyruvate acts as a competitive inhibitor to α-ketoglutarate, a substrate of prolyl hydroxylase, the enzyme which hydroxylates prolyl residues of HIF-1α, thus targeting HIF-1α for proteosomal degradation

(Semenza et al, 2007; Ryou et al., 2012). In Mongolian gerbils, intracerebroventricular delivery of EPO, immediately following restoration of blood flow after 5-min bilateral occlusion of the common carotid arteries, reduced brain edema, neuronal death, and nitrite and nitrate content at 6h post ischemia (Calapai et al., 2000). In rat, rhEPO, injected *i.p.* at the time of carotid artery occlusion, markedly dampened monocyte and macrophage infiltration, and microglia activation (Villa et al, 2003). In addition, appreciable reductions of the pro-inflammatory cytokines: TNF-α, IL-6, and monocyte chemoattractant protein 1 (MCP-1) were detected at the ischemic area in rhEPO-treated group compared to non-treated controls. Increased HIF-1α expression drives EPO production, which prevents cellular damage and death via Akt pathway (Siren et al, 2000). Exogenous EPO has been shown to traverse the BBB, yet 5 - 17 h were required for EPO to access the neurons (Brines et al, 2000). Intense EPO mRNA expression was evident at 4 h ROSC and in the corresponding sham controls, although this expression subsided by 3 d post-arrest. Thus it appears that surgical stress per se, regardless of cardiac arrest-resuscitation, may have elicited EPO expression. It is especially surprising that EPO mRNA increased in spite of the hyperoxic condition imposed by O_2-enriched ventilation. Many factors during the experiments can impact EPO production: isoflurane anesthesia, hyperoxia-associated oxidative stress, and/or surgical preparation. While isoflurane inhalation, the anesthetic used in our experiments, inhibits HIF-1α, HIF-2α, and EPO in rat and mouse brains (Tanaka et al., 2011, Kai et al., 2014), high oxygen ventilation can be detrimental to the already vulnerable ischemic brain (Friedman, 2015). A transient increase in EPO expression may serve to protect cells from reactive oxygen species generated by hyperoxic O_2 ventilation.

Cytoprotective heat-shock protein-70 (Hsp-70) is inducible by ischemia in neurons, astrocytes, microglia, and endothelial cells. The most vulnerable neurons were among the first to

express Hsp70 in rat subjected to 10 min of global ischemia and 24 h reperfusion, and survival of these neurons exceeded that of acid fuchsin stained (indicating dying/dead) neurons (Gaspary et al., 1995). Hsp-70 expression, however, returns to baseline by 3 d ROSC (Hata et al., 2000). At 3d ROSC, HIF-1α expression is associated with increased hsp-70 gene expression in cultured cardiomyocyte (Date et al., 2005). At 3 d after cardiac arrest-resuscitation, hippocampal Hsp-70 tended to increase compared to the sham value, although the difference was not statistically significant. Increased hsp-70 comtent may contribute to an advantageous outcome in these animals.

Pro-apoptotic markers and Purkinje cell death

At 3 d ROSC, a substantial loss of Purkinje cells was evident in cardiac arrest + NaCl group, but pyruvate treatment during the first hour of resuscitation preserved Purkinje cells. Cerebellar cell death as a result of cardiac arrest has been documented in human and rat (Horn and Schlote, 1992; Brasko et al, 1995). We examined whether apoptotic signaling was associated with the loss of Purkinje cells. Cytochrome c (CYTc), a protein normally residing in the mitochondria intermembrane space, is released into the cytosol during ischemia/reperfusion and once released, initiates apoptosis via activation of caspases-9 and -3. However, content of the pro-apoptotic markers CYTc, caspase-3, and caspase-9 content did not differ at 3 d ROSC vs. Sham. Also, cardiac arrest has been shown to reversibly inactivate myocardial enzymes of the glutathione antioxidant system, including glutathione reductase (GR) (Sharma et al., 2007). At 1 h ROSC, cerebellar GR activity decreased in both NaCl and pyruvate treated pigs and recovered by 3d. Thus, pyruvate protection of Purkinje cells could not be ascribed to cytoprotective enzymes or an impact on the mitochondrial apoptotic cascade.

Neurological outcome

All animals consistently scored 1 in the CPC scale, indicating optimal neurological recovery. Additional neurological assessment and memory evaluation supports this result. Cardiac arrest may result in deficits in memory and motor functions with variable executive impairment (Lim et al., 2004), which can be difficult to evaluate in an animal model, although many tests have been applied on swine to assess learning and memory. A systemic approach is lacking and further research on pigs' behaviors is necessary (Gieling et al, 2011).

Despite extensive research, no clinical trial has shown improved outcomes resulting from pharmacological interventions superimposed on standard CCR. Therapeutic hypothermia, despite its compelling results in neurological recovery, is controversial and has many exclusion factors, such as major surgery within the preceding 14 days, systemic infection/sepsis, or known bleeding problems (American Heart Association guidelines). Pyruvate can be readily administered *iv*, and it has been found to protect post-ischemic myocardium and brain, in association with increased expression of EPO and decreased neuronal apoptosis.

Limitations and future direction

Neurological function was not appreciably compromised in any of the swine subjected to cardiac arrest. The absence of neurological impairment may be due to the use of healthy, juvenile swine used in this study. Although juvenile swine provided a compliant, compressible thoracic chamber facilitating quality CCR, they might not accurately represent the typical adult human suffering cardiac arrest, many of whom have comorbidities that complicate the resuscitation and recovery process such as age, coronary artery disease, arrhythmia, diabetes, and hypertension (Piscator et al., 2016). Indeed, fewer comorbidities have been associated with better neurological

recovery after cardiac arrest (Kragholm et al, 2015). The pathophysiological progression of cardiac arrest due to ventricular fibrillation is considered to have 3 phases: Electrical (0-5 minutes), circulatory (5-15 min), and metabolic phase (> 15 min) (Ewy, 2005). In the electrical phase, the most effective intervention is prompt defibrillation. During the circulatory phase, generation of adequate coronary and cerebral perfusion by chest compression is crucial and recovery may depend on the duration of arrest. In the metabolic phase, outcomes are almost always dismal. Thus, 6 min of untreated cardiac arrest in healthy juvenile swine may be associated with favorable outcomes. In the future, studies of longer durations of pre-intervention arrest and in older animals with cardiometabolic comorbidities may be more representative of clinical cardiac arrest scenarios.

ACKOWLEDGEMENTS

This work was supported by research grant R01 NS076975 from the National Institute of Neurological Disorders and Stroke. AQN was supported by the D.O./Ph.D. scholarship from the University of North Texas Health Science Center. This work was conducted in partial fulfillment of the requirements for the Ph.D. degree for AQN.

REFERENCES

2005 American Heart Association Guidelines for Cardiopulmonary Resuscitation and Emergency Cardiovascular Care. *Circulation*. 2005 Dec 13. 112(24 Suppl):IV1-203.

Bahcekapili N, Uzum G, Gokkusu C, Kuru A, Ziylan Y. The relationship between erythropoietin pretreatment with blood-brain barrier and lipid peroxidation after ischemia/reperfusion in rats. *Life science*2007; **80**: 1245 – 1251.

Bareyre F, Wahl F, McIntosh TK, Stutzmann JM. Time course of cerebral edema after traumatic brain injury in rats: effects of riluzole and mannitol. *J Neurotrauma* 1997; **14**(11): 839 – 849.

Brasko J, Rai P, Sabol MK, Patrikios P, Ross DT. The AMPA antagonist NBQX provides partial protection of rat cerebellar Purkinje cells after cardiac arrest and resuscitation. *Brain Research* 1995; **699**: 133 – 138.

Brines ML, Ghezzi P, Keenan S, Agnello D, de Lanerolle NC, Cerami C, Itri LM, Cerami A. Erythropoietin crosses the blood-brain barrier to protect against experimental brain injury. PNAS 200; 97(19): 10526 – 10531.

Broughton BRS, Reutens DC, Sobey CG. Apoptotic mechanisms after cerebral ischemia. Stroke 2009; 40: e331 – e339.

Calapai G, Marciano MC, Corica F, Allegra A, Parisi A, Frisina N, Caputi A, Buemi M. Erythropoietin protects against brain ischemic injury by inhibition nitric oxide formation. *European Journal of Pharmacology* 2000; **401**: 349 – 356.

Cherry BH, Nguyen AQ, Hollrah RA, Williams AG Jr, Hoxha B, Olivencia-Yurvati AH, Mallet RT. Pyruvate stabilizes electrocardiographic and hemodynamic function in pigs recovering from cardiac arrest. *Exp Biol Med.* 2015 Dec; **240**(12):1774-84.

Conn AR, Steele RD: Transport of alpha-keto analogues of amino acids across blood-brain barrier in rats. *Am J Physio* 1982; l**243** :E272 –E277.

Date T, Mochizuki S, Belanger Aj, Yamakawa M, Luo Z, Vincent KA, Cheng SH, Gregory RJ, Jiang C. Expression of constitutively stable hybrid hypoxia-inducible factor-1α protects cultured rat cardiomyocytes against simulated ischemia-reperfusion injury. *American Journal of Physiology- Cell Physiology* 2005; **288**(2): C314 – C320.

Ehrenreich H, Weissenborn K, Prange H, Schneider D, Weimar C, Wartenberg K, Schellinger PD, Bohn M, Becker H, Wegrzyn M, *et al*. Recombinant human erythropoietin in the treatment of acute ischemic stroke**.** *Stroke* 2009; **40:** e647-e656. 10.1161/STROKEAHA.109.564872.

Esiri M, Perl D. Oppenheimer's diagnostic neuropathology: A practical manual. New York: Hodder Arnold, 2006. Print.

Ewy GA. Cardiocerebral resuscitation: The new cardiopulmonary resuscitation. Circulation 2005; 111: 2134 – 2142.

Fujimoto M, Takagi Y, Aoki T, Hayase M, Marumo T, Gomi M, Nishimura M, Kataoka H, Hashimoto N, Nozaki K. Tissue inhibitor of metalloproteinases protect blood-brain barrier disruption in focal cerebral ischemia. *J Cereb Blood Flow Metab.* 2008 Oct; **28**(10):1674-85.

Friedman, S. Less oxygen for cardiac arrest patients is better. *Crit Care & Shock* 2015; **18**: 92 – 96.

Gaspary H, Graham SH, Sagar SM, Sharp FR. Hsp70 heat shock protein induction following global ischemia in the rat. *Molecular brain research* 1995; **34**: 327 – 332.

Gieling ET, Nordquist RE, van der Staay FJ. Assessing learning and memory in pigs. *Anim Cogn.* 2011; **14**(2): 151 – 173.

Hata R, Maeda K, Hermann D, Mies G, Hossmann KA. Dynamics of regional brain metabolism and gene expression after middle cerebral artery occlusion in mice. *J Cereb Blood Flow Metab.* 2000; **20**(2): 306 – 315.

Horn M, Schlote W. Delayed neuronal death and delayed neuronal recovery in the human brain following global ischemia. *Acta Neuropathol* 1992; **85**: 79 – 87.

Jiao H, Wang Z, Liu Y, Wang P, Xue Y. Specific role of tight junction proteins claudin-5, occludin, and ZO-1 of the blood-brain barrier in a focal cerebral ischemic insult. *J Mol Neurosci* 2011; **44**: 130 – 139.

Kai S, Tanaka T, Matsuyama T, Suzuki K, Hirota K. The volatile anesthetic isoflurane differentially suppresses the induction of erythropoietin sysnthesis elicited by acute anemia and systemic hypoxemia in mice in a hypoxia-inducible factor-2-dependent manner. *Eur J Pharmacol*. 2014 Jun 5;**732**:43-49.

Kirino, T. Delayed neuronal death. Neuropathology 2000; 20: S95 – S97

Kragholm K, Wissenberg M, Mortensen N, Fonager K, Jensen SE, Rajan S, Lippert FK, Christensen EF, Handen PA, Lang-Jensen T, Hendriksen OM, Kober L, Gislason G, Torp-Pedersen C, Rasmussen BS. Return to work in out-of-hospital cardiac arrest survivors: A nationwide register-based follow-up study. Circulation 2015; 131: 1682-1690. DOI: 10.1161/CIRCULATIONAHA.114.011366.

Lakhan SE, Kirchgessner A, Tepper D, Leonard A. Matrix metalloproteinases and blood-brain barrier disruption in acute ischemic stroke. Front neurol. 2013; **4**: 32.

Lee JY, Kim YH, Koh JY: Protection by pyruvate against transient forebrain ischemia in rats. *J Neurosci* 2001; **21** :RC171.

Lee SR, Tsuji K, Lee SR, Lo EH. Role of Matrix Metalloproteinases in delayed neuronal damage after transient global cerebral ischemia. *The Journal of Neuroscience*, 2004: **24**(3): 671 – 678.

Lim C, Alexander MP LaFleche G, Schnyer DM, Verfaellie M. The neurological and cognitive sequelae of cardiac arrest. *Neurology* 2004; **63**(10): 1774 – 1778

Lochhead JJ, McCaffrey G, Quigley CE, Finch J, DeMarco KM, Nametz N, Davis TP. Oxidative stress increases blood-brain barrier permeability and induces alterations in occluding during hypoxia-reoxygenation. *J of Cerebral Blood Flow & Metabolism* 2010; **30**: 1625 – 1636.

Mallet RT, Sun J, Knott EM, Sharma AB, Olivencia-Yurvati AH. Metabolic cardioprotection by pyruvate: recent progress. *Exp Biol Med* 2005 Jul; **230**(7):435-43.

Mallet RT. Pyruvate: metabolic protector of cardiac performance. *Proc Soc Exp Biol Med*. 2000; **223**:136–148.

Mallet RT, Sun J. Antioxidant properties of myocardial fuels. Mol Cell Biochem. 2003; **253**:103–111.

Masuda S, Okano M, Yamagishi K, Nagao M, Ueda M, Sasaki R. A novel site of erythropoietin production. Oxygen-dependent production in cultured rat astrocytes. *The Journal of Biological Chemistry* 1994; **269**: 19488 – 19493.

Matsuo Y, Onodera H, Shiga Y, Nakamura M, Ninomiya M, Kihara T, Kogure K. Correlation between myeloperoxidase-quantified neutrophil accumulation and ischemic brain injury in the rat. Effects of neutrophil depletion. *Stroke* 1994; **25**(7): 1469 – 1475.

Mellergard P, Bengtsson F, Smith ML, Riesenfeld V, Siiesjo BK. Time course of early brain edema following reversible forebrain ischemia in rats. *Stroke* 1989; **20**(11): 1565 – 1570.

Miller LP, Oldendorf WH. Regional kinetic constants for blood–brain barrier pyruvic acid transport in conscious rats by the monocarboxylic acid carrier. *J Neurochem*. 1986; **46**: 1412–1416.

Nguyen AQ, Cherry BH, Scott GF, Ryou MG, Mallet RT. Erythropoietin: Powerful protection of ischemic and post-ischemic brain. *Exp Biol Med* 2014: 1-15. DOI: 10.1177/1535370214523703.

Okamoto T, Akuta T, Tamura F, Van Der Vliet A, Akaike T. Molecular mechanism for activation and regulation of matrix metalloproteinases during bacterial infections and respiratory inflammation. *Biol. Chem*. 2004; Vol. **385**, Issue 11: 997 – 1006.

Oldendorf WH: Carrier-mediated blood-brain barrier transport of short-chain monocarboxylic organic acids. *Am J Physiol* 1973; **224** :1450 –1453.

Pérez-Pinzón MA, Xu GP, Born J, Lorenzo J, Busto R, Rosenthal M, Sick TJ. Cytochrome C is released from mitochondria into the cytosol after cerebral anoxia or ischemia. *J Cereb Blood Flow Metab.* 1999; **19**(1): 39 – 43.

Pfeffer MA, Burdmann EA, Chen CY, Cooper ME, de Zeeuw D, Eckardt KU, Feyzi JM, Ivanovich P, Kewalramani R, Levey AS, *et al*.: A trial of darbepoetin alfa in type 2 diabetes and chronic kidney disease**.** *N Engl J Med* 2009; **361:** 2019–2032. 10.1056/NEJMoa0907845.

Piscator E, Hedberg P, Goransson K, Djarv T. Survival after in-hospital cardiac arrest is highly associated with the Age-combined Charlson Co-morbidity index in a cohort study from a two-site Swedish University hospital. *Resuscitation* 2016; **99**: 79 – 83.

Rajdev S, Hara K, Kokubo Y, Mestril R, Dillmann W, Weinstein PR, Sharp FR. Mice overexpressing rat heat shock protein 70 are protected against cerebral infarction. Annals of neurology 200; 47(6): 782 – 791.

Rosenberg GA, Estrada EY, Dencoff JE, Stetler-Stevenson WG. Tumor necrosis factor-α-induced gelatinase B causes delayed opening of the blood-brain barrier: an expanded therapeutic window. *Brain Research* 1995; **703**: 151 – 155.

Rosenberg GA, Estrada EY, Dencoff JE. Matrix metalloproteinases and TIMPs are associated with blood-brain barrier opening after reperfusion in rat brain. *Stroke* 1998; **29**: 2189 – 2195.

Ryou MG, Choudhury GR, Winters A, Xie L, Mallet RT, Yang SH. Pyruvate minimizes rtPA toxicity from in vitro oxygen-glucose deprivation and reoxygenation. *Brain Res.* 2013; **1530**: 66 – 75.

Ryou MG, Flaherty DC, Hoxha B, Sun J, Gurji H, Rodriguez S, Bell G, Olivencia-Yurvati AH, Mallet RT. Pyruvate-fortified cardioplegia evokes myocardial erythropoietin signaling in swine undergoing cardiopulmonary bypass. *Am J Physiol Heart Circ Physiol.* 2009; **297** (5): H1914 – H1922.

Ryou MG, Flaherty DC, Hoxha B, Gurji H, Sun J, Hodge LM, Olivencia-Yurvati AH, Mallet RT. Pyruvate-enriched cardioplegia suppresses cardiopulmonary bypass-induced myocardial inflammation. *The Annals of Thoracic Surgery* 2010; Vol. **90**, Issue 5: 1529 – 1535.

Ryou, MG, Liu R, Ren M, Sun J, Mallet RT, Yang SH. Pyruvate protects the brain against ischemia-reperfusion injury by activating the erythropoietin signaling pathway. *Stroke*. 2012; **43**: 1101-1107.

Sakanaka M, Wen TC, Matsuda S, Masuda S, Morishita E, Nagao M, Sasaki R. *In vivo* evidence

that erythropoietin protects neurons from ischemic damage. *PNAS* 1998; **95**(8): 4635 – 4640.

Semenza GL. Hypoxia-inducible factor 1 (HIF-1) pathway. Sci STKE.2007;2007:cm8.

Sharma AB, Sun J, Howard LL, Williams AG, Mallet RT. Oxidative stress reversibly inactivates myocardial enzymes during cardiac arrest. American Journal of Physiology- Heart and Circulatory Physiology 2007; 292(1): H198 – H206.

Shichita T, Sakaguchi R, Suzuki M, Yoshimura A. Post-ischemic inflammation in the brain. *Frontiers in immunology* 2012; Vol. **3**, Article 132: 1 – 7.

Siren Al, Fratelli M, Brines M, Goemans C, Casagrande S, Lewczuk P, Keenan S, Gleiter C, Pasquali C, Capobianco A, Mennini T, Heumann R, Cerami A, Ehrenreich H, Ghezzi P. Erythropoietin prevents neuronal apoptosis after cerebral ischemia and metabolic stress. *PNAS* 2001; **98**(7): 4044 – 4049.

Tanaka T, Kai S, Koyama T, Daijo H, Adachi T, Fukuda K, Hirota K. General anesthetics inhibit erythropoietin induction under hypoxic conditions in the mouse brain. *PLOS* 2011 Dec. http://dx.doi.org/10.1371/journal.pone.0029378.

Villa P, Bigina P, Mennini T, Agnello D, Laragione T, Cagnotto A, Viviani B, Marinovich M, Cerami A, Coleman T, Brines M, Ghezzi. Erythropoietin selectively attenuates cytokine production and inflammation in cerebral ischemia by targeting neuronal apoptosis. *J. Exp. Med.* 2003; Volume **198**, Number 6: 971 – 975.

Vries HW, Bloom-Roosemalen MCM, Oosten MV, Boer AG, Berkel TJC, Breimer DD, Kuiper J. The influence of cytokines on the integrity of the blood-brain barrier in vitro. *Jounal of Neuroimmunology* 1996; **64**: 37 – 43.

Wang L, Zhang ZG, Zhang RL, Gregg SR, Hozeska-Solgot A, LeTourneau Y, Wang Y, Chopp M. Matrix metalloproteinase 2 (MMP2) and MMP9 secreted by erythropoietin-activated endothelial cells promote neural progenitor cell migration. The Journal of Neuroscience 2006, 26(22): 5996 – 6003.

Weisfeldt ML, Becker LB. Resuscitation after cardiac arrest: a 3-phase time-sensitive model. *JAMA.* 2002; **288**: 3035–3038.

Xin H, Liang W, Mang J, Lin L, Guo N, Zhang F, Xu Z. Relationship of gelatinases-tight junction proteins and blood-brain barrier permeability in the early stage of cerebral ischemia and reperfusion. *Neural Regen Res.* 2012 Nov 5; **7**(31):2405-12.

Yang Y, Estrada EY, Thompson JF, Liu W, Rosenberg GA. Matrix metalloproteinase-mediated

disruption of tight junction proteins in cerebral vessels is reversed by synthetic matrix metalloproteinase inhibitor in focal ischemia in rat. *Journal of Cerebral Blood Flow & Metabolism* 2007; **27**: 697 – 709.

Yatsiv I, Grigoriadis N, Simeonidou C, Stahel PF, Schmidt OI, Alexandrovich AG, Tsenter J, Shohami E. Erythropoietin is neuroprotective, improves functional recovery, and reduces neuronal apoptosis and inflammation in a rodent model of experimental closed head injury. The FASEB Journal 2005. Doi: 10.1096/fj.05-390.

FIGURE LEGENDS

Figure 1. *Experimental timeline*. Cardiac arrest was induced by ventricular fibrillation. Cardiocerebral resuscitation was performed at 6-10 min arrest, and then transthoracic countershock were applied to restore sinus rhythm. Animal was recovered at 4h and euthanized at 3d post cardiac arrest. Open triangles: blood sampling at pre-arrest baseline and at 5, 15, 30, 60, 120, 180, and 240 min ROSC. Filled triangles: the animals were sacrificed and brain biopsies obtained at 1, 4, or 3d ROSC.

Figure 2. Cerebral water content (ml/100g tissue) at 1 h (filled bars), 4 h (hatched bars), and 3 d (dotted bars) ROSC. Values are mean $\pm$ SEM. Single-factor ANOVA: P= 0.38 (1 h), P= 0.5 (4 h), P= 0.25 (3 d). Two-factor ANOVA: P= 0.2 (time); P= 0.3 (treatment); P= 0.6 (time and treatment).

Figure 3. *Matrix metalloproteinases*. MMP-2 and MMP-9 activities and content. Panels A,B: Hippocampal MMP-2 activities and content (P= 0.4, P= 0.6). Panels C,D: hippocampal MMP-9 activity and content (P= 0.8; P= 0.6). Panels E,F: Cerebellar MMP-2 activity and content (P=0.4, P=0.6). Panels G,H: cerebellar MMP-9 activity and content (P= 0.3, P= 0.7). Panels I,J: hippocampal TIMP-2 content at 3d ROSC (left, P= 0.2), cerebellar TIMP-2 content at 3 d ROSC (right, P= 0.4). Values are mean $\pm$ SEM.

Figure 4. *Myeloperoxidase*. Hippocampal (Panel A) and cerebellar (Panel B) MPO contents, and cerebellar MPO activity (Panel C) at 3d ROSC, expressed as relative density against actin. Values are mean $\pm$ SEM. One-way ANOVA: Hippocampal MPO content: P=0.4; cerebellar MPO content: P= 0.7; cerebellar MPO activity: P= 0.7.

Figure 5. *Zona Occludens-1*. Hippocampal (Panel A) and cerebellar (Panel B) ZO-1 content at 3d ROSC, normalized to actin content. Values are mean ± SEM. Single-factor ANOVA: Hippocampus: P=0.3; cerebellum: P= 0.3.

Figure 6. *Heat shock protein-70*. Hippocampal (Panel A) and cerebellar (Panel B) Hsp-70 contents at 3d ROSC, normalized to actin content. Values are mean ± SEM. Single-factor ANOVA: Hippocampus: P=0.056; cerebellum: P= 0.5.

Figure 7. *Pro-apoptotic proteins 3 d after cardiac arrest-resuscitation*. Panels A, B: Procaspase-3: hippocampus (P= 0.8), cerebellum (P= 0.4); Panels C, D: Caspase-3: hippocampus (P= 0.14), cerebellum (P= 0.4); Panel D, E: Caspase-9: hippocampus (P= 0.8), cerebellum (P= 0.3) (P= 0.4 (left) and P= 0.37 (right), expressed in relative density against actin. Values are mean ± SEM.

Figure 8. *Cytochrome c*. Cytochrome c in the hippocampus (panel A) and cerebellum (panel B) at 3d ROSC, expressed as immunoblot density vs. actin. Values are mean ± SEM. Single-factor ANOVA P= 0.5 and P= 0.2, respectively.

Figure 9. *Hippocampal HIF-1α and EPO mRNA expression at 4h and 3d ROSC*. Panel A: Hippocampal HIF-1α expression at 4 h (hatched bar) and 3 d (dotted bar). Panel B: Hippocampal EPO expression at 4 h (hatched bar) and 3 d (dotted bar) Values are mean ± SEM, expressed in $2^{-\Delta\Delta Ct}$. Two-factor ANOVA, *post hoc* Holm-Sidak method. *: P< 0.05 4h vs. 3d.

Figure 10. *Glutathione peroxidase and reductase in the cerebellum*. Glutathione peroxidase (Panel A) and glutathione reductase (Panel B) activities in the cerebellum at 3d ROSC (P= 0.09 and P= 0.8, respectively). Enzyme activities are expressed as nmol/min/mg. Values are mean ± SEM.

Figure 11. *Glutathione reductase in the cerebellum*. Cerebellar glutathione reductase activities at 1h, 4h, and 3d ROSC, are expressed as nmol/min/mg protein. Mean values ± SEM. *: $P < 0.05$ between 1h and 3d; +: $P < 0.05$ between sham vs. CPR and sham vs. CPR+P in 1h protocol. ANOVA 2-factor for treatment and time, *post hoc* Holm-Sidak method.

Figure 12. *Purkinje cells count per high power field*. Number of Purkinje cells per high power field (100x objective) among sham (n=5), CPR (n=5), and CPR+P (n=4), expressed as average number of cells per field. +: $P < 0.05$ between sham vs. CPR; *: $P < 0.05$ between CPR vs. CPR+P. ANOVA single-factor, *post hoc* Holm-Sidak method.

Figure 13. *Neurocognitive function test*. Animals were placed in a separate room from housing for training. Distance (top) and time (bottom) that animals travel to the food source were recorded. Animals completed 5 trials to locate food at baseline, then another 5 trials 24 h after cardiac arrest. Values are mean ± SEM.

TABLES AND FIGURES

Group	24 h ROSC	48 h ROSC	72 h ROSC
Sham (n=5)	1 ± 0	1 ± 0	1 ± 0
Sham+P (n=3)	1 ± 0	1 ± 0	1 ± 0
CPR (n=11)	1 ± 0	1 ± 0	1 ± 0
CPR+P (n=10)	1 ± 0	1 ± 0	1 ± 0

Table 1. *Cerebral performance categories*. An adapted neurological evaluation, used clinically, was used to access function at 24 h, 24 h, and 48 h, scored between 1 (best) and 5 (worse). Data are means ± SEM.

	Baseline				24 h ROSC				48 h ROSC				72 h ROSC			
Categories	Sham	CPR	CPR+P	P	Sham	CPR	CPR+P	P	Sham	CPR	CPR+P	P	Sham	CPR	CPR+P	P
Total score	**57 ± 0**	**57 ± 0**	**57 ± 0**	**NS**	**56.0 ±0.6**	**55.3 ± 0.5**	**54.7± 1.0**	**NS**	**56.8 ± 0.1**	**56.7 ± 0.1**	**56.5 ±0.3**	**NS**	**56.9 ±0.1**	**56.7 ±0.2**	**56.9 ±0.0**	**NS**
Mental status	5 ± 0	5 ± 0	5 ± 0	NS	5 ± 0	5 ± 0	5 ± 0	NS	5 ± 0	5 ± 0	5 ± 0	NS	5 ± 0	5 ± 0	5 ± 0	NS
Limb posture	5 ± 0	5 ± 0	5 ± 0	NS	4.8 ±0.08	4.8 ±0.07	4.9 ± 0.1	NS	5 ± 0	4.9 ±0.06	4.9± 0.07	NS	5 ± 0	4.8 ±0.09	5 ± 0	NS
Gait	5 ± 0	5 ± 0	5 ± 0	NS	4.9 ±0.1	4.8 ± 0.1	4.8 ± 0.1	NS	4.9 ± 0.1	4.9 ± 0.1	5 ± 0	NS	5 ± 0	5 ± 0	5 ± 0	NS
Proprioception	3 ± 0	3 ± 0	3 ± 0	NS	3 ± 0	3 ± 0	3 ± 0	NS	3 ± 0	3 ± 0	3 ± 0	NS	3 ± 0	3 ± 0	3 ± 0	NS
Menace response	3 ± 0	3 ± 0	3 ± 0	NS	2.8	2.6 ±0.2	2.5 ± 0.3	NS	5 ± 0	2.9 ±0.08	2.9± 0.07	NS	5 ± 0	2.9 ±0.08	5 ± 0	NS
Pupil symmetry	5 ± 0	5 ± 0	5 ± 0	NS	5 ± 0	5 ± 0	5 ± 0	NS	5 ± 0	5 ± 0	4.9 ± 0.1	NS	5 ± 0	5 ± 0	5 ± 0	NS
Pupil size	5 ± 0	5 ± 0	5 ± 0	NS	5 ± 0	5 ± 0	5 ± 0	NS	5 ± 0	5 ± 0	5 ± 0	NS	5 ± 0	5 ± 0	5 ± 0	NS
Pupil light reflex	3 ± 0	3 ± 0	3 ± 0	NS	3 ± 0	3 ± 0	3 ± 0	NS	3 ± 0	3 ± 0	3 ± 0	NS	3 ± 0	3 ± 0	3 ± 0	NS
Facial sensation	5 ± 0	5 ± 0	5 ± 0	NS	5 ± 0	4.4 ±0.2	3.9 ± 0.6	NS	5 ± 0	5 ± 0	5 ± 0	NS	5 ± 0	5 ± 0	5 ± 0	NS
Ocular positioning	5 ± 0	5 ± 0	5 ± 0	NS	5 ± 0	5 ± 0	5 ± 0	NS	5 ± 0	5 ± 0	5 ± 0	NS	5 ± 0	5 ± 0	5 ± 0	NS
Nystagmus	5 ± 0	5 ± 0	5 ± 0	NS	5 ± 0	5 ± 0	5 ± 0	NS	5 ± 0	5 ± 0	5 ± 0	NS	5 ± 0	5 ± 0	5 ± 0	NS
Positional nystagmus	5 ± 0	5 ± 0	5 ± 0	NS	5 ± 0	4.9 ± 0.08	5 ± 0	NS	5 ± 0	5 ± 0	4.6 ± 0.4	NS	5 ± 0	5 ± 0	5 ± 0	NS
Palpebral reflex	3 ± 0	3 ± 0	3 ± 0	NS	3 ± 0	3 ± 0	3 ± 0	NS	3 ± 0	3 ± 0	3 ± 0	NS	3 ± 0	3 ± 0	3 ± 0	NS

Table 2. *Individual component of neurological scores*. Functions were examined and scored. Total and individual scores for each categories are reported, among Sham, CPR, CPR+P groups at baseline, 24 h ROSC, 48 h ROSC, and 72 h ROSC. NS: statistically non-significance.

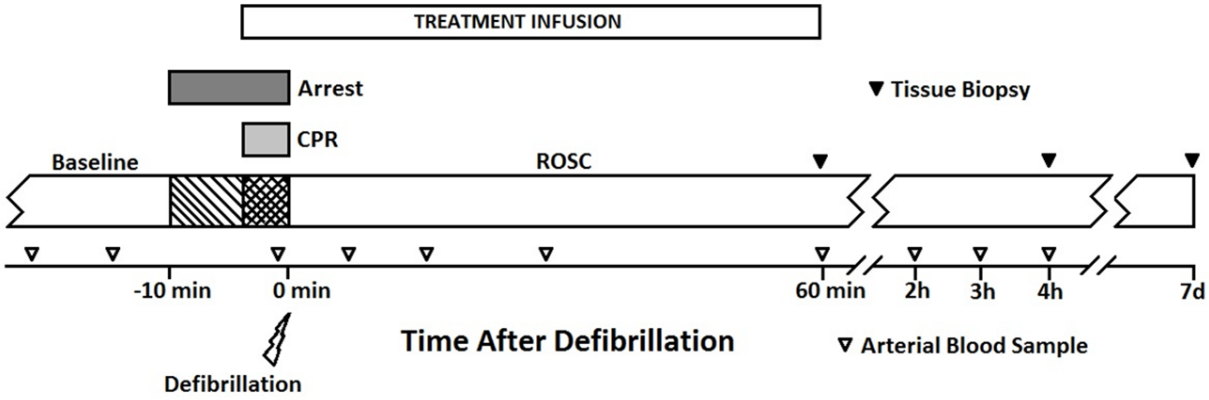

Figure 1. *Experimental timeline*. Cardiac arrest was induced by ventricular fibrillation. Cardiocerebral resuscitation was performed at 6-10 min arrest, and then transthoracic countershock were applied to restore sinus rhythm. Animal was recovered at 4h and euthanized at 3d post cardiac arrest. Open triangles: blood sampling at pre-arrest baseline and at 5, 15, 30, 60, 120, 180, and 240 min ROSC. Filled triangles: the animals were sacrificed and brain biopsies obtained at 1, 4, or 3d ROSC.

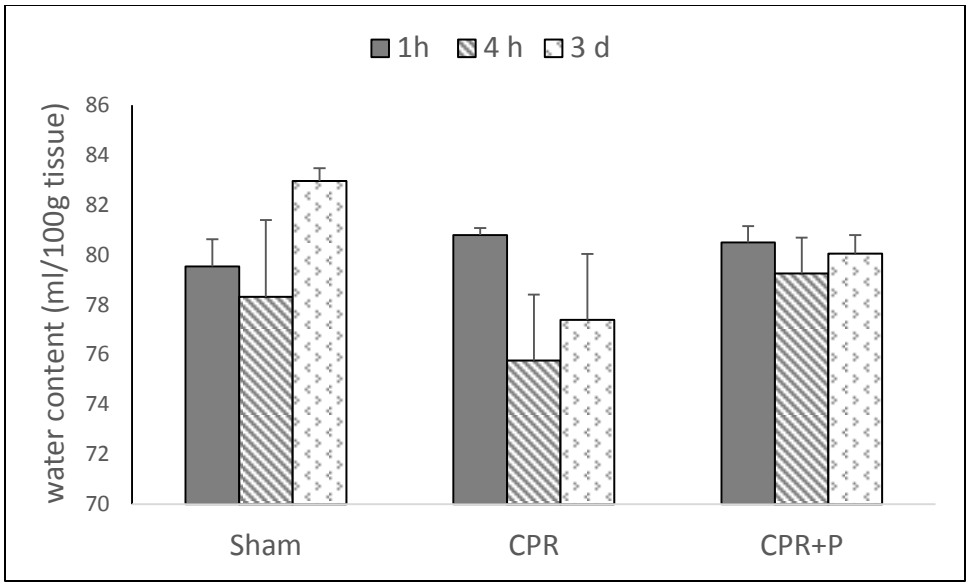

Figure 2. Cerebral water content (ml/100g tissue) at 1 h (filled bars), 4 h (hatched bars), and 3 d (dotted bars) ROSC. Values are mean ± SEM. Single-factor ANOVA: P= 0.38 (1 h), P= 0.5 (4 h), P= 0.25 (3 d). Two-factor ANOVA: P= 0.2 (time); P= 0.3 (treatment); P= 0.6 (time and treatment).

A 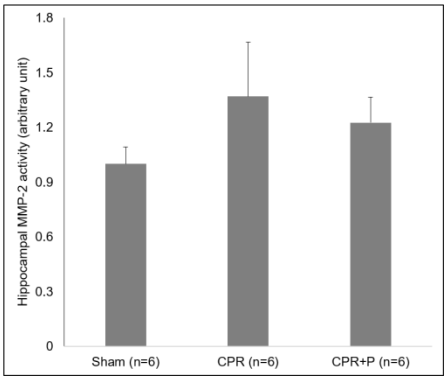
Hippocampal MMP-2 activity (arbitrary unit)
1.8
1.5
1.2
0.9
0.6
0.3
0
Sham (n=6)
CPR (n=6)
CPR+P (n=6)

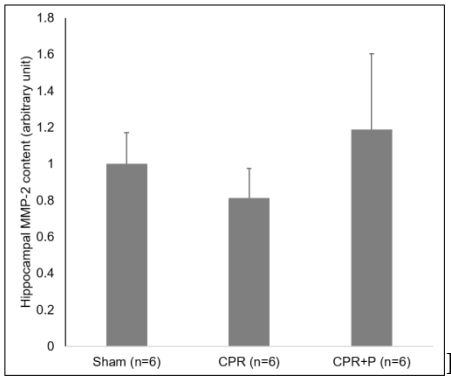
Hippocampal MMP-2 content (arbitrary unit)
1.8
1.6
1.4
1.2
1
0.8
0.6
0.4
0.2
0
Sham (n=6)
CPR (n=6)
CPR+P (n=6)
B

C 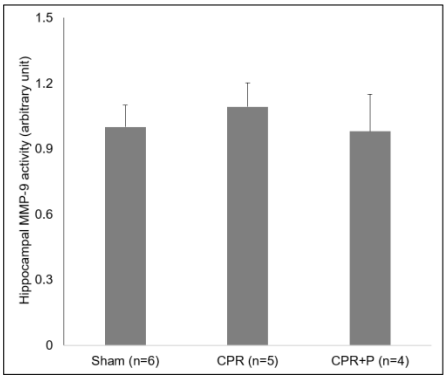
Hippocampal MMP-9 activity (arbitrary unit)
1.5
1.2
0.9
0.6
0.3
0
Sham (n=6)
CPR (n=5)
CPR+P (n=4)

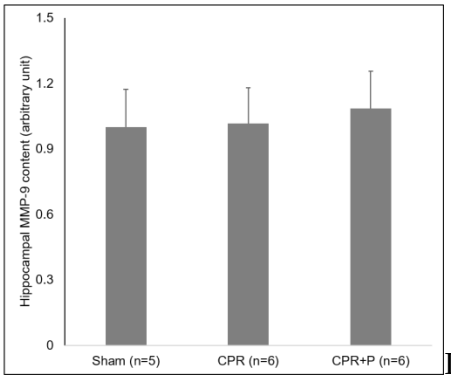
Hippocampal MMP-9 content (arbitrary unit)
1.5
1.2
0.9
0.6
0.3
0
Sham (n=5)
CPR (n=6)
CPR+P (n=6)
D

E 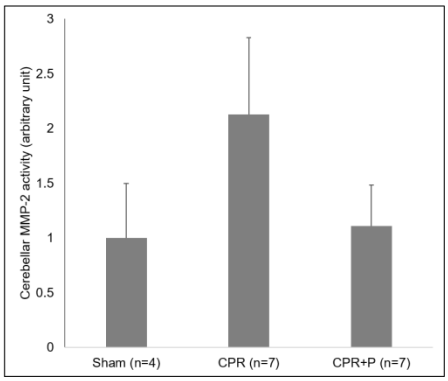
Cerebellar MMP-2 activity (arbitrary unit)
3
2.5
2
1.5
1
0.5
0
Sham (n=4)
CPR (n=7)
CPR+P (n=7)

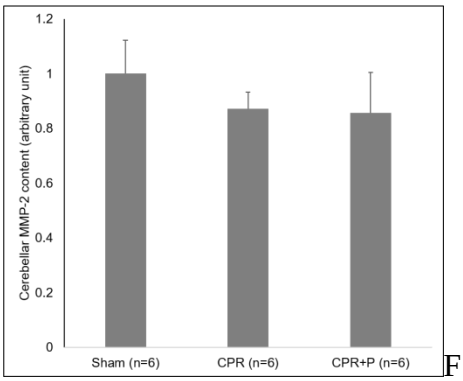
Cerebellar MMP-2 content (arbitrary unit)
1.2
1
0.8
0.6
0.4
0.2
0
Sham (n=6)
CPR (n=6)
CPR+P (n=6)
F

G 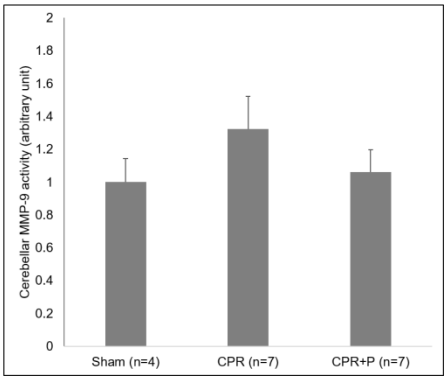
Cerebellar MMP-9 activity (arbitrary unit)
2
1.8
1.6
1.4
1.2
1
0.8
0.6
0.4
0.2
0
Sham (n=4)
CPR (n=7)
CPR+P (n=7)

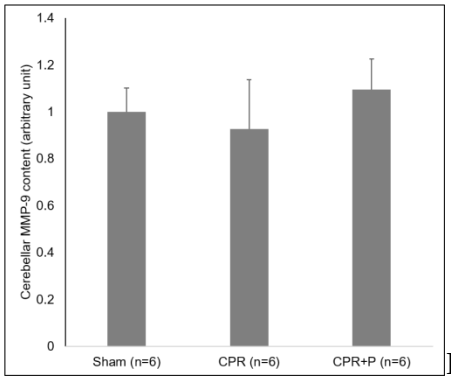
Cerebellar MMP-9 content (arbitrary unit)
1.4
1.2
1
0.8
0.6
0.4
0.2
0
Sham (n=6)
CPR (n=6)
CPR+P (n=6)
H

I 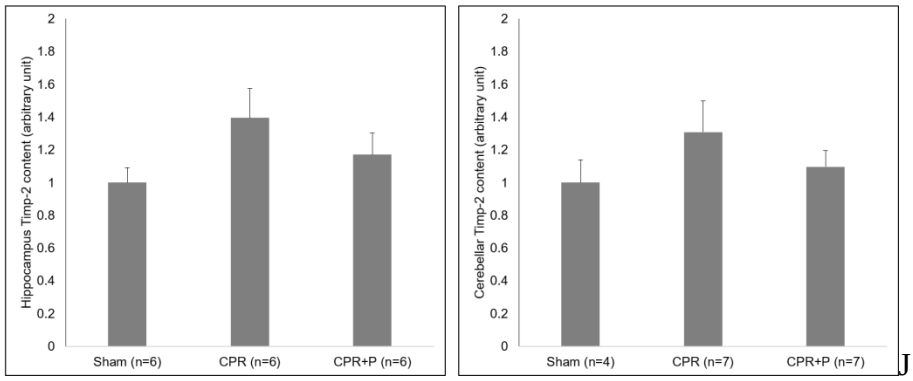

J

Figure 3. *Matrix metalloproteinases*. MMP-2 and MMP-9 activities and content. Panels A,B: Hippocampal MMP-2 activities and content (P= 0.4, P= 0.6). Panels C,D: hippocampal MMP-9 activity and content (P= 0.8; P= 0.6). Panels E,F: Cerebellar MMP-2 activity and content (P=0.4, P=0.6). Panels G,H: cerebellar MMP-9 activity and content (P= 0.3, P= 0.7). Panels I,J: hippocampal TIMP-2 content at 3d ROSC (left, P= 0.2), cerebellar TIMP-2 content at 3 d ROSC (right, P= 0.4). Values are mean $\pm$ SEM.

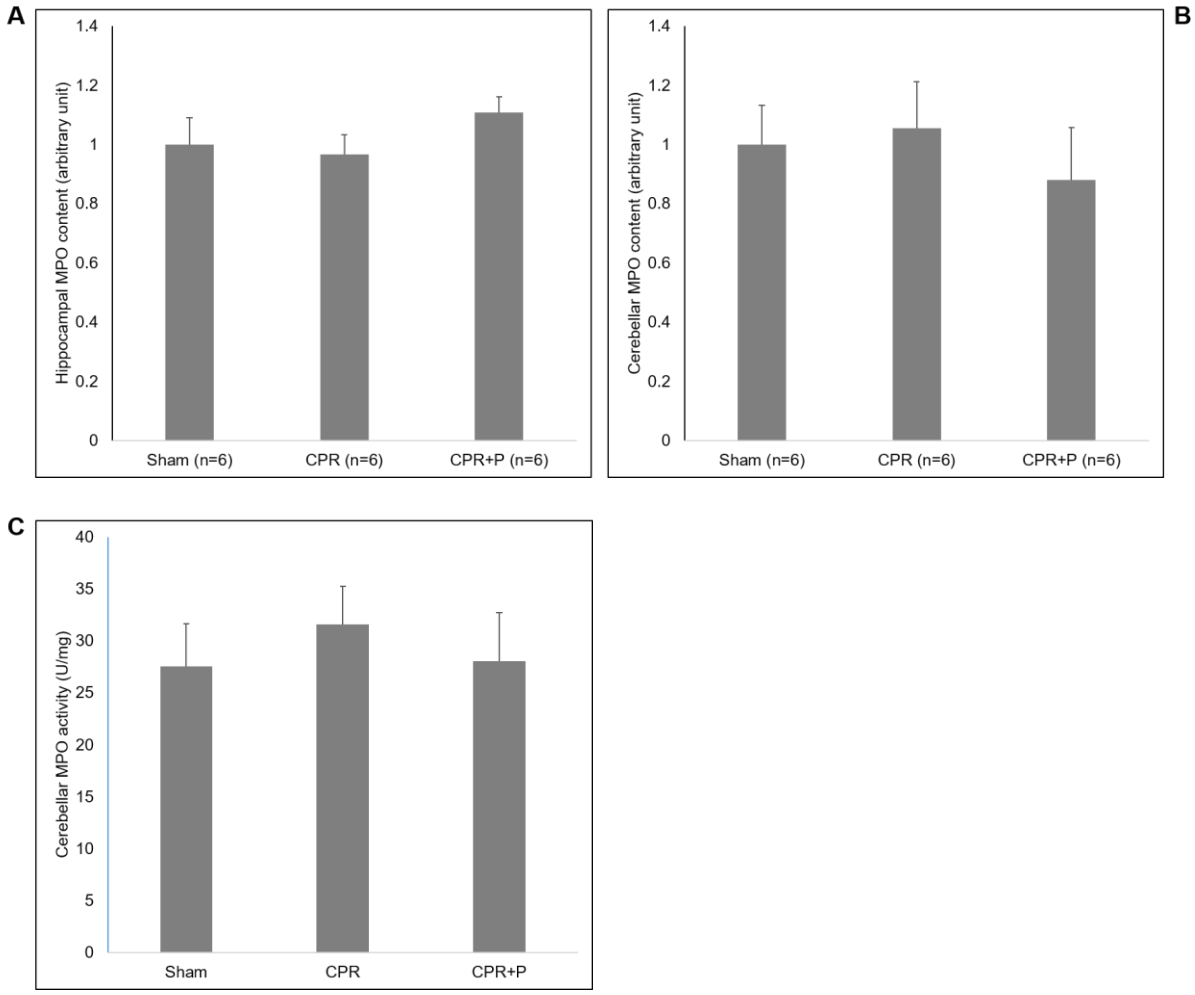

Figure 4. *Myeloperoxidase*. Hippocampal (Panel A) and cerebellar (Panel B) MPO contents, and cerebellar MPO activity (Panel C) at 3d ROSC, expressed as relative density against actin. Values are mean $\pm$ SEM. One-way ANOVA: Hippocampal MPO content: P=0.4; cerebellar MPO content: P= 0.7; cerebellar MPO activity: P= 0.7.

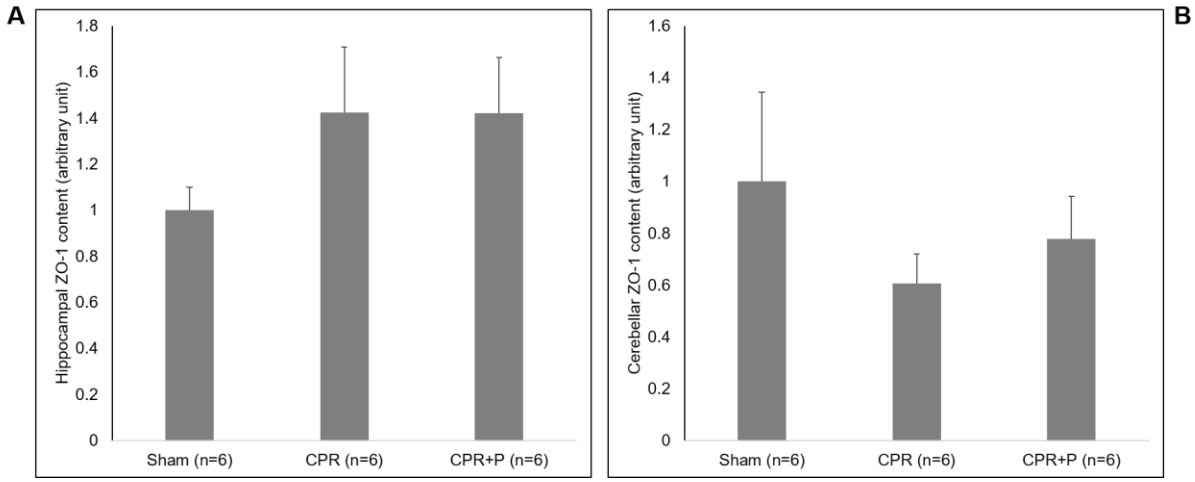

Figure 5. *Zona Occludens-1*. Hippocampal (Panel A) and cerebellar (Panel B) ZO-1 content at 3d ROSC, normalized to actin content. Values are mean ± SEM. Single-factor ANOVA: Hippocampus: P=0.3; cerebellum: P= 0.3.

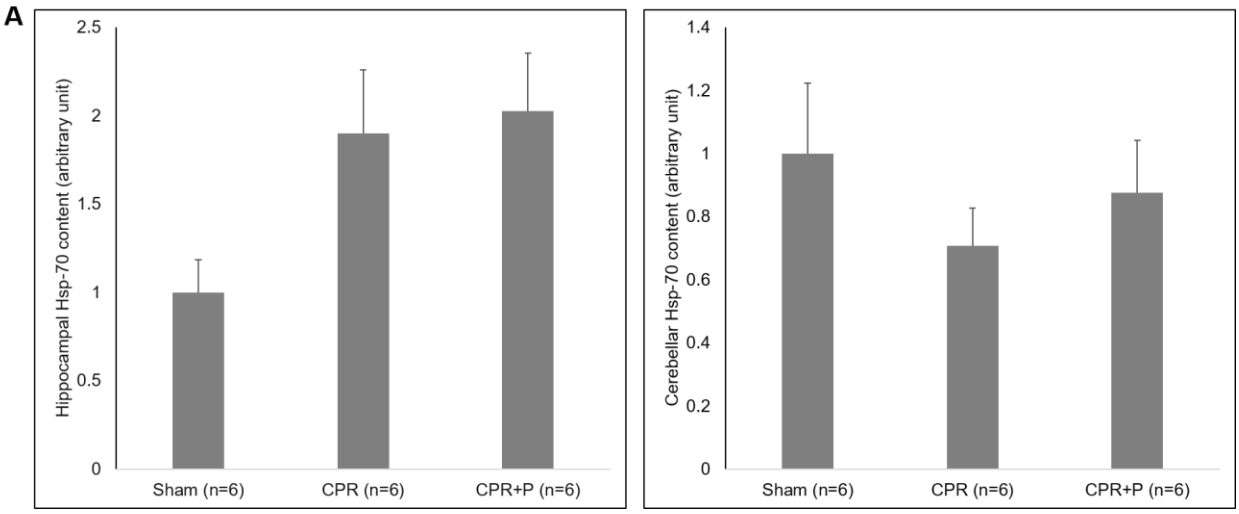

Figure 6. *Heat shock protein-70*. Hippocampal (Panel A) and cerebellar (Panel B) Hsp-70 contents at 3d ROSC, normalized to actin content. Values are mean ± SEM. Single-factor ANOVA: Hippocampus: P=0.056; cerebellum: P= 0.5.

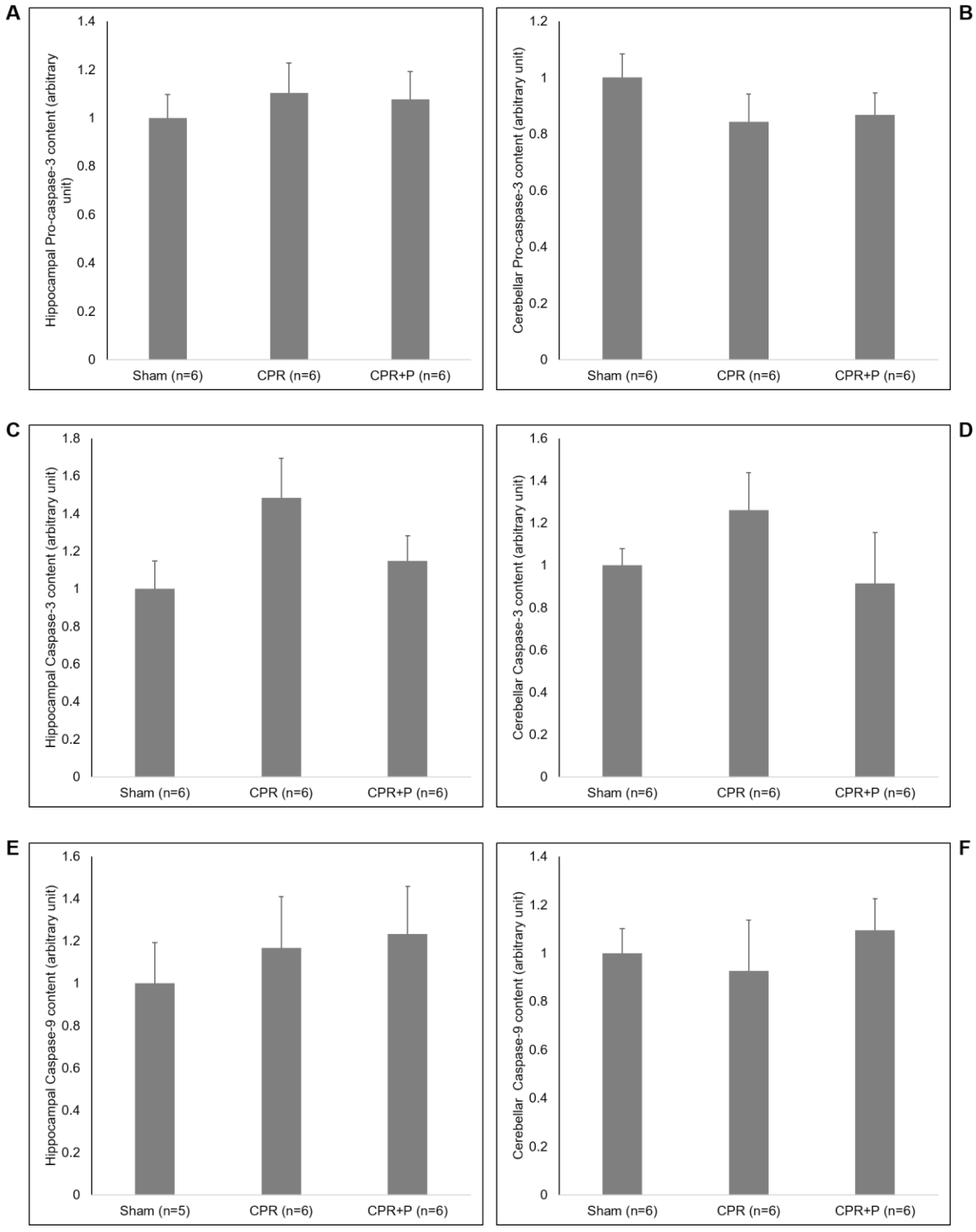

Figure 7. *Pro-apoptotic proteins 3 d after cardiac arrest-resuscitation*. Panels A, B: Procaspase-3: hippocampus (P= 0.8), cerebellum (P= 0.4); Panels C, D: Caspase-3: hippocampus (P= 0.14), cerebellum (P= 0.4); Panel D, E: Caspase-9: hippocampus (P= 0.8), cerebellum (P= 0.3) (P= 0.4 (left) and P= 0.37 (right), expressed in relative density against actin. Values are mean $\pm$ SEM.

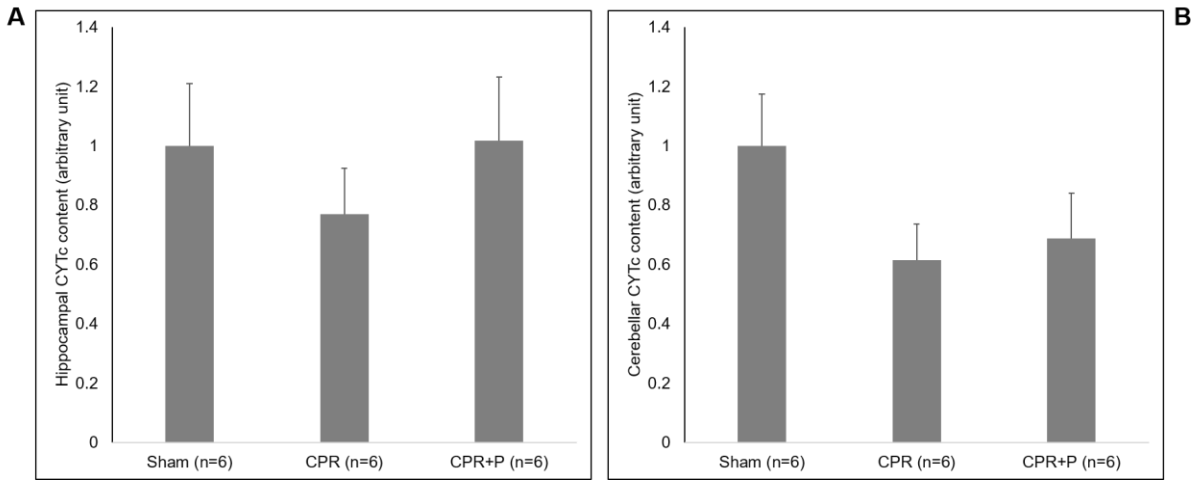

Figure 8. *Cytochrome c*. Cytochrome c in the hippocampus (panel A) and cerebellum (panel B) at 3d ROSC, expressed as immunoblot density vs. actin. Values are mean ± SEM. Single-factor ANOVA P= 0.5 and P= 0.2, respectively.

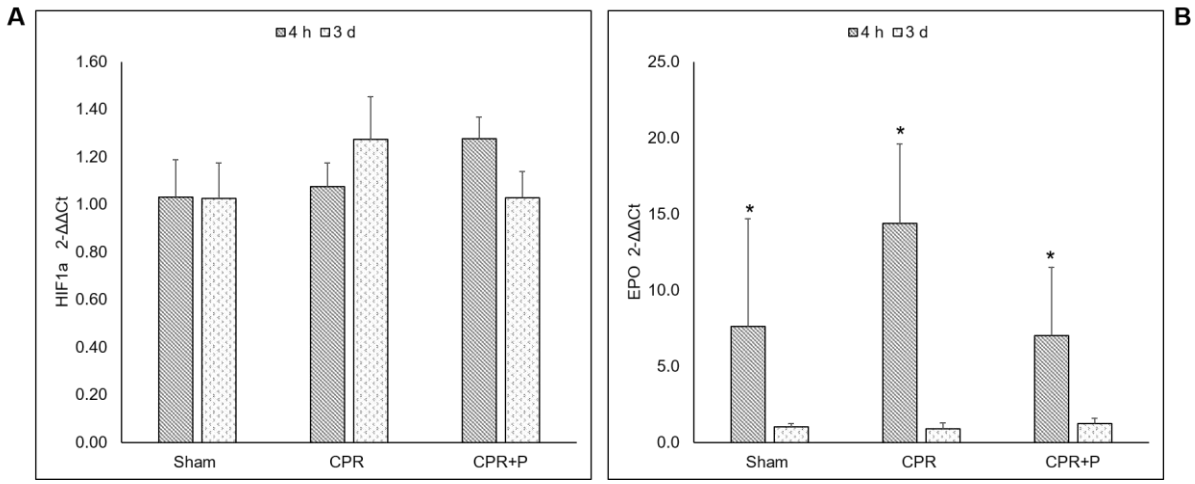

Figure 9. *Hippocampal HIF-1α and EPO mRNA expression at 4h and 3d ROSC*. Panel A: Hippocampal HIF-1α expression at 4 h (hatched bar) and 3 d (dotted bar). Panel B: Hippocampal EPO expression at 4 h (hatched bar) and 3 d (dotted bar) Values are mean ± SEM, expressed in $2^{-\Delta\Delta Ct}$. Two-factor ANOVA, *post hoc* Holm-Sidak method. *: P< 0.05 4h vs. 3d.

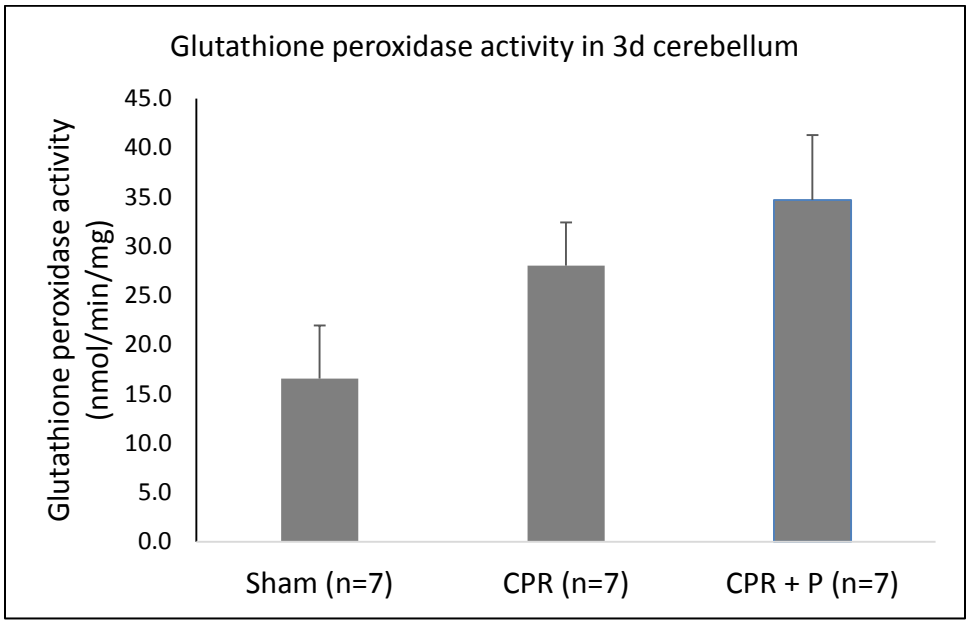

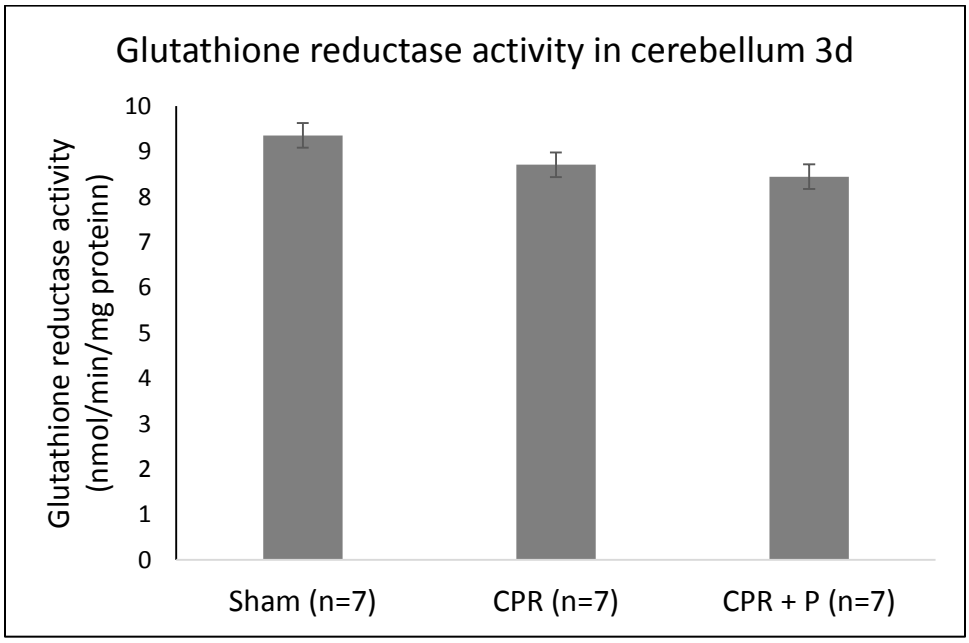

Figure 10. *Glutathione peroxidase and reductase in the cerebellum*. Glutathione peroxidase (Panel A) and glutathione reductase (Panel B) activities in the cerebellum at 3d ROSC (P= 0.09 and P= 0.8, respectively). Enzyme activities are expressed as nmol/min/mg. Values are mean ± SEM.

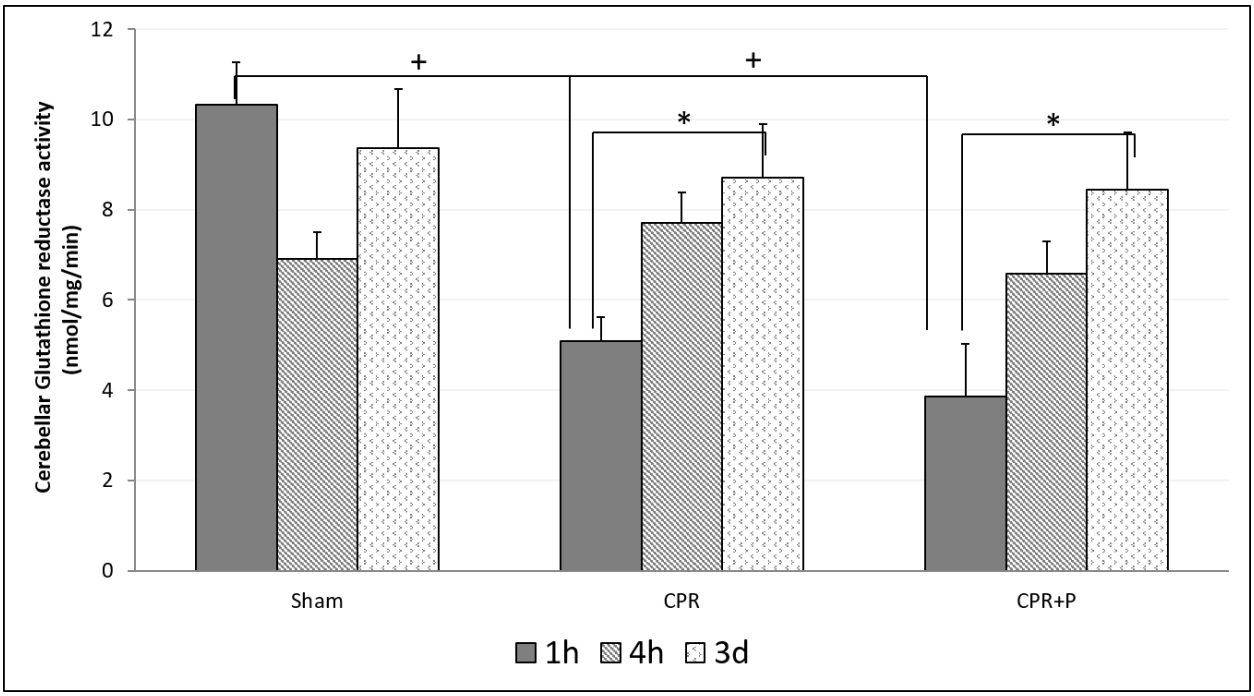

Figure 11. *Glutathione reductase in the cerebellum*. Cerebellar glutathione reductase activities at 1h, 4h, and 3d ROSC, are expressed as nmol/min/mg protein. Mean values ± SEM. *: P <0.05 between 1h and 3d; +: P <0.05 between sham vs. CPR and sham vs. CPR+P in 1h protocol. ANOVA 2-factor for treatment and time, *post hoc* Holm-Sidak method.

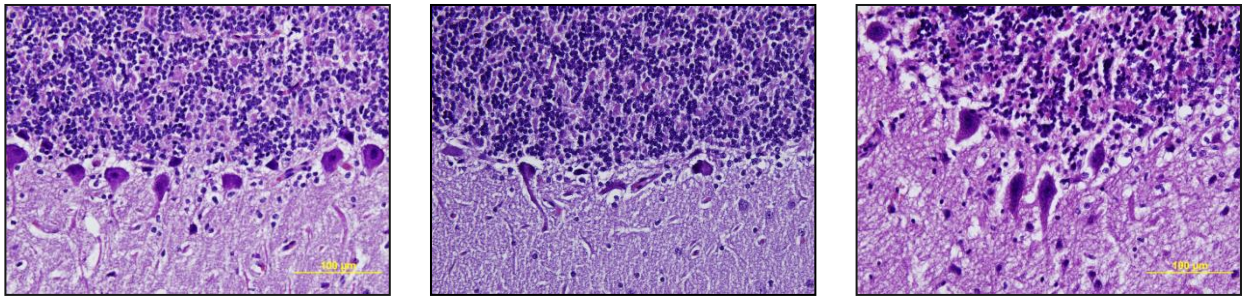

Sham CPR CPR + P

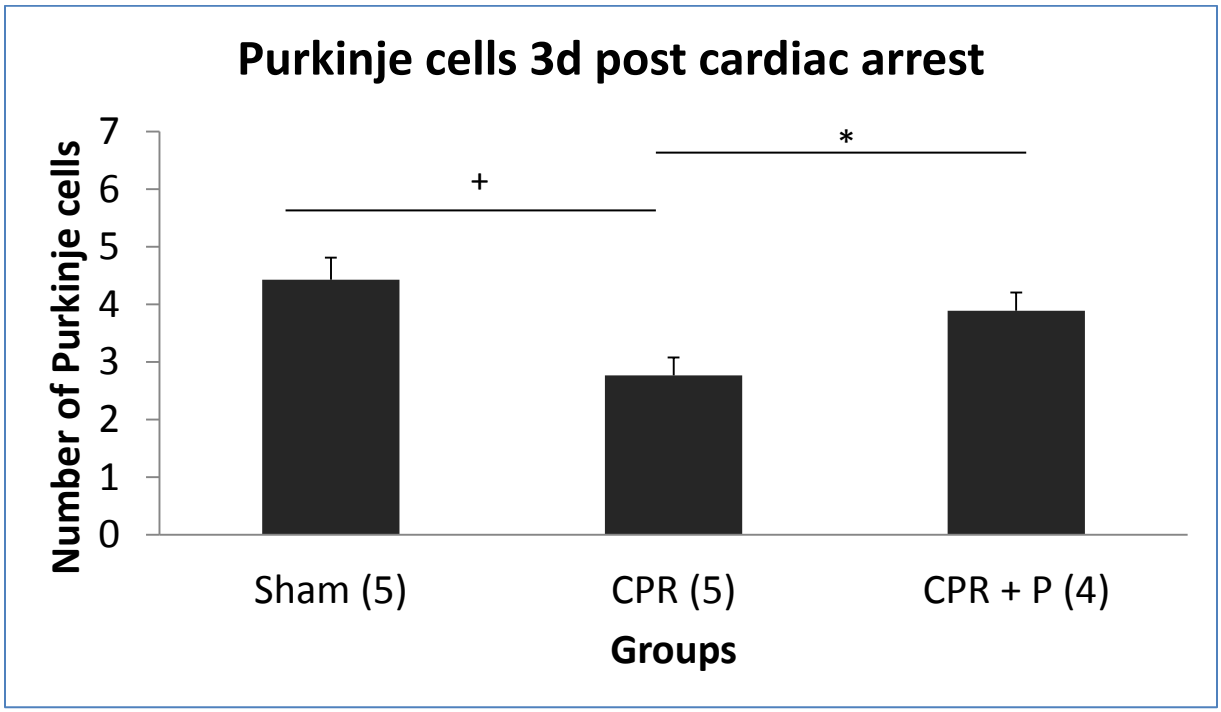

Figure 12. *Purkinje cells count per high power field*. Number of Purkinje cells per high power field (100x objective) among Sham (n=5), CPR (n=5), and CPR+P (n=4), expressed as average number of cells per field. +: P <0.05 between sham vs. CPR; *: P< 0.05 between CPR vs. CPR+P. ANOVA single-factor, *post hoc* Holm-Sidak method.

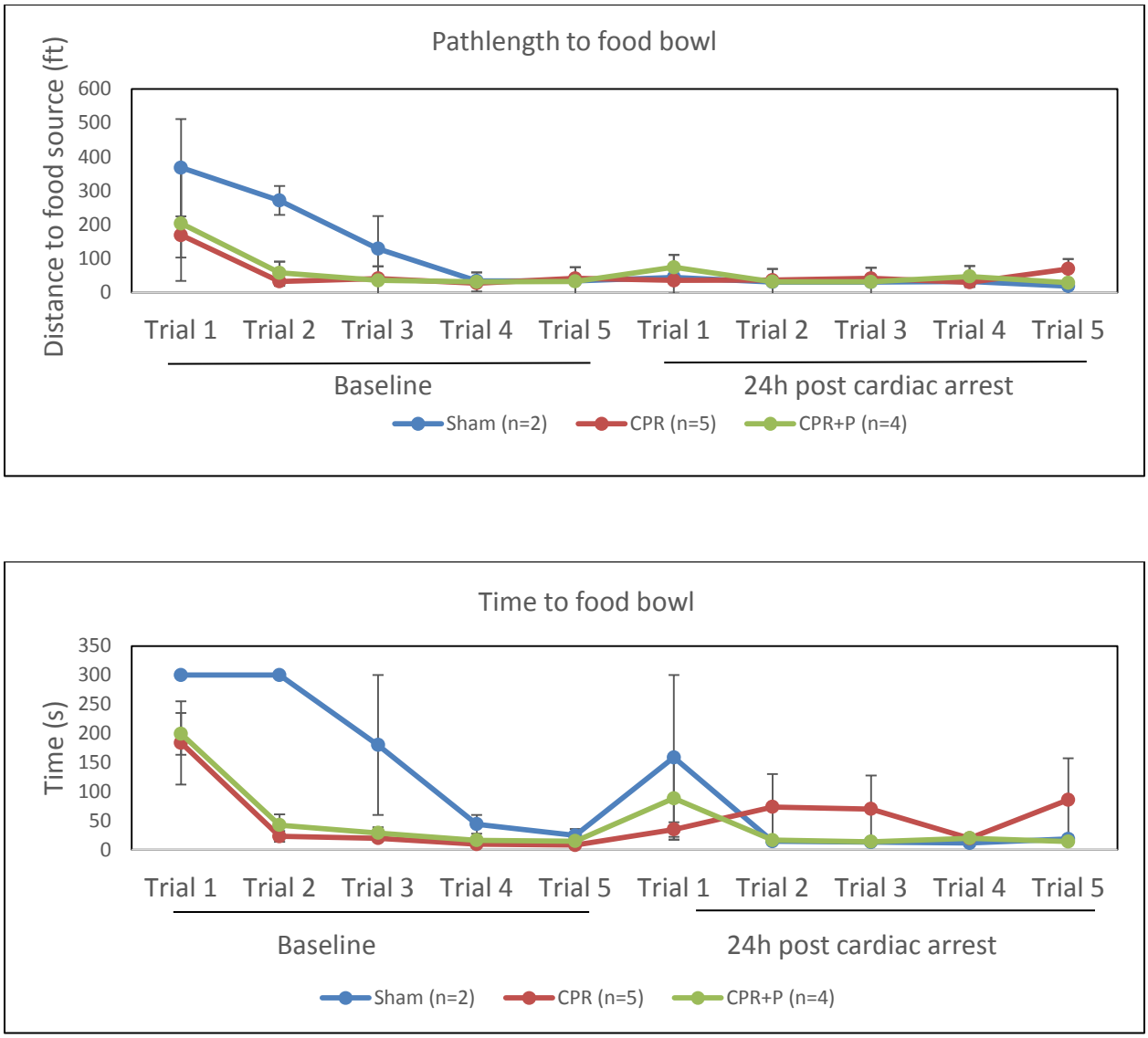

Figure 13. *Neurocognitive function test*. Animals were placed in a separate room from housing for training. Distance (top) and time (bottom) that animals travel to the food source were recorded. Animals completed 5 trials to locate food at baseline, then another 5 trials 24 h after cardiac arrest. Values are mean ± SEM.

Chapter IV

IMPACT OF CARDIAC ARREST AND CARDIOCEREBRAL RESUSCITATION ON HEMODYNAMICS AND NEUROPROTECTIVE MECHANISMS IN SWINE

Anh Q. Nguyen[1], Myoung-Gwi Ryou[3], Roger A. Hollrah[1], Gary F. Scott[4], Arthur G. Williams Jr.[1], Albert H. Olivencia-Yurvati[1,2], Robert T. Mallet[1,2]

[1]Institute of Cardiovascular and Metabolic Diseases and [2]Department of Surgery, Univ. North Texas Health Science Center, Fort Worth, TX; [3]Department of Medical Laboratory Sciences, Tarleton State Univ., Fort Worth, TX; [4]Department of Science, Wiley College, Marshall, TX

Address for Correspondence:

Robert T. Mallet, Ph.D.

Department of Integrative Physiology

University of North Texas Health Science Center

3500 Camp Bowie Boulevard

Fort Worth, TX 76107-2699 USA

Telephone: 817-735-2260

Fax: 817-735-5084

Email: robert.mallet@unthsc.edu

ABSTRACT

Recovery from cardiac arrest depends on many factors, including duration of cardiac arrest, timely delivery and quality of cardiocerebral resuscitation (CCR). Despite improvements in clinical outcomes from cardiac arrest as a result of therapeutic hypothermia, survival is still dismal. Additional interventions to be used alone or in combination with therapeutic hypothermia that can be administered readily to cardiac arrest victims could potentially save many lives. Pyruvate, a metabolic intermediate in mammalian cells, has been proven to be neuroprotective when acutely administered *iv*. The neuroprotective capabilities and mechanism of pyruvate were examined in domestic swine subjected to 10 min pre-intervention cardiac arrest and 4 min CCR, delivered by precordial compressions followed by defibrillatory countershocks. After ROSC was achieved, animals were recovered for 4 h. Sodium pyruvate (CPR+P group) was infused *iv* to produce circulatory pyruvate concentration of 3.5 mM during CCR and the first 60 min ROSC; controlled received equimolar NaCl infusion (CPR+NaCl group). Brain biopsies were collected to examine the effects of global ischemia and pyruvate treatment on the brain metabolism. At 4h ROSC, hippocampal activities of the oxyradical-sensitive enzyme aconitase decreased in cardiac arrest vs. sham control pigs. Matrix metalloproteinase-2 (MMP-2) activity were lowered with cardiac arrest vs. sham control in both hippocampus and cerebellum. Furthermore, cerebellar erythropoietin (EPO) content markedly declined following cardiac arrest group vs. sham control, and pyruvate treatment did not restore EPO content. There was no appreciable change in pro-apoptotic proteases in the hippocampus and cerebellum at 4 h ROSC. In conclusion, cardiac arrest-resuscitation resulted decreased hippocampal and brain MMP-2 activities and cerebellar EPO at 4 h ROSC. Pyruvate infusion did not produce appreciable

difference vs. NaCl-treated pigs. Pharmacological intervention restoring MMP-2 activity and EPO content merit investigations.

Key words: cardiac arrest, cardiopulmonary resuscitation, cardiocerebral resuscitation, apoptosis, erythropoietin, pyruvate, matrix metalloproteinase

Abbreviations: ANOVA: analysis of variance; ATP: adenosine triphosphate; ADP: adenosine diphosphate; AMP: adenosine monophosphate; BBB: blood-brain barrier; CA1: *cornus ammonis* region 1 of hippocampus; CPR: cardiopulmonary resuscitation; CCR: Cardiocerebral resuscitation; CYTc: cytochrome c; ECG: electrocardiogram; EPO: Erythropoietin; GAPDH: glyceraldehyde-3 phosphate dehydrogenase; HIF-1α: hypoxia inducible factor-1α; MAP: mean aortic pressure; MMP: matrix metalloproteinase; MPO: myeloperoxidase; ROSC: recovery of spontaneous circulation; ZO-1: zona occludens-1

INTRODUCTION

Survival and neurological recovery from cardiac arrest-resuscitation is critically dependent on effective resuscitation, including forceful chest compression and timely application of defibrillatory countershocks (Y et al., 2002; Pierce et al., 2015; Yannopoulos et al., 2015). In a study of 200 out-of-hospital cardiac arrest victims for whom early defibrillation resources were available, the time from 911 call to administration of 1^{st} shock is significantly less (5.7 ± 1.6 min) compared to non-survivors (6.6 ± 1.5) (Bunch et al., 2003). However, even initially successful resuscitation and restoration of effective brain perfusion initiates massive production of reactive oxygen species which damages vulnerable cellular components, including biomolecules and organelles, thereby exacerbating brain injury (Holger and Tobias, 2011). Another factor that adversely impacts cardiac arrest outcome is the lethal postcardiac arrest syndrome, which typically presents at 4-24 h after initial resuscitation and embodies a constellation of physiological derangements including cardiogenic shock, neurological dysfunction, and multiple organ failure(Mongardon, 2011).

Pyruvate infusion during the first hour following 6-min untreated cardiac arrest stabilizes blood pressure and arterial electrolytes (Cherry et al., 2015). In an *in vitro* preparation model of oxidative damage, exposure of isolated hearts to H_2O_2 results in impaired contractile performance and inactivation of aconitase and glyceraldehyde 3-phosphate dehydrogenase (GAPDH). Aconitase and GAPDH spontaneously recovered during H_2O_2 wash-out. Pyruvate treatment restored contractile performance and unexpectedly inhibited GAPDH (Mallet et al., 2002). On the other hand, pyruvate treatment during reperfusion potentiates β-adrenergic responses in stunned guinea-pig myocardium (Tejero-Taldo et al., 1998) and in an *in vitro* preparation of human myocardium (Hermann et al., 2002).

In a swine model of 6 min untreated cardiac arrest and 4 min CCR, at 3 d ROSC, both hippocampus and cerebellum did not show appreciable inflammatory responses including activities of matrix metalloproteinases and myeloperoxidase, and neurological recovery was essentially complete. The full neurological recovery and the absence of inflammation or metabolic derangements left scant opportunity for further improvement by pyruvate. In order to examine the effect of cardiac arrest on brain inflammation, and pyruvate's putative anti-inflammatory effects, in the current study, cardiac arrest was extended to 10 min. A second objective was to examine the effect of pyruvate when its administration was delayed until 1-2h ROSC, thereby modeling the scenario of initiating intravenous treatment after the victim's arrival at the emergency department.

MATERIALS AND METHODS

Surgical preparation

This preclinical study was designed to elucidate the impact of cardiac arrest and cardiocerebral resuscitation (CCR) on injury in ischemia-susceptible brain regions, and whether intravenous pyruvate treatment mitigates this damage. All animal care, surgery, and experimental procedures were conducted in accordance with the National Research Council's *Guide for the Care and Use of Laboratory Animals*, and were approved by the University of North Texas Health Science Center Institutional Animal Care and Use Committee, protocol # 2012/13-29-A10.

Surgical preparation and cardiac arrest protocol were conducted as previously described (Cherry et al., 2015). Yorkshire swine (25 kg – 35kg) were anesthetized with *im* 5.56 mg/kg Telazol (Tiletamine HCl and zolazepam HCl, NADA 106-111) and 1.11 mg/kg Anased (xylazine, NADA 139-236) cocktail. The surgical anesthetic plane was maintained by continuous administration of 1-3% isoflurane (Isothesia, NDC 11695-6776-2, Narkovet Delux Anesthesia System) in oxygen. Animals were mechanically ventilated (MDS Matrx, Model 3000) at a tidal volume of 12-15 ml/kg, 12 – 16 cycles/min to keep end tidal PCO_2 at 35 - 40 mmHg. Core temperature was monitored with a rectal probe. A catheter was introduced into the right jugular vein and a pacing wire was advanced via this catheter into the right ventricle. The catheter also was used for treatment solution administration. A retrograde catheter was inserted rostrally to measure the jugular venous pressure and to collect venous blood. The left femoral artery and vein were cannulated for blood pressure monitoring and medication/fluid administration, respectively.

Cardiac arrest protocol

Cardiac arrest was induced by passing a train of 60–70V, 4 Hz electrical impulses to the right ventricular endocardium. Mechanical ventilation was then suspended and the pacing wire withdrawn. At 9 min of cardiac arrest, 10 mEq of $NaHCO_3$ was injected into the femoral vein. Treatments were infused from 9.5 min of cardiac arrest until 60 min after recovery of spontaneous circulation (ROSC). Precordial chest compressions were delivered at 10 to 14 min arrest at the rate of 100-110 compressions/min at a depth of approximately 2 inches. 0.167 to 0.267 U/kg vasopressin (Pitressin, 20 units/ml, NDC 42023-117-25) was bolus-injected into the jugular catheter at 1 min CCR to provide vasoconstrictor support during CPR. The defibrillation protocol was begun at 14 min arrest, it consisted of single countershocks at 30 s intervals with intervening CCR until ROSC was achieved, following this sequence: 1-3 200J countershocks, then 1-3 300 J countershocks, then 1-3 360J countershocks. If ROSC could not be achieved after countershocks, a rescue dose of epinephrine was administered before the next shock. Experiment was terminated if spontaneous cardiac rhythm was not restored by the 9^{th} countershock. The ventilator was reconnected and 1 ml lidocaine (20mg/ml) was given as soon as ROSC was confirmed by spontaneous recovery of arterial pressure and the presence of discernable electromechanical rhythm. The depth and frequency of ventilator cycles were adjusted to keep end-tidal P_{CO2} between 35-45 mmHg. Mean blood pressure was maintained at a minimum of 70mmHg by administering intravenous phenylephrine (phenylephrine HCl, 10 mg/ml, NDC 66758-017-01), diluted to 0.2 mg/ml in normal saline (Braun, NDC 0264-7800-20). Arterial and venous blood was sampled at: baseline (before cardiac arrest and after completion of surgery), and at 5, 15, 30, 60, 120, 180, and 240 ROSC, and immediately analyzed in a blood gas laboratory (Instrumentation Laboratory, GEM Premier 3000). Partial pressures of O_2 and CO_2,

and pH of arterial samples informed ongoing management of these variables. 10 ml of blood was centrifuged at 7500 rpm for 10 min to sediment formed elements, and then plasma was aliquoted in 1.5 ml centrifuge tubes, flash frozen in liquid nitrogen, and stored at -80^{o}C for future analysis.

Another set of experiments was conducted to test the effect of pyruvate when its administration was delayed until 1-2 h ROSC. Pyruvate solution was prepared and infused at the same rate as above. Blood sampling and euthanization followed the same timeline as described above.

At 4 h ROSC, the animals were euthanized and tissues were biopsied. The thoracic cavity was accessed by an incision in the left 5th or 6th intercostal space. The pericardium was incised, exposing the heart. To sacrifice the anesthetized animal, 60V direct current was applied to the left ventricle epicardium to induce ventricular fibrillation. The descending aorta was cross-clamped. A 0.5 cm incision was made in the ascending aorta, approximately 2 cm rostral to the clamp, for insertion of a catheter to deliver perfusion fluid to the brain. Ice-cold (4^{o}C) 0.9% NaCl + heparin sulfate (1000U/L) was delivered via peristatic pump at a rate of 1 ml/g tissue/minute for 10 min. Afterwards, the brain was exposed by craniotomy, dissected, and biopsies were excised. Other organs were biopsied in sequence: left and right ventricles, left and right lungs, kidney, and liver. Brain was further dissected to sample frontal and temporal cortex, hippocampus, cerebellum, pons, and medulla. Excised tissues were freeze-clamped with aluminum blocks precooled in liquid N_2 and were stored at -80^{o}C (Thermo Scientific) for biochemical analysis, or fixed in 10% formalin for paraffin embedding.

Protein extraction

Frozen tissues were pulverized with precooled mortar and pestle under liquid N_2. 100 mg powder was then added to a tube containing 1 ml of phosphate buffer (0.1M KH_2PO_4) and 5 µl protease inhibitor (Sigma-Aldrich, P8340) and then homogenized for 1 min at 4^oC using a Teflon piston. The suspension was then centrifuged at 25,000 rpm at 4^oC for 20 min (Thermo Scientific Ultracentrifuge). The supernatant was saved and the pellet was re-suspended in 0.4 ml of phosphate buffer, and again homogenized and centrifuged. The supernatants were combined, aliquoted, and stored at -80^oC.

Protein concentrations in the extracts were measured using Bradford reagent (Sigma-Aldrich, B6916). A standard curve was constructed with sequential dilutions of bovine serum albumin in ddH_2O (Thermo Scientific, Cat# 23209), diluted in ddH_2O to concentration of 0.25 mg/ml to 2 mg/ml. 5µl of samples and 250 µl Bradford reagent were combined in each well on a 96-well plate, which was then incubated for 30 min at room temperature. Absorbance was read at wavelength 595 nm using a spectrophotometer plate reader (Bio-Tek).

Immunoblotting

Running gel (10% SDS-PAGE) and 4% stacking gel were casted. Tissue extracts were electrophoretically separated using the Mini-PROTEAN Tetra cell system (BioRad, Cat#1658001EDU) with the following ingredients: Acrylamide/Bis solution 37.5:1 (BioRad, Cat#1610158), 1.5M Tris: pH 8.8 (BioRad, Cat#1610798), SDS (BioRad, Cat#1610418), ammonium persulfate (BioRad, Cat#161-0700), and Temed (BioRad, Cat#161-0800). Precision Plus Protein All blue Standards (BioRad, Cat# 161-0373) were utilized for molecular mass (kDa)

reference. 30 µg of proteins were loaded into each well and were separated by size and charge at 100V for 100 min in Tris/Glycine/SDS (BioRad, cat# 161-0772).

After electrophoresis, proteins were transferred electrophoretically overnight at 30V in 4^{o}C Tris/Glycine solution (BioRad, Cat# 161-0771) onto nitrocellulose membranes. Complete transfer was confirmed by Ponceau S staining of the membrane (Sigma-Aldrich, Cat#P7170). he membrane was incubated with 5% non-fat milk (Bio-Rad, Cat#1706404XTU) at room temperature for 1 h to block non-specific binding, and then exposed to primary antibodies overnight at 4^{o}C. Appropriate secondary antibodies (1:5000 dilution) were applied at room temperature for 1 h. In order to visualize protein bands, the membrane was first incubated with chemiluminescent substrate (Thermo Scientific, Cat#PI34080). X-ray films of membranes were taken using an imaging system (Thermo Scientific). Densitometry was performed with the AlphaEaseFC (Alpha Innotech) digital program.

Primary and secondary antibodies were purchased from commercial vendors: β-actin (Genscript, Cat# A00702), HIF-1α (Santa Cruz, Cat# Sc-10790), zona occludens-1 (Santa Cruz, Cat# Sc-10804), erythropoietin (Santa Cruz, Cat# Sc-7956), MMP-2 (Santa Cruz, Cat# Sc6838), cytochrome c (Novus, Cat# NB100-56503), caspase-3 (Bioss, Cat# Bs-0081R), caspase-9 (Biovision, Cat# 3016-100). Secondary antibodies included donkey anti-goat horseradish peroxidase (HRP), goat anti-rabbit HRP, and goat anti-mouse HRP (Jackson Immuno Research, Cat# 705-035-0003, 111-035-003, and 115-001-003, respectively).

Gelatin zymography of matrix metalloproteinases

Matrix metalloproteinase-2 and -9 (Gelatinase) activities were examined by gelatin zymography as previously described (Frankowski et al., 2012). Briefly, 8% SDS-PAGE with 0.1% gelatin was casted, and extracts (30 µg protein) were run at 100V in 4^{o}C buffer solution for

3 h. The gel was washed in 2.5% TritonX-100 buffer (50 mM Tris-HCl-pH 7.5, 5mM $CaCl_2$, 1 µM $ZnCl_2$) at 37^oC for 48 hours to activate MMP proteins. Gels were stained with Coomassie Blue solution (0.25% Coomassie Blue, 45% methanol, 10% acetic acid) for 1-2 h, and destained in 30% methanol, 10% acetic acid for 30 minutes, or until clear bands were revealed. The destained gel was scanned with a digital scanner with grayscale setting for photography.

Brain water content

Brain edema was assessed indirectly from the difference between wet weight and dry weight of brain tissue, a measure of tissue water content. Approximately 1 cm^3 of cerebral and cerebellar tissue was collected in glass jars and weighed. The jars were placed in a dry oven and the tissue desiccated at 110^oC overnight, and then re-weighed.

Plasma pyruvate concentration measurement

Flash-frozen plasma samples were placed on ice and allowed to thaw slowly. Plasma proteins were precipitated by combining thawed plasma with 1 volume of Solution A (1M $HClO_4$ and 2mM EDTA), and then centrifuged at 10,000 rpm for 5 minutes at 4^oC to removed denatured protein precipitate. To neutralize and precipitate the $HClO_4$, 400 µl supernatant was added to 122 µl of solution B (2M KOH + 0.3M MOPS), chilled on ice for 30 min, and centrifuged again to sediment the $KClO_4$ precipitate. Pyruvate was measured in the supernatant.

Plasma pyruvate was measured with a UV-VIS spectrophotometric assay previously described (Bergmeyer et al., 1983; Passonneau et al., 1993). In this assay, the reduction of pyruvate to lactate is stoichiometrically coupled to the oxidation of NADH to NAD^+, monitored as the decrease in absorbance at 339 nm. Lactate dehydrogenase is added to trigger the reaction. The change of absorbance is proportional to the pyruvate concentration in the reaction medium.

$$\text{Pyruvate} + \text{NADH} + \text{H}^+ \overset{lactate\ dehydrogenase}{\Longleftrightarrow} \text{lactate} + \text{NAD}^+$$

Enzyme activity assays in tissue

Aconitase and glyceraldehyde-3-phosphate dehydrogenase (GAPDH) activities were measured by spectrophotometric assay following the linear change in absorbance at 340 nm at 37^{o}C for 30 min according to an established colorimetric method (Bergmeyer et al., 1983) using a UV spectrophotometer (Shimadzu, UV-1800). In the aconitase assay, the aconitase reaction, which converts citrate to isocitrate, is coupled to the reduction of NAD^+ to NADH by isocitrate dehydrogenase. The rate of reduction of NAD^+ to NADH, monitored at 340 nm, is proportional to rate of isocitrate formation, which is directly proportional to aconitase activity.

$$\text{Citrate} \xrightarrow{aconitase,\text{Fe2+}} \text{Isocitrate}$$

$$\text{Isocitrate} + \text{NAD}^+ \xrightarrow{Isocitrate\ dehydrogenase} \alpha\text{-ketoglutarate} + \text{CO}_2 + \text{NADH} + \text{H}^+$$

The GAPDH assay monitors the reduction of NAD^+ to NADH in the presence of excess concentration of glyceraldehyde 3-phosphate and inorganic phosphate. The rate of increase in absorbance at 340 nm is proportional to GAPDH-catalyzed conversion of glyceraldehyde 3-phosphate to 1,2-*bis*phosphoglycerate.

$$\text{Glyceraldehyde-3-phosphate} + \text{PO}_4^{3-} + \text{NAD}^+ \xrightarrow{GAPDH} \text{1,3-}bis\text{phosphoglycerate} + \text{NADH} + \text{H}^+$$

One unit of enzyme activity was defined as amount of enzyme required to catalyze the conversion of 1 µmol of substrate to product per minute. Enzyme activities are expressed per mg of protein.

Statistical analysis

Data are expressed as mean values $\pm$ standard error of mean (SEM). Single factor (treatment) analysis of variance (ANOVA) was used to compare enzyme activities and

immunoblot values among groups. An appropriate *post-hoc* test was applied to identify statistically treatment effects. Two-factor ANOVA (time, treatment) with repeated measures on time and appropriate *post hoc* tests were applied to analyze hemodynamics variable, and plasma chemistry values. P values < 0.05 were required to reject the null hypothesis. Statistical analysis was performed using Sigma Stat 3.5 (Systat Software, Inc.).

RESULTS

Hemodynamics

Body weight, mean aortic pressure, core temperature, and arterial hemoglobin O_2 saturation (SpO_2) did not differ among non-arrested sham, NaCl-infused cardiac arrest CCR (CPR), and pyruvate-infused cardiac arrest CCR (CPR+P) groups at baseline, or at 1h, 4h ROSC. Heart rates were similar among the groups at baseline as expected. However, at 1h ROSC, heart rates in NaCl-treated animals were appreciably higher than those of the pyruvate-treated and Sham pigs. However, by 4h ROSC, heart rates in the post-arrest pigs that earlier received NaCl or sodium pyruvate infusions were similar and no longer differed significantly from those of non-arrested sham groups (Table 1).

At the onset of ROSC, arterial pressure increased abruptly, due at least in part to the increased circulatory catecholamines released in response to the cardiac arrest, and the lingering effects of the powerful vasoconstrictor, vasopressin. As these neurohormones cleared, arterial pressure fell, indicating cardiac dysfunction ("stunning") resulting from the ischemic stress imposed by cardiac arrest. Intravenous infusion of the α-adrenergic agonist phenylephrine was initiated at 15-30 min ROSC to maintain mean arterial pressure at $\geq$ 70 mmHg, and thereby, stabilize organ perfusion. The total phenylephrine dosage required to maintain arterial pressure was significantly lower in pyruvate-treated vs. NaCl-treated pigs. A similar trend toward decreased phenylephrine requirement was observed when pyruvate treatment was delayed until 1 h ROSC, although the Dunn's *post-hoc* pairwise analysis did not detect statistical significance ($P > 0.05$) (Figure 2).

Plasma pyruvate concentration

When pyruvate was infused *iv* during chest compressions and the first 60 min ROSC, its arterial plasma concentration increased to 3.6 $\pm$ 0.3 mM at 5 min ROSC, and stabilized at 3-4 mM until the infusion was discontinued (Figure 3A). Arterial pyruvate concentration subsided over the remaining 3 h ROSC (Figure 3A). Jugular venous pyruvate concentration followed a similar time course, peaking at 5' ROSC (2.80 $\pm$ 0.27 mM) and remaining elevated throughout pyruvate infusion (Figure 3B). An arteriovenous decrease in pyruvate was evident throughout pyruvate infusion, indicating net uptake of the compound by the head and neck region.

Brain water content

There were no significant differences in the cerebral or cerebellar water contents among the different treatment groups at 4h ROSC, even when pyruvate infusion was delayed until 1-2 h ROSC (CPR+DP group) (P= 0.07 and P= 0.8, respectively) (Figure 4). Brain edema often results from inflammation, although it may not be fully manifested until 24 h after the ischemic insult (Mellergard et al., 1989; Bareyre et al., 1997). Therefore, the similar brain water contents among the post-arrest groups and the non-arrested sham group was not unexpected at 4 h ROSC.

Aconitase and GAPDH activities

Cardiac arrest-resuscitation imposes oxidative stress that may inactivate metabolic enzymes. The catalytic activities of two well-recognized oxyradical targets, aconitase and glyceraldehyde 3-phosphate dehydrogenase (GAPDH), were assessed in brain at 4 h ROSC. In the hippocampus, cardiac arrest produced a significant decrease in aconitase activity vs. sham (Figure 5A). Neither cardiac arrest nor pyruvate treatment altered aconitase activity in cerebellum. Interestingly, aconitase activity in the hippocampus was markedly lower than the cerebellum in all 3 groups ($P< 0.001$).

Hippocampal and cerebellar GAPDH activities were not significantly different among sham or the NaCl-treated (P= 0.4) and pyruvate treated (P=0.8) cardiac arrest groups. As in the case of aconitase, GAPDH activity was appreciably less in the hippocampus than the cerebellum (Figure 5B).

Arterial and venous blood gas and chemistry

Cardiac arrest produced the expected acid-base disturbances. Arterial pH fell from 7.44 $\pm$ 0.04 at baseline to 7.14 $\pm$ 0.04 at 5 min ROSC. Pyruvate treatment hastened subsequent recovery of arterial pH to baseline by 1 h ROSC while sustained acidemia was evident up to 4 h ROSC in the NaCl-infused cardiac arrest group (Figure 6A). As expected, jugular venous pH was slightly below the corresponding arterial values in all 3 groups. Pyruvate treatment restored venous pH to that of the sham animals.

Cardiac arrest produced robust increases in systemic arterial and jugular venous pCO_2, lasting up to 4 h ROSC (Figure 7). Meanwhile, there were no statistical differences in arterial pO_2 among the groups. Venous pO_2 was significantly lower in both cardiac groups vs. sham, from 30 min through 4 h ROSC (Figure 8), indicating the expected O_2 uptake as brain metabolism recovered from cardiac arrest.

Cardiac arrest induces arterial and jugular venous hypernatremia, first evident at 15 min ROSC and lasting up to 4 h ROSC. Pyruvate treatment suppressed this hypernatremia (Figure 9). Cardiac arrest produced a transitory hyperkalemia, which resolved by 15 min ROSC in both the NaCl and pyruvate groups (Figure 10). Calcium, in both arterial and venous, decreased with cardiac arrest compared to sham up to 3 h ROSC (Figure 11).

Systemic arterial and jugular venous glucose concentrations increased during cardiac arrest-resuscitation, an effect that persisted until 1 h ROSC (Figure 12). Both arterial and venous lactate appreciably increased with cardiac arrest and remained elevated up to 3 h ROSC. Pyruvate treatment is associated with significantly higher lactate concentrations than NaCl (Figure 13), reflecting the expected conversion of some of the pyruvate to lactate by circulating lactate dehydrogenase. Arterial and venous lactate/pyruvate ratios also increase with cardiac arrest, lasting until 30 min ROSC (Figure 14). Pyruvate treatment lowered the lactate/pyruvate ratios, as expected.

Arterial and venous $NaHCO_3$ fell with cardiac arrest, indicating the expected metabolic acidosis resulting from the global ischemia insult. Pyruvate infusion quietly restored plasma HCO_3^-, while HCO_3^- concentration remained below the sham values in the NaCl-infused post-CCR group (Figure 15).

Inflammation after cardiac arrest-resuscitation

At 4h ROSC, cardiac arrest was associated with decreased hippocampal MMP-2 activity, particularly with pyruvate treatment ($P< 0.05$), and MMP-2 protein content followed a similar trend (Figure 16 A). Cerebellar MMP-2 activity was lower in NaCl vs. pyruvate treated group ($P< 0.05$). Cerebellar MMP-2 content was similar in the NaCl and pyruvate treatment groups, yet cardiac arrest with NaCl treatment produced a statistically significant reduction in cerebellar MMP-2 content vs. sham (Figure 16B).

Zona occludens-1, a structural component of the tight junction complex, is crucial to maintain the integrity of the blood-brain barrier (BBB). In rats subjected to 2 h of unilateral middle cerebral artery occlusion, ZO-1 expression and content decreased by 3 h reperfusion, and

loss of continuous ZO-1 distribution was observed, indicating BBB compromise (Jiao et al., 2011). In this study, the effect of cardiac arrest on ZO-1 protein was examined at 4 h ROSC. There were no appreciable changes in ZO-1 content in the hippocampus and cerebellum as a result of cardiac arrest-resuscitation or pyruvate treatment (Figure 17).

Next, the effect of cardiac arrest-resuscitation on HIF-1α/EPO, a cellular defense mechanism against oxidative stress, was studied. Cardiac arrest-resuscitation and pyruvate treatment did not alter HIF-1α content in the cerebellum and hippocampus (Figure 18 A and C). Hippocampal EPO content did not change at 4 h ROSC in cardiac arrest-resuscitated animals vs. sham control (Figure 18B). Interestingly, cardiac arrest lowered cerebellar erythropoietin (EPO) content, regardless of treatment (Figure 18D).

Pro-apoptotic markers were also examined. Cytochrome c (CYTc), a protein abundant in the mitochondrial intermembrane space, is released into the cytoplasm when cells are under oxidative stress and initiates the mitochondrial apoptosis pathway involving sequential activation of caspase-9 and caspase-3. Hippocampal CYTc tended to increase after cardiac arrest, and pyruvate treatment dampened this effect, although the differences were not statistically significant ($P= 0.09$). There were no differences in CYCc content in the cerebellum at 4 h ROSC (Figure 19). Pro-apoptotic proteases, pro-caspase-3 ($P= 0.6$) and caspase-3 ($P= 0.4$) were unaltered by cardiac arrest or treatment in the cerebellum (Figure 20 A and B). Neither pro-caspase-9 ($P= 0.07$) nor caspase-9 ($P= 0.15$) contents differed among NaCl-treated and pyruvate-treated cardiac arrest animals vs. sham control.

DISCUSSION

Effect of cardiac arrest and pyruvate treatment on hemodynamics

Cardiac arrest leads to hemodynamics and electrolyte derangements (Chazan et al, 1968; Cherry et al, 2015). Acute metabolic acidosis impairs cardiac contractility, decreasing cardiac output (Kraut and Madias, 2010). In this study, pyruvate treatment restored arterial pH by 60 min ROSC vs. NaCl-infused control. Timely recovery of pH afforded by pyruvate treatment could potentially increase cardiac performance and thus, cerebral perfusion. In support of this scenario, pyruvate treatment lowered the amount of vasoconstrictor phyenylephrine required to maintain arterial pressure.

Persistent elevation of plasma lactate concentration is associated with unfavorable outcomes in cardiac arrest (Mullner et al., 1997). However, lactate is a neuronal energy source and is preferentially oxidized when lactate and glucose are present in anesthetized rat (Wyss et al., 2011). Utilization of lactate as an energy source for brain was demonstrated in humans suffering from traumatic brain injury (Glenn et al., 2015). Therefore, transient elevation of plasma lactate during the first 3 h ROSC as a result of pyruvate treatment may be advantageous to the brain. On the other hand, lactate/pyruvate ratio, reflecting cytoplasmic NADH/NAD^+, is a more accurate measure of oxido-reduction state. Under hypoxia, lactate/pyruvate ratio increases, correlating with higher NADH/NAD^+ (Debray et al., 2007), whereas increased cytosolic pyruvate is correlated with lower NADH/NAD^+ via the lactate dehydrogenase equilibrium (Veech et al., 1979). In this study, both arterial and venous lactate/pyruvate fell with pyruvate infusion vs. sham and NaCl-treated cardiac arrest-resuscitation control, partly due to increased plasma pyruvate concentration. Pyruvate treatment during cardiac arrest stabilizes blood pressure

and potentiates myocardial contractility and thus, may protect the brain by maintaining cerebral perfusion pressure after resuscitation.

Effect of cardiac arrest on brain glycolytic enzyme activities

Enzyme activities, including glycolytic glyceraldehyde-3-phosphate (GAPDH) and aconitase of the Krebs cycle, were investigated in the myocardium in dogs suffered from cardiac arrest (Sharma et al., 2006). While no change in GAPDH was detected up to 3 h ROSC, aconitase activity fell with cardiac arrest but recovered by the end of chest compression and maintained through 3 h ROSC. ROS induced aconitase dysfunction is associated with neurodegenerative diseases, including Alzheimer's and Parkinson's (Marcus et al., 1998; Liang et al., 2004). Its inactivation by H_2O_2 in rat primary cell culture was associated with increased neuronal death (Cantu et al., 2009). Here we demonstrated aconitase inactivation in an acute setting, which may contribute to energy depletion that may compromise post-arrest recovery of brain function. However, pyruvate treatment did not preserve aconitase activity at 4 h ROSC.

Besides its well-recognized glycolytic function, GAPDH contributes to with tRNA transport, DNA replication and DNA repair (Meyer-Siegler et al., 1991; Singh and Green, 1993). GAPDH nuclear translocation was associated with increased neuronal cell death (Sawa et al., 1997). In rats subjected to 2 h of middle cerebral artery occlusion, increased GAPDH positive neurons were observed in the ischemic brain region vs. the non-ischemic hemisphere; moreover, double staining revealed co-localization of nuclear GAPDH and TUNEL in the ischemic penumbra 48 h after reperfusion, indicating active cellular apoptosis (Tanaka et al., 2002). In this study, GAPDH activity was unaltered at 4 h ROSC in the hippocampus and cerebellum. Stability of GAPDH activity was not unexpected, as similar result was detected in the myocardium

(Sharma et al., 2006). Immunohistochemistry to visualize intracellular GAPDH location would be necessary to demonstrate a role of GAPDH translocation in brain injury inflicted by cardiac arrest-resuscitation.

Cardiac arrest affects brain inflammation and EPO

Cardiac arrest lowered MMP-2 activities in the hippocampus and cerebellum at 4 h ROSC. Gelatinases, including MMP-2 and MMP-9, have been implicated in ischemia-reperfusion injury and there activation is correlated with worse neurological outcome in many experimental models (Kurzepa et al, 2014; Aoki et al, 2002; Rosnell 2006). Moreover, MMP-2 gene variants were studied in in 546 stroke patients, and certain MMP-2 alleles were found to be associated with better functional outcome at 3 months after ischemic stroke (Manso et al., 2010). On the other hand, EPO has been shown to decrease neuronal apoptosis. In mice, transgenic over- expression of human EPO in brain decreased infarct volume by 84%, diminished edema, and ameliorated neurological deficit following 90 min of middle cerebral artery occlusion with 24 h reperfusion (Kilic et al., 2005).

In an *in vitro* preparation of co-culturing neural progenitor cells and vascular endothelial cells, recombinant human EPO activated secretion of MMP-2 and MMP-9 by endothelial cells, resulting in more robust progenitor cell migration (Wang et al., 2006). In the current study, the decrease in cerebellar MMP-2 activity may be associated with the lower EPO content. This result suggests potential opportunities for treatment intervention that increase EPO content and MMP-2 activities, thereby fostering brain recovery from ischemia-reperfusion injuries.

In conclusion, at 4 h ROSC after 10 min untreated cardiac arrest and 4 min CCR, hippocampal aconitase activity fell appreciably in pyruvate-treated and NaCl-infused cardiac

arrest groups vs. sham control. MMP-2 activities fell in the hippocampus and cerebellum, and Cerebellar EPO content was appreciably reduced vs. sham control. Pyruvate treatment did not alter hippocampal MMP-2 activity or cerebellar EPO content vs. NaCl-infused control at 4 h ROSC.

LIMITATION

With longer duration of untreated cardiac arrest, recovery of animal to longer time period, such as 3 d, was not optimal due to ethical concern and limited financial and human resources. Therefore, we were unable to study prolonged neurological recovery in this group of animals. Ischemia-reperfusion injury from cardiac arrest-resuscitation has been correlated with subtle neurological impairments and may not be fully manifested until later in life. In a study of 200 patients who suffered from out-of-hospital cardiac arrest where early defibrillation resources were available, at 5-year follow-up, one-third of survivors filled out SF-36 score, a survey emphasized on quality of life, and there was no significant difference compared to the U.S. general population except for decrease vitality score- a measurement of the extent one feels tired or worn out (Bunch, 2003). In another study extending to 6 month after hospital discharge, quality of life was assessed with the Health Utilities Index mark 3, which described health as a utility score on a scale from perfect (score=1) to death (score=0). In these patients, the mean time between collapse and initiation of CCR was 2.2 $\pm$ 2.6 min. Health Utilities Index was higher among patients who had a shorter duration of resuscitation (less than 2 min) than those resuscitated for 3-10 min, and the score is worse than those of the general population, though most claimed to have acceptable health-related quality of life (Nichol, 1999). Another study in patients who had intrahospital cardiac arrest or a myocardial infarction (MI), showed that among cardiac arrest survivors, 30% suffered from anxiety, 15% depression, and 19% post-traumatic stress disorder; while the proportions of these disorders were lower in the post is post-MI patients (O'Reilly et al, 2004). Assessing subtle changes in neurological functions, as described above, is challenging in animal models.

REFERENCES

Aoki T, Sumii T, Mori T, Wang X, Lo EH. Blood-brain barrier disruption and matrix metalloproteinase-9 expression during reperfusion injury. *Stroke* 2002; **33**: 2711 – 2717.

Bareyre F, Wahl F, McIntosh TK, Stutzmann JM. Time course of cerebral edema after traumatic brain injury in rats: effects of riluzole and mannitol. *J Neurotrauma* 1997; **14**(11): 839 – 849.

Bunch TJ, White RD, Gersh BJ, Meverden RA, Hodge DO, Ballman KV, Hammill SC, Shen WK, Packer DL. Long-term outcome of out-of-hospital cardiac arrest after successful early defibrillation. *N Engl J Med* 2003; **348**:2626-2633.

Cantu D, Schaack J, Patel M. Oxidative Inactivation of Mitochondrial Aconitase Results in Iron and H_2O_2-Mediated Neurotoxicity in Rat Primary Mesencephalic Cultures. PLOS 2009; http://dx.doi.org/10.1371/journal.pone.0007095.

Chazan JA, Stenson R, Kurland GS. The acidosis of cardiac arrest. *N Engl J Med* 1968**; 278**: 360 – 364.

Cherry BH, Nguyen AQ, Hollrah RA, Williams AG Jr, Hoxha B, Olivencia-Yurvati AH, Mallet RT. Pyruvate stabilizes electrocardiographic and hemodynamic function in pigs recovering from cardiac arrest. *Exp Biol Med* 2015 Dec; **240**(12):1774-84.

Cherry BH, Nguyen AQ, Hollrah RA, Olivencia-Yurvati AH, Mallet RT. Modeling cardiac arrest and resuscitation in the domestic pig. *World J Crit Care Med.* 2015; **4**(1):1 – 12.

Cousins TR, O'Donnell JM. Arterial cannulation: A critical review. AANA Journal 2004; 72(4): 267 – 271.

Debray FG, Mithell GA, Allard P, Robinson BH, Hanley JA, Lambert M. Diagnostic accuracy of blood lactate-to-pyruvate molar ratio in the differential diagnosis of congenital lactic acidosis. *Clinical Chemistry* 2007; **53**(5): 916 – 921.

Glenn, T.C., N. A. Martin, D. A. Hovda, P. Vespa, M. A. Horning, D. L. MacArthur, and G.A. Brooks. Lactate: Brain Fuel following Traumatic Brain Injury. *J Neurotrauma* 2015; **32**: 820-382.

Hermann HP, Zeitz O, Lehnart SE, Keweloh B, Datz N, Hasenfuss G, Janssen PM. Potentiation of beta-adrenergic inotropic response by pyruvate in failing human myocardium. *Cardiovasc Res.* 2002; **53**(1): 116 – 23.

Holger KE and Tobias E. Ischemia and reperfusion- from mechanism to translation. Nat Med. 2011 Nov 7; 17(11): 10.1038/nm.2507.

Jiao H, wang Z, Liu Y, Wang P, Xue Y. Specific role of tight junction proteins claudin-5, occluding, and ZO-1 of the blood-brain barrier in a focal cerebral ischemic insult. *J Mol Neurosci* 2011; **44**: 130 – 139.

Kilic E, Kilic U, Soliz J, Claudio BL, Gassmann M, Hermann DM. Brain-derived erythropoietin protects from focal cerebral ischemia by dual activation of ERK-1/-2 and Akt pathways. *The FASEB Journal* 2005; Vol. **19**: 2026 – 2028.

Kraut JA and Madias NE. Metabolic acidosis: pathophysiology, diagnosis and management. Nature Reviews Nephrology 2010; 6: 274 – 285.

Kurzepa J, Kurzepa J, Golab P, Czerska S, Bielewicz. The significance of matrix metalloproteinase (MMP)-2 and MMP-9 in the ischemic stroke. *International Journal of Neuroscience* 2014; **124** (10): 1 – 10.

Liang LP, Patel M. Iron-sulfur enzyme mediated mitochondrial superoxide toxicity in experimental Parkinson's disease. *J Neurochem* 2004; **90**: 1076–1084.

Mallet RT, Sun J, Knott EM, Sharma AB, Olivencia-Yurvati AH. Metabolic cardioprotection by pyruvate: recent progress. *Exp Biol Med* 2005 Jul; **230**(7):435-43.

Mallet RT, Squires JE, Bhatia S, Sun J. Pyruvate restores contractile function and antioxidant defenses of hydrogen peroxide-challenged myocardium. *J Mol Cell Cardiol.* 2002 Sep; **34**(9):1173-84.

Mallet RT. Pyruvate: metabolic protector of cardiac performance. *Proc Soc Exp Biol Med*. 2000; **223**:136–148.

Manso H, Krug T, Sobral J, Albergaria I, Gaspar G, Ferro JM, Oliveira SA, Vicente AM. Variants of the matrix metalloproteinase-2 but not the matrix metalloproteinase-9 gene significantly influence functional outcome after stroke. BMC Medical Genetics 2010; 11: 1-9.

Marcus DL, Thomas C, Rodriguez C, Simberkoff K, Tsai JS, et al. Increased peroxidation and reduced antioxidant enzyme activity in Alzheimer's disease. Exp Neurol 1998; 150: 40–44.

Mellergard P, Bengtsson F, Smith ML, Riesenfeld V, Siiesjo BK. Time course of early brain edema following reversible forebrain ischemia in rats. *Stroke* 1989; **20**(11): 1565 – 1570.

Meyer-Siegler K, Mauro DJ, Seal G, Wurzer J, Deriel JK, Shirover MA. A human nuclear uracil DNA glycosylase is the 37-kd subunit of glyceraldehyde-3-phosphate dehydrogenase. *Proc Natl Acad Sci U S A* 1991; **88**:8460–8464.

Mongan PD, Capacchione J, Fontana JL, West S, Bünger R. Pyruvate improves cerebral metabolism during hemorrhagic shock. *Am J Physiol Heart Circ Physiol.* 2001 Aug; **281**(2):H854-64.

Müllner M, Sterz F, Domanovits H, Behringer W, Binder M, Laggner AN. The association between blood lactate concentration on admission, duration of cardiac arrest, and functional neurological recovery in patients resuscitated from ventricular fibrillation. *Intensive Care Med.* 1997 Nov; **23**(11):1138-43.

Nguyen AQ, Cherry BH, Scott GF, Ryou MG, Mallet RT. Erythropoietin: powerful protection of ischemic and post-ischemic brain. *Exp Biol Med* 2014; **239**(11): 1461 – 1475.

Nichol G, Stiell IG, Hebert P, Wells GA, Vandemheen K, Laupacis A. What is the quality of life for survivors of cardiac arrest? A prospective study. *Acad Emerg Med* 1999; **6**:95-102.

Olivencia-Yurvati AH, Blair JL, Baig M, Mallet RT. Pyruvate-enhanced cardioprotection during surgery with cardiopulmonary bypass. *J Cardiothorac Vasc Anesth.* 2003 Dec; **17**(6):715-20.

O'Reilly SM, Grubb N, O'Carroll RE. Long-term emotional consequences of in-hospital cardiac arrest and myocardial infarction. *Br J Clin Psychol 2004*; **43**:83-95.

Pierce AE, Roppolo LP, Owens PC, Pepe PE, Idris AH. The need to resume chest compressions immediately after defibrillation attempts: an analysis of post-shock rhythms and duration of pulselessness following out-of-hospital cardiac arrest. *Resuscitation.* 2015 Apr; **89**:162-8.

Rosell A, Ortega-Aznar A, Alvarez-Sabin J, Fernandez-Cadenas I, Ribo M, Molina CA, Lo EH, Montaner J. Increased brain expression of matrix metalloproteinase-9 after ischemic and hemorrhagic human stroke. *Stroke* 2006; **37**(6): 1399 – 1406.

Sawa A, Khan AA, Hester LD, Snyder SH. Glyceraldehyde-3-phosphate dehydrogenase: Nuclear translocation participates in neuronal and non-neuronal cell death. *Proc Natl Acad Sci U S A* 1997; **94**:11669–11674.

Sharma AB, Sun J, Howard LL, Williams AG Jr, Mallet RT. Oxidative stress reversibly inactivates myocardial enzymes during cardiac arrest. *Am J Physiol Heart Circ Physiol.* 2007 Jan; **292**(1):H198-206. Epub 2006 Aug 18.

Singh R., Green M.R. Sequence-specific binding of transfer RNA by glyceraldehyde-3-phosphate dehydrogenase. *Science* 1993; **259**:365–368.

Tanaka R, Mochizuki H, Suzuki A, Katsube N, Ishitani R, Mizuno Y, Urabe T. Induction of glyceraldehyde-3-phosphate dehydrogenase (GAPDH) expression in rat brain after focal ischemia/reperfusion. *J Cereb Blood Flow Metab* 2002; **22**(3): 280 – 288.

Veech RL, Lawson JWR, Cornell NW, Krebs HA. Cytosolic phosphorylation potential. *J Biol Chem* 1979; **254**:6538–6547.

Wang L, Zhang ZG, Xhang RL, Gregg SR, Hozeska-Solgot A, LeTourneau Y, Wang Y, Chopp M. Matrix metalloproteinases 2 (MMP2) and MMP9 secreted by erythropoietin-activated endothelial cells promote neural progenitor cell migration. *The Journal of Neuroscience* 2006; **26**(22): 5996 – 6003.

Wyss MT, Jolivet R, Buck A, Magistretti PJ, Weber B. *In vivo* evidence for lactate as a neuronal energy source. *The Journal of Neuroscience* 2011; **31**(20): 7477 – 7485.

Yannopoulos D, Aufderheide TP, Abella BS, Duval S, Frascone RJ, Goodloe JM, Mahoney BD, Nadkarni VM, Halperin HR, O'Connor R, Idris AH, Becker LB, Pepe PE. Quality of CPR: An important effect modifier in cardiac arrest clinical outcomes and intervention effectiveness trials. *Resuscitation*. 2015 Sep; **94**:106-13.

Y X, Liachenko S, Tang P. dependence of early cerebral reperfusion and long-term outcome on resuscitation efficiency after cardiac arrest in rats. *Stroke* 2002; **33**(3): 837 – 43.

	Sham (n=9)	CPR (n=6)	CPR+P (n=7)	*P* value
Body weight (kg)	25.5 ± 1.3	29.7 ± 1.7	25.4 ± 1.0	0.06
Baseline hemodynamic status				
Mean aortic pressure (mmHg)	78.6 ± 4.5	76.3 ± 2.5	82.0 ± 3.0	0.60
Heart rate (bpm)	98.4 ± 6.1	104.0 ± 6.0	103.4 ± 12.4	0.87
Core temperature (^{o}C)	37.1 ± 0.3	37.0 ± 0.4	36.8 ± 0.2	0.70
SpO_2	94.1 ± 1.4	94.2 ± 1.3	95.7 ± 1.2	0.65
1h ROSC hemodynamic status				
Mean aortic pressure (mmHg)	79.7 ± 5.1	78.5 ± 1.5	86.4 ± 4.3	0.43
Heart rate (bpm)	99.6 ± 5.0	125.8 ± 5.2	116.0 ± 6.2	0.009*
Core temperature (^{o}C)	36.8 ± 0.3	37.0 ± 0.4	36.4 ± 0.4	0.61
SpO_2	94.0 ± 1.5	95.2 ± 0.7	95.1 ± 1.1	0.74
4h ROSC hemodynamic status				
Mean aortic pressure (mmHg)	74.3 ± 2.6	80.3 ± 3.1	81.6 ± 3.5	0.19
Heart rate (bpm)	96.4 ± 6.9	116.3 ± 6.4	106.9 ± 9.2	0.23
Core temperature (^{o}C)	36.6 ± 0.3	37.3 ± 0.6	36.4 ± 0.2	0.35
SpO_2	96.7 ± 0.9	96.0 ± 1.0	95.6 ± 1.3	0.75

Table 1. *Hemodynamic characteristics at baseline, 1h ROSC, and 4h ROSC*. Data are presented as means ± SEM. * P<0.05, Holm-Sidak *post hoc* test showed significant different between CPR and Sham. "CPR": NaCl-infused CCR, "CPR+P": pyruvate-infused CCR, "SpO_2": oxygen saturation.

Figure Legends

Figure 1. *Experiment timeline*. Ventricular fibrillation was induced for 10 minutes. CCR was performed for 4 minutes. Surgery for catheter placement was completed before blood was drawn for baseline measurement. Blood gas and blood was also drawn at 5 min, 15 min, 30 min, 60 min, 120 min, 180 min, and 240 min ROSC (open triangle). Tissue biopsy was collected at 240 min (filled triangle).

Figure 2. Amount of phenylephrine needed to maintain MAP $\geq$ 70mmHg during the first 4 hours ROSC. Values are Mean $\pm$ SEM. *: $P < 0.05$ vs CPR+P, ✦: $P < 0.05$ vs CPR+DP

Figure 3. Arterial (upper) and venous (lower) pyruvate concentration at baseline and any time points up to 4 h ROSC. Two way (treatment and time) repeated measure (time) ANOVA was conducted with Holm-Sidak for pairwise comparison.*: $P< 0.05$ vs. Sham and CPR.

Figure 4. Cerebral and cerebellar water content at 4h ROSC after 14 min cardiac arrest. $P = 0.07$ (top) and $P= 0.8$ (bottom). DP: delayed pyruvate infusion. Values are Mean $\pm$ SEM.

Figure 5. Aconitase and GAPDH activities 4h ROSC after 14 min arrest. Data was presented as Mean $\pm$ SE (U/mg). Two-way ANOVA for tissue and treatment. Aconitase (panel A): ✦: *post hoc* Holm-Sidak Method showed statistically different between hippocampus (filled bar) and cerebellum (dotted bar) ($P< 0.001$), +: Sham vs. CPR ($P= 0.02$), ❖: Sham vs. CPR+P ($P= 0.02$). GAPDH (panel B): ✦: *post hoc* Holm-Sidak Method showed statistically different between hippocampus (filled bar) and cerebellum (dotted bar) ($P= 0.007$).

Figure 6. Arterial and venous pH at baseline and at ROSC. "+", "*", "❖" indicates statistically significant ($P<0.05$) between Sham vs. CPR, CPR vs. CPR+P, and Sham vs. CPR+P, respectively.

Figure 7. Arterial and venous pCO_2 at baseline and at ROSC. "+", "*", "❖" indicates statistically significant (P<0.05) between Sham vs. CPR, CPR vs. CPR+P, and Sham vs. CPR+P, respectively.

Figure 8. Arterial and venous pO_2 at baseline and at ROSC. "+", "*", "❖" indicates statistically significant (P<0.05) between Sham vs. CPR, CPR vs. CPR+P, and Sham vs. CPR+P, respectively.

Figure 9. Arterial and venous sodium at baseline and at ROSC. "+", "*", "❖" indicates statistically significant (P<0.05) between Sham vs. CPR, CPR vs. CPR+P, and Sham vs. CPR+P, respectively.

Figure 10. Arterial and venous potassium at baseline and at ROSC. "+", "*", "❖" indicates statistically significant (P<0.05) between Sham vs. CPR, CPR vs. CPR+P, and Sham vs. CPR+P, respectively.

Figure 11. Arterial and venous calcium at baseline and at ROSC. "+", "*", "❖" indicates statistically significant (P<0.05) between Sham vs. CPR, CPR vs. CPR+P, and Sham vs. CPR+P, respectively.

Figure 12. Arterial and venous glucose at baseline and at ROSC. "+", "*", "❖" indicates statistically significant (P<0.05) between Sham vs. CPR, CPR vs. CPR+P, and Sham vs. CPR+P, respectively.

Figure 13. Arterial and venous lactate at baseline and at ROSC. "+", "*", "❖" indicates statistically significant (P<0.05) between Sham vs. CPR, CPR vs. CPR+P, and Sham vs. CPR+P, respectively.

Figure 14. Arterial and venous lactate/pyruvate ratio at baseline and at ROSC. "+", "*", "❖" indicates statistically significant (P<0.05) between Sham vs. CPR, CPR vs. CPR+P, and Sham vs. CPR+P, respectively.

Figure 15. Arterial and venous bicarbonate at baseline and at ROSC. "+", "*", "❖" indicates statistically significant (P<0.05) between Sham vs. CPR, CPR vs. CPR+P, and Sham vs. CPR+P, respectively.

Figure 16. *Matrix metalloproteinase*. A: Hippocampal MMP-2 activity at 4h ROSC. One-way ANOVA, *post hoc* Dunn's test indicated statistically significant between Sham and CPR+P. B: Hippocampal MMP-2 content; One-way ANOVA, *post hoc* Holm-Sidak P< 0.05 Sham vs CPR and Sham vs. CPR+P. C: Cereb MMP-2 activity; One-way ANOVA, *post hoc* Holm-Sidak, P< 0.05 CPR vs CPR+P. D: MMP-2 content, One-way ANOVA, *post hoc* Dunn's Sham vs CPR.

Figure 17. *ZO-1*. Hippocampal (A) and cerebellar (B) ZO-1 content. One-way ANOVA P= 0.2 and P= 0.12, respectively.

Figure 18. *HIF-1α and EPO*. Hippocampal Hif-1α and EPO 4h ROSC. One-way ANOVAP=0.7 (A) and P=0.9 (B). Cerebellar HIF-1α (Panel C, One-way ANOVA P = 0.16) and EPO (Panel D, One-way ANOVA and *post hoc* Holm-Sidak, P< 0.05 Sham vs. CPR and Sham vs. CPR+P)

Figure 19. *Cytochrome c*. Hippocampal (A) and cerebellar (B) cytochrome c. One-way ANOVA P= 0.09 and P= 0.14, respectively.

Figure 20. *Cerebellar caspase 3 and hippocampal caspase-9*. Cerebellar pro-caspase-3 (A) and caspase-3 (B) in the cerebellum at 4 h ROSC. One-way ANOVA P= 0.6 and P= 0.4, respectively.

Hippocampal pro-caspase 9 (C) and caspse-9 (D) in the hippocampus at 4h ROSC. Single-factor ANOVA P= 0.07 and P= 0.15, respectively.

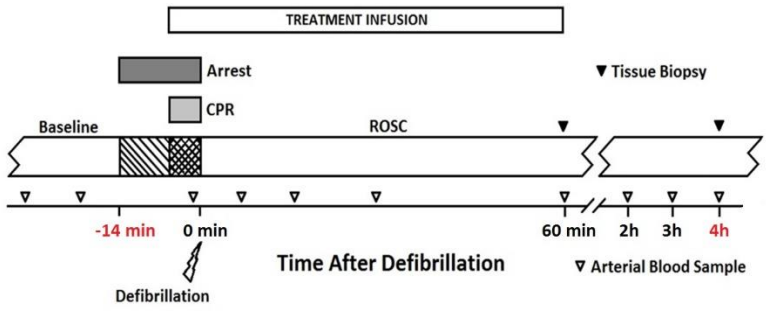

Figure 1. *Experiment timeline*. Ventricular fibrillation was induced for 10 minutes. CCR was performed for 4 minutes. Surgery for catheter placement was completed before blood was drawn for baseline measurement. Blood gas and blood was also drawn at 5 min, 15 min, 30 min, 60 min, 120 min, 180 min, and 240 min ROSC (open triangle). Tissue biopsy was collected at 240 min (filled triangle).

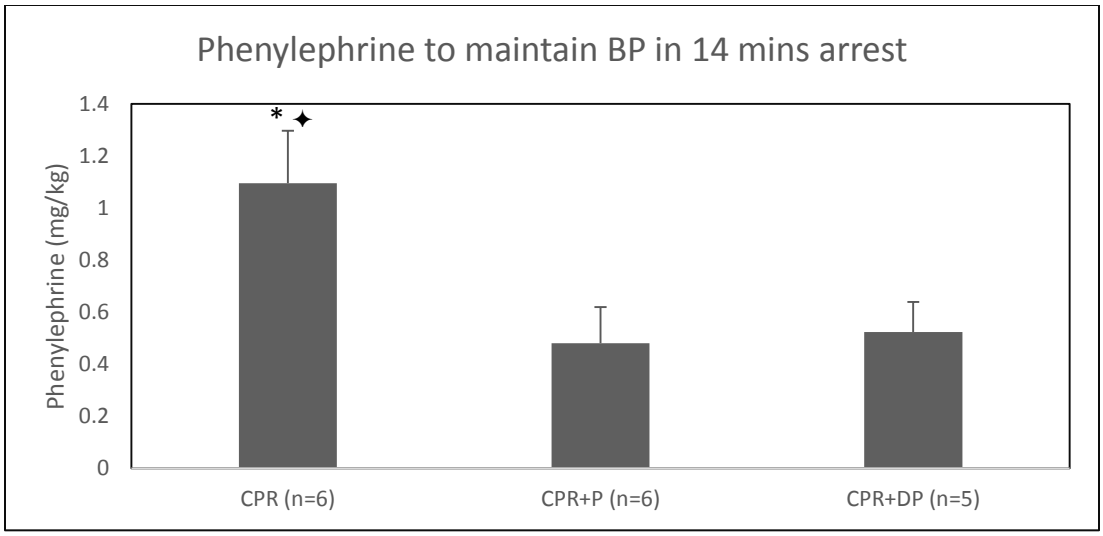

Figure 2. Amount of phenylephrine needed to maintain MAP $\geq$ 70mmHg during the first 4 hours ROSC. Values are Mean $\pm$ SEM. *: $P < 0.05$ vs CPR+P, ✦: $P < 0.05$ vs CPR+DP.

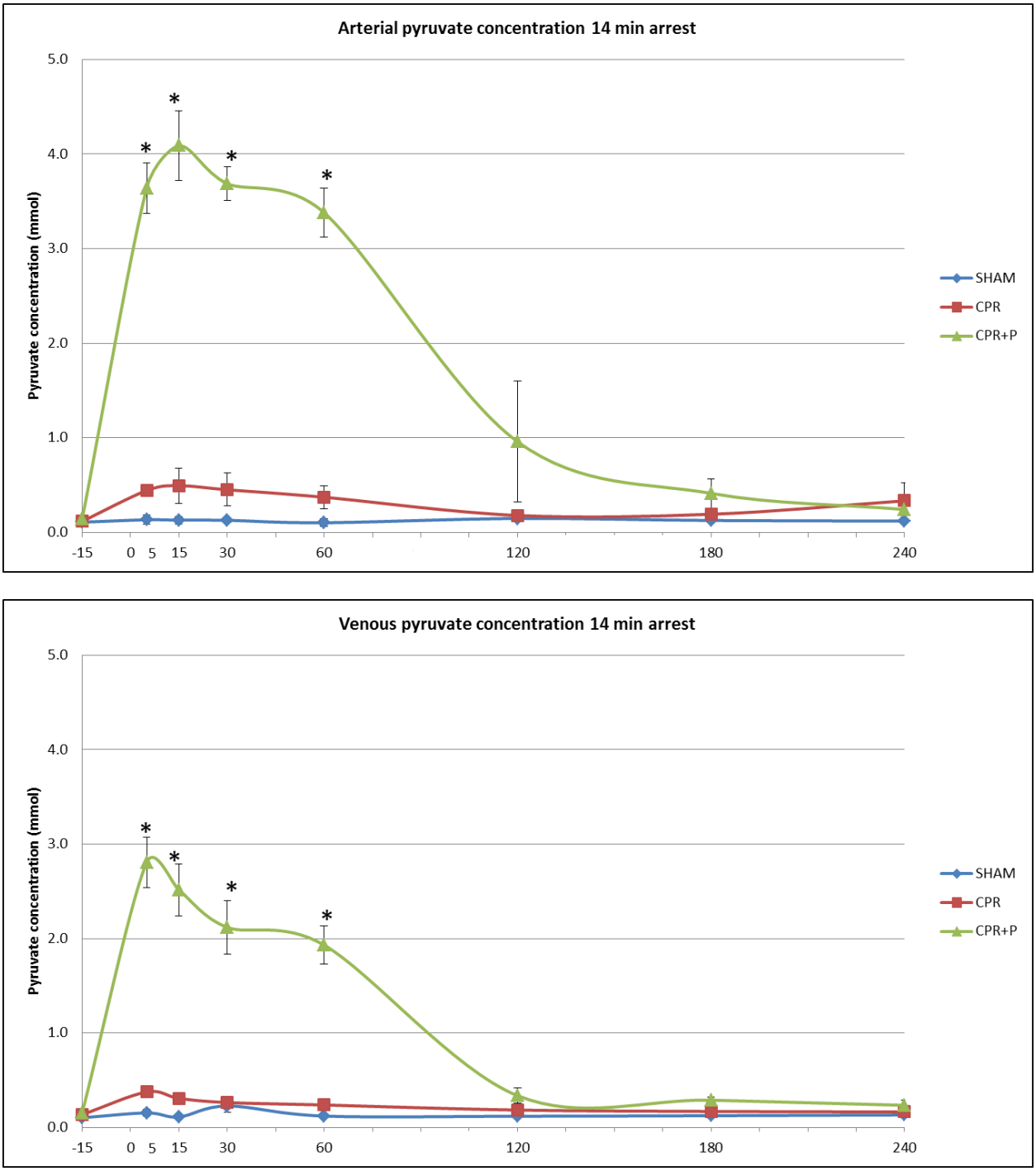

Figure 3. Arterial (upper) and venous (lower) pyruvate concentration at baseline and any time points up to 4 h ROSC. Two way (treatment and time) repeated measure (time) ANOVA was conducted with Holm-Sidak for pairwise comparison.*: P< 0.05 vs. Sham and CPR.

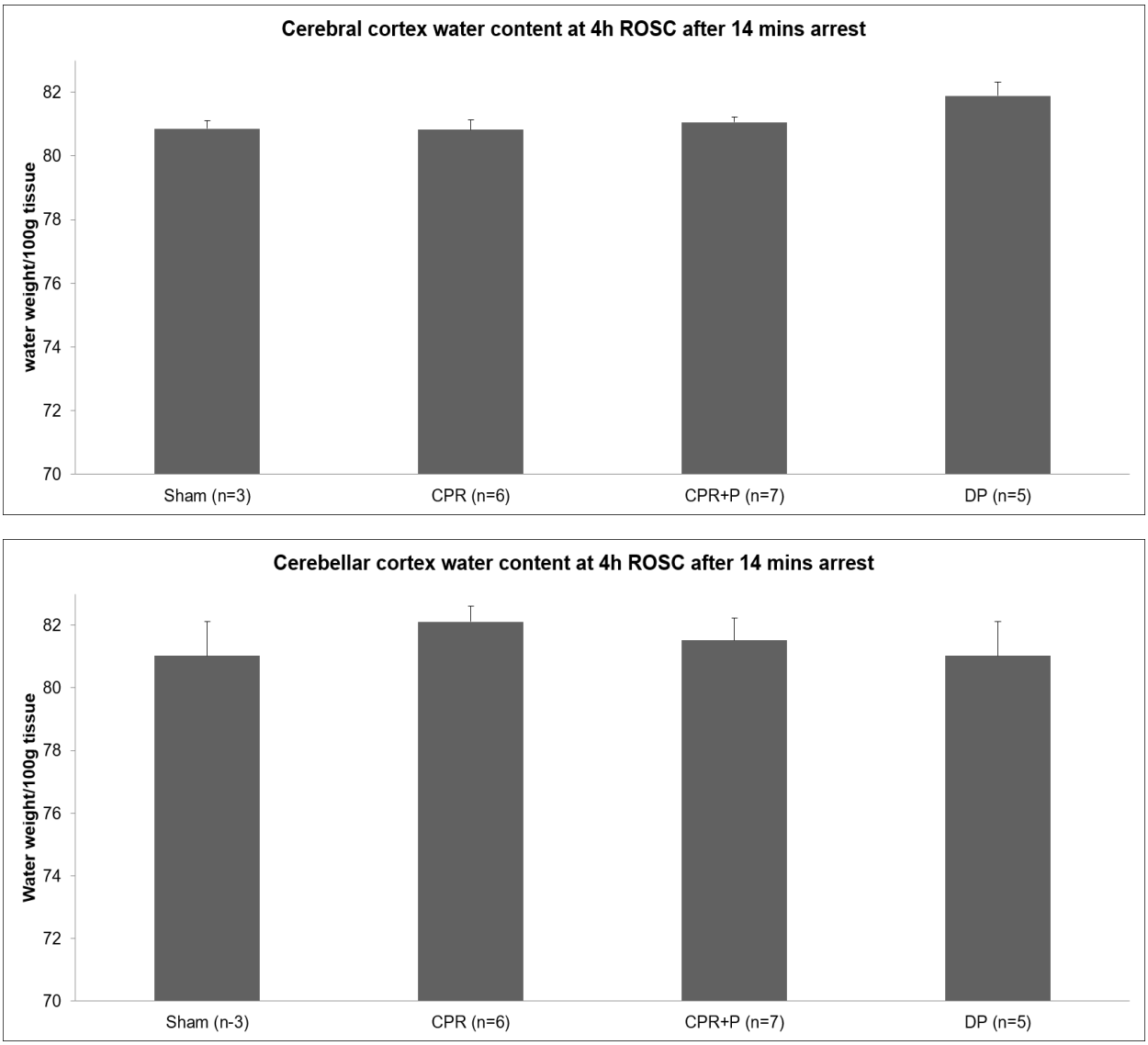

Figure 4. Cerebral and cerebellar water content at 4h ROSC after 14 min cardiac arrest. P = 0.07 (top) and P= 0.8 (bottom). DP: delayed pyruvate infusion. Values are Mean ± SEM.

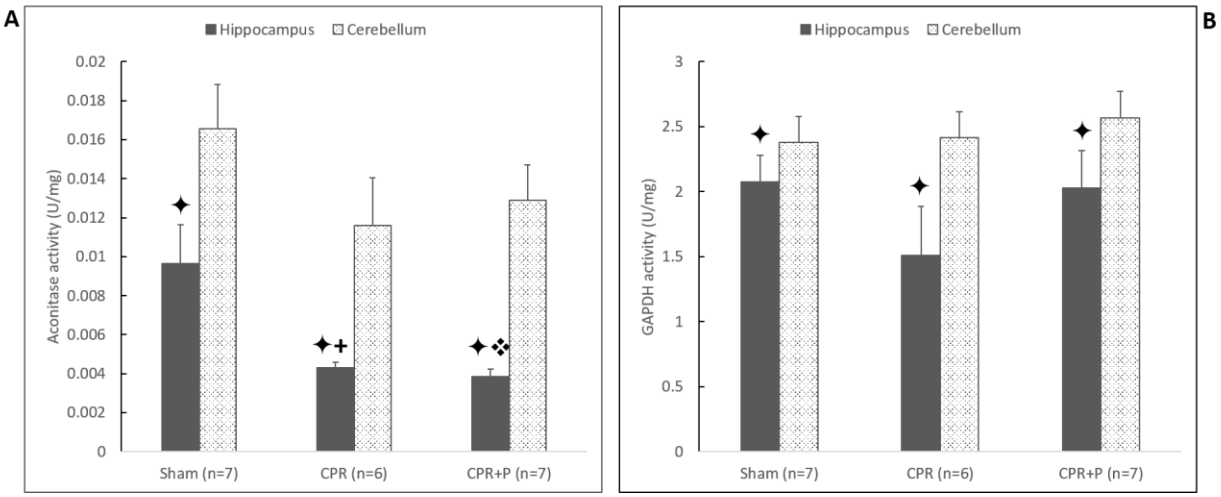

Figure 5. Aconitase and GAPDH activities 4h ROSC after 14 min arrest. Data was presented as Mean ± SE (U/mg). Two-way ANOVA for tissue and treatment. Aconitase (panel A): ✦: *post hoc* Holm-Sidak Method showed statistically different between hippocampus (filled bar) and cerebellum (dotted bar) (P< 0.001), +: Sham vs. CPR (P= 0.02), ❖: Sham vs. CPR+P (P= 0.02). GAPDH (panel B): ✦: *post hoc* Holm-Sidak Method showed statistically different between hippocampus (filled bar) and cerebellum (dotted bar) (P= 0.007).

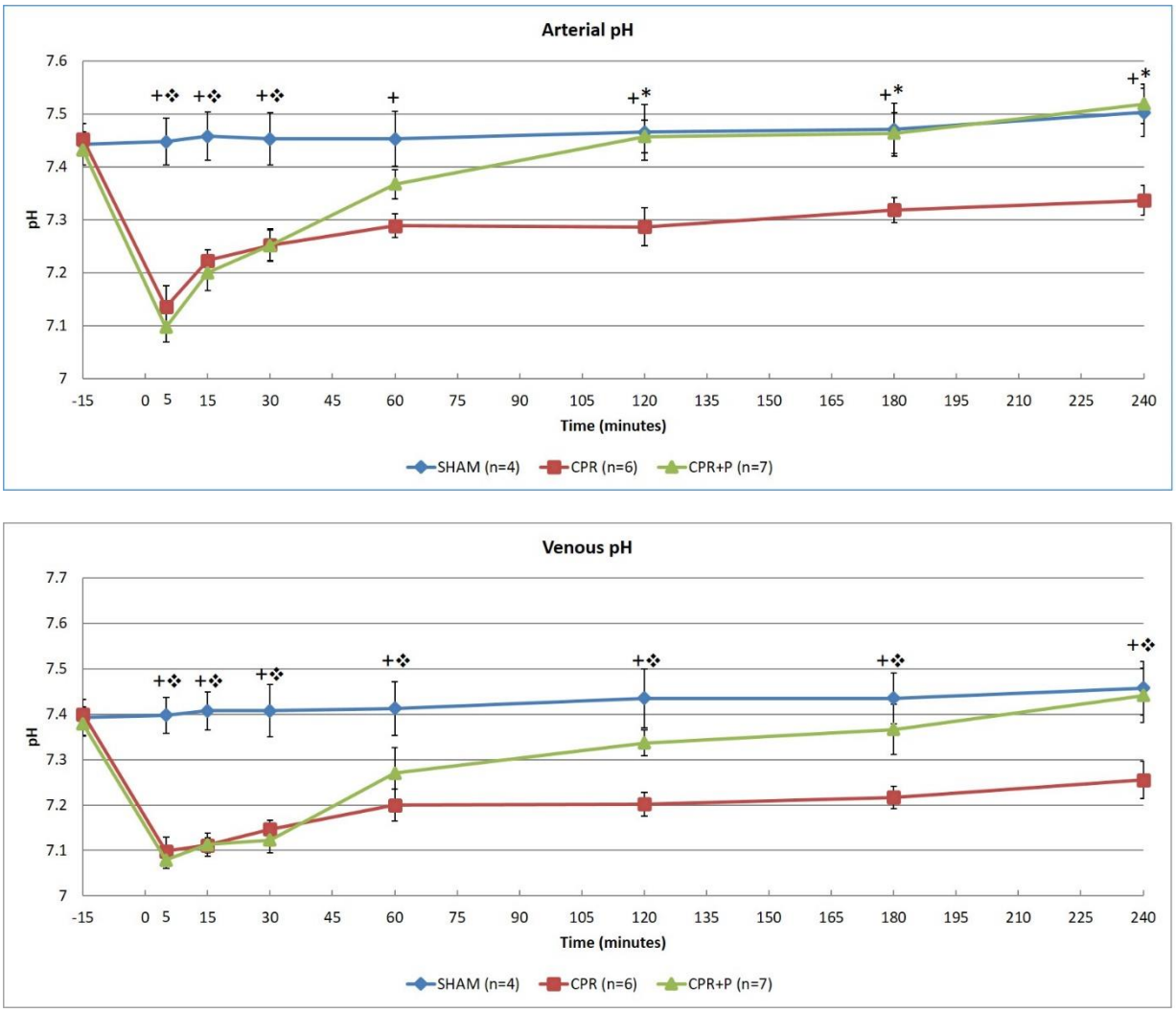

Figure 6. Arterial and venous pH at baseline and at ROSC. "+", "*", "❖" indicates statistically significant ($P<0.05$) between Sham vs. CPR, CPR vs. CPR+P, and Sham vs. CPR+P, respectively.

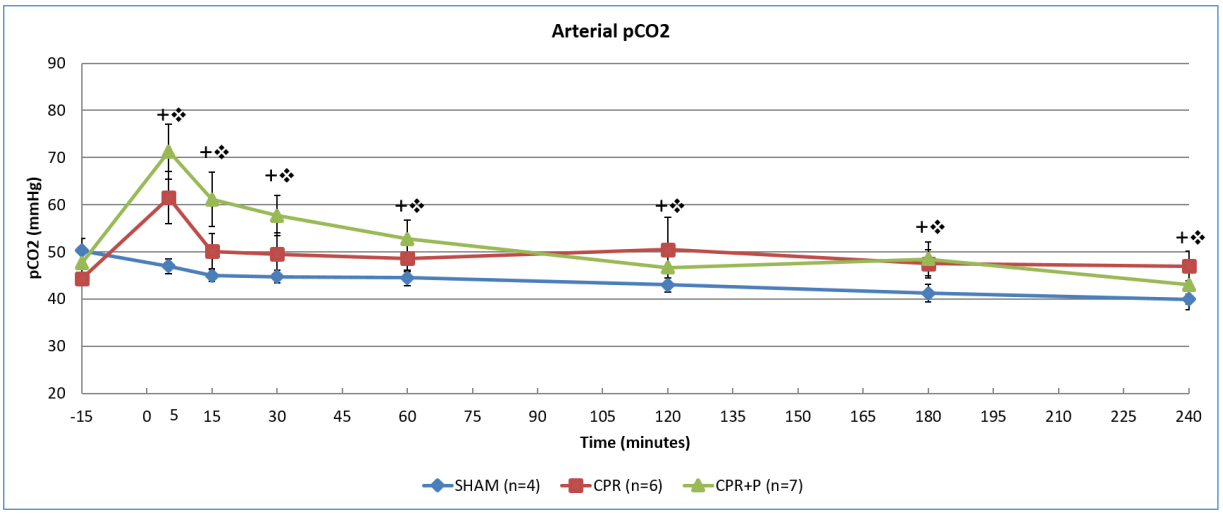

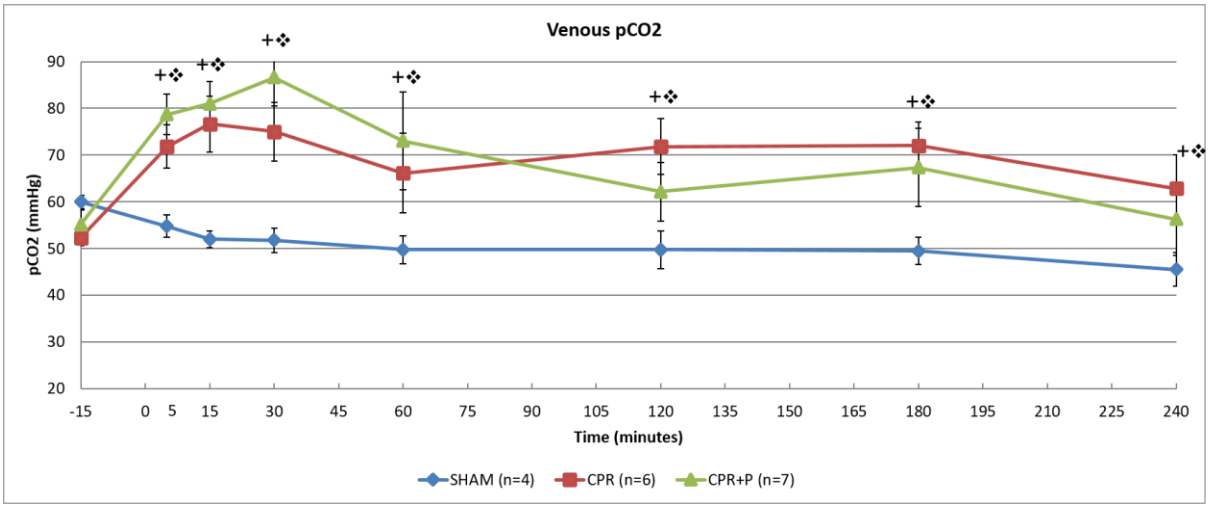

Figure 7. Arterial and venous pCO_2 at baseline and at ROSC. "+", "*", "❖" indicates statistically significant ($P<0.05$) between Sham vs. CPR, CPR vs. CPR+P, and Sham vs. CPR+P, respectively.

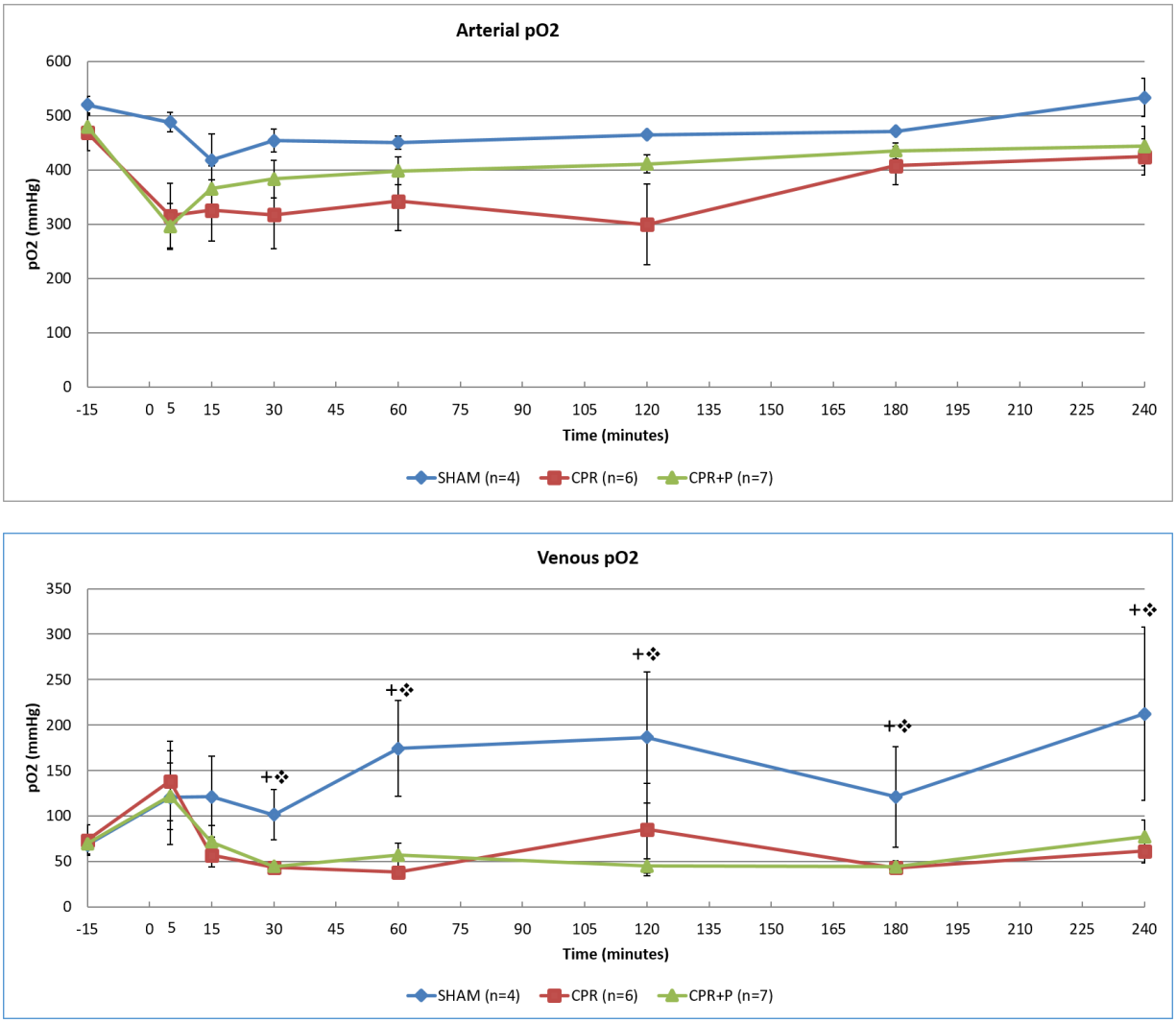

Figure 8. Arterial and venous pO_2 at baseline and at ROSC. "+", "*", "❖" indicates statistically significant ($P<0.05$) between Sham vs. CPR, CPR vs. CPR+P, and Sham vs. CPR+P, respectively.

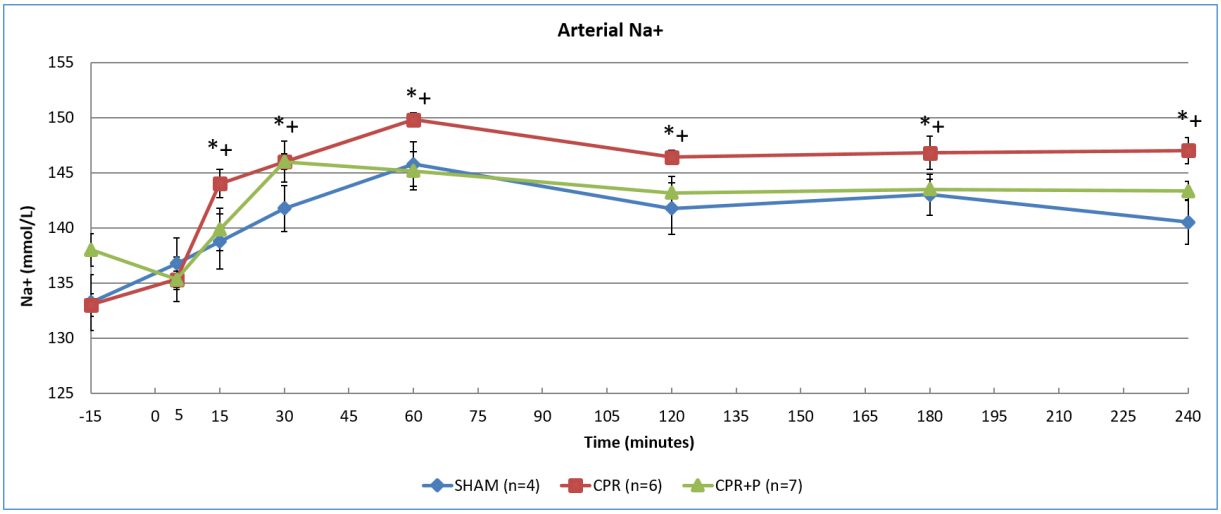

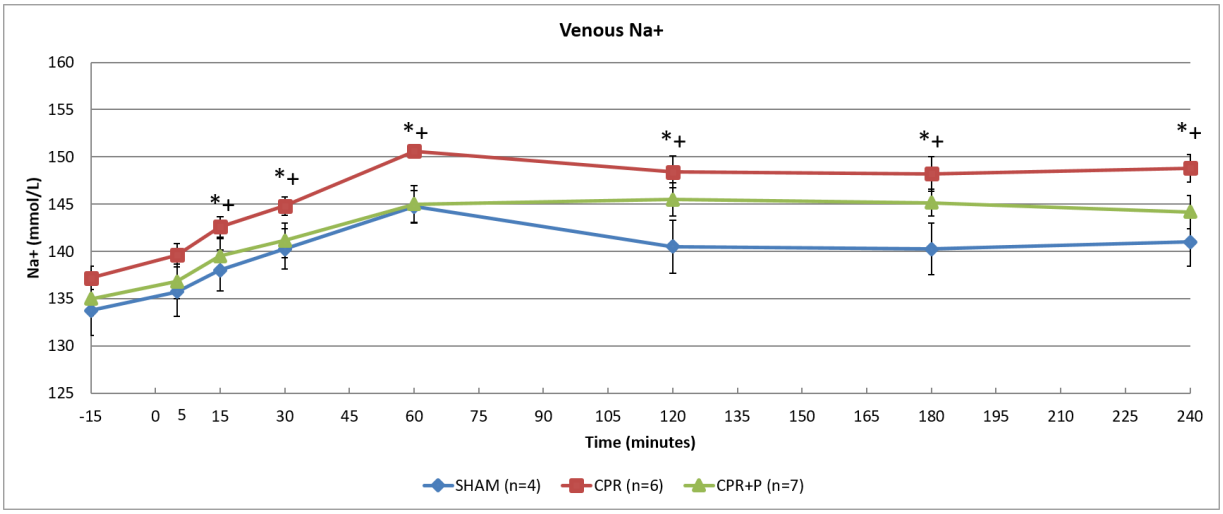

Figure 9. Arterial and venous sodium at baseline and at ROSC. "+", "*", "❖" indicates statistically significant (P<0.05) between Sham vs. CPR, CPR vs. CPR+P, and Sham vs. CPR+P, respectively.

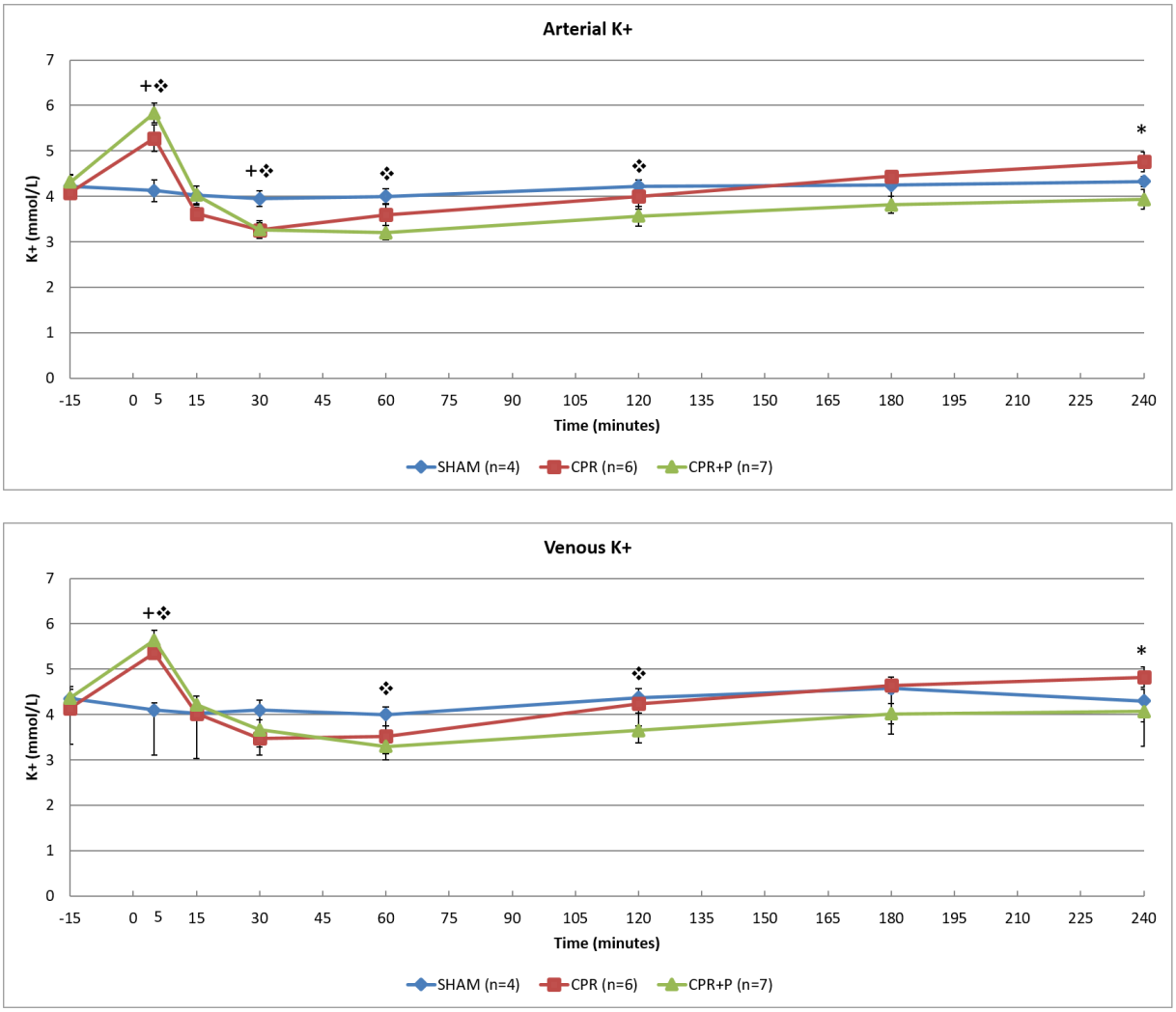

Figure 10. Arterial and venous potassium at baseline and at ROSC. "+", "*", "❖" indicates statistically significant (P<0.05) between Sham vs. CPR, CPR vs. CPR+P, and Sham vs. CPR+P, respectively.

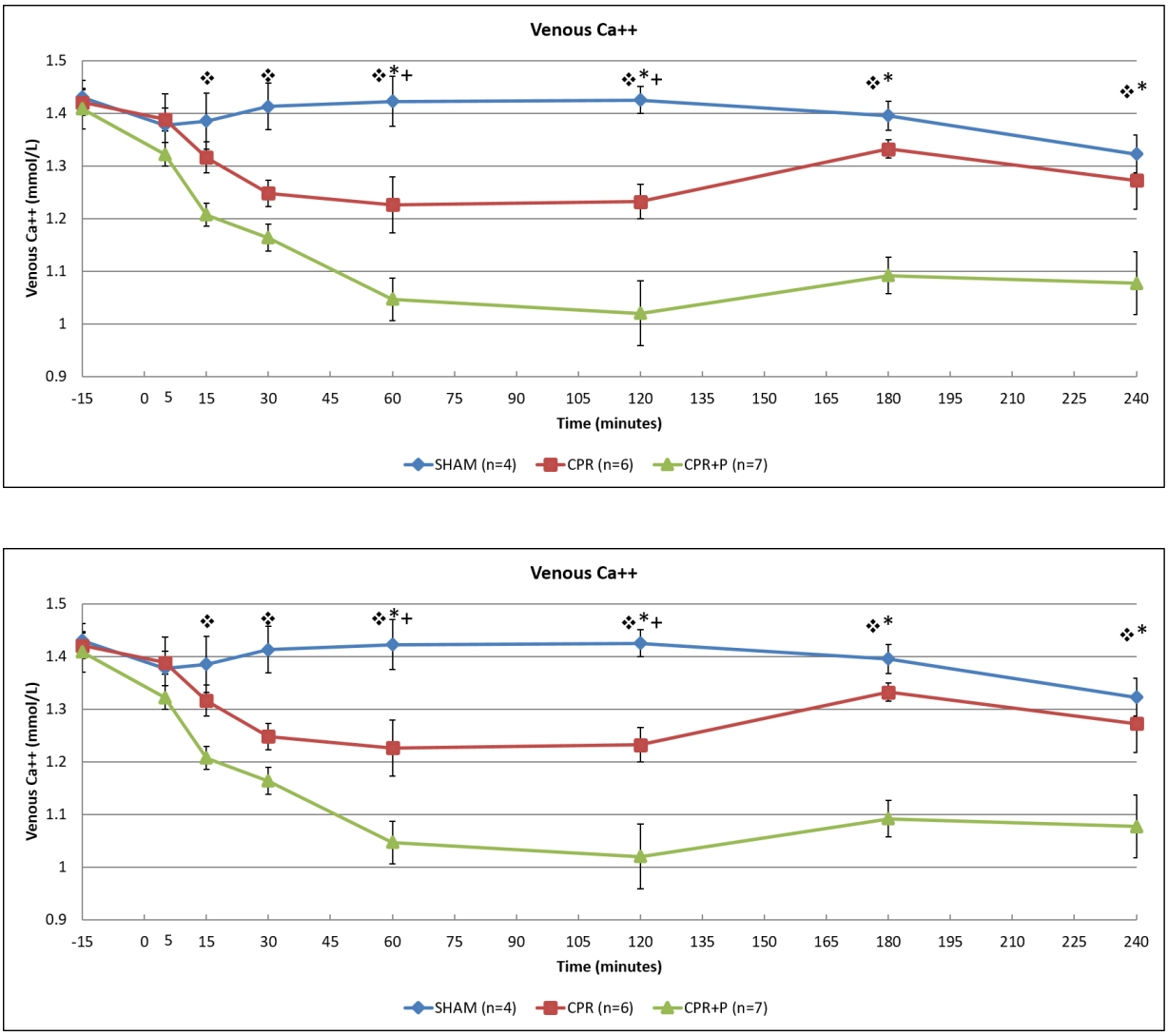

Figure 11. Arterial and venous calcium at baseline and at ROSC. "+", "*", "❖" indicates statistically significant (P<0.05) between Sham vs. CPR, CPR vs. CPR+P, and Sham vs. CPR+P, respectively.

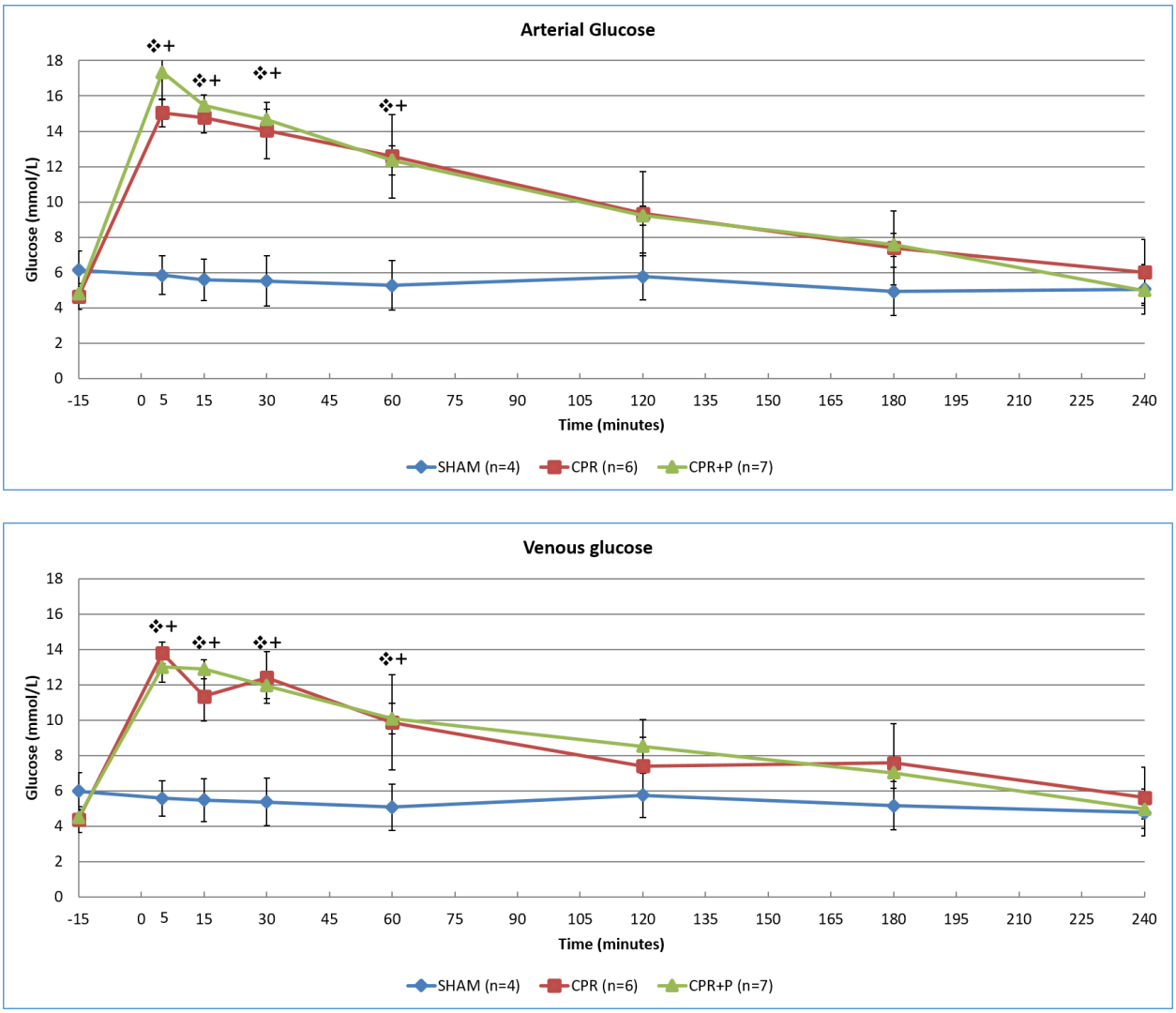

Figure 12. Arterial and venous glucose at baseline and at ROSC. "+", "*", "❖" indicates statistically significant (P<0.05) between Sham vs. CPR, CPR vs. CPR+P, and Sham vs. CPR+P, respectively.

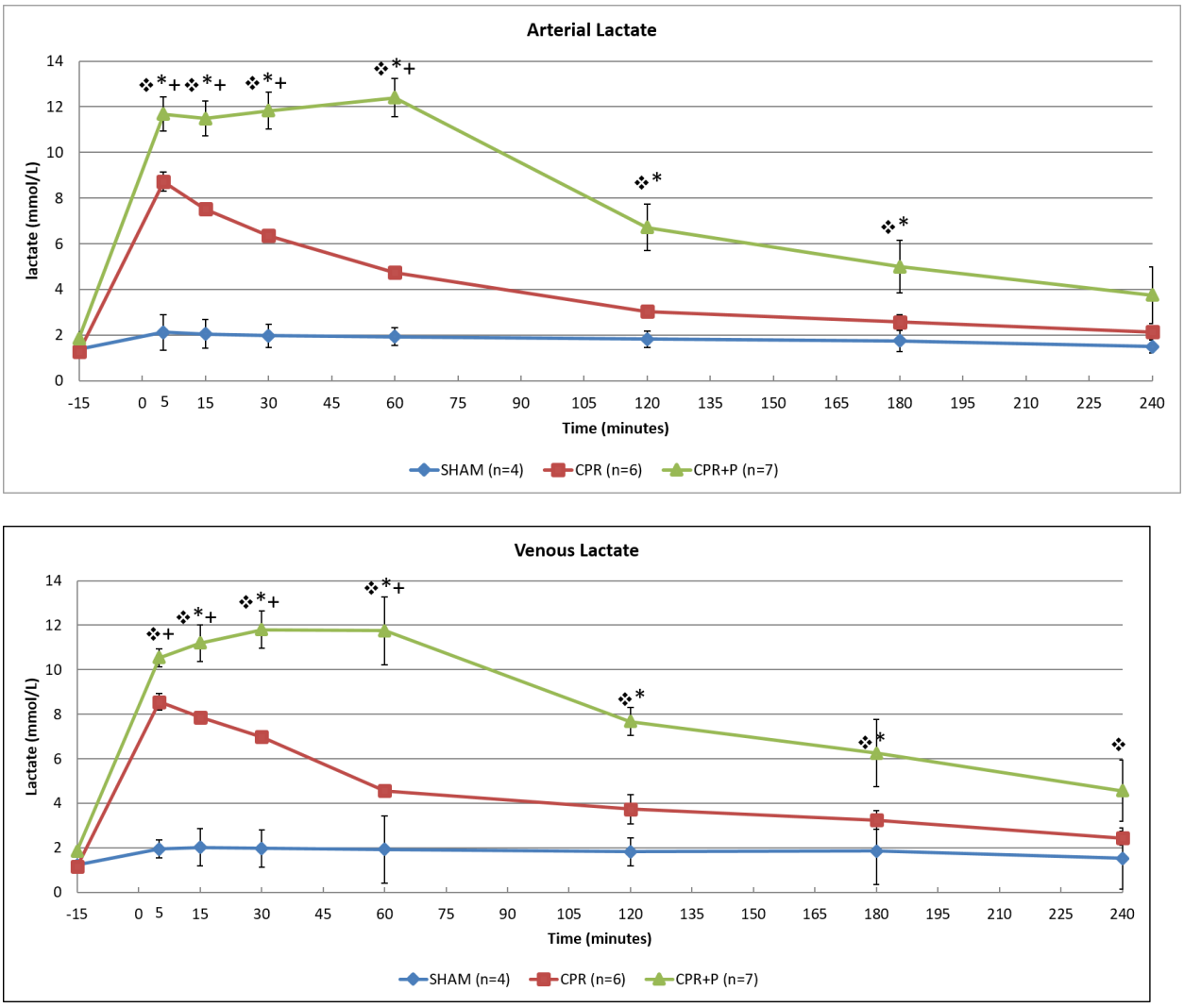

Figure 13. Arterial and venous lactate at baseline and at ROSC. "+", "*", "❖" indicates statistically significant (P<0.05) between Sham vs. CPR, CPR vs. CPR+P, and Sham vs. CPR+P, respectively.

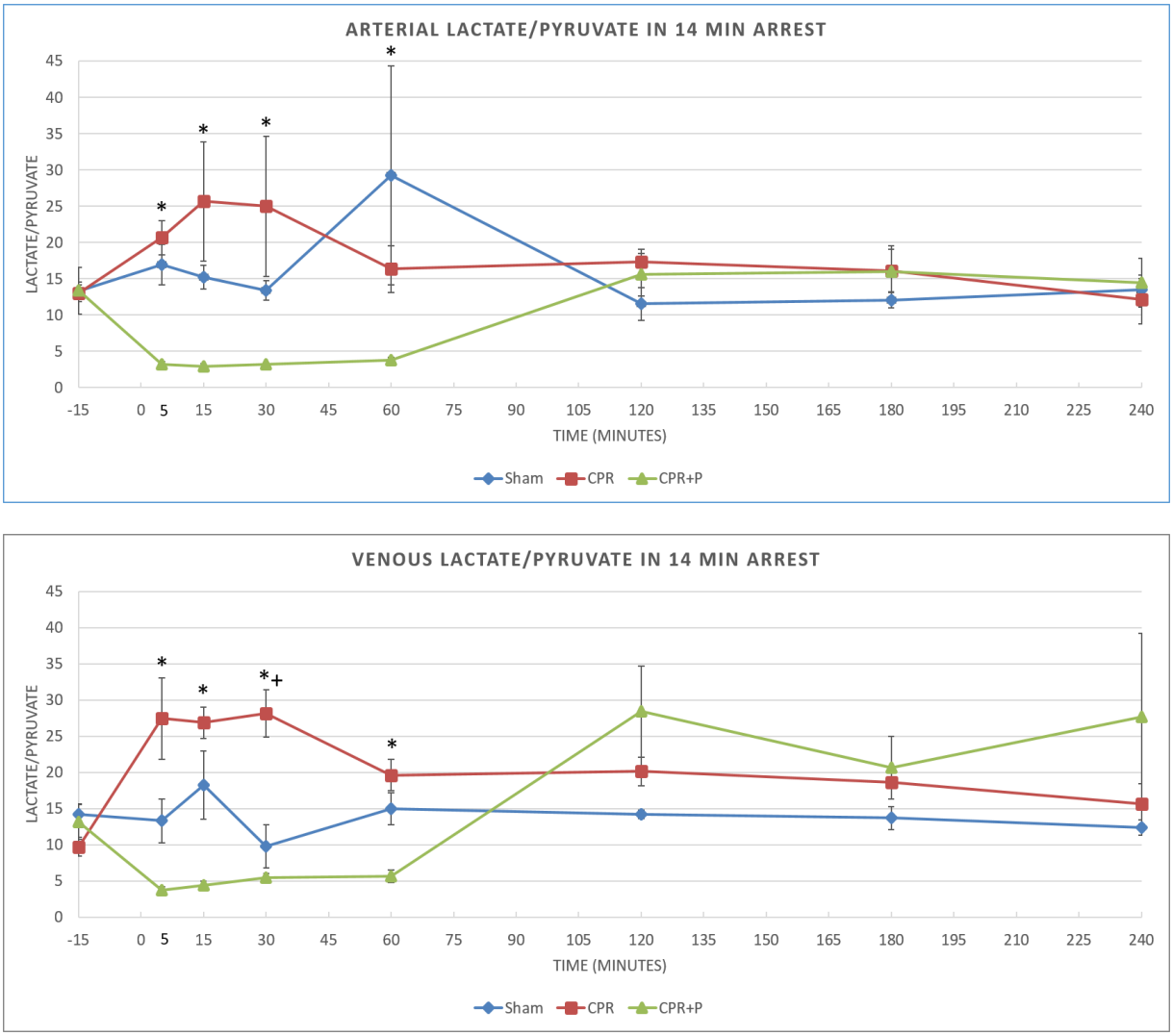

Figure 14. Arterial and venous lactate/pyruvate ratio at baseline and at ROSC. "+", "*", "❖" indicates statistically significant (P<0.05) between Sham vs. CPR, CPR vs. CPR+P, and Sham vs. CPR+P, respectively.

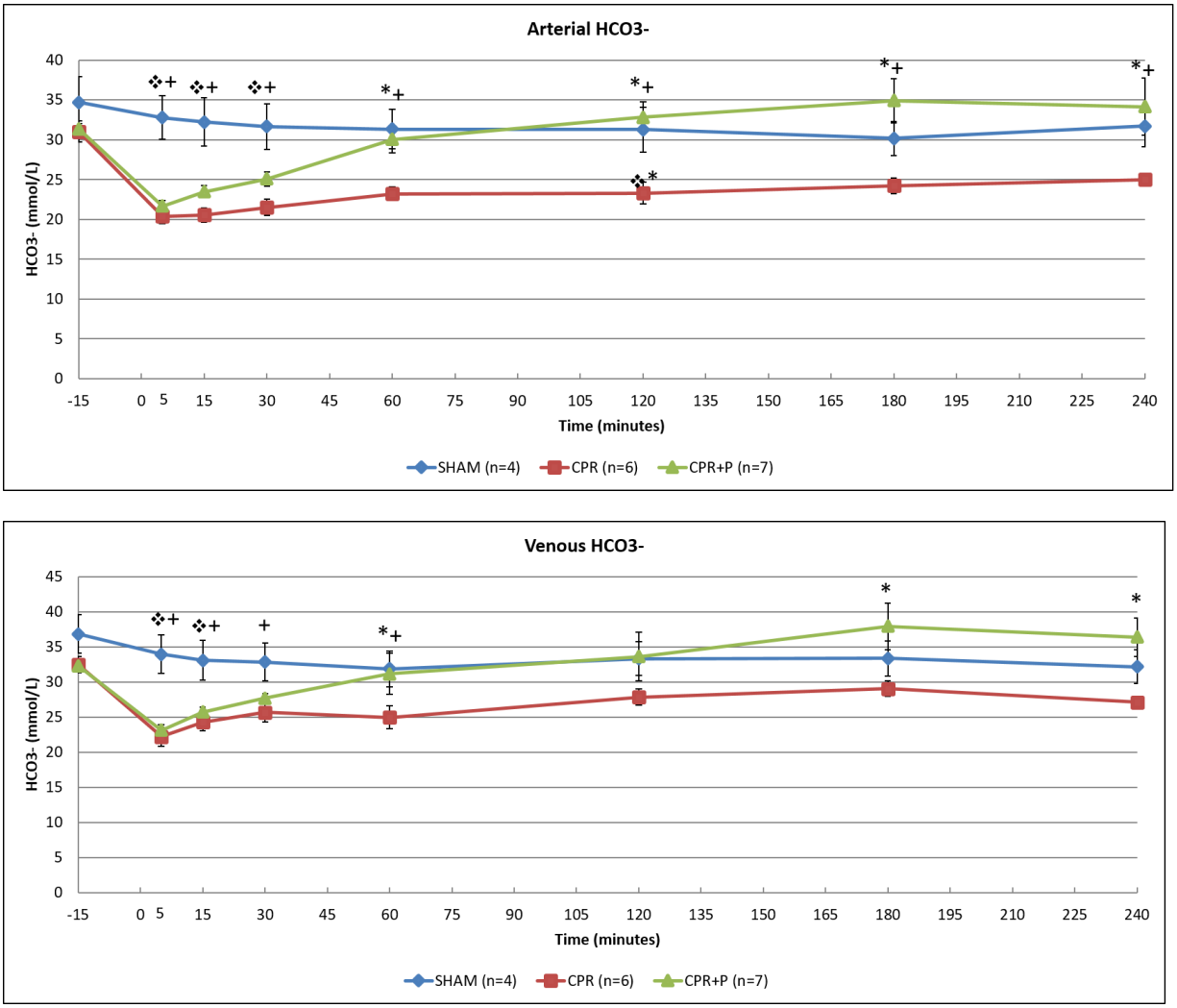

Figure 15. Arterial and venous bicarbonate at baseline and at ROSC. "+", "*", "❖" indicates statistically significant (P<0.05) between Sham vs. CPR, CPR vs. CPR+P, and Sham vs. CPR+P, respectively.

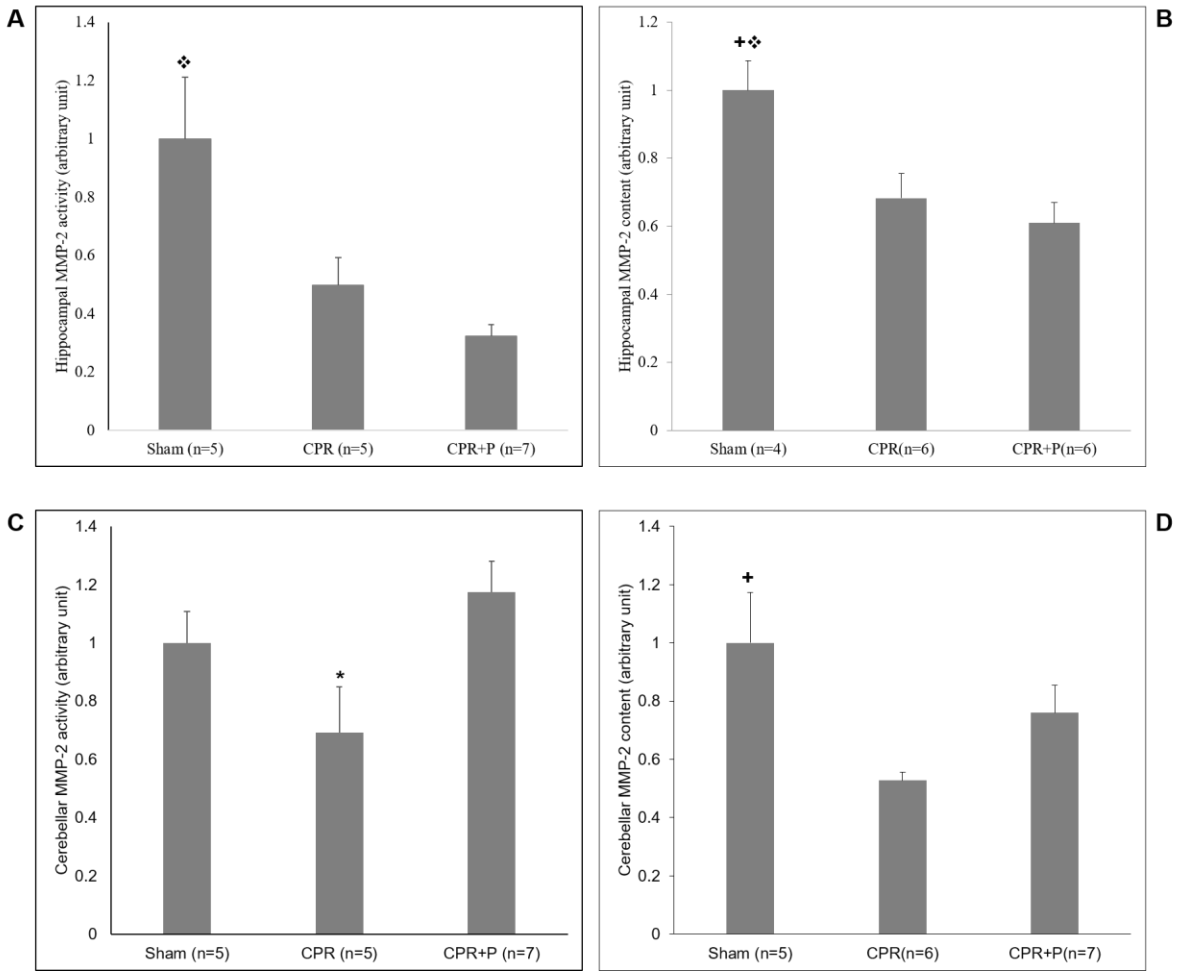

Figure 16. *Matrix metalloproteinase*. A: Hippocampal MMP-2 activity at 4h ROSC. One-way ANOVA, *post hoc* Dunn's test indicated statistically significant between Sham and CPR+P. B: Hippocampal MMP-2 content; One-way ANOVA, *post hoc* Holm-Sidak $P < 0.05$ Sham vs CPR and Sham vs. CPR+P. C: Cereb MMP-2 activity; One-way ANOVA, *post hoc* Holm-Sidak, $P < 0.05$ CPR vs CPR+P. D: MMP-2 content, One-way ANOVA, *post hoc* Dunn's Sham vs CPR.

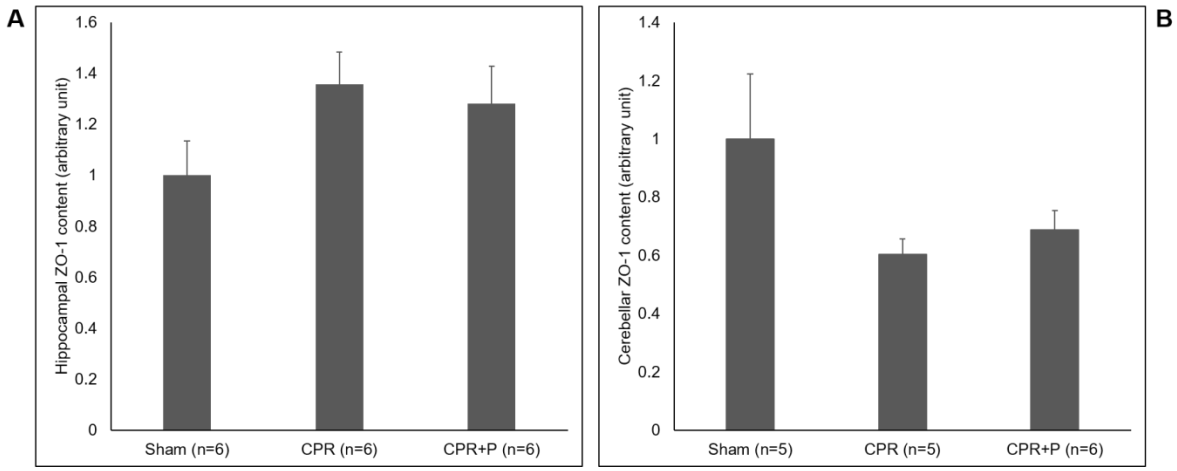

Figure 17. *ZO-1*. Hippocampal (A) and cerebellar (B) ZO-1 content. One-way ANOVA P= 0.2 and P= 0.12, respectively.

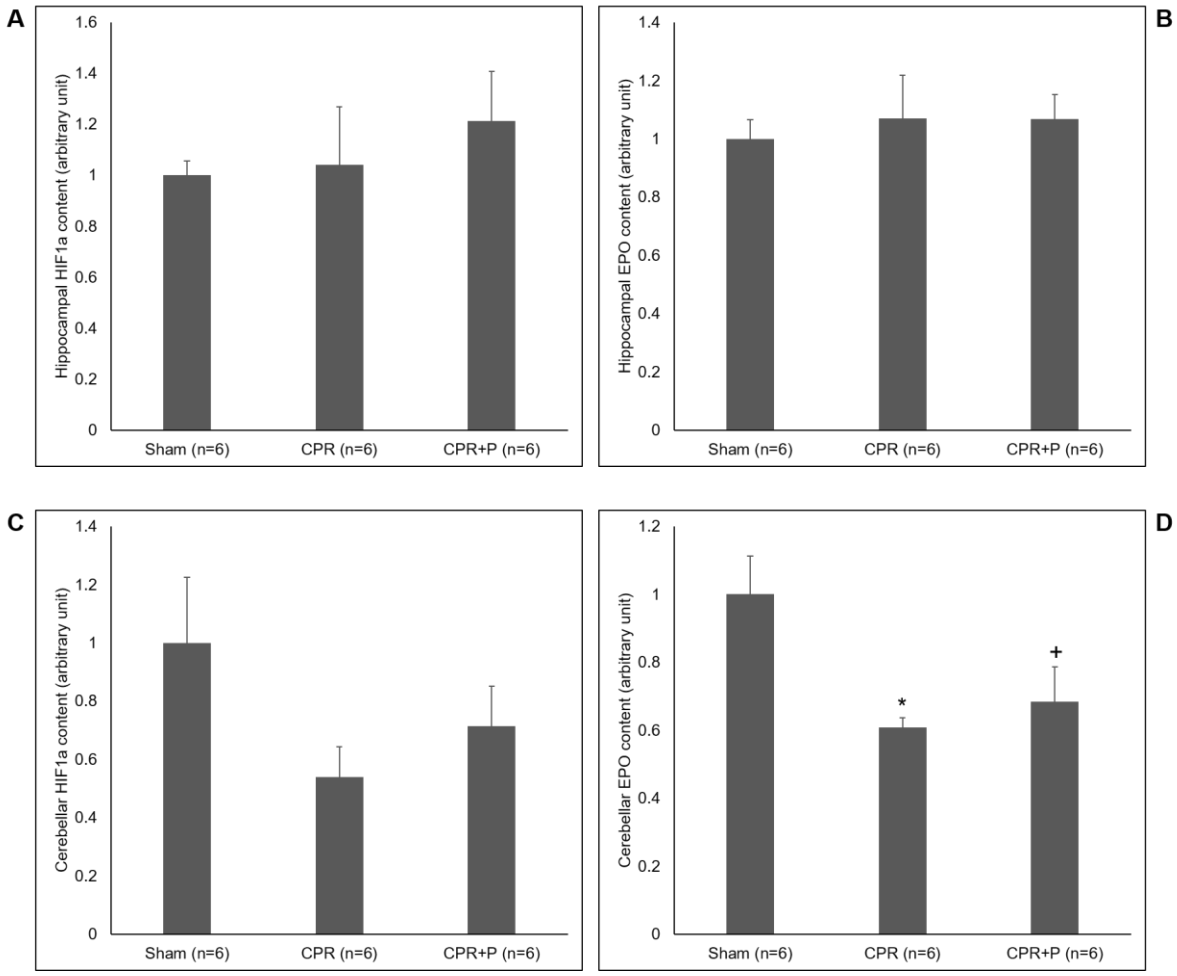

Figure 18. *HIF-1α and EPO*. Hippocampal Hif-1α and EPO 4h ROSC. One-way ANOVAP=0.7 (A) and P=0.9 (B). Cerebellar HIF-1α (Panel C, One-way ANOVA P = 0.16) and EPO (Panel D, One-way ANOVA and *post hoc* Holm-Sidak, P< 0.05 Sham vs. CPR and Sham vs. CPR+P.

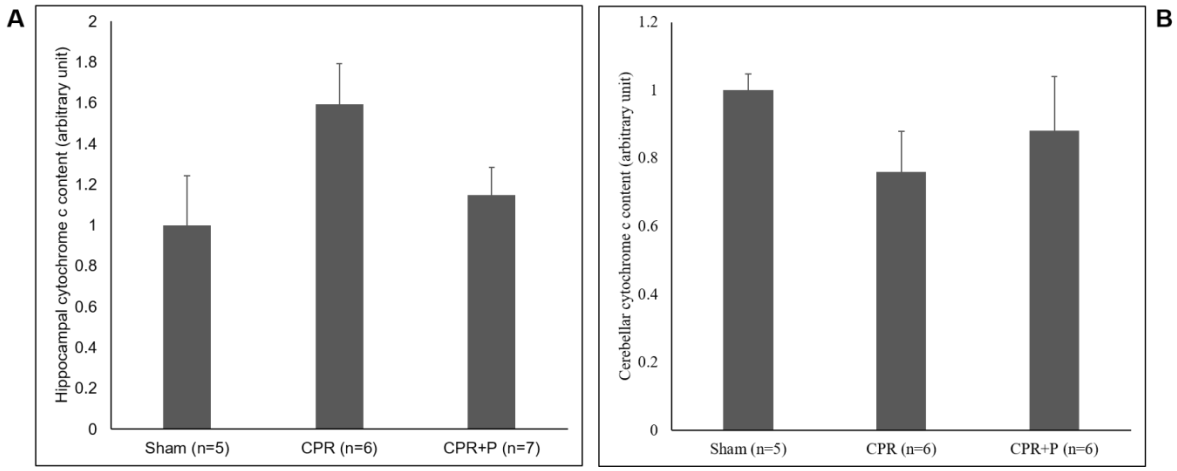

Figure 19. *Cytochrome c*. Hippocampal (A) and cerebellar (B) cytochrome c. One-way ANOVA P= 0.09 and P= 0.14, respectively.

A

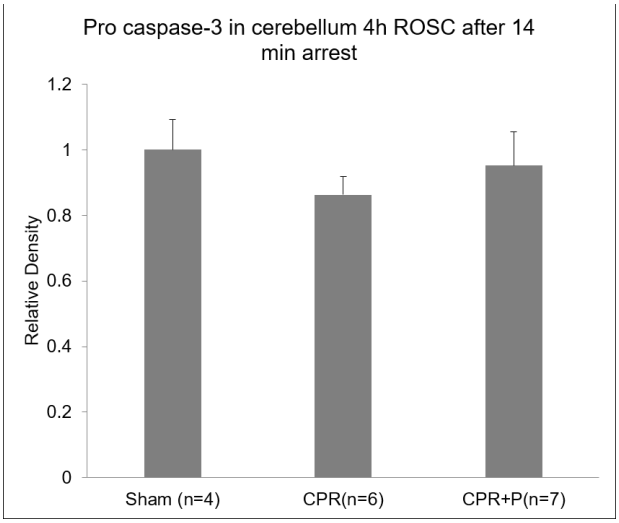

B

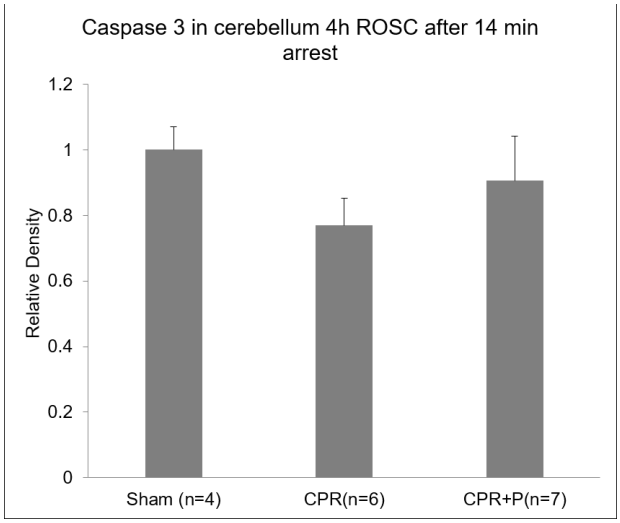

C

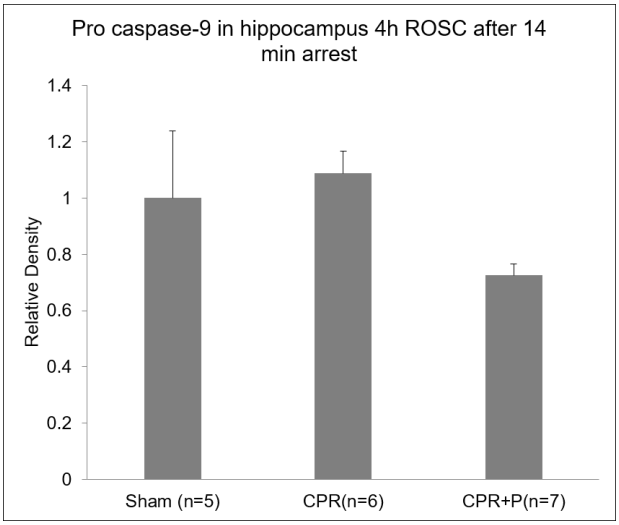

D

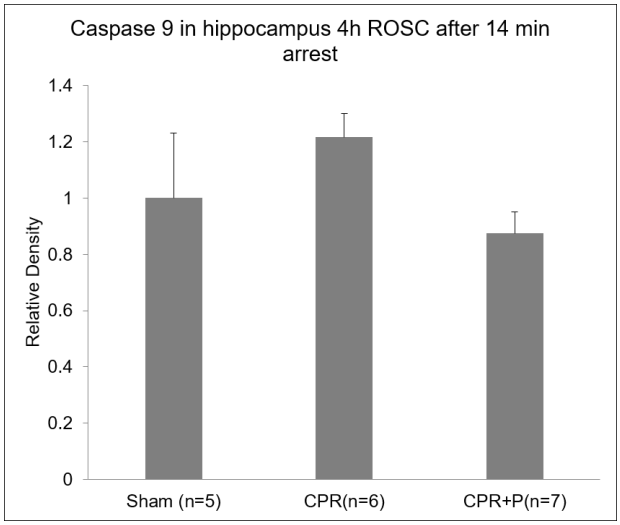

Figure 20. *Cerebellar caspase 3 and hippocampal caspase-9*. Cerebellar pro-caspase-3 (A) and caspase-3 (B) in the cerebellum at 4 h ROSC. One-way ANOVA P= 0.6 and P= 0.4, respectively. Hippocampal pro-caspase 9 (C) and caspse-9 (D) in the hippocampus at 4h ROSC. Single-factor ANOVA P= 0.07 and P= 0.15, respectively.

CHAPTER V

CONCLUSIONS

At 3 d recovery from 6 min of untreated cardiac arrest, the number of histologically intact cerebellar Purkinje cells per high power field decreased vs. sham control. Pyruvate treatment preserved cerebellar Purkinje cells vs. NaCl infused pigs. Changes in cerebellar Purkinje cells by cardiac arrest and protection of these cells with pyruvate treatment could not be explained through differences in the mechanisms of brain injuries by content and activities of MMPs, MPO, and content of pro-apoptotic proteases (caspase-3 and caspase-9), or by differences in cellular defense mechanisms, including Hsp-70 content and Hif-1α/EPO expression. There were no differences in neurological outcome scores and memory assessment in pigs surviving cardiac arrest vs. Sham control, regardless of treatment infusion. Thus, preservation of Purkinje cells by pyruvate treatment may have been due to discrete cytoprotective effect of pyruvate in these neurons, rather than global biochemical effects of pyruvate throughout the brain.

At 4 h recovery from 10 min of untreated cardiac arrest, hippocampal aconitase activity was lower in both cardiac arrest groups vs. the sham control. On the other hand, decreased MMP-2 activities were observed in both hippocampus and cerebellum of cardiac arrest animals at 4 h ROSC. Cardiac arrest-resuscitation depleted cerebellar EPO content, noticeable at 4 h ROSC. Pyruvate treatment did not preserve EPO content, a finding that has important implications for future studies to identify an intervention that protects the brain from ischemia-reperfusion injuries through protective mechanisms activated by EPO. Combined therapy of pyruvate with other potentially cerebroprotective intervention merit investigation.

CHAPTER VI

LIMITATIONS and FUTURE DIRECTIONS

Cardiac arrest is a profound insult to the body. Despite excessive research efforts and several clinical trials, no single pharmacological treatment has been identified that meaningfully alters the outcome. As a proof of concept, our experiments focused on the effect of pyruvate on cerebral ischemia-reperfusion injury, and pyruvate's impact on study endpoints was limited. Instead, a bundle therapy, combining several interventions that alone may have limited therapeutic effect, could be more effective than monotherapy for cerebral resuscitation (Bartos et al., 2015). Thus, combined treatment with pyruvate ad other interventions, e.g. intermittent hypoxia conditioning (Manukhina et al., 2016) or brain cooling (Andrews et al., 2015) may merit study.

The healthy, juvenile swine used in our experiments does not represent the majority of clinical cardiac arrest patients, many of whom have significant multiple comorbidities that complicate the resuscitation and recovery process, including age, coronary artery disease, arrhythmia, diabetes, hypertension, chronic obstructive pulmonary disease and renal insufficiency (Piscator et al., 2016). Fewer and less severe comorbidities are associated with better recovery of neurological functions after cardiac arrest. In a study of 4354 cardiac arrest patients in Denmark, 796 patients aged 18 - 65 years who survived beyond 30 days were examined (Kragholm et al., 2015). The factors most associated with return to work for more than 6 months of sustainable employment were advanced cardiac care that focused on the chest

component and use of therapeutic hypothermia (from 2006-2011 compared to 2001-2005, triple the survival rate), age, gender (male), bystander-witnessed arrest, and bystander CPR. In this study, implementation of chest-oriented care and hypothermia (2006-2011) tripled the survivor rate vs. the immediate pre-study period (2001-2005). The increased survival is correlated with a greater proportion of patients returning to their previous work without any major relapses or extensive sick leave (Kragholm et al., 2015). This clinical study indicates that optimal delivery of effective CCR and other proven measures can increase survival with good neurological functions in many patients.

However, within the laboratory setting, clinically relevant alternatives to large animal models of cardiac arrest are not readily available. A potential large animal model, with metabolic syndrome, a risk factor for cardiac arrest, is the Ossabaw pig (Neeb et al., 2010); but the electrocardiographic fragility of these large animals, and their predisposition to suffer lethal arrhythmia under anesthesia make them poor candidates for controlled cardiac arrest experimentation (personal communication with Dr. Jonathan Tune, Indiana University). Many neurological complications of cardiac arrest arise later in life, even years after cardiac arrest (Cronberg et al., 2009; Cherry et al., 2014). The 3 d recovery period in this study did not permit complete assessment of the long-term sequelae of cardiac arrest in our model. Thus, a future study of more prolonged post-arrest recovery may be required. Many cardiac arrest survivors experience subtle changes in their neurological function such as language or problem-solving skills, or temperament. It is important to note that, none of those aspects could be thoroughly tested in animals, especially the higher order ones like pigs, since there is not a sensitive and specific test to evaluate neurobehavioral status of a pigs (Gieling et al., 2011). Also, it should be

noted that fully mature domestic swine are very large, weighing several hundred pounds, and their chest walls might not be sufficiently compliant for effective chest compression.

Inhaled anesthetics such as isoflurane have been shown to be neuroprotective in many *in vitro* and *in vivo* models of ischemia-reperfusion injuries (Burchell et al., 2013). In rat subjected to permanent unilateral middle cerebral arterial occlusion, 30 min isoflurane treatment 24 h before the ischemic event reduced brain infarct size and improved neurological deficit scores at 6, 24, and 72 h after reperfusion (Zheng and Zuo, 2004). A highly effective anesthetic, isoflurane was used in all the experiments in this project. On the other hand, isoflurane may have minimized ischemia-reperfusion injuries in some brain regions, which may account for the non-significant differences in some biochemical markers of brain injury.

We attempted to recover a subset of animals which suffered 14 mins of cardiac arrest. Out of 6 animals, cardioversion could not be achieved in 2 animals, another 2 had respiratory failure and could not be weaned from mechanical ventilation, 1 recovered with intact motor function, and 1 was paralyzed. Because of the high costs of the experiment, limited resources for intensive care, and ethical concerns, we decided to not study further long-term recovery after the longer cardiac arrest.

A small subset of experiments was conducted on female pigs, allowing a preliminary analysis of the effect of gender on brain biochemical responses to global ischemia. It is commonly accepted that women are protected from cardiovascular disease until menopause, possibly due to the presence of the female sex hormones, particularly estrogen (McCullough et al., 2003). We used juvenile pigs (30 -40 kg, or approximately 90 days old). In pigs, the age of onset of puberty is 170-220 days old (~90kg in weight), and the pig's oestrous cycle is 18-24

days (Soede et al., 2011). We found that after 4h ROSC after 10 min cardiac arrest in male pigs, MMP-2 activity was lower than in the sham male counterparts. On the other hand, there was not a significant difference among the female cardiac arrest and sham groups. Statistical power was not sufficient for conclusive comparison of males vs. females. However, robust comparisons of male vs. female responses to cardiac arrest-resuscitation would be a valuable extension of this project, especially in light of the intense focus on gender differences at NIH and other funding agencies.

REFERENCES

Andrews PJ, Sinclair HL, Rodriguez A, Harris BA, Battison CG, Rhodes JK, Murray GD, Eurotherm3235 Trial Collaborators. Hypothermia for intracranial hypertension after traumatic brain injury. *N Engl J Med.* 2015; **373**(25): 2403 – 2412.

Bartos JA, Matsuura TR, Sarraf M, Youngquist ST, McKnite SH, Rees JN, Sloper DT, Bates FS, Segl N, Debaty G, Lurie KG, Neumar RW, etzger JM, Riess ML, Yannopoulos D. Bundled postconditioning therapies improve hemodynamics and neurologic recovery after 17 min of untreated cardiac arrest. *Resuscitation* 2015; **87**: 7 – 13.

Burchell SR, Dixon BJ, Tang J, Zhang JH. Isoflurane provides neuroprotection in neonatal hypoxic ischemic brain injury. *J Investig Med*. 2013; **61**(7): 1078 – 1083.

Cronberg t, Lilja G, Rundgren M, Friberg H, Widner H. Long-term neurological outcome after cardiac arrest and therapeutic hypothermia. *Resuscitation* 2009; **80**: 1119 – 1123.

Gieling ET, Nordquist RE, Van der Staay FJ. Assessing learning and memory in pigs. *Anim Cogn.* 2011; **14**(2):151-173.

Kragholm K, Wissenberg M, Mortensen N, Fonager K, Jensen SE, Rajan S, Lippert FK, Christensen EF, Handen PA, Lang-Jensen T, Hendriksen OM, Kober L, Gislason G, Torp-Pedersen C, Rasmussen BS. Return to work in out-of-hospital cardiac arrest survivors: A nationwide register-based follow-up study. Circulation 2015; 131: 1682-1690. DOI: 10.1161/CIRCULATIONAHA.114.011366.

Manukhina EB, Downey HF, Shi XR, Mallet RT. Intermittent hypoxia training protects cerebrovascular function in Alzheimer's disease. *Exp Biol Med* 2016; in press.

McCullough LD, Hurn PD. Estrogen and ischemic neuroprotection: an integrated view. *Trends in endocrinology and metabolism* 2003; **24**(5): 228 – 235.

Neeb ZP, Edwards JM, Alloosh M, Long X, Mokelke EA, Sturek M. Metabolic syndrome and coronary artery disease in Ossabaw compared with Yucatan swine. *Comp Med*. 2010; **60**(4): 300 – 315.

Piscator E, Hedberg P, Goransson K, Djarv T. Survival after in-hospital cardiac arrest is highly associated with the Age-combined Charlson Co-morbidity index in a cohort study from a two-site Swedish University hospital. *Resuscitation* 2016; **99**: 79 – 8.3

Soede NM, Langerdijk P, Kemp B. Reproductive cycles in pigs. *Animal reproduction science* 2011; **124**(3-4): 251 – 258.

Zheng S and Zuo Z. isoflurane preconditioning induces neuroprotection against ischemia via activation of P38 mitogen-activated protein kinases. *Molecular Pharmacology* 2004; **65**(5): 1172 – 1180.

APPENDIX A

FIGURES

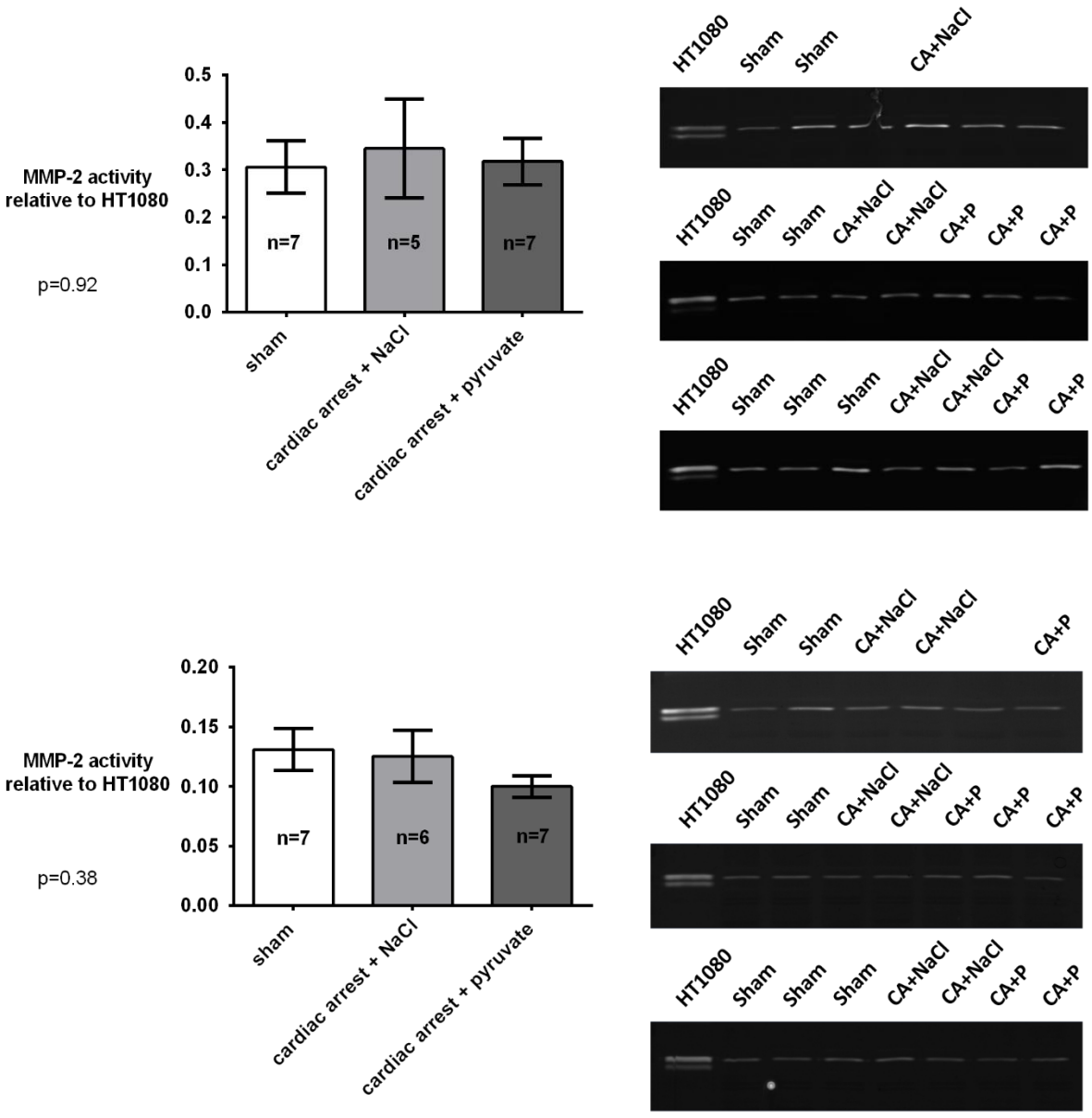

Figure 1. *Matrix metalloproteinase activity in the myocardium*. MMP-2 activity in the right ventricle (top panel) and left ventricle (bottom panel) at 4h ROSC. MMP activity is expressed as an arbitrary unit, relative to HT1080.

Cardiac arrest, regardless of treatment, did not affect MMP-2 activity at 4h ROSC, compared to Sham, in right and left ventricle. MMP-2 activity, however, was greater in the right ventricle versus left ventricle. This is a new finding in swine and has not been reported in literature. We

speculated that the finding might be due to differences in mechanical stress on left and right ventricle walls. It was reported that mechanism of remodeling was different in left (increased in collagen production) and right (decreased MMP-2 expression was correlated with reduction in extracellular matrix degradation) ventricle 4 weeks following myocardial infarction in rats (Stefanon et al., 2013).

Reference

Stefanon I, Valero-Munoz V, Fernandes AA, Ribeiro Jr. RF, Rodriguez C, Miana M, Martinez-Gonzalez J, Spalenza JS, Lahera V, Vassallo PF, Cachofeiro V. Left and right ventricle late remodeling following myocardial infarction in rats. PLOS 2013; http://dx.doi.org/10.1371/journal.pone.0064986.

A B

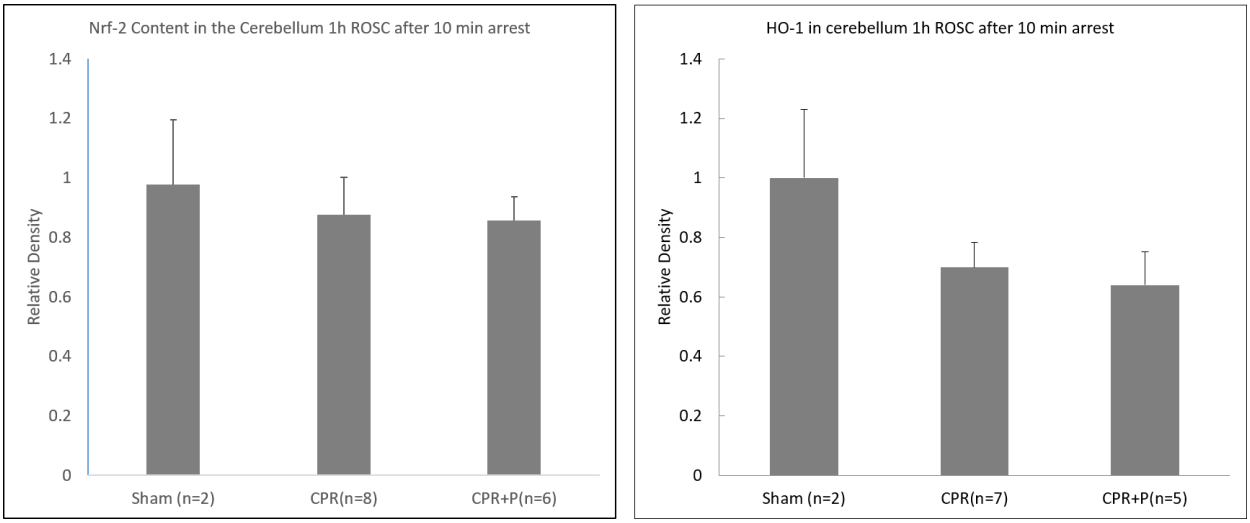

C D

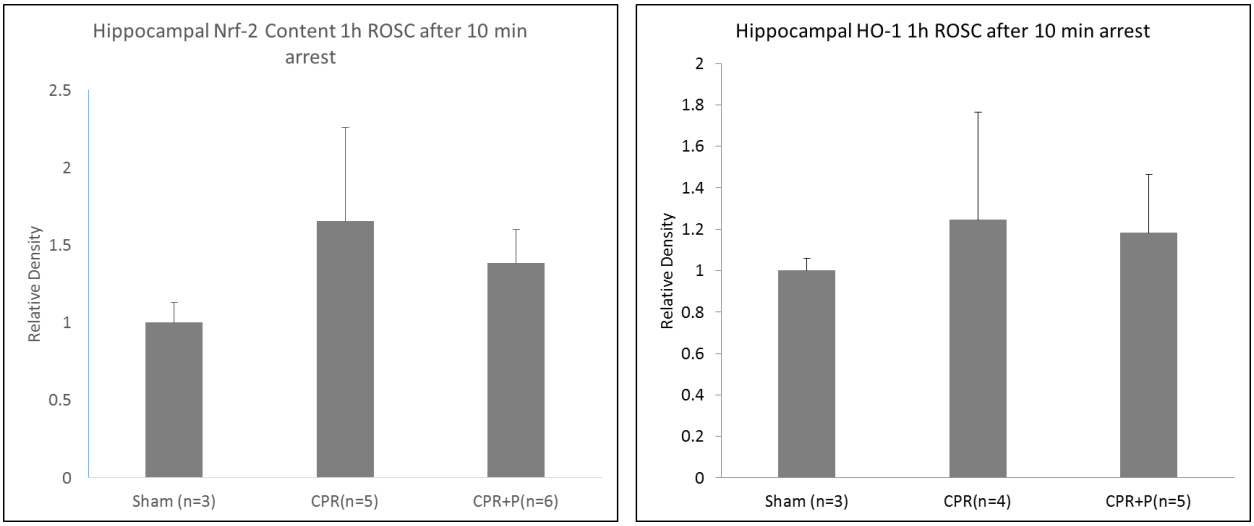

Figure 2. *Nrf-2 and HO-1 content 3 d after cardiac arrest- resuscitation*. Nrf-2 and HO-1 content in the cerebellum (A,B) and hippocampus (C,D) 1 h ROSC after 6 min untreated cardiac arrest and 4 min CCR. Single-factor ANOVA. Cerebellum: P= 0.8 (A) and P= 0.2 (B). Hippocampus: P= 0.6 (C) and P= 0.9 (D).

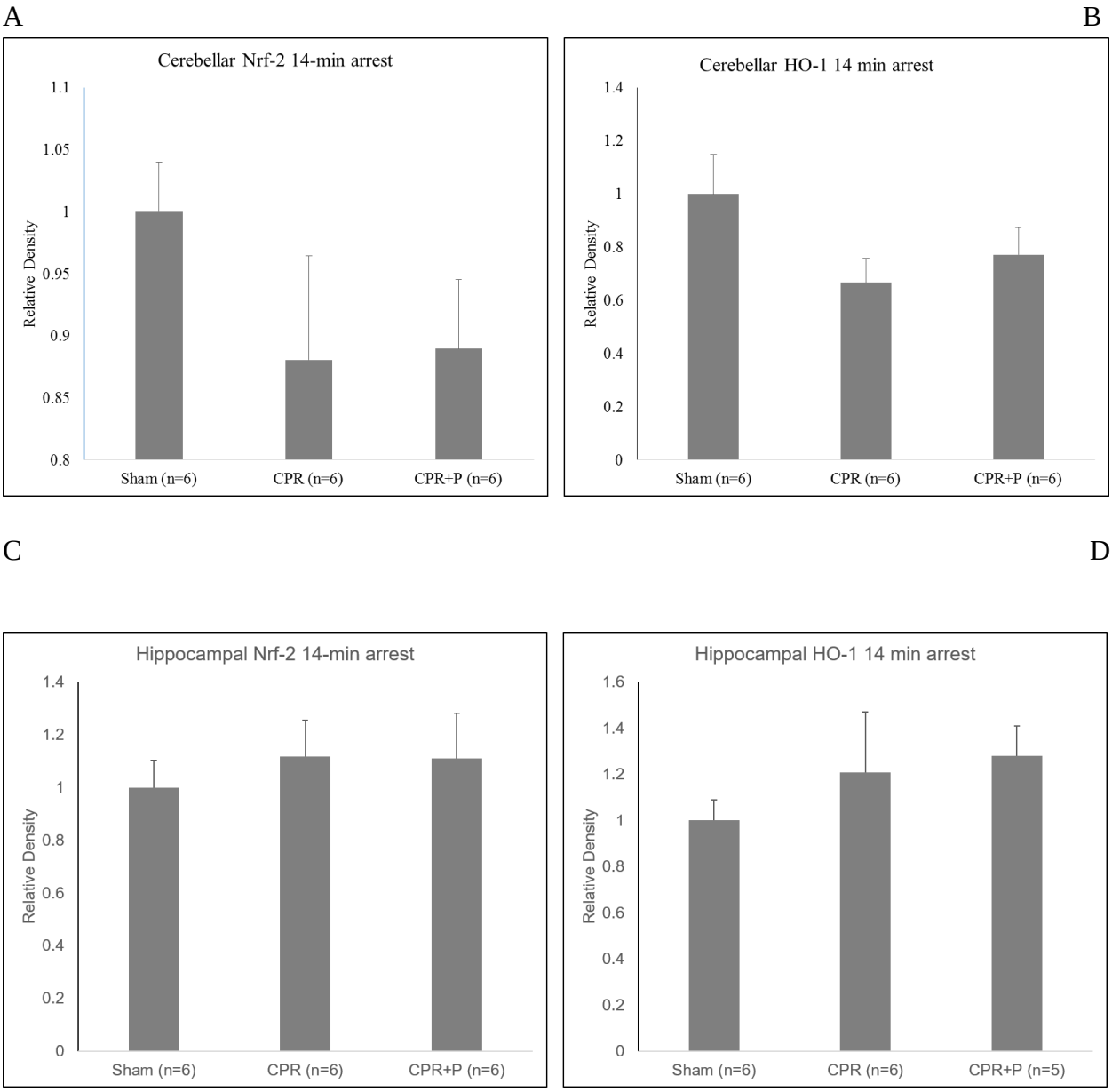

Figure 3. *Nrf-2 and HO-1 content 4 h after 10 min untreated cardiac arrest and 4 min CCR.* Nrf-2 and HO-1 content in the cerebellum (A,B) and hippocampus (C,D) 4 h ROSC after 10 min untreated cardiac arrest and 4 min CCR. Single-factor ANOVA. Cerebellum: P= 0.3 (A) and P= 0.2 (B). Hippocampus: P= 0.8 (C) and P= 0.6 (D).

A B C

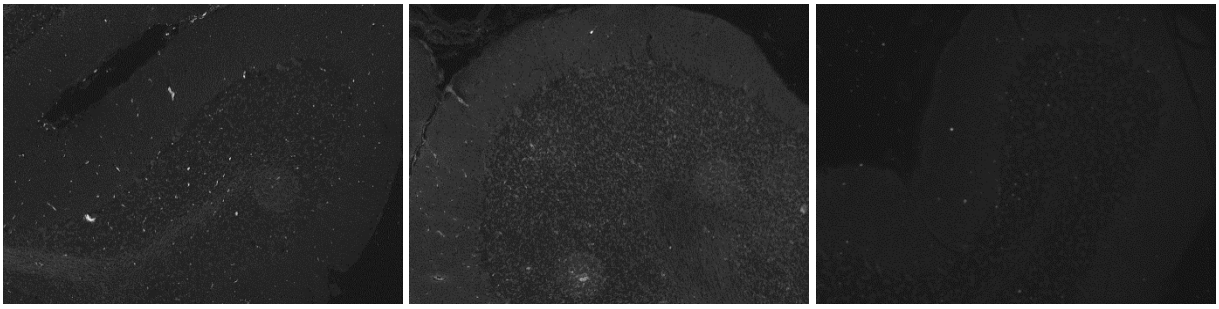

Figure 4. Representative TUNEL stain of the cerebellum at 3 d ROSC. A: sham, B: CPR, C: CPR+P

APPENDIX B

MINIREVIEW

Nguyen AQ, Cherry BH, Gary SF, Ryou MG, Mallet RT. Erythropoietin: powerful protection of ischemic and post-ischemic brain. *Exp Biol Med* 2014; **239** (11): 1461 – 1475

MINIREVIEW

Erythropoietin: Powerful Protection of Ischemic and Post-Ischemic Brain

Anh Q. Nguyen, M.S.,* Brandon H. Cherry, B.A.,* Gary F. Scott, Ph.D., Myoung-Gwi Ryou, M.S., Ph.D., Robert T. Mallet, Ph.D.

Department of Integrative Physiology and Cardiovascular Research Institute

University of North Texas Health Science Center

Fort Worth, TX

*These authors contributed equally to the preparation of this manuscript.

Running title: Brain Protection by Erythropoietin

Address for Correspondence:

Robert T. Mallet, Ph.D.

Department of Integrative Physiology

University of North Texas Health Science Center

3500 Camp Bowie Boulevard

Fort Worth, TX 76107-2699 USA

Telephone: 817-735-2260

Fax: 817-735-5084

Email: robert.mallet@unthsc.edu

Abstract

Ischemic brain injury inflicted by stroke and cardiac arrest ranks among the leading causes of death and long-term disability in the United States. The brain consumes large amounts of metabolic substrates and oxygen to sustain its energy requirements. Consequently, the brain is exquisitely sensitive to interruptions in its blood supply, and suffers irreversible damage after 10-15 minutes of severe ischemia. Effective treatments to protect the brain from stroke and cardiac arrest have proven elusive, due to the complexities of the injury cascades ignited by ischemia and reperfusion. Although recombinant tissue plasminogen activator and therapeutic hypothermia have proven efficacious for stroke and cardiac arrest, respectively, these treatments are constrained by narrow therapeutic windows, potentially detrimental side effects and the limited availability of hypothermia equipment. Mounting evidence demonstrates the cytokine hormone erythropoietin (EPO) to be a powerful neuroprotective agent and a potential adjuvant to established therapies. Classically, EPO originating primarily in the kidneys promotes erythrocyte production by suppressing apoptosis of proerythroid progenitors in bone marrow. However, the brain is capable of producing EPO, and EPO's membrane receptors and signaling components also are expressed in neurons and astrocytes. EPO activates signaling cascades that increase the brain's resistance to ischemia-reperfusion stress by stabilizing mitochondrial membranes, limiting formation of reactive oxygen and nitrogen intermediates, and suppressing pro-inflammatory cytokine production and neutrophil infiltration. Collectively, these mechanisms preserve functional brain tissue and, thus, improve neurocognitive recovery from brain ischemia. This article reviews the mechanisms mediating EPO-induced brain protection, critiques the clinical utility of exogenous EPO to preserve brain threatened by ischemic stroke and cardiac arrest, and discusses the prospects for induction of EPO production within the brain by the intermediary metabolite, pyruvate.

Keywords: apoptosis, blood brain barrier, hypoxia-inducible factor, nitric oxide synthase, peroxynitrite, pyruvate

Abbreviations: AMPA: α-amino-3-hydroxy-5-methyl-4-isoazolepropionic acid; BBB: blood brain barrier; cIAP2: c-inhibitor of apoptosis-2; CNS: central nervous system; CPR: cardiopulmonary resuscitation; EPO: erythropoietin; ΔG_{ATP}: Gibbs free energy of ATP hydrolysis; HIF: hypoxia-inducible factor; Keap1: Kelch-like ECH-associated protein 1; MCA: middle cerebral artery; MMP: matrix metalloproteinase; NF-κB: nuclear factor κB; NMDA: *N*-methyl-*D*-aspartate; NOS: nitric oxide synthase (eNOS: endothelial NOS; iNOS: inducible NOS; nNOS: neuronal NOS); Nrf2: nuclear factor erythroid 2-related factor 2; RONS: reactive oxygen and nitrogen species; ROSC: recovery of spontaneous circulation; rtPA: recombinant tissue plasminogen activator; TIMP: tissue inhibitor of metalloproteinase; TUNEL: terminal deoxynucleotidyl transferase dUTP nick end labeling; XIAP: X-linked inhibitor of apoptosis

Authors' contributions: AQN, BHC, GFS, MGR and RTM researched the literature and wrote the manuscript; AQN and RTM created the figures; RTM edited the manuscript.

Acknowledgements: This work was supported by research grant R01 NS076975 from the National Institute of Neurological Disorders and Stroke. AQN and BHC were supported by predoctoral fellowships from the UNTHSC Physician Scientist Program and the UNTHSC Neurobiology of Aging Program, respectively. GFS was supported by a Postdoctoral Fellowship from the National Institute of Neurological Disorders and Stroke.

Introduction

Ischemic syndromes of the central nervous system (CNS) are devastating to the victims and exact an enormous cost on society. Each year nearly 800,000 Americans experience a new or recurrent stroke, of which 87% are ischemic strokes.[1] The fourth leading cause of death and the leading cause of long-term disability in the United States, ischemic stroke kills approximately 130,000 Americans annually,[1,2] and many survivors experience persistent neurocognitive deficits that profoundly impact their quality of life. Nearly 7 million living American adults have suffered a stroke.[2]

Cardiac arrest, *i.e*. sudden cardiac death, which interrupts blood flow to the entire body including the CNS, kills approximately 350,000-400,000 Americans per year, many succumbing to massive brain injury inflicted by the ischemic insult.[3,4] Of the 70,000 cardiac arrest victims initially resuscitated each year in the U.S., approximately 70% of these victims die in the hospital, due primarily to extensive brain damage.[4-6] 40% of initial survivors of cardiac arrest enter a permanent vegetative state, and 80% of them die within 1 year of the event.[7] Only 5-14% of resuscitated victims of cardiac arrest survive without significant cerebral impairment.[8,9] As the American Heart Association's 2008 consensus statement on cardiac arrest laments, "*…little evidence exists to suggest that the in-hospital mortality rate of patients who achieve recovery of spontaneous circulation (ROSC) after cardiac arrest has changed significantly in the past half-century.*"[10]

In 2000, White *et al*. commented "*There are as yet no clinically effective therapeutic protocols for amelioration of brain damage by ischemia and reperfusion.*"[11] Regrettably this statement still holds true 14 years later. Aside from early restoration of cerebral perfusion, few interventions have been found to prevent ischemic brain injury, despite enormous investments in preclinical and clinical research. Indeed, recombinant tissue plasminogen activator (rtPA) and therapeutic hypothermia are the only interventions with proven clinical efficacy for ischemic stroke and

cardiac arrest, respectively. The challenge to any prospective treatment for CNS ischemia is the sheer complexity of the injury cascade triggered by ischemia-reperfusion. This article summarizes research conducted in the last two decades that has demonstrated the natural cytokine erythropoietin to be a potentially powerful neuroprotectant capable of intervening at multiple points in the injury cascade.

Mechanisms of injury in ischemic and post-ischemic brain

Ischemia and reperfusion ignite a complex cascade of brain injury (Figure 1) mediated by glutamate, intracellular Ca^{2+} overload, and reactive oxygen and nitrogen intermediates (RONS). The brain requires continuous delivery of oxygen and energy substrates via the cerebral circulation to sustain its high rate of ATP turnover. Occlusion of cerebral arteries or cardiac arrest interrupts oxidative metabolism, precipitating an abrupt decrease in the cytosolic Gibbs free energy of ATP hydrolysis (ΔG_{ATP}), the immediate energy source for the ion pumps that manage cytosolic free Ca^{2+} and repolarize the cell membrane. Depolarization of ischemic neurons causes excessive release of the excitatory amino acid neurotransmitter, glutamate.[12-14] Astrocytes normally protect neurons from glutamate toxicity by ATP-dependent sequestration of the neurotransmitter.[15] Loss of ΔG_{ATP} can cause reversal of glutamate transport, so astrocytes release glutamate. Moreover, RONS attack and disable glutamate transporters.

Glutamate binding to α-amino-3-hydroxy-5-methyl-4-isoazolepropionic acid (AMPA) and *N*-methyl-*D*-aspartate (NMDA) receptors located on neurons, glia and cerebrovascular endothelium[3] provokes additional depolarization and intense Ca^{2+} entry, sufficient to activate destructive Ca^{2+}-dependent proteases and phospholipases, culminating in cellular injury and death.[11,13,14] Among the Ca^{2+}-activated proteins is calcineurin, which activates the pro-apoptotic protein, Bad, a promoter of mitochondrial permeability transition, and the inducible nitric oxide synthase (NOS) isoform, iNOS, which catalyzes cytotoxic peroxynitrite ($ONOO^-$) formation.[11]

Intracellular Ca^{2+} overload also damages neurons by precipitating mitochondrial dysfunction. A spike in cytosolic Ca^{2+} concentration above 0.5 μM increases mitochondrial Ca^{2+} uptake, which provokes sequential opening of the mitochondrial permeability transition pores, collapse of the inner mitochondrial membrane potential, failure of oxidative phosphorylation, and generation of RONS.[14]

By binding to NMDA receptors, glutamate activates NOS[16,17] to produce excessive amounts of NO which condense with superoxide ($\bullet O_2^-$), yielding a cytotoxic product, $ONOO^-$.[18] At the onset of reperfusion there is a burst of RONS formation in the brain,[19] with microglia as a major source of NO.[20,21] In addition, ischemia-reperfusion can induce iNOS in astrocytes, causing these cells to release toxic amounts of NO. $ONOO^-$ initiates peroxidation of membrane phospholipids, nitrosylates tyrosine and cysteine residues in proteins, and depletes the intracellular antioxidant, glutathione.[18,22] Moreover, $\bullet O_2^-$ reacts with heme, liberating Fe^{2+} which catalyzes lipid peroxidation.[11] Hypothermic circulatory arrest in dogs activated cerebrocortical neuronal NOS (nNOS), which peaked at five times the pre-ischemic activity at 20 h post-arrest.[23] In a rat model of *status epilepticus*, bilateral microinjection of kainate induced hippocampal NO, $\bullet O_2^-$ and $ONOO^-$ formation, which led, sequentially, to inactivation of mitochondrial respiratory complex I, cytochrome *c* release, initiation and propagation of caspase activity and, finally, DNA fragmentation.[24]

Calcium[25] and RONS[26,27] induce astrocytes,[25,26,28] microglia[25] and cerebrovascular endothelium[29-31] to secrete matrix metalloproteinases (MMPs), a class of enzymes that degrade protein components of the extracellular matrix and of the tight junctions within the capillary endothelium that comprise the blood-brain barrier (BBB).[32-35] By oxidizing cysteine residues in the autoinhibitory domain of proMMPs, RONS activate MMPs by the 'cysteine switch' mechanism.[36] MMPs have been implicated in BBB disruption and brain edema and inflammation.[37,38] Interstitial brain edema, which develops within 1 hour after cardiac arrest or

stroke[3] is associated with poor neurological outcome. Brain edema increases intracranial pressure, which compresses the brain, lowers cerebral perfusion pressure and decreases cerebral blood flow. Moreover, BBB disruption allows neutrophils to infiltrate the brain parenchyma, where they release RONS and MMPs that further compromise the BBB. In rats subjected to cardiac arrest – CPR, neutrophils were detected in the susceptible brain regions within 6 h ROSC.[9]

Neuronal apoptosis after brain ischemia and reperfusion

Brain ischemia triggers two general processes of neuronal death: necrosis and apoptosis.[39,40] Which process predominates depends on the duration and intensity of the ischemic insult. In focal ischemia, necrosis is the major cause of cell death in the intensely ischemic core.[41] The core is surrounded by the less severely ischemic penumbra, where neurons primarily die by apoptosis, a highly regulated mechanism of cell death.[39,40,42,43] Because apoptosis is orchestrated by specific signaling elements, and because its measured pace affords time to initiate treatment, there are opportunities to salvage penumbral cells threatened by ischemic stroke.

Two distinct apoptotic cascades operate in the CNS (Figure 2).[39,40,44] In the extrinsic pathway, Fas ligand secreted by neurons, glia and inflammatory leukocytes binds its receptor, Fas, which, via its Fas-activated death domain, activates caspase 8, a protease that mediates apoptosis by activating caspase 3, the major 'executioner' caspase, and cleaves Bid to truncated Bid (*t*Bid), which combines with Bad in the mitochondrial membrane forming a channel. The release of cytochrome *c* through this channel initiates the intrinsic apoptotic pathway. In the cytosol, cytochrome *c* combines with Apaf-1, dATP and procaspase 9, forming the apoptosome which activates caspase 9 by cleavage of its procaspase. In a similar manner, caspase 9 activates caspase 3, which cleaves numerous targets culminating in the cell's destruction.

Neuronal apoptosis is well documented in animal models of cardiac arrest. For example, in rabbits placed on cardiopulmonary bypass and subjected to 2 h hypothermic circulatory arrest, 4 h reperfusion, hippocampal CA1 neurons exhibited caspase-3 activation and DNA fragmentation detectable by terminal deoxynucleotidyl transferase dUTP nick end labeling (TUNEL).[45] Böttiger, Teschendorf *et al*.[46,47] examined the progression of apoptotic cell death in rat brain over the first 7 d recovery from cardiac arrest – CPR. Post-arrest caspase activity followed different time-courses in different brain regions. In *nucleus reticularis thalami*, cortex and striatum, caspase activity and DNA fragmentation detected by TUNEL were already maximal at 6 h ROSC. In the hippocampal CA1 subregion, TUNEL-positive cells were first detected at 3 d, and increased further at 7 d. Thus, cardiac arrest activates caspases and apoptosis in vulnerable brain regions. A strong correlation emerged, both in extent and time-course, between caspase activation and DNA fragmentation.

Nitric oxide generated by the neuronal and inducible NOS isoforms has been implicated in CNS apoptosis following cardiac arrest. Incubation of hippocampal neurons with the NO donor sodium nitroprusside lowered Bcl-2 content and increased Bax content, and activated caspase-3.[48] In astrocyte-neuron cocultures, NOS inhibition by *L*-NMMA increased neuronal survival and prevented the decrease in Bcl-2 and increase in Bax initiated by hypoxia-reoxygenation.[49]

Erythropoietin: cerebroprotective cytokine

Erythropoietin, a 165 amino acid, 30.4 kDa glycoprotein with four oligosaccharide chains, was identified over 30 years ago as the hormone responsible for inducing erythropoiesis.[50] The liver is the major source of EPO during the prenatal period. Postpartum, 90% of EPO production shifts to the kidneys,[51] where peritubular interstitial fibroblasts near the corticomedullary border synthesize and secrete EPO in response to hypoxemia.[52-54] EPO circulates to the bone marrow, where it suppresses apoptosis of colony-forming unit erythroid cells, promoting the proliferation

and development of these cells into mature erythrocytes.[50,55] EPO's anti-apoptotic protection of erythroid precursors was an early indication that the cytokine might similarly protect cells in other tissues, including brain.

Studies in a variety of animal models of CNS ischemia-reperfusion[56,57] have defined EPO's robust neuroprotective properties in brain.[58-61] In stroke-prone spontaneously hypertensive rats, cerebroventricular infusion of EPO salvaged cerebral cortex and motor function following permanent middle cerebral artery (MCA) occlusion.[62] The abundance of mRNA encoding the EPO receptor was elevated in the ischemic penumbra, potentially enhancing the neuroprotective capabilities of EPO and preventing infarct expansion. Injection of EPO (5,000 IU/kg, *ip*) at the start of 60 min MCA occlusion in rats decreased infarct size by 75% and suppressed apoptosis in the ischemic penumbra.[63] Erythropoietin (1,000 IU/kg, *ip*) decreased ethanol-induced apoptosis in cerebellum, prefrontal cortex, and hippocampus of mice given subcutaneous ethanol injections.[64] In gerbils subjected to 5 min bilateral carotid artery occlusion,[65] recombinant human EPO, when injected (50 or 100 IU, *ip*) at the time of reperfusion, attenuated hippocampal edema, lipid peroxidation and neuronal death, and suppressed NO formation. Thus, EPO treatment may protect sensitive brain regions, at least in part by suppressing NOS.

Transgenic human EPO expression in mouse brain doubled cerebrocortical and striatal EPO content *vs.* wild type, and decreased infarct volume by 84% following 90 min middle cerebral artery occlusion and 72 h reperfusion.[66] In this study, TUNEL-positive and caspase-3-positive neurons were decreased by ~50 and ~75%, respectively, in transgenic *vs.* wild-type striatum. EPO expression sharply increased phosphor-activation of Erk-1, Erk-2 and Akt; the Erk inhibitor PD98059 and the PI3K/Akt inhibitor Wortmannin both prevented the reduction in TUNEL- and caspase-3-positive neurons, implicating both kinases in the neuroprotective cascade.

EPO has been found to be cerebroprotective even when its administration is delayed. In rats, exogenous EPO decreased infarct volume even when given 6 h after MCA occlusion-reperfusion.[67] In a rat model of traumatic brain injury, EPO (5,000 IU/kg, ip) given 24 h post-injury produced significant improvement in neurological function and decreased neuronal loss in the hippocampal CA3 subregion, and increased neurogenesis in the injured cortex and dentate gyrus.[68] Erythropoietin, injected *ip* in rats subjected to MCA occlusion, reduced infarct volume by 70-75% whether given 24 h before, during or 3 h after occlusion.[63] EPO also sharply lowered TUNEL-positive cells in the ischemic penumbra of these rats. Importantly, some protection was still seen when EPO was administered as late as 6 h post-occlusion, although not at 9 h post-occlusion. EPO's neuroprotective efficacy for at least the first several h after the ischemic insult expands opportunities for its therapeutic application for acute CNS ischemia.

Although the preponderance of preclinical evidence shows EPO to be neuroprotective, a study in rats subjected to 6 min pre-treatment ventricular fibrillation, 2 min CPR, defibrillatory countershocks and up to 7 d recovery yielded less favorable outcomes.[69] EPO (5000 IU/kg), given *iv* 5 min before cardiac arrest, then injected *ip* at 24 and 72 h post-arrest, failed to suppress total caspase or caspase-3 activities, prevent DNA fragmentation and neuronal degeneration in the hippocampal CA1 subregion, or improve neurological deficit score at 1, 3 or 7 d recovery. These negative findings merit attention in light of the equivocal results of clinical trials of EPO for CNS ischemia described below.

Mechanisms of erythropoietin neuroprotection

Erythropoietin is an especially promising neuroprotectant because it potentially intervenes at several points in the apoptotic pathway (Figure 2). Brain neurons express homodimeric EPO receptors; EPO binding triggers reciprocal auto-phosphorylation of the two monomers, which in turn phosphorylate and activate the signaling kinase, Jak-2.[70] Multiple protein kinases are

recruited to the EPO receptor and phosphorylated by activated Jak2, initiating a complex anti-apoptotic signaling cascade (Figure 2). Several cytoprotective mechanisms activated by EPO signaling are summarized in the following subsections.

Increased anti-apoptotic proteins and Bcl-X_L/Bax ratio

The relative cellular contents of anti- *vs*. pro-apoptotic members of the Bcl protein family exert a profound effect on cell survival *vs*. apoptosis.[71,72] EPO enhancement of neuronal Bcl-X_L content plays a pivotal role in EPO's anti-apoptotic neuroprotection.[60] In cultured rat cortical microglia and astrocytes, EPO shifted the Bcl/Bax ratio in favor of anti-apoptotic Bcl.[73] In gerbils subjected to CNS ischemia, EPO up-regulated Bcl-X_L mRNA and protein in hippocampal CA1 neurons, and prevented learning disability.[74] Transgenic over-expression of human EPO in murine striatum enhanced ischemic induction of Bcl-X_L.[66] Activated Akt phosphorylates the pro-apoptotic protein, Bad, preventing the latter's insertion into the mitochondrial membrane.[75] Phosphorylated STAT5 activates nuclear factor κB (NF-κB), which promotes expression of the anti-apoptotic proteins X-linked inhibitor of apoptosis (XIAP) and c-inhibitor of apoptosis-2 (cIAP2) in cultured cerebrocortical neurons.[76] c-IAP2 suppresses caspases 3, 8 and 9;[77] XIAP binds and suppresses caspases 3 and 9,[78] and inhibits activation of procaspase 9 within the apoptosome.[79]

Enhancement of the brain's antioxidant defenses

Preclinical studies have demonstrated EPO induction of key components of the brain's antioxidant armamentarium. In rats, *ip* injection of 1,000 IU/kg EPO at 8 h intervals beginning 5 min after induction of subarachnoid hemorrhage increased gene expression and content of the antioxidant enzymes glutathione *S*-transferase, NAD(P)H:quinone oxidoreductase-1 and heme oxygenase-1, and blunted cerebrocortical apoptosis, brain edema and BBB disruption 48 h later.[80] EPO (1,000 IU/kg, *ip*) increased glutathione peroxidase activity and decreased lipid

peroxidation in the brains of ethanol-intoxicated mice.[64] In brains of rats subjected to hyperoxia-imposed oxidative stress, EPO (20,000 IU/kg, *ip*) upregulated heme oxygenase-1, dampened lipid peroxidation, and prevented the decline in glutathione redox state.[81]

Recent studies implicate the transcription factor nuclear factor erythroid 2-related factor 2 (Nrf2) in EPO's induction of antioxidant enzymes. Nrf2 activates expression of a gene program encoding several phase II defense enzymes that afford antioxidant and anti-inflammatory cytoprotection,[82,83] including heme oxygenase-1, peroxiredoxin, superoxide dismutase, glutathione peroxidase, NAD(P)H:quinone oxidoreductase-1, and the glutathione synthesizing enzyme glutamate-cysteine ligase.[80,84,85] Binding of a regulatory protein, Keap1, sequesters Nrf2 in the cytoplasm, targeting Nrf2 for polyubiquitinylation and proteasomal degration and, thus, silencing the Nrf2 gene program.[86-88] RONS oxidize Keap1 sulfhydryls,[83] liberating Nrf2 which translocates to the nucleus and binds the antioxidant response element in the promoter of phase II response genes. EPO is proposed[89] to activate Nrf2 by activating Akt and Erk, which in turn phosphor-activate eNOS, thereby increasing NO formation in the neuronal cytosol (Figure 2). NO or its derivative $ONOO^-$ release Nrf2 by nitrosylating Keap1's regulatory sulfhydryls.[90] Accordingly, pharmacological inhibition of Akt and Erk blunted EPO-induced nuclear translocation of Nrf2 and heme oxygenase-1 expression in cultured human neural cells.[84]

Suppression of matrix metalloproteinases and inflammation

Li *et al*.[91] studied mice subjected to intracerebral hemorrhage, a pro-inflammatory event. EPO (*ip* injection), given during the first 3 d post-hemorrhage, preserved the BBB, prevented tissue edema, preserved collagen, restrained increases in MMP-2 content and enhanced content of the endogenous MMP inhibitor, tissue inhibitor of metalloproteinase-2 (TIMP-2). In human erythroid progenitor cells, EPO suppressed MMP-9 secretion and induced TIMP-1 expression and secretion.[92] ERK1/2 inhibitors PD98059 and U0126 and PI3K inhibitor LY294002 blocked

EPO suppression of MMP-9 and induction of TIMP-1. These findings are empirical evidence that EPO preserves the extracellular matrix and prevents CNS injury by inducing TIMPs and suppressing MMPs. In rats undergoing MCA occlusion, EPO (5000 IU/kg body wt, *ip*) decreased astrocyte activation and recruitment of leukocytes and microglia into the infarct, and suppressed formation of the pro-inflammatory cytokines IL-6, TNF and monocyte chemoattractant protein-1 by >50%.[93]

Erythropoietin dampens glutamate excitotoxicity

The excitatory amino acid glutamate provokes neuronal Ca^{2+} entry via NMDA and AMPA channels. Excessive glutamatergic activity in ischemic and post-ischemic brain provokes cytotoxic Ca^{2+} overload. EPO suppressed glutamate release from hippocampal and cerebellar neurons exposed to 'chemical ischemia' produced by excess Ca^{2+} or ionomycin,[94] in spinal neurons exposed to excitotoxic kainic acid[95] and in electrically stimulated hippocampal slices.[96] By dampening glutamate release, EPO may ameliorate NMDA- and AMPA-channel-mediated Ca^{2+} entry, thereby preventing excitoxicity and minimizing ATP demands for Ca^{2+} extrusion by the energy-depleted neurons.

Erythropoietin modulation of nitric oxide synthase

Erythropoietin exerts divergent effects on the three NOS isoforms. EPO dampened expression of iNOS in oligodendrocytes exposed to inflammatory stimuli.[89] Transgenic expression of human EPO in murine brain suppressed nNOS and iNOS expression in striatal neurons.[66] In gerbils subjected to bilateral carotid occlusion, post-ischemic EPO injection (*c*. 800-1500 100 IU/kg, *ip*) 60 min after reperfusion lowered NO formation in the hippocampus, in parallel with EPO's suppression of lipid peroxidation and tissue edema.[65] Neuronal NOS is Ca^{2+}-activated, so EPO's suppression of glutamatergic signaling and the resultant Ca^{2+} overload may contribute

to the decreased NOS activity. In contrast, EPO has been shown to activate the endothelial NOS isoform (eNOS), which generates the moderate amounts of NO which activate Nrf2.[84,89,90]

Clinical trials: exogenous erythropoietin for brain ischemia

As Pytte and Steen[97] noted, "*...the last three decades have been filled with disappointments regarding pharmacological treatment of cardiac arrest patients*." Indeed, an array of potential treatments has failed to impart significant clinical benefit, including treatments which afforded substantial neuroprotection in animal models. Clinical trials of EPO for brain ischemia have yielded mixed outcomes. Ehrenreich *et al*.[98] conducted a pioneering clinical trial in which *iv* injections of 33,000 IU EPO, daily for the first 3 days after stroke, improved recovery of neurocognitive function and decreased the persistent neurological deficit evident 18-30 d after stroke. EPO was efficacious when the first dose was given up to 8 h after the onset of stroke symptoms, but massive doses of EPO were required for clinical benefit.

Cariou *et al*.[99] conducted a clinical trial of EPO for brain protection following cardiac arrest. Five intravenous injections of 40,000 IU EPO at 12 h intervals, beginning 42-72 min after out-of-hospital cardiac arrest, failed to improve neurological recovery assessed at day 28 post-arrest. EPO did produce modest increases in hematocrit and hemoglobin content at 14 d post-arrest *vs.* non-EPO controls. A small trial by Grmec *et al*.[100] showed that a single, massive *iv* bolus of EPO (90,000 IU), given by emergency responders within 1-2 min of initiating CPR, did increase rates of initial defibrillation, survival to ICU admission, 24 h survival and survival to hospital discharge. Despite these promising short-term outcomes, EPO treatment did not improve neurological outcome.

Ehrenreich *et al*.[101] studied 460 patients with stroke in the MCA perfusion territory. Patients received three *iv* injections of 40,000 IU EPO, at 6, 24 and 48 h after onset of symptoms. EPO increased death rate (16.4%; 42/256) *vs*. placebo (9.0%; 24/266) and incidence of

cerebrovascular hemorrhage. These adverse effects were seen almost entirely in patients receiving recombinant tissue plasminogen activator (rtPA) beyond its therapeutic window, which is limited to the first 4.5 h after stroke onset.[102,103]

A recent preclinical study by Jia *et al*.[104] provided valuable insights regarding the detrimental interaction of rtPA and EPO. Rats were subjected to embolic MCA occlusion, followed by EPO (5000 IU/kg, *ip* injection) and rtPA treatment (10 mg/kg, *iv* injection) at 2 or 6 h MCA occlusion. When administered at 2 h MCA occlusion, EPO and rtPA were similarly effective at reducing infarct size, but the combination of the two afforded no additional protection over the separate treatments. When administered at 6 h MCA occlusion, although EPO alone decreased infarct size, neither rtPA alone or combined with EPO afforded protection. Indeed, rtPA increased intracerebral hemorrhage at 6 h MCA occlusion *vs*. saline-injected control rats, and the combined EPO + rtPA treatment increased intracerebral hemorrhage even more than rtPA alone. The combined treatments, but not EPO or rtPA alone, activated MMP-9 via nuclear factor κB (NF-κB) signaling in cerebral microvessels at 6 h MCA occlusion. Thus, when EPO and rtPA are coadministered beyond rtPA's therapeutic window, the result is activation of MMP-9, culminating in cerebral hemorrhage and infarct expansion.

How readily does erythropoietin traverse the blood-brain barrier?

The transfer of systemically administered EPO from the cerebral circulation across the BBB into the brain parenchyma is less than 1% efficient;[67,105,106] consequently, high doses are required to achieve therapeutically effective EPO concentrations within the brain.[60] In mice a tiny fraction of intravenously injected EPO, 0.05-0.1% of the injected dose, entered the brain parenchyma, an efficiency that approximated that of albumin.[105] In fetal sheep and monkeys injected with high doses of EPO, the EPO activity in the cerebrospinal fluid was only about 2% of the circulating activity.[106] Similar results were reported in humans;[107] indeed, the dosages of recombinant EPO

required to produce neuroprotection (1,000-30,000 IU/kg) are well above those (<500 IU/kg) used to treat anemia.[108] Other studies showed that circulating EPO can only enter the brain if the BBB has been compromised. In patients with traumatic brain injury, the appearance of EPO in the ventricular cerebrospinal fluid correlated with the extent of BBB disruption.[109] In a patient undergoing resection of a brain tumor, a single *iv* injection of 6000 IU recombinant human EPO increased serum EPO activity from *c*. 13 to >6500 IU/l for at least 60 min, but there was no increase in EPO activity in the cerebrospinal fluid.[110] Collectively, these studies demonstrate that circulating EPO does not efficiently cross the intact BBB, but can pass from blood to brain if the BBB is disrupted. The high doses of exogenous EPO necessary to surmount the intact BBB may increase blood coagulability enough to precipitate thrombotic events[111] and, when combined with tPA therapy, produce deadly hemorrhagic transformation.[104,112]

Erythropoietin expression within the brain

Noguchi *et al*.[75] stated "*EPO production in neural cells can increase the local bioavailability of EPO independent of transit through the blood-brain barrier*." The brain possesses the molecular machinery to manufacture EPO intrinsically, on the "leeward" side of the blood-brain barrier.[59,113-115] Indeed, EPO mRNA abundance in the cerebellum, pituitary gland and cerebrocortex rivaled that of the conventionally EPO-expressing liver and kidneys.[116] Substantial EPO expression was detected in several brain regions[116] and spinal cord[117] in preterm human fetuses. Nagai *et al*.[118] examined expression of EPO and its receptors in cultured human astrocytes, neurons, microglia and oligodendrocytes. Only the astrocytes expressed EPO mRNA. Neurons, astrocytes and microglia possessed EPO receptors; the oligodendrocytes did not. In gerbils, sequestration of intrinsic EPO by injection of soluble EPO receptors into the cerebral ventricles intensified neuronal death in the hippocampus following a moderate, ordinarily non-injurious ischemic challenge,[119] suggesting that EPO production within the brain contributed to a basal level of neuroprotection.

As in kidney,[120,121] hypoxia is a powerful inducer of EPO expression in brain.[94,122] This induction is mediated by hypoxia inducible factor-1 (HIF-1), an O_2-regulated transcription factor that activates the expression of an extensive gene program encoding proteins that increase cellular resistance to hypoxia and ischemia.[51,123] HIF-1 is a heterodimer containing two subunits: a constitutive β subunit and an α subunit which is also constitutively expressed but, in well-oxygenated tissues, rapidly undergoes prolyl hydroxylase-catalyzed, Fe^{2+}- and α-ketoglutarate-dependent hydroxylation of two prolyl residues, earmarking the subunit for poly-ubiquitinylation and proteosomal degradation (Figure 2).[124] Hypoxia stabilizes HIF-1α in two ways:[114] it deprives prolyl hydroxylase of the O_2 required for HIF-1α hydroxylation, and it causes the mitochondrial electron transport chain to generate RONS which convert Fe^{2+} to Fe^{3+}, removing the source of electrons for the prolyl hydroxylase reaction. Thus stabilized, HIF-1α diffuses from the cytosol to the nucleus and combines with the β subunit, forming the active HIF-1 transcription factor. HIF-1 then binds the hypoxia response element in the promoter regions of an extensive array of genes, including EPO, vascular endothelial growth factor, the entire glycolytic enzyme sequence, and a host of other proteins which, collectively, increase cellular resistance to hypoxia and ischemia.[114] Thus, embryonic mouse neocortical neurons and astrocytes expressed EPO mRNA and protein when exposed to hypoxia or the hypoxia-mimetic chemicals desferrioxamine or cobalt chloride.[125] While EPO is intensely expressed by astrocytes, its membrane receptors are predominantly located in neurons and cerebrovascular endothelium. EPO secreted by astrocytes may function in a paracrine manner (Figure 2).

By effectively surmounting the BBB, while potentially avoiding the untoward effects of massive systemic EPO dosages, intrinsic EPO expression within the brain parenchyma addresses the important limitations of exogenous EPO. However, a strategy of subjecting critically ill patients to systemic hypoxia in the midst of an acute CNS ischemic event would be dangerous and

clinically unacceptable. Is there a safe, simple means of inducing EPO expression in the brain for treatment of acute CNS ischemia?

Neuroprotection by exogenous pyruvate

The neuroprotective capabilities of pyruvate, a natural intermediary metabolite and energy substrate, have been demonstrated in a variety of brain preparations. Although an exhaustive review of these studies is beyond the scope of this article, several reports exemplifying the neuroprotection afforded by pyruvate are summarized here. Lee *et al*.[126] subjected rats to 12 min forebrain ischemia by bilateral occlusion of the carotid arteries. Sodium pyruvate (250, 500 or 1000 mg/kg) sharply lowered mortality to 1 of 26 rats *vs*. 18 of 31 NaCl-injected control rats when injected *ip* at 30 min or 1 h reperfusion, but was ineffective when given at 2 or 3 h reperfusion. In the NaCl-injected rats, extensive cell death was detected in the post-ischemic brain 72 h after ischemia-reperfusion; pyruvate (500 mg/kg) prevented cell death. Thus, pyruvate injected *ip* protected brain from ischemia, even when given 30 or 60 min after reperfusion. In a swine model of hemorrhagic shock, Mongan *et al*.[127] showed that intravenous resuscitation with sodium pyruvate suppressed excitotoxic glutamate release within the cerebral cortex and slowed the post-hemorrhage decline in cortical electrical activity. Kim *et al*.[128] studied kainate-induced epileptic seizures in rats. Sodium pyruvate (500 mg/kg, *ip*) was injected 30 or 150 min after kainate (10 mg/kg, *ip*). Pyruvate sharply lowered, by 60-85%, cell death in hippocampal CA1, CA3 and dentate gyrus. Zinc injures neurons by activating metallothioneins, interfering with mitochondrial respiration, inducing ROS formation by the respiratory chain, and activating NADPH oxidase to produce $\cdot O_2^-$. Pyruvate prevented intracellular zinc accumulation in the studies of Lee *et al*.[126] and Kim *et al*.[128]

In a study by Sharma *et al*.,[129] pyruvate prevented simulated ischemia-induced damage and death of cultured rat astrocytes subjected to simulated ischemia-reperfusion. Cells were

challenged by 6 h profound, substrate-free hypoxia, then reoxygenated for another 6 h in presence of pyruvate or glucose. Pyruvate maintained cellular morphology, prevented lactate dehydrogenase leakage, a measure of membrane rupture and cell death, and suppressed early apoptotic events including mitochondrial cytochrome *c* release, caspase-3 cleavage and activation, and poly(ADP-ribose) polymerase (PARP) cleavage, in a manner superior to glucose.

In anesthetized dogs, Sharma *et al*.[130] evaluated pyruvate protection of the brain threatened by cardiac arrest and resuscitation. The heart was arrested by epicardial shock, then, after 5 min arrest, cardiac massage was performed for 5 min before defibrillation by epicardial countershocks. Sodium pyruvate or NaCl were infused *iv* (0.125 mmol • kg^{-1} • min^{-1}) during cardiac massage and the first 60 min recovery, and then the dogs were recovered for 3 days. The pyruvate infusion increased arterial plasma pyruvate concentration from 0.22 ± 0.02 to 3.6 ± 0.2 mM; pyruvate concentration subsided within 30 min post-infusion.[131] Pyruvate sharply lowered neurological deficit 24 and 48 h post-arrest, particularly the deficits in motor function, *vs*. the NaCl-infused dogs. Pyruvate also lowered neuronal death and caspase-3 activity in the hippocampal CA1 subregion and prevented degeneration of cerebellar Purkinje cells.

Fukushima *et al*.[132] demonstrated pyruvate protection of brain in a rat model of cortical contusion injury. Sodium pyruvate was injected (500 or 1000 mg/kg, *ip*) 5 min after contusion. Intracerebral pyruvate detected by microdialysis plateaued at 30-75 min after pyruvate injection, confirming that pyruvate traversed the BBB in this model. Both doses of pyruvate sharply lowered the intensity of cortical cell death at 6 h post-contusion.

Recently, Ryou *et al*.[133] examined pyruvate's neuroprotective capabilities in a rat model of ischemic stroke, in which the left MCA was occluded by advancing a suture into the artery for 120 min; suture withdrawal abruptly reperfused the ischemic tissue. Sodium pyruvate or NaCl

control were infused *iv* from 60 min occlusion until 30 min reperfusion. Analyses of brains harvested at 24 h reperfusion revealed that pyruvate infusion produced an 84% reduction in infarct volume and 80% reduction in apoptotic nuclei *vs*. the respective control values. Indeed, the reduction in infarct volume afforded by pyruvate was nearly identical to that produced by transgenic human EPO expression in Kilic *et al*.'s studies in mice subjected to MCA occlusion-reperfusion.[66] Collectively, these and other reports demonstrate that timely administration of pyruvate can minimize brain injury from ischemia-reperfusion and other stresses.

Pyruvate traverses the blood brain barrier

Many potentially cerebroprotective compounds have proven ineffective due to their inability to surmount the BBB. In contrast, pyruvate is readily transferred across the BBB by a high-affinity, proton-linked monocarboxylate transport mechanism in the vascular endothelium (Figure 3).[134,135] Monocarboxylate transporters also are abundant in the plasma membranes of neurons and astrocytes,[136] affording pyruvate uptake by the brain parenchyma. Using cerebrocortical microdialysis in a pig model of hemorrhagic shock, Mongan *et al*.[127] showed that intravenous pyruvate (0.9 mmol • kg^{-1} bolus followed by 0.08 mmol • kg^{-1} • min^{-1} infusion), producing a sustained arterial plasma pyruvate concentration of 5-6 mM, increased pyruvate concentration in cerebrocortical microdialysate from 0.09 to 0.43 mM. Although the fractional recovery of pyruvate in the microdialysate wasn't reported, the results suggest pyruvate does indeed cross the blood-brain barrier, but doesn't equilibrate. On the other hand, the neurons and astroglia may have avidly taken up the pyruvate, keeping the interstitial concentration low. Cerebrocortical microdialysis studies in rats by Fukushima *et al*.[132] confirmed that pyruvate, injected *ip* appeared in the brain parenchyma over a period of several minutes. Additional evidence that pyruvate cerebroprotection requires pyruvate transport was reported by Wang *et al*.,[137] who showed *ip* injections of 500 mg/kg sodium pyruvate decreased infarct size nearly

50% in rats subjected to 65 min MCA occlusion, and that this cerebroprotective effect was blunted by the monocarboxylate transporter antagonist α-cyano-4-hydroxycinnamate.

Cerebroprotective mechanisms of pyruvate

Pyruvate may preserve post-ischemic brain by several mechanisms. An energy-yielding, oxidizable fuel,[138,139] pyruvate augments oxidative metabolism, thereby generating ATP and phosphocreatine[127] and, thus, increasing ΔG_{ATP}, the thermodynamic driving force for cellular function. Pyruvate also affords three general antioxidant mechanisms:[139,144] (1) as an alpha-keto carboxylate, pyruvate can react with and directly detoxify H_2O_2, lipid peroxides and $ONOO^-$;[140-142] (2) pyruvate oxidizes the cytosolic NADH/NAD^+ redox couple, thereby decreasing availability of NADH to NADH oxidase, which generates $\bullet O_2^-$;[143] (3) pyruvate bolsters intracellular antioxidant defenses by increasing NADPH/$NADP^+$ and, thus, glutathione redox state, the major intracellular antioxidant system.[131,145] Pyruvate suppressed DNA fragmentation, a critical event in the progression of apoptosis (Figure 2) in a cultured renal tubular epithelial cell line subjected to antimycin A-induced chemical hypoxia,[146] as well as in H_2O_2-challenged mouse thymocytes[147] and post-ischemic rat liver.[148] Pyruvate suppression of H_2O_2-induced glutathione depletion, caspase activation and death of cultured human umbilical vein endothelial cells[149,150] paralleled intense Erk1/2 phosphorylation[150] as well as increased Bcl-2 and decreased Bax contents and, thus, increased anti-apoptotic Bcl-2/Bax ratio.[149] Although pyruvate's actions in cerebrovascular endothelium are not yet known, effects such as these could stabilize integrity of the cerebrovascular endothelium and blood brain barrier in the face of ischemia-reperfusion.

Several reports over the past decade have demonstrated pyruvate's antioxidant and anti-apoptotic actions in brain preparations. Wang *et al*.[151] showed that cultured astrocytes released pyruvate which protected co-cultured neurons from copper-catalyzed cysteine autoxidation, a source of hydroxyl radicals. In rat primary neurons, 2.5 mM pyruvate suppressed β-amyloid-

induced dichlorofluorescein fluorescence, a measure of ROS formation.[152] In another study[153] pyruvate protected murine neuroblastoma cells from cell death triggered by H_2O_2 and 6-hydroxydopamine, an inducer of H_2O_2 formation. Wang *et al*.[154] exposed cultured human neuroblastoma SK-N-SH cells to 150 μM H_2O_2, which provoked mitochondrial superoxide formation, collapsed the mitochondrial membrane potential, and killed 85% of the cells. Pyruvate concentration-dependently suppressed cell death; 1-4 mM pyruvate completely prevented H_2O_2-induced cell death, even when its administration was delayed until 1 h after H_2O_2 exposure. Pyruvate also suppressed H_2O_2-induced intracellular and mitochondrial RONS formation, with 2 mM pyruvate exerting near-complete prevention of RONS. Massive mitochondrial depolarization by 3 mM H_2O_2 was prevented by 1 mM pyruvate.

Pyruvate's anti-inflammatory actions have been demonstrated in several organs, including brain. Cardiopulmonary bypass provokes a systemic inflammatory response that damages internal organs and compromises post-surgical recovery.[155,156] In pigs subjected to cardioplegia-induced cardiac arrest and maintained on-pump, pyruvate-fortified cardioplegia suppressed the pro-inflammatory C-reactive protein, enhanced anti-inflammatory cytokine IL-10, prevented activation of MMP-9, suppressed neutrophil infiltration into the myocardial parenchyma, and blunted nitrotyrosine formation, a measure of nitrosative stress.[157] These effects were seen 4 h after pyruvate treatment. In dogs, cardiac arrest and cardiopulmonary resuscitation produced a striking increase in hippocampal MMP activity 3 d later; pyruvate infusion during cardiac massage and the first 60 min recovery suppressed this MMP activation by 80%.[130] Sharma and Mongan[158] examined the anti-inflammatory capabilities of low-volume, hypertonic sodium pyruvate resuscitation in a rat model of hemorrhagic shock. The pyruvate treatment ameliorated liver injury, suppressed serum and hepatic pro-inflammatory cytokines, NOS and cyclooxygenase-2 activities, caspase-3 activation and poly(ADP ribose) polymerase cleavage and lipid peroxidation, and attenuated liver injury. Thus, pyruvate can supply energy

substrate, detoxify RONS and suppress inflammation and apoptosis in CNS threatened by acute ischemia-reperfusion.

Induction of erythropoietin and neuroprotection by pyruvate

Studies in a cultured human glioma cell line revealed a novel action of pyruvate: the stabilization of HIF-1α despite the presence of abundant O_2.[159,160] Here, pyruvate and oxaloacetate, an α-keto carboxylate structural analogue and product of mitochondrial pyruvate carboxylation (Figure 3),[139] suppressed prolyl hydroxylase activity, apparently by competing with the enzyme's natural substrate, α-ketoglutarate, for access to the enzyme's catalytic domain.[161] These findings raised the possibility that pyruvate could suppress prolyl hydroxylation and subsequent polyubiquitination and degradation of HIF-1α and, thus, augment expression of HIF-1-activated genes, including EPO, in normal tissue.

Ryou *et al*.'s studies in a porcine cardiopulmonary bypass model revealed, for the first time, pyruvate induction of EPO synthesis in a mammalian organ, the heart.[162] Here, pyruvate-enriched cardioplegia stabilized HIF-1α content, which paralleled robust myocardial mRNA expression and synthesis of EPO. Elements of EPO's intracellular signaling cascades, Erk and eNOS, were activated following pyruvate cardioplegia. Thus, temporary (60 min) pyruvate treatment evoked EPO expression and its cytoprotective signaling cascades that persisted several h after treatment. Indeed, the myocardium released EPO into the coronary venous effluent for at least 4 h after crossclamp release and washout of the pyruvate-enriched cardioplegia.

In Ryou *et al*.'s rat model of ischemic stroke,[133] pyruvate treatment increased cerebral EPO content severalfold, in the ischemic tissue as well as the contralateral, non-ischemic hemisphere. Additional experiments were conducted in glioma and neuronal cell lines subjected to oxygen-glucose deprivation and reoxygenation, a cell culture model of ischemia-

reperfusion, to assess the roles of HIF-1α, EPO and the downstream signaling in pyruvate's neuroprotection.[133] Five and 10 mM pyruvate afforded significant cytoprotection, paralleled by marked increases in HIF-1α and EPO contents and phosphor-activation of Akt but not Erk. Incubation with soluble EPO receptor, and siRNA suppression of HIF-1α expression, blunted pyruvate's cytoprotection. Collectively, these results support the hypothesis that pyruvate prevents ischemic injury of brain, at least in part by stabilizing HIF-1α, thereby increasing EPO synthesis and activating the cytoprotective Akt signaling cascade.

Recently Ryou *et al*. tested pyruvate's ability to limit rtPA toxicity in a cultured neuronal cell line and primary microvascular endothelial cells.[163] Six and 10 h of oxygen-glucose deprivation produced marked neuronal cell death which was exacerbated by rtPA. Pyruvate (8 mM) prevented cell death in the absence of rtPA, dampened cell death in the rtPA-exposed cells, suppressed rtPA-induced RONS formation, and sharply lowered basal and rtPA-induced MMP-2 content, while inducing Akt and Erk phosphorylation. Interestingly, pyruvate alone or combined with rtPA increased cellular content of monocarboxylate transporter-2 *vs*. the respective pyruvate-free conditions. These results suggested that pyruvate might extend rtPA's therapeutic window by dampening rtPA-induced cytotoxicity; it is essential to test this interaction in intact animals.

Conclusion and perspectives

Cardiac arrest and stroke, two of the leading causes of death and long-term disability in the United States and Europe, heretofore have proven refractory to pharmacological interventions. Extensive preclinical research has identified EPO as a potentially powerful treatment to limit the ischemic damage to the CNS inflicted by these scourges. Unlike agents that failed to protect the CNS in clinical trials, EPO is not a "one trick pony;" it activates several intracellular mechanisms that intervene at multiple steps in the cascade of ischemia-reperfusion injury

(Figure 2). However, despite favorable outcomes in early clinical trials, two factors threaten to limit EPO's clinical utility for stroke and cardiac arrest: its potentially dangerous interaction with rtPA inducing hemorrhagic transformation within the cerebral circulation, and the high dosages of EPO required to surmount the BBB.

The brain's intrinsic ability to express and synthesize EPO may afford an alternative strategy: the administration of compounds that promote EPO gene expression within the brain by stabilizing the transcription factor HIF-1, the principal activator of EPO gene expression. Pyruvate offers several advantages as an enhancer of HIF-1-driven EPO expression in the CNS: a natural intermediary metabolite, pyruvate is nontoxic at cerebroprotective dosages; aside from its EPO induction, pyruvate is a physiological antioxidant and energy-yielding, oxidizable fuel; pyruvate is efficiently transferred from the circulation to the brain parenchyma by monocarboxylate transporters within the cerebrovascular endothelium and in the plasma membranes of neurons and glia, delivering it to the sites of ischemia-reperfusion injury and of EPO synthesis; pyruvate is highly water soluble, so that aqueous solutions of concentrated sodium pyruvate suitable for intravenous infusion[164] are readily prepared. Thus, pyruvate therapy may offer a facile means of evoking EPO expression and cytoprotection within the CNS. It should be noted that pyruvate has been shown to be safe and efficacious as an intracoronary intervention in patients with congestive heart failure[165,166] and cardiogenic shock,[167] and as a component of cardioplegia in patients undergoing coronary revascularization on cardiopulmonary bypass.[168]

Potential limitations of pyruvate therapy must be acknowledged. Given HIF-1's fundamental role in promoting survival and growth of solid tumors,[159] protracted pyruvate treatment might impose unacceptable risks in cancer patients. However, this concern would not apply to a single pyruvate treatment for acute CNS ischemia. It has been argued[169,170] that pyruvate may be unsuitable for protracted storage due to its chemical instability. However, pyruvate can be

kept indefinitely in powder form and, as noted above, dissolved to high concentrations immediately before its administration. Esterified derivatives of pyruvate, most notably ethyl pyruvate, have been found to be highly stable in aqueous solution, although these compounds are somewhat less soluble than authentic pyruvate,[139] and to suppress systemic inflammation in rat models of endotoxemia[171] and hemorrhagic shock.[172] However, it has been reported that ethyl-pyruvate resuscitation affords no short-term energetic and hemodynamic advantages over standard lactated Ringer's.[173] Moreover, the ability of these pyruvate derivatives to traverse the BBB has not yet been established.

References

1. Go AS, Mozaffarian D, Roger VL; American Heart Association Statistics Committee and Stroke Statistics Subcommittee. Heart disease and stroke statistics – 2013 update. *Circulation* 2013;**127:**e6-245
2. Roger VL, Go AS, Lloyd-Jones DM; American Heart Association Statistics Committee and Stroke Statistics Committee. Heart disease and stroke statistics – 2012 update. *Circulation* 2012;**125:**e2-220
3. Xiao F. Bench to bedside: brain edema and cerebral resuscitation: the present and future. *Acad Emerg Med* 2002;**9:**933-46
4. Idris AH, Roberts LJ II, Caruso L, Showstark M, Layon AJ, Becker LB, Vanden Hoek T, Gabrielli A. Oxidant injury occurs rapidly after cardiac arrest, cardiopulmonary resuscitation, and reperfusion. *Crit Care Med* 2005;**33:**2043-8
5. Nadkarni VM, Larkin GL, Peberdy MA, Carey SM, Kaye W, Mancini ME, Nichol G, Lane-Truitt T, Potts J, Ornato JP, Berg RA, National Registry of Cardiopulmonary Resuscitation Investigators. First documented rhythm and clinical outcome from in-hospital cardiac arrest among children and adults. *JAMA* 2006;**295:**50-7
6. Nolan JP, Laver SR, Welch CA, Harrison DA, Gupta V, Rowan K. Outcome following admission to UK intensive care units after cardiac arrest: a secondary analysis of the ICNARC Case Mix Programme Database. *Anesthesia* 2007;**62:**1207-16
7. Madl C, Holzer M. Brain function after resuscitation from cardiac arrest. *Curr Opin Crit Care* 2004;**10:**213-7
8. Westfal RE, Reissman S, Doering G. Out-of-hospital cardiac arrests: an 8-year New York City experience. *Am J Emerg Med* 1996;**14:**364-8
9. Böttiger BW, Grabner C, Bauer H, Bode C, Weber T, Motsch J, Martin E. Long term outcome after out-of-hospital cardiac arrest with physician staffed emergency medical services: the Utstein style applied to a midsized urban/suburban area. *Heart* 1999;**82:**674-9
10. Neumar RW, Nolan JP, Adrie C, Aibiki M, Berg RA, Böttiger BW, Callaway C, Clark RSB, Geocadin RG, Jauch EC, Kern KB, Laurent I, Longstreth WT Jr., Merchant RM, Morley P, Morrison LJ,

Nadkarni V, Peberdy MA, Rivers EP, Rodriguez-Nunez A, Sellke FW, Spaulding C, Sunde K, Vanden Hoek T. Post-cardiac arrest syndrome: epidemiology, pathophysiology, treatment, and prognostication. *Circulation* 2008;**118:**2452-83

11. White BC, Sullivan JM, DeGracia DJ, O'Neil BJ, Neumar RW, Grossman LI, Rafols JA, Krause GS. Brain ischemia and reperfusion: molecular mechanisms of neuronal injury. *J Neurol Sci* 2000;**179:**1-33
12. Guyot LL, Diaz FG, O-Regan MH, Song D, Phillis JW. The effect of streptozotocin-induced diabetes on the release of excitotoxic and other amino acids from the ischemic rat cerebral cortex. *Neurosurgery* 2011;**48:**385-90
13. Belousov AB. Novel model for the mechanisms of glutamate-dependent excitotoxicity: role of neuronal gap junctions. *Neurosci Lett* 2012;**524:**16-9
14. Konstady BB. The role of glutamate in neuronal ischemic injury: the role of spark in fire. *Neurol Sci* 2012;**33:**223-37
15. Swanson RA, Ying W, Kauppinen TM. Astrocyte influences on ischemic neuronal death. *Curr Molec Med* 2004;**4:**193-205
16. Mayhan WG, Didion SP. Glutamate-induced disruption of the blood-brain barrier in rats. Role of nitric oxide. *Stroke* 1996;**27:**965-9
17. Nicotera P, Lipton SA. Excitotoxins in neuronal apoptosis and necrosis. *J Cereb Blood Flow Metab* 1999;**19:**583-91
18. Manukhina EB, Downey HF, Mallet RT. Role of nitric oxide in cardiovascular adaptation to intermittent hypoxia. *Exp Biol Med* 2006;**231:**343-65
19. Basu S, Liu X, Nozari A, Rubertsson S, Miclescu A, Wiklund L. Evidence for time-dependent maximum increase of free radical damage and eicosanoid formation in the brain as related to duration of cardiac arrest and cardio-pulmonary resuscitation. *Free Radic Res* 2003;**37:**251-6
20. Chao CC, Hu S, Molitor TW, Shaskan EG, Peterson PK. Activated microglia mediate neuronal cell injury via a nitric oxide mechanism. *J Immunol* 1992;**149:**2736-41
21. Boje KM, Arora PK. Microglial-produced nitric oxide and reactive nitrogen oxides mediate neuronal cell death. *Brain Res* 1992;**587:**250-6

22. Guix FX, Uribesalgo I, Coma M, Muñoz FJ. The physiology and pathophysiology of nitric oxide in the brain. *Progr Neurobiol* 2005;**76:**126-52

23. Brock MV, Blue ME, Lowenstein CJ, Northington FA, Lange MS, Johnston MV, Baumgartner WA. Induction of neuronal nitric oxide after hypothermic circulatory arrest. *Ann Thorac Surg* 1996;**62:**1313-20

24. Chuang Y-C, Chen S-D, Liou C-W, Lin T-K, Chang W-N, Chan SHH, Chang AYW. Contribution of nitric oxide, superoxide anion, and peroxynitrite to activation of mitochondrial apoptotic signaling in hippocampal CA3 subfield following experimental temporal lobe status epilepticus. *Epilepsia* 2009;**50:**731-46

25. Neria F, del Carmen Serrano-Perez M, Velasco P, Urso K, Tranque P, Cano E. NFATc3 promotes Ca^{2+}-dependent MMP3 expression in astroglial cells. *Glia* 2013;**61:**1052-66

26. Ralay Ranaivo H, Hodge JN, Choi N, Wainwright MS. Albumin induces upregulation of matrix metalloproteinase-9 in astrocytes via MAPK and reactive oxygen species-dependent pathways. *J Neuroinflammation* 2012;**9:**68

27. Hsieh HL, Chi PL, Lin CC, Yang CC, Yang CM. Up-regulation of ROS-dependent matrix metalloproteinase-9 from high-glucose-challenged astrocytes contributes to the neuronal apoptosis. *Mol Neurobiol* 2014; in press

28. Gottschall PE, Deb S. Regulation of matrix metalloproteinase expressions in astrocytes, microglia and neurons. *Neuroimmunomodulation* 1996;**3:**69-75

29. Harkness KA, Adamson P, Sussman JD, Davies-Jones GA, Greenwood J, Woodroofe MN. Dexamethasone regulation of matrix metalloproteinase expression in CNS vascular endothelium. *Brain* 2000;**123:**698-709

30. Lee JM, Yin KJ, Hsin I, Chen S, Fryer JD, Holtzman DM, Hsu CY, Xu J. Matrix metalloproteinase-9 and spontaneous hemorrhage in an animal model of cerebral amyloid angiopathy. *Ann Neurol* 2003;**54:**379-82

31. Wang L, Zhang ZG, Zhang RL, Gregg SR, Hozeska-Solgot A, LeTourneau Y, Wang Y, Chopp M. Matrix metalloproteinase 2 (MMP2) and MMP9 secreted by erythropoietin-activated endothelial cells promote neural progenitor cell migration. *J Neurosci* 2006;**26:**5996-6003

32. Gidday JM, Gasche YG, Copin JC, Shah AR, Perez RS, Shapiro SD, Chan PH, Park TS. Leukocyte-derived matrix metalloproteinase-9 mediates blood-brain barrier breakdown and is proinflammatory after transient focal cerebral ischemia. *Am J Physiol Heart Circ Physiol* 2005;**289:**H558-68

33. Lischper M, Beuck S, Thanabalasundaram G, Pieper C, Galla HJ. Metalloproteinase mediated occluding cleavage in the cerebral microcapillary endothelium under pathological conditions. *Brain Res* 2010;**1326:**114-27

34. Lehner C, Gehwolf R, Tempfer H, Krizbai I, Hennig B, Bauer HC, Bauer H. Oxidative stress and blood-brain barrier dysfunction under particular consideration of matrix metalloproteinases. *Antioxid Redox Signal* 2011;**15:**1305-23

35. Abdul Muneer PM, Alikunju S, Szlachetka AM, Haorah J. The mechanism of cerebral vascular dysfunction and neuroinflammation by MMP-mediated degradation of VEGFR-2 in alcohol ingestion. *Arterioscler Thromb Vasc Biol* 2012;**32:**1167-77

36. Okamoto T, Akuta T, Tamura F, van der Vliet A, Akaike T. Molecular mechanism for activation and regulation of matrix metalloproteinases during bacterial infections and respiratory inflammation. *Biol Chem* 2004;**385:**997-1006

37. Gasche Y, Soccal PM, Kanemitsu M, Copin JC. Matrix metalloproteinases and diseases of the central nervous system with a special emphasis on ischemic brain. *Front Biosci* 2006;**11:**1289-1301

38. Planas AM, Solé S, Justicia C. Expression and activation of matrix metalloproteinase-2 and -9 in rat brain after transient focal cerebral ischemia. *Neurobiol Dis* 2001;**8:**834-46

39. Broughton BR, Reutens DC, Sobey CG. Apoptotic mechanisms after cerebral ischemia. *Stroke* 2009;**40:**e331-9

40. Sims NR, Muyderman H. Mitochondria, oxidative metabolism and cell death in stroke. *Biochim Biophys Acta* 2010;**1802:**80-92

41. Belayev L, Zhao WZ, Busto R, Ginsberg MD. Transient middle cerebral artery occlusion by intraluminal suture. 1. Three-dimensional autoradiographic analysis of local cerebral glucose

metabolism-blood flow interrelationships during ischemia and early recirculation. *J Cereb Blood Flow Metab* 1997;**17:**1266-80

42. Ferrer I, Planas AM. Signaling of cell death and cell survival following cerebral ischemia: life and death struggle in the penumbra. *J Neuropathol Exp Neurol* 2003;**62:**329-39
43. Jordan J, de Groot PW, Galindo MF. Mitochondria: the headquarters in ischemis-induced neuronal death. *Cent Nerv Syst Agents Med Chem* 2011;**11:**98-106
44. Bredesen DE, Mehlen P, Rabizadeh S. Apoptosis and dependence receptors: a molecular basis for cellular addiction. *Physiol Rev* 2004;**84:**411-30
45. Yeh CH, Wang YC, Wu YC, Lin YM, Lin PJ. Ischemic preconditioning or heat shock pretreatment ameliorates neuronal apoptosis following hypothermic circulatory arrest. *J Thorac Cardiovasc Surg* 2004;**128:**203-10
46. Böttiger BW, Schmitz B, Wiessner C, Vogel P, Hossman K-A. Neuronal stress response and neuronal cell damage after cardiocirculatory arrest in rats. *J Cereb Blood Flow Metab* 1998;**18:**1077-87
47. Teschendorf P, Padosch SA, Spöhr F, Albertsmeier M, Schneider A, Vogel P, Choi Y-H, Böttiger BW, Popp E. Time course of caspase activation in selectively vulnerable brain areas following *global* cerebral ischemia due to cardiac arrest in rats. *Neurosci Lett* 2008;**448:**194-9
48. Tamatani M, Ogawa S, Nunez G, Tohyama M. Growth factors prevent changes in Bcl-2 and Bax expression and neuronal apoptosis induced by nitric oxide. *Cell Death Differ* 1998;**5:**911-9
49. Tamatani M, Ogawa S, Niitsu Y, Tohyama M. Involvement of Bcl-2 family and caspase-3-like protease in NO-mediated neuronal apoptosis. *J Neurochem* 1998;**71:**1588-96
50. Fisher JW. Landmark advances in the development of erythropoietin. *Exp Biol Med* 2010;**235:**1398-1411
51. Semenza GL. Regulation of erythropoietin production. New insights into molecular mechanisms of oxygen homeostasis. *Hematol Oncol Clin North Am* 1994;**8:**863-84
52. Ishii Y, Sawada T, Murakami T, Sakuraoka Y, Shiraki T, Shimizu A, Kubota K, Fuchinoue S, Teraoka S. Renoprotective effect of erythropoietin against ischaemia-reperfusion injury in a non-human primate model. *Nephrol Dial Transplant* 2011;**26:**1157-62

53. Moore E, Bellomo R. Erythropoietin (EPO) in acute kidney injury. *Ann Intensive Care* 2011; **1**:3

54. Benderro GF, LaManna JC. Kidney EPO expression during chronic hypoxia in aged mice. *Adv Exp Med Biol* 2013;**765:**9-14

55. Fisher JW. Erythropoietin: physiology and pharmacology update. *Exp Biol Med* 2003;**228:**1-14

56. Chong ZZ, Kang J-Q, Maiese K. Erythropoietin fosters both intrinsic and extrinsic neuronal protection through modulation of microglia, Akt1, Bad, and caspase-mediated pathways. *Brit J Pharmacol* 2003;**138:**1107-18

57. Maiese K, Li F, Chong ZZ. New avenues of exploration for erythropoietin. *JAMA* 2005;**293:**90-5

58. Hasselblatt M, Ehrenreich H, Sirén A-L. The brain erythropoietin system and its potential for therapeutic exploitation in brain disease. *J Neurosurg Anesthesiol* 2006;**18:**132-8

59. McPherson RJ, Juul SE. Recent trends in erythropoietin-mediated neuroprotection. *Int J Devel Neurosci* 2008;**26:**103-11

60. Rabie T, Marti HH. Brain protection by erythropoietin: a manifold task. *Physiology* 2008;**23:**263-74

61. Mammis A, McIntosh TK, Maniker AH. Erythropoietin as a neuroprotective agent in traumatic brain injury. *Surg Neurol* 2009;**71:**527-31

62. Sadamoto Y, Igase K, Sakanaka M, Sato K, Otsuka H, Sasaki S, Masuda S, Sasaki R. Erythropoietin prevents place navigation disability and cortical infarction in rats with permanent occlusion of the middle cerebral artery. *Biochem Biophys Res Commun* 1998;**253:**26-32

63. Sirén A, Fratelli M, Brines M, Goemans C, Casagrande S, Lewczuk P, Keenan S, Gleiter C, Pasquali C, Capobianco A, Mennini T, Heumann R, Cerami A, Ehrenreich H, Ghezzi P. Erythropoietin prevents neuronal apoptosis after cerebral ischemia and metabolic stress. *Proc Natl Acad Sci USA* 2001;**98:**4044-9

64. Kumral A, Tugyan K, Gonenc S, Genc K, Genc S, Sonmez U, Yilmaz O, Duman N, Uysal N, Ozkan H. Protective effects of erythropoietin against ethanol-induced apoptotic neurodegeneration and oxidative stress in the developing C57BL/6 mouse brain. *Devel Brain Res* 2005;**160:**146-56

65. Calapai G, Marciano MC, Corica F, Allegra A, Parisi A, Frisina N, Caputi AP, Buemi M. Erythropoietin protects against brain ischemic injury by inhibition of nitric oxide formation. *Eur J Pharmacol* 2000;**401:**349-56

66. Kilic E, Kilic Ü, Soliz J, Bassetti CL, Gassmann M, Hermann DM. Brain-derived erythropoietin protects from focal cerebral ischemia by dual activation of ERK-1/-2 and Akt pathways. *FASEB J* 2005;**19:**2026-8

67. Brines ML, Ghezzi P, Keenan S, Agnello D, de Lanerolle NC, Cerami C, Itri LM, Cerami A. Erythropoietin crosses the blood-brain barrier to protect against experimental brain injury. *Proc Natl Acad Sci USA* 2000;**97:**10526-31

68. Xiong Y, Mahmood A, Meng Y, Zhang Y, Qu C, Schallert T, Chopp M. Delayed administration of erythropoietin reducing hippocampal cell loss, enhancing angiogenesis and neurogenesis, and improving functional outcome following traumatic brain injury in rats: comparison of treatment with single and triple dose. *J Neurosurg* 2010;**113:**598-608

69. Popp E, Vogel P, Teschendorf P, Böttiger BW. Effects of the application of erythropoietin on cerebral recovery after cardiac arrest in rats. *Resuscitation* 2007;**74:**344-51

70. Witthuhn BA, Quelle FW, Silvennoinen O, Yi T, Tang B, Miura O, Ihle JN. JAK2 associates with the erythropoietin receptor and is tyrosine phosphorylated and activated following stimulation with erythropoietin. *Cell* 1993;**74:**227-36

71. Crow MT, Mani K, Nam Y-J, Kitsis RN. The mitochondrial death pathway and cardiac myocyte apoptosis. *Circ Res* 2004;**95:**957-70

72. Baines CP. The cardiac mitochondrion: nexus of stress. *Annu Rev Physiol* 2010;**72:**61-80

73. Vairano M, Russo CD, Pozzoli G, Battaglia A, Scambia G, Tringali G, Aloe-Spiriti MA, Preziosi P, Navara P. Erythropoietin exerts anti-apoptotic effects on rat microglial cells *in vitro*. *Eur J Neurosci* 2002;**16:**584-92

74. Wen TC, Sadamoto Y, Tanaka J, Zhu PX, Nakata K, Ma YJ, Hata R, Sakanaka M. Erythropoietin protects neurons against chemical hypoxia and cerebral ischemic injury by up-regulating Bcl-xL expression. *J Neurosci Res* 2002;**67:**795-803

75. Noguchi CT, Asavaritikrai P, Teng R, Jia Y. Role of erythropoietin in the brain. *Crit Rev Oncol Hematol* 2007;**64:**159-71

76. Digicaylioglu M, Lipton SA. Erythropoietin-mediated neuroprotection involves cross-talk between Jak2 and NF-kappaP signaling cascades. *Nature* 2001;**412:**641-7

77. Genc S, Koroglu TF, Genc K. Erythropoietin as a novel neuroprotectant. *Restor Neurol Neurosci* 2004;**22:**105-19

78. Deveraux QL, Roy N, Stennicke HR, Van Arsdale T, Zhou Q, Srinivasula SM, Alnemri ES, Salvesen GS, Reed JC. IAPs block apoptotic events induced by caspase-8 and cytochrome c by direct inhibition of distinct caspases. *EMBO J* 1998;**17:**2215-23

79. Shiozaki EN, Chai J, Rigotti DJ, Riedl SJ, Li P, Srinivasula SM, Alnemri ES, Fairman R, Shi Y. Mechanism of XIAP-mediated inhibition of caspase-9. *Mol Cell* 2003;**11:**519-27

80. Zhang J, Zhu Y, Zhou D, Wang Z, Chen G. Recombinant human erythropoietin (rhEPO) alleviates early brain injury following subarachnoid hemorrhage in rats: possible involvement of Nrf2-ARE pathway. *Cytokine* 2010;**52:**252-7

81. Sifringer M, Brait D, Weichelt U, Zimmerman G, Endesfelder S, Brehmer F, von Haefen C, Friedman A, Soreq H, Bendix I, Gerstner B, Felderhoff-Mueser U. Erythropoietin attenuates hyperoxia-induced oxidative stress in the developing rat brain. *Brain Behav Immun* 2010;**24:**792-9

82. Innamorato NG, Rojo AI, Garcia-Yagüe AJ, Yamamoto M, de Ceballos ML, Cuadrado A. The transcription factor Nrf2 is a therapeutic target against brain inflammation. *J Immunol* 2008;**181:**680-9

83. Zhang GL, Wang W, Kang YX, Xue Y, Yang H, Zhou CM, Shi GM. Chronic testosterone propionate supplement activated the Nrf2-ARE pathway in the brain and ameliorated the behaviors of age rats. *Behav Brain Res* 2013;**252:**388-95

84. Genc K, Egrilmez MY, Genc S. Erythropoietin induces nuclear translocation of Nrf2 and heme oxygenase-1 expression in SH-SY5Y cells. *Cell Biochem Funct* 2010;**28:**197-201

85. Jin R, Song Z, Yu S, Piazza A, Nanda A, Penninger JM, Granger DN, Li G. Phosphatidylinositol-3-kinase gamma plays a central role in blood-brain barrier dysfunction in acute experimental stroke. *Stroke* 2011;**42:**2033-44

86. McMahon M, Itoh K, Yamamoto M, Hayes JD. Keap1-dependent proteasomal degradation of transcription factor Nrf2 contributes to the negative regulation of antioxidant response element-driven gene expression. *J Biol Chem* 2003;**278:**21592-600

87. Villeneuve NF, Lau A, Zhang DD. Regulation of the Nrf2-Keap1 antioxidant response by the ubiquitin proteasome system: an insight into cullin-ring ubiquitin ligases. *Antioxid Redox Signal* 2010;**13:**1699-1712

88. Uruno A, Motohashi H. The Keap1-Nrf2 system as an in vivo sensor for electrophiles. *Nitric Oxide* 2011;**25:**153-60

89. Genc S. Endothelial nitric oxide-mediated Nrf2 activation as a novel mechanism for vascular and neuroprotection by erythropoietin in experimental subarachnoid hemorrhage. *Med Hypotheses* 2006;**67:**424

90. Buckley BJ, Li S, Whorton AR. Keap1 modification and nuclear accumulation in response to *S*-nitrosocysteine. *Free Radic Biol Med* 2008;**44:**692-8

91. Li Y, Ogle ME, Wallace GC 4th, Lu ZY, Yu SP, Wei L. Erythropoietin attenuates intracerebral hemorrhage by diminishing matrix metalloproteinases and maintaining blood-brain barrier integrity in mice. *Acta Neurochir* 2008;**105 (suppl):**105-12

92. Kadri Z, Petitfrère E, Boudot C, Freyssinier J-M, Fichelson S, Mayeux P, Emonard H, Hornebeck W, Haye B, Billat C. Erythropoietin induction of tissue inhibitors of metalloproteinase-1 expression and secretion is mediated by mitogen-activated protein kinase and phsphatidylinositol 3-kinase pathways. *Cell Growth Differen* 2000;**11:** 573-80

93. Villa P, Bigini P, Mennini T, Agnello D, Laragione T, Cagnotto A, Viviani B, Marinovich M, Cerami A, Coleman TR, Brines M, Ghezzi P. Erythropoietin selectively attenuates cytokine production and inflammation in cerebral ischemia by targeting neuronal apoptosis. *J Exp Med* 2003;**198:**971-75

94. Kawakami M, Sekiguchi M, Sato K, Kozaki S, Takahashi M. Erythropoietin receptor-mediated inhibition of exocytotic glutamate release confers neuroprotection during chemical ischemia. *J Biol Chem* 2001;**276:**39469-75

95. Won YJ, Yoo JY, Lee JH, Hwang SJ, Kim D, Hong HN. Erythropoietin is neuroprotective on GABAergic neurons against kainic acid-excitotoxicity in the rat spinal cell cultures. *Brain Res* 2007;**1154:**31-9

96. Kamal A, Al Shaibani T, Ramakers G. Erythropoietin decreases the excitatory neurotransmitter release probability and enhances synaptic plasticity in mice hippocampal slices. *Brain Res* 2011;**1410:**33-7

97. Pytte M, Steen PA. Are we closer to a new strategy in the treatment of cardiac arrest? *Resuscitation* 2009;**80:**613-4

98. Ehrenreich H, Hasselblatt M, Dembowski C, Cepek L, Lewczuk P, Stiefel M, Rustenbeck H-H, Breiter N, Jacob S, Knerlich F, Bohn M, Poser W, Rüther E, Kochen M, Gefeller O, Gleiter C, Wessel TC, De Ryck M, Itri L, Prange H, Cerami A, Brines M, Sirén A-L. Erythropoietin therapy for acute stroke is both safe and beneficial. *Molec Med* 2002;**8:**495-505

99. Cariou A, Claessens Y-E, Pène F, Marx J-S, Spaulding C, Hababou C, Casadevall N, Mira J-P, Carli P, Hermine O. Early high-dose erythropoietin therapy and hypothermia after out-of-hospital cardiac arrest: a matched control study. *Resuscitation* 2008;**76:**397-404

100. Grmec Š, Strnad M, Kupnik D, Sinkovič A, Gazmuri RJ. Erythropoietin facilitates the return of spontaneous circulation and survival in victims of out-of-hospital cardiac arrest. *Resuscitation* 2009;**80:**631-7

101. Ehrenreich H, Weissenborn K, Prange H, Schneider D, Weimar C, Wartenberg K, Schellinger PD, Bohn M, Becker H, Wegrzyn M, Jähnig P, Herrmann M, Knauth M, Bähr M, Heide W, Wagner A, Schwab S, Reichmann H, Schwendemann G, Dengler R, Kastrup A, Bartels C, EPO Stroke Trial Group. Recombinant human erythropoietin in the treatment of acute ischemic stroke. *Stroke* 2009;**40:**e647-56

102. Green AR. Pharmacological approaches to acute ischaemic stroke: reperfusion certainly, neuroprotection possibly. *Br J Pharmacol* 2008;**153:**S325-38

103. Hacke W, Kaste M, Bluhmki E, Brozman M, Davalos A, Guidetti D, Larrue V, Lees KR, Medeghri Z, Machnig T, Schneider D, von Kummer R, Wahlgren N, Toni D, ECASS Investigators. Thrombolysis with alteplase 3 to 4.5 h after acute ischemic stroke. *N Engl J Med* 2008;**359:**1317-29

104. Jia L, Chopp M, Zhang L, Lu M, Zhang Z. Erythropoietin in combination of tissue plasminogen activator exacerbates brain hemorrhage when treatment is initiated 6 hours after stroke. *Stroke* 2010;**41:**2071-6

105. Banks WA, Jumbe NL, Farrell CL, Niehoff ML, Heatherington AC. Passage of erythropoietic agents across the blood-brain barrier: a comparison of human and murine erythropoietin and the analog darbepoietin alfa. *Eur J Pharmacol* 2004;**505:**93-101

106. Juul SE, McPherson RJ, Farrell FX, Jolliffe L, Ness DJ, Gleason CA. Erythropoietin concentrations in cerebrospinal fluid of nonhuman primates and fetal sheep following high-dose recombinant erythropoietin. *Biol Neonate* 2004;**85:**138-44

107. Dame C, Juul SE, Christensen RD. The biology of erythropoietin in the central nervous system and its neurotrophic and neuroprotective potential. *Biol Neonate* 2001;**79:**228-35

108. Haiden N, Klebermass K, Cardona F, Schwindt J, Berger A, Kohlhauser-Vollmuth C, Jilma B, Pollak A. A randomized, controlled trial of the effects of adding vitamin B12 and folate to erythropoietin for the treatment of anemia of prematurity. *Pediatrics* 2006;**118:**180-8

109. Marti HH, Gassmann M, Wenger RH, Kvietikova I, Morganti-Kossmann MC, Kossmann T, Trentz O, Bauer C. Detection of erythropoietin in human liquor: intrinsic erythropoietin production in the brain. *Kidney Int* 1997;**51:**416-8

110. Buemi M, Allegra A, Corica F, Floccari F, D'Avella D, Aloisi C, Calapai G, Iacopino G, Frisina N. Intravenous recombinant erythropoietin does not lead to an increase in cerebrospinal fluid erythropoietin concentration. *Nephrol Dial Transplant* 2000;**15:**422-3

111. McPherson RJ, Juul SE. Recent trends in erythropoietin-mediated neuroprotection. *Int J Devel Neurosci* 2008;**26:**103-11

112. García-Yébenes I, Sobrado M, Zarruk JG, Castellanos M, Pérez de la Ossa N, Dávalos A, Serena J, Lizasoain I, Moro MA. A mouse model of hemorrhagic transformation by delayed tissue plasminogen activator administration after in situ thromboembolic stroke. *Stroke* 2011;**42:**196-203

113. Baciu I, Oprisiu C, Deverenco P, Vasile V, Muresan A, Hriscu M, Chris I. The brain and other sites of erythropoietin production. *Rom J Physiol* 2000;**37:**3-14

114. Marti HH. Erythropoietin and the hypoxic brain. *J Exp Biol* 2004;**207:**3233-42

115. Benderro GF, Sun X, Kuang Y, LaManna JC. Decreased VEGF expression and microvascular density, but increased HIF-1 and 2α accumulation and EPO expression in chronic moderate hyperoxia in the mouse brain. *Brain Res* 2012;**1471:**46-55

116. Dame C, Bartmann P, Wolber E-M, Fahnenstich H, Hofmann D, Fandrey J. Erythropoietin gene expression in different areas of the developing human central nervous system. *Dev Brain Res* 2000;**125:**69-74

117. Juul SE, Anderson DK, Li Y, Christensen RD. Erythropoietin and erythropoietin receptor in the developing human central nervous system. *Pediatr Res* 1998;**43:**40-4

118. Nagai A, Nakagawa E, Choi HB, Hatori K, Kobayashi S, Kim SU. Erythropoietin and erythropoietin receptors in human CNS neurons, astrocytes, microglia, and oligodendrocytes grown in culture. *J Neuropathol Exp Neurol* 2001;**60:**386-92

119. Sakanaka M, Wen TC, Matsuda S, Masuda S, Morishita E, Nagao M, Sasaki R. *In vivo* evidence that erythropoietin protects neurons from ischemic damage. *Proc Natl Acad Sci USA* 1998;**95:**4635-40

120. Nangaku M, Eckardt KU. Hypoxia and the HIF system in kidney disease. *J Mol Med (Berl)* 2007;**85:**1325-30

121. Haase VH. Regulation of erythropoiesis by hypoxia-inducible factors. *Blood Rev* 2013;**27:**41-53

122. Fandrey J. Oxygen-dependent and tissue-specific regulation of erythropoietin gene expression. *Am J Physiol Regul Integr Comp Physiol* 2004;**286:**R977-88

123. Semenza GL. Expression of hypoxia-inducible factor 1: mechanisms and consequences. *Biochem Pharmacol* 2000;**59:**47-53

124. Jelkmann W. Regulation of erythropoietin production. *J Physiol* 2011;**589:**1251-8

125. Bernaudin M, Bellail A, Marti HH, Yvon A, Vivien D, Duchatelle I, Mackenzie ET, Petit E. Neurons and astrocytes express EPO mRNA: oxygen-sensing mechanisms that involve the redox-state of the brain. *Glia* 2000;**30:**271-8

126. Lee J-Y, Kim Y-H, Koh J-Y. Protection by pyruvate against transient forebrain ischemia in rats. *J Neurosci* 2001;**21:**RC171(1-6)

127. Mongan PD, Capacchione J, Fontana JL, West S, Bünger R. Pyruvate improves cerebral metabolism during hemorrhagic shock. *Am J Physiol Heart Circ Physiol* 2001;**281:**H854-64

128. Kim T-Y, Yi J-S, Chung S-J, Kim D-K, Byun H-R, Lee J-Y, Koh J-Y. Pyruvate protects against kainite-induced epileptic brain damage in rats. *Exp Neurol* 2007;**208:**159-67

129. Sharma P, Karian J, Sharma S, Liu S, Mongan PD. Pyruvate ameliorates post ischemic injury of rat astrocytes and protects them against PARP mediated cell death. *Brain Res* 2003;**992:**104-13

130. Sharma AB, Barlow MA, Yang SH, Simpkins JW, Mallet RT. Pyruvate enhances neurological recovery following cardiopulmonary arrest and resuscitation. *Resuscitation* 2008;**76:**108-19

131. Sharma AB, Knott EM, Bi J, Martinez RR, Sun J, Mallet RT. Pyruvate improves cardiac electromechanical and metabolic recovery from cardiopulmonary arrest and resuscitation. *Resuscitation* 2005;**66:**71-81

132. Fukushima M, Lee SM, Moro N, Hovda DA, Sutton RL. Metabolic and histologic effects of sodium pyruvate treatment in the rat after cortical contusion injury. *J Neurotrauma* 2009;**26:**1095-110

133. Ryou MG, Liu R, Ren M, Sun J, Mallet RT, Yang SH. Pyruvate protects the brain against ischemia-reperfusion injury by activating the erythropoietin signaling pathway. *Stroke* 2012;**43:**1101-7

134. Miller LP, Oldendorf WH. Regional kinetic constants for blood-brain barrier pyruvic acid transport in conscious rats by the monocarboxylic acid carrier. *J Neurochem* 1986;**46:**1412-6

135. Steele RD. Blood-brain barrier transport of the alpha-keto acid analogs of amino acids. *Fed Proc* 1986;**45:**2060-4

136. Lin T, Koustova E, Chen H, Rhee PM, Kirkpatrick J, Alam HB. Energy substrate-supplemented resuscitation affects brain monocarboxylate transporter levels and gliosis in a rat model of hemorrhagic shock. *J Trauma* 2005;**59:**1191-1202

137. Wang Y, Guo SZ, Bonen A, Li RC, Kheirandish-Gozal L, Zhang SX, Brittian KR, Gozal D. Monocarboxylate transporter 2 and stroke severity in a rodent model of sleep apnea. *J Neurosci* 2011;**31:**10241-8

138. Mallet RT. Pyruvate: metabolic protector of cardiac performance. *Proc Soc Exp Biol Med* 2000;**223:**136-48

139. Mallet RT, Sun J, Knott EM, Sharma AB, Olivencia-Yurvati AH. Metabolic cardioprotection by pyruvate: recent progress. *Exp Biol Med* 2005;**230:**435-43

140. Constantopoulos G, Barranger JA. Nonenzymatic decarboxylation of pyruvate. *Anal Biochem* 1984;**139:**353-8

141. DeBoer LW, Bekx PA, Han L, Steinke L. Pyruvate enhances recovery of rat hearts after ischemia and reperfusion by preventing free radical generation. *Am J Physiol Heart Circ Physiol* 1993;**265:**H1571-6

142. Vásquez-Vivar J, Denicola A, Radi R, Augusto O. Peroxynitrite-mediated decarboxylation of pyruvate to both carbon dioxide and carbon dioxide radical anion. *Chem Res Toxicol* 1997;**10:**786-94

143. Bassenge E, Sommer O, Schwemmer M, Bünger R. Antioxidant pyruvate inhibits cardiac formation of reactive oxygen species through changes in redox state. *Am J Physiol Heart Circ Physiol* 2000;**279:**H2431-8

144. Mallet RT, Sun J. Antioxidant properties of myocardial fuels. *Mol Cell Biochem* 2003;**253:**103-11

145. Tejero-Taldo MI, Caffrey JL, Sun J, Mallet RT. Antioxidant properties of pyruvate mediate its potentiation of β-adrenergic inotropism in stunned myocardium. *J Mol Cell Cardiol* 1999;**31:**1863-72

146. Hagar H, Ueda N, Shah S. Role of reactive oxygen metabolites in DNA damage and cell death in chemical hypoxic injury to LLC-PK1 cells. *Am J Physiol Renal Fluid Electrolyte Physiol* 1996;**271:**F209-15

147. Ramakrishnan N, Chen R, McClain DE, Bünger R. Pyruvate prevents hydrogen peroxide-induced apoptosis. *Free Radic Res* 1998;**29:**283-95

148. Sileri P, Schena S, Morini S, Rastellini C, Pham S, Benedetti E, Cicalese L. Pyruvate inhibits hepatic ischemia-reperfusion injury in rats. *Transplantation* 2001;**72:**27-30

149. Lee YJ, Kang IJ, Bünger R, Kang YH. Mechanisms of pyruvate inhibition of oxidant-induced apoptosis in human endotelial cells. *Microvasc Res* 2003;**66:**91-101

150. Lee YJ, Kang IJ, Bünger R, Kang YH. Enhanced survival effect of pyruvate correlates MAPK and NF-κB activation in hydrogen peroxide-treated human endothelial cells. *J Appl Physiol* 2004;**96:**793-801

151. Wang XF, Cynader MS. Pyruvate released by astrocytes protects neurons from copper-catalyzed cysteine neurotoxicity. *J Neurosci* 2001;**21:**3322-31

152. Alvarez G, Ramos M, Ruiz F, Satrústegui J, Bogónez E. Pyruvate protection against β-amyloid-induced neuronal death: role of mitochondrial redox state. *J Neurosci Res* 2003;**73:**260-9

153. Mazzio EA, Soliman KF. Cytoprotection of pyruvic acid and reduced beta-nicotinamide adenine dinucleotide against hydrogen peroxide toxicity in neuroblastoma cells. *Neurochem Res* 2003;**28:**733-41

154. Wang X, Perez E, Liu R, Yan L-J, Mallet RT, Yang S-H. Pyruvate protects mitochondria from oxidative stress in human neuroblastoma SK-N-SH cells. *Brain Res* 2007;**1132:**1-9

155. Levy JH, Tanaka KA. Inflammatory response to cardiopulmonary bypass. *Ann Thorac Surg* 2003;**75(Suppl):**715-20

156. Van Harten AE, Scheeren TW, Absalom AR. A review of postoperative cognitive dysfunction and neuroinflammation associated with cardiac surgery and anaesthesia. *Anaesthesia* 2012;**67:**280-93

157. Ryou MG, Flaherty DC, Hoxha B, Gurji H, Sun J, Hodge LM, Olivencia-Yurvati AH, Mallet RT. Pyruvate-enriched cardioplegia suppresses cardiopulmonary bypass-induced myocardial inflammation. *Ann Thorac Surg* 2010;**90:**1529-35

158. Sharma P, Mongan PD. Hypertonic sodium pyruvate solution is more effective than Ringers ethyl pyruvate in the treatment of hemorrhagic shock. *Shock* 2010;**33:**532-40

159. Lu H, Forbes RA, Verma A. Hypoxia-inducible factor 1 activation by aerobic glycolysis implicates the Warburg effect in carcinogenesis. *J Biol Chem* 2002;**277:**23111-5

160. Dalgard CL, Lu H, Mohyeldin A, Verma A. Endogenous 2-oxoacids differentially regulate expression of oxygen sensors. *Biochem J* 2004;**380:**419-24

161. Lu H, Dalgard CL, Mohyeldin A, McFate T, Tait AS, Verma A. Reversible inactivation of HIF-1 prolyl hydroxylases allows cell metabolism to control basal HIF-1. *J Biol Chem* 2005; **280:**41928-39

162. Ryou MG, Flaherty DC, Hoxha B, Sun J, Gurji H, Rodriguez S, Bell G, Olivencia-Yurvati AH, Mallet RT. Pyruvate-fortified cardioplegia evokes myocardial erythropoietin signaling in swine undergoing cardiopulmonary bypass. *Am J Physiol Heart Circ Physiol* 2009;**297:**H1914-22

163. Ryou MG, Choudhury GR, Winters A, Xie L, Mallet RT, Yang SH. Pyruvate minimizes rtPA toxicity from in vitro oxygen0glucose deprivation. *Brain Res* 2013;**1530:**66-75

164. Gurji HA, White DW, Hoxha B, Sun J, Harbor JP, Schulz DR, Williams AG Jr., Olivencia-Yurvati AH, Mallet RT. Pyruvate-enriched resuscitation: metabolic support of post-ischemic hindlimb muscle in hypovolemic goats. *Exp Biol Med* 2014;in press

165. Hermann HP, Pieske B, Schwarzmüller E, Keul J, Just H, Hasenfuss G. Haemodynamic effects of intracoronary pyruvate in patients with congestive heart failure: an open study. *Lancet* 1999;**353:**1321-3

166. Hermann HP, Arp J, Pieske B, Kögler H, Baron S, Janssen PM, Hasenfuss G. Improved systolic and diastolic myocardial function with intracoronary pyruvate in patients with congestive heart failure. *Eur J Heart Fail* 2004;**6:**213-8

167. Schillinger W, Hünlich M, Sossalia S, Hermann HP, Hasenfuss G. Intracoronary pyruvate in cardiogenic shock as an adjunctive therapy to catecholamines and intra-aortic balloon pump shows beneficial effects on hemodynamics. *Clin Res Cardiol* 2011;**100:**433-8

168. Olivencia-Yurvati AH, Blair JL, Baig M, Mallet RT. Pyruvate-enhanced cardioprotection during surgery with cardiopulmonary bypass. *J Cardiothorac Vasc Anesth* 2003;**17:**715-20

169. Fink MP. Ringer's ethyl pyruvate solution: a novel resuscitation fluid. *Minerva Anesthesiol* 2001;**67:**190-2

170. Fink MP. Ethyl pyruvate: a novel anti-inflammatory agent. *J Intern Med* 2007;**261:**349-62

171. Venkataraman R, Kellum JA, Song M, Fink MP. Resuscitation with Ringer's ethyl pyruvate solution prolongs survival and modulates plasma cytokine and nitrite/nitrate concentrations in a rat model of lipopolysaccharide-induced shock. *Shock* 2002;**18:**507-12

172. Yang R, Gallo DJ, Baust JJ, Uchiyama T, Watkins SK, Delude RL, Fink MP. Ethyl pyruvate modulates inflammatory gene expression in mice subjected to hemorrhagic shock. *Am J Physiol Gastrointest Liver Physiol* 2002;**283:**G212-21

173. Mulier KE, Beilman GJ, Conroy MJ, Taylor JH, Skarda DE, Hammer BE. Ringer's ethyl pyruvate in hemorrhagic shock and resuscitation does not improve early hemodynamics or tissue energetics. *Shock* 2005;**23:**248-52

Figure legends

Figure 1. *Cascade of injury in ischemic and post-ischemic brain.* By interrupting cerebrovascular delivery of energy substrates and O_2, CNS ischemia depletes Gibbs free energy of ATP hydrolysis (ΔG_{ATP}), thus impairing neuronal Ca^{2+} management and provoking excitotoxic glutamate signaling. Subsequent reperfusion triggers intense formation of reactive oxygen and nitrogen species. These compounds and Ca^{2+} overload combine to trigger mitochondrial permeability transition, cytochrome *c* release and energetic collapse, and activate matrix metalloproteinases that degrade the extracellular matrix, allowing neutrophil infiltration in response to pro-inflammatory cytokines and provoking brain edema. See text for details.

Figure 2. *Anti-apoptotic mechanisms of erythropoietin.* Ischemia-reperfusion activates intrinsic and extrinsic apoptotic cascades, the elements of which are indicated by solid and broken gray outlines, respectively, which converge on caspase-3 as the common effector. Erythropoietin (EPO) activates anti-apoptotic signaling in neurons by binding its membrane receptors. This event initiates a complex cascade of intracellular signaling events, mediated by protein kinases, that (1) prevent formation of Bad-*t*Bid channels that release cytochrome *c* from mitochondria; (2) blunt the activation of pro-apoptotic caspases; and (3) evoke Nrf2- and NF-κB driven expression of cytoprotective genes that increase neuronal resistance to ischemia-reperfusion stress. Collectively, these mechanisms suppress the intrinsic and extrinsic apoptotic pathways. EPO expression, primarily in astrocytes, is driven by hypoxia-inducible factors (HIF) interacting on hypoxia response elements (HRE) in the promoter regions of EPO and other genes. HIF, in turn, is activated by stabilization of its O_2-regulated α subunit. Pyruvate interferes with HIF-α hydroxylation by prolyl hydroxylase (PHD), thereby preventing proteosomal degradation of the subunit and promoting EPO expression.

Figure 3. *Metabolism and cytoprotective mechanisms of pyruvate in brain.* Pyruvate is carried across the cerebrovascular endothelium and cell and mitochondrial membranes within the brain parenchyma my monocarboxylate transporters (MCT). In addition to its induction of EPO expression (Figure 2), pyruvate affords cytoprotection by (1) supporting oxidative metabolism and mitochondrial ATP production; (2) directly detoxifying hydrogen peroxide, lipid peroxides (LOOH) and peroxynitrite; (3) increasing mitochondrial citrate formation, which, when exported to the cytosol by the tricarboxylate transporter (TCT), suppresses phosphofructokinase (PFK) activity, thereby diverting glycolytic flux into the hexose monophosphate shunt, the source of NADPH reducing power by glucose 6-phosphate dehydrogenase (G6PDH) and 6-phosphogluconate dehydrogenase; (4) cytosolic citrate lyase degrades citrate to acetate and oxaloacetate, which, like pyruvate, competitively inhibits prolyl hydroxylase.

Figure 1

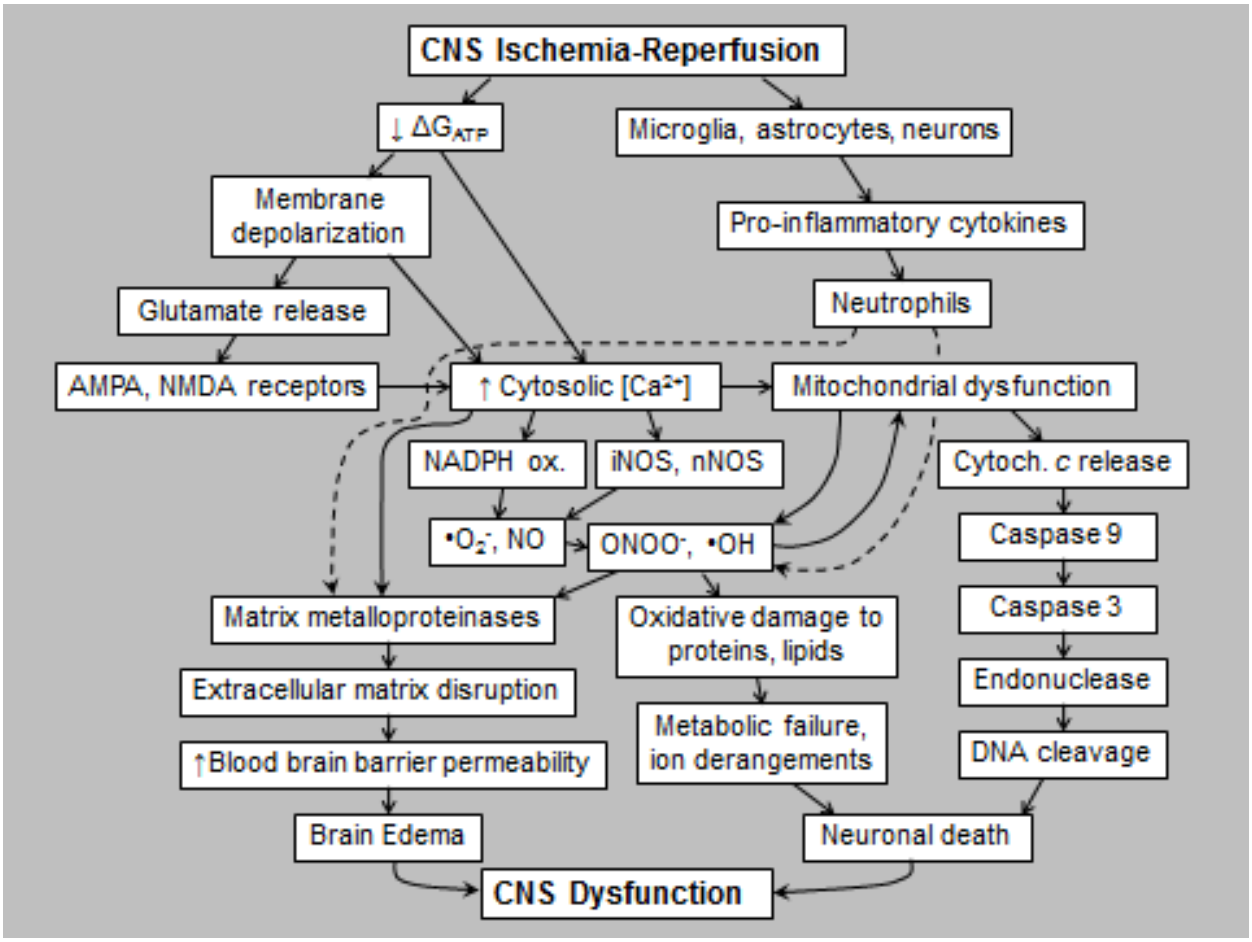

Figure 1. *Cascade of injury in ischemic and post-ischemic brain.* By interrupting cerebrovascular delivery of energy substrates and O_2, CNS ischemia depletes Gibbs free energy of ATP hydrolysis (ΔG_{ATP}), thus impairing neuronal Ca^{2+} management and provoking excitotoxic glutamate signaling. Subsequent reperfusion triggers intense formation of reactive oxygen and nitrogen species. These compounds and Ca^{2+} overload combine to trigger mitochondrial permeability transition, cytochrome *c* release and energetic collapse, and activate matrix metalloproteinases that degrade the extracellular matrix, allowing neutrophil infiltration in response to pro-inflammatory cytokines and provoking brain edema. See text for details.

Figure 2

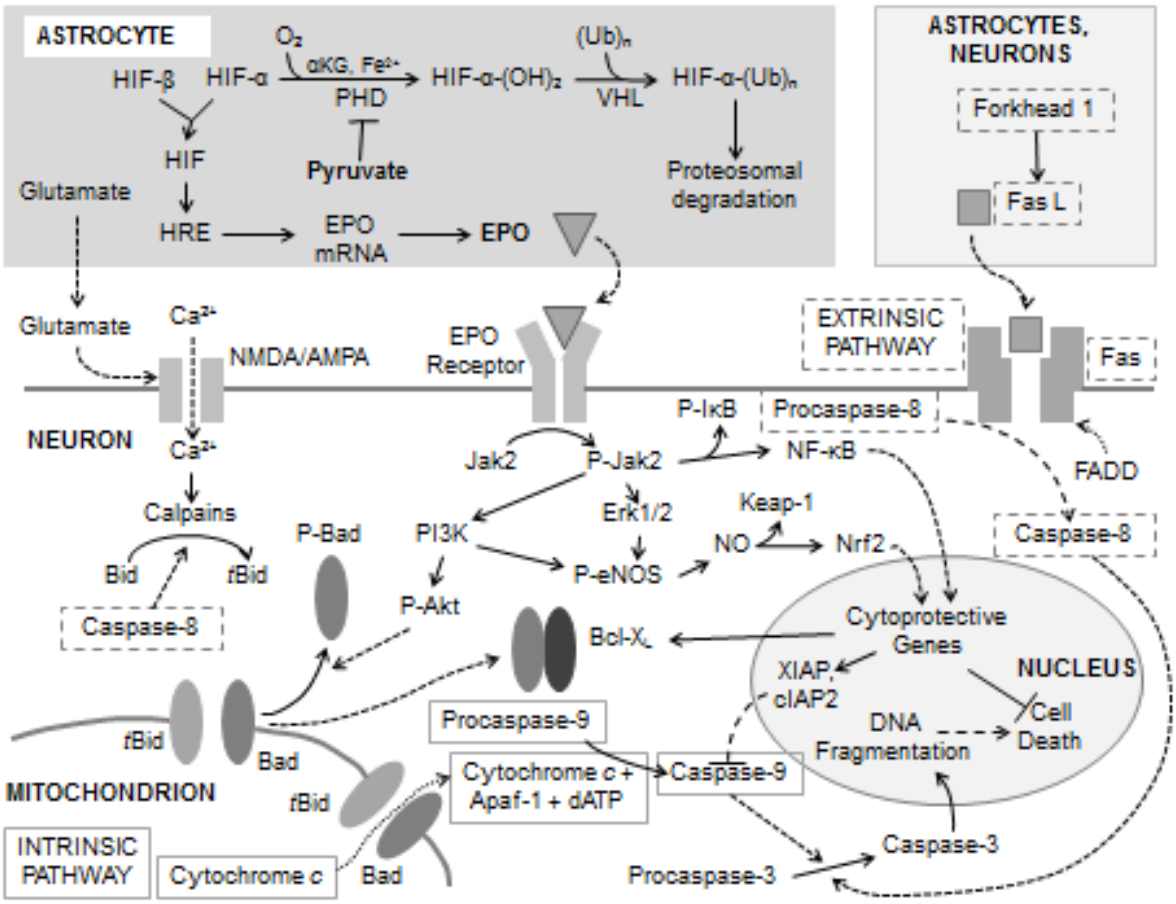

Figure 2. *Anti-apoptotic mechanisms of erythropoietin.* Ischemia-reperfusion activates intrinsic and extrinsic apoptotic cascades, the elements of which are indicated by solid and broken gray outlines, respectively, which converge on caspase-3 as the common effector. Erythropoietin (EPO) activates anti-apoptotic signaling in neurons by binding its membrane receptors. This event initiates a complex cascade of intracellular signaling events, mediated by protein kinases, that (1) prevent formation of Bad-*t*Bid channels that release cytochrome *c* from mitochondria; (2) blunt the activation of pro-apoptotic caspases; and (3) evoke Nrf2- and NF-κB driven expression of cytoprotective genes that increase neuronal resistance to ischemia-reperfusion stress. Collectively, these mechanisms suppress the intrinsic and extrinsic apoptotic pathways. EPO expression, primarily in astrocytes, is driven by hypoxia-inducible factors (HIF) interacting on hypoxia response elements (HRE) in the promoter regions of EPO and other genes. HIF, in turn, is activated by stabilization of its O_2-regulated α subunit. Pyruvate interferes with HIF-α hydroxylation by prolyl hydroxylase (PHD), thereby preventing proteosomal degradation of the subunit and promoting EPO expression.

Figure 3

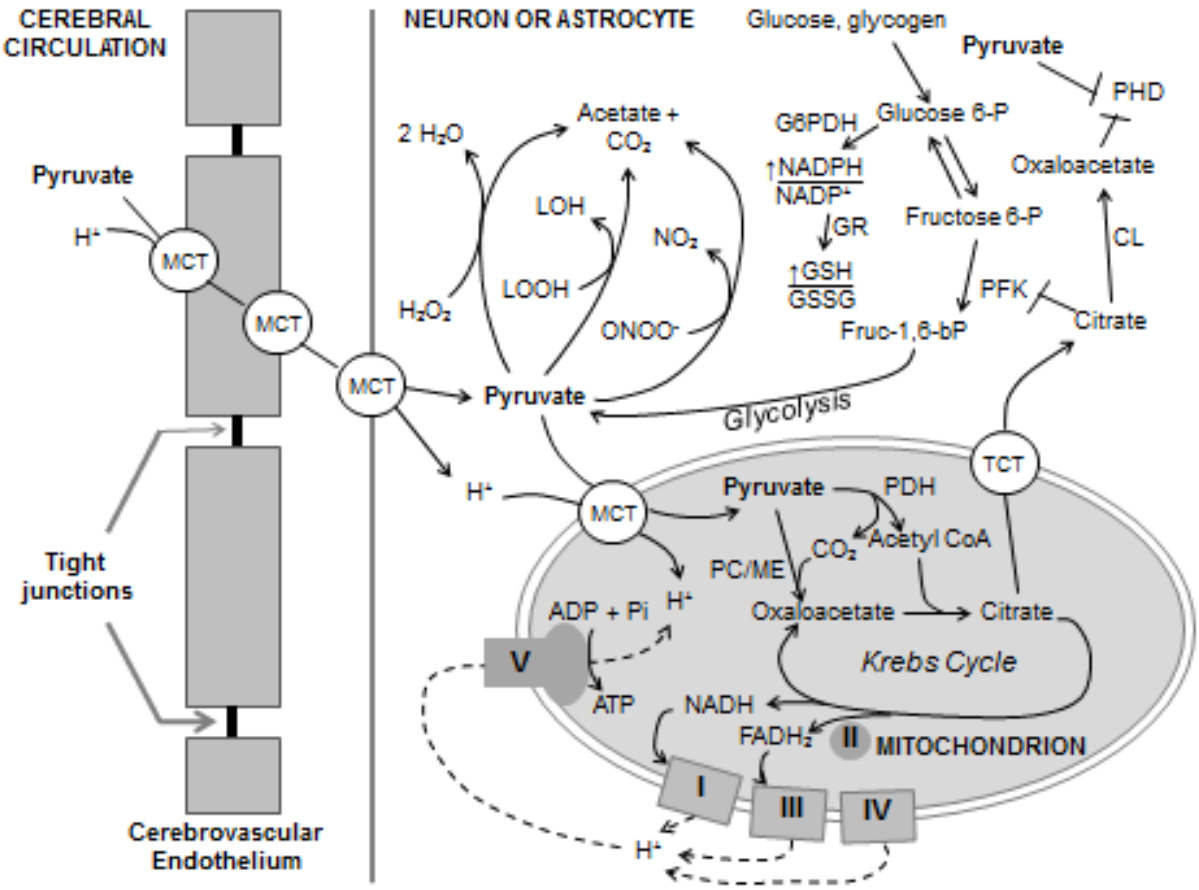

Figure 3. *Metabolism and cytoprotective mechanisms of pyruvate in brain.* Pyruvate is carried across the cerebrovascular endothelium and cell and mitochondrial membranes within the brain parenchyma my monocarboxylate transporters (MCT). In addition to its induction of EPO expression (Figure 2), pyruvate affords cytoprotection by (1) supporting oxidative metabolism and mitochondrial ATP production; (2) directly detoxifying hydrogen peroxide, lipid peroxides (LOOH) and peroxynitrite; (3) increasing mitochondrial citrate formation, which, when exported to the cytosol by the tricarboxylate transporter (TCT), suppresses phosphofructokinase (PFK) activity, thereby diverting glycolytic flux into the hexose monophosphate shunt, the source of NADPH reducing power by glucose 6-phosphate dehydrogenase (G6PDH) and 6-phosphogluconate dehydrogenase; (4) cytosolic citrate lyase degrades citrate to acetate and oxaloacetate, which, like pyruvate, competitively inhibits prolyl hydroxylase.